TRANSPORTATION RESEARCH

RECORD

No. 1382

Materials and Construction

PART 1

1993 TRB Distinguished Lecture

BRYANT MATHER

PART 2

Developments in Concrete Technology

A peer-reviewed publication of the Transportation Research Board

TRANSPORTATION RESEARCH BOARD
NATIONAL RESEARCH COUNCIL

NATIONAL ACADEMY PRESS
WASHINGTON, D.C. 1993

Transportation Research Record 1382
Price: $22.00

Subscriber Category
IIIB materials and construction

TRB Publications Staff
Director of Reports and Editorial Services: Nancy A. Ackerman
Senior Editor: Naomi C. Kassabian
Associate Editor: Alison G. Tobias
Assistant Editors: Luanne Crayton, Norman Solomon, Susan E. G. Brown
Graphics Specialist: Terri Wayne
Office Manager: Phyllis D. Barber
Senior Production Assistant: Betty L. Hawkins

Printed in the United States of America

Library of Congress Cataloging-in-Publication Data
National Research Council. Transportation Research Board.

1993 TRB distinguished lecture/Bryant Mather. Developments in concrete technology: a peer-reviewed publication of the Transportation Research Board / Transportation Research Board, National Research Council.
p. cm.—(Transportation research record, ISSN 0361-1981; no. 1382)
ISBN 0-309-05451-6
1. Concrete. 2. Concrete—Testing. 3. Pavements, Concrete. I. Mather, Bryant. II. National Research Council (U.S.). Transportation Research Board. III. Series: Transportation research record; 1382.
TA439.A16 1993
625.8'4—dc20 93-8533
CIP

Sponsorship of Transportation Research Record 1382

GROUP 2—DESIGN AND CONSTRUCTION OF TRANSPORTATION FACILITIES

Group 2 Council
Chairman: Charles T. Edson, Greenman Pederson
Mike Acott, Thomas J. Barnard, David B. Beal, Robert L. Clevenger, Donald J. Flemming, Raymond A. Forsyth, Donn E. Hancher, Scott B. Harvey, Robert D. Holtz, J. M. Hoover, Rosemary M. Ingram, Michael G. Katona, Joe P. Mahoney, William B. O'Sullivan, Thomas J. Pasko, Jr., Harold R. Paul, M. Lee Powell, III, Hayes E. Ross, Jr., Earl C. Shirley

Concrete Section
Chairman: Thomas J. Pasko, Jr., Federal Highway Administration

Committee on Performance of Concrete
Chairman: Donald J. Janssen, University of Washington
M. Arockiasamy, Philip D. Cady, William P. Chamberlin, Glenn William De Puy, Philip H. DeCabooter, John W. Figg, Kenneth C. Hover, Inam Jawed, Joseph F. Lamond, James W. Mack, Richard C. Meininger, Roger P. Northwood, John T. Paxton, Steven A. Ragan, V. Ramakrishnan, John Ryell, David Stark, Joyce M. Susa, Richard Edwin Weyers

Committee on Mechanical Properties of Concrete
Chairman: Michael M. Sprinkel, Virginia Transportation Research Council
Archie F. Carter, Jr., W. Charles Greer, Jr., James D. Grove, Lloyd E. Hackman, Inman Jawed, Lawrence I. Knab, Louis A. Kuhlmann, Joseph F. Lamond, Colin Lobo, V. M. Malhotra, Edward G. Nawy, Steven A. Ragan, V. Ramakrishnan, Masood Rasoulian, Gary L. Robson, M. Reza Salami, Charles F. Scholer, Raymond J. Schutz, S. P. Shah, James M. Shilstone, Sr., Parviz Soroushian, D. Gerry Walters, Dan G. Zollinger

Committee on Chemical Additions and Admixtures for Concrete
Chairman: H. Celik Ozyildrim, Virginia Department of Transportation
Bernard C. Brown, John W. Bugler, Ramon L. Carrasquillo, Henry H. Duval, Jr., Richard D. Gaynor, R. Douglas Hooton, Kenneth C. Hover, Inam Jawed, Daniel P. Johnston, Kamal Henri Khayat, T. J. Larsen, Mosongo Moukwa, Michael F. Pistilli, V. Ramakrishnan, Jere Rose, Maris A. Sermolins, A. Haleem Tahir, Samuel S. Tyson, Suneel N. Vanikar, Thomas G. Weil, David Whiting

Construction Section
Chairman: Donn E. Hancher, University of Kentucky

Committee on Rigid Pavement Construction and Rehabilitation
Chairman: Sanford P. Lahue, American Concrete Pavement Association
Woodrow J. Anderson, Curt A. Beckemeyer, Bernard C. Brown, Yves Charonnat, Lawrence W. Cole, Michael I. Darter, Howard J. Durham, John E. Eisenhour, Jr., Ronald M. Guntert, Jr., Jim W. Hall, Jr., Ira J. Huddleston, L. S. Ingram, Carlos Kraemer, Louis R. Marais, John E. McChord, Jr., Dennis A. Morian, James J. Murphy, Wayne F. Murphy, Theodore L. Neff, M. Lee Powell III, William G. Prince, Carl W. Rapp, Terry W. Sherman, William L. Trimm, Steven Tritsch, Dan G. Zollinger

Frederick D. Hejl, Transportation Research Board staff

Sponsorship is indicated by a footnote at the end of each paper. The organizational units, officers, and members are as of December 31, 1992.

Transportation Research Record 1382

Contents

PART 1

1993 TRB Distinguished Lecture

Part 1
Foreword

In 1990 the Transportation Research Board Executive Committee approved the establishment of the Distinguished Lectureship Series to recognize the career contributions and achievements of an individual in one of four areas covered by the Board's Technical Activities Division: transportation systems planning and administration (Group 1); design and construction of transportation facilities (Group 2); operation, safety, and maintenance of transportation facilities (Group 3); and legal resources (Group 4).

Those selected are provided a forum at the TRB Annual Meeting to present an overview of their technical area, including evolution, present status, and prognosis. Bryant Mather, Director of the Structures Laboratory at the U.S. Army Corps of Engineers Waterways Experiment Station, is the second to be honored with the TRB Distinguished Lectureship. His lecture, entitled *Concrete in Transportation: Desired Performance and Specifications*, was sponsored by Group 2 and presented at the 1993 Annual Meeting. It is published in this Record.

Bryant Mather, 1993 TRB Distinguished Lecturer

BRYANT MATHER

Bryant Mather is the director of the Structures Laboratory at the U.S. Army Corps of Engineers Waterways Experiment Station in Vicksburg, Mississippi.

An employee of the Corps of Engineers since 1941, Mr. Mather first worked as a geologist and later as an engineer. Throughout his career, he has specialized in concrete research. His first assignment was with the Central Concrete Laboratory at the U.S. Military Academy, West Point, and at Mount Vernon, New York. He has been affiliated with the Waterways Experiment Station since 1946.

He received a bachelor's degree in geology from Johns Hopkins University, where he also did graduate work in geology. He also did graduate work in economics at American University. Mr. Mather received an honorary doctorate from Clarkson University in 1978.

Throughout his career, Mr. Mather has been active in ASTM, the American Concrete Institute (ACI), and TRB. He is a member of several ASTM committees and has more than 162 years of service on nine ACI technical committees. He is one of only three individuals to have served as president of both ASTM and ACI.

For TRB, Mr. Mather served as Chairman of the Curing Concrete Committee from 1971 to 1974 and Chairman of the Concrete Division from 1963 to 1969. He received the Roy W. Crum Distinguished Service Award in 1966. His colleagues elected him to honorary membership of the TRB concrete committees, on which he remains active. He also served for many years on the NCHRP SP20-5 Panel on Synthesizing Information on Highway Projects. Additionally, he has been a member of the Cement and Concrete/Structures Advisory Committee of the Strategic Highway Research Program since the program's inception in 1984.

As one of the foremost experts on concrete, Mr. Mather has received many government and industry awards. His awards include the Department of the Army's Meritorious Civilian Service Award and the Decoration for Exceptional Civilian Service. President Carter made him a charter member of the government's Senior Executive Service in 1979. ASTM has bestowed on Mr. Mather its Award of Merit, the Sanford E. Thompson Award, the William T. Cavanaugh Award, the Frank E. Richart Award, the Charles B. Dudley Award, and honorary membership. ACI presented him with the Henry C. Turner Medal and honorary membership. He is an honorary fellow of England's Institute of Concrete Technology. In 1992 he was elected to the National Academy of Engineering.

Mr. Mather was the Henry M. Shaw Lecturer at North Carolina State University in 1967, the Stanton Walker Lecturer at the University of Maryland in 1969, the ASTM Edgar Marburg Lecturer in 1970, the IBM Visiting Scholar at Northeastern University in 1985, and a visiting professor at the Science University of Tokyo, Japan, in 1988. He is author or co-author of more than 500 technical reports and papers.

Mr. Mather is recognized internationally as "Mr. Concrete" because of his great contributions and dedicated interest in concrete technology transfer. With more than 50 years of a highly committed and most productive career for the U.S. Army Corps of Engineers, he continues to be a world-renowned researcher, lecturer, consultant, and activist in consensus standards-writing organizations.

Concrete in Transportation: Desired Performance and Specifications

BRYANT MATHER

This lecture is about concrete—specifically, hydraulic-cement concrete. If one starts with the dry powder that is hydraulic cement—usually the particular class of hydraulic cement known as portland cement—and adds water, what results, depending on the amount of water added, is cement paste or grout. Grout can be poured like gravy. If fine aggregate is added, the result is mortar or sanded grout. If both fine aggregate and coarse aggregate are added, the result is concrete. As the Supreme Court of Pennsylvania once wrote in a decision dealing with cement-manufacturing plants, "cement is to concrete as flour is to fruitcake." My first point is, to get proper concrete, get the terminology right. There is no such thing as a cement mixer. And sand is not a synonym for fine aggregate; sand is a class of fine aggregate produced by nature rather than by rock crushers and grinding mills.

Having dealt briefly with terminology, I will provide the procedure for obtaining concrete that has the desired performance. It is, simply, to include the relevant requirements in the contract documents and ensure through proper contractor quality control and proper owner quality assurance that the requirements of the specifications are followed. In fewer words, order the concrete that you need and make sure that you get it.

DEVELOPMENT OF HARDENED CONCRETE PROPERTIES

Robert Philleo, who in 1986, as chairman, signed the certificates making Katherine Mather and me honorary members of the Concrete Section of TRB and all of its committees, also in 1986 described the fundamental features of concrete. The following is paraphrased from his papers (*1*,*2*). For concrete to stiffen, harden, and develop strength, there must be a chemical reaction between the constituents of the cement and the mixing water. This reaction causes the anhydrous calcium silicates in the cement to be converted into calcium silicate hydrate (CSH), the cement gel or hydrated cement. The critical feature of this reaction is that if the ratio of the volume of water to the volume of cement is 1.2, then all the water and all the cement can combine and all the originally mixing water–filled space can be filled with hydration product. A water-cement ratio (w/c) of 1.2 by volume is 0.4 by mass. If the w/c is higher than 0.4, even if all the cement hydrates, there will always be some residual originally mixing water–filled space that can hold freezable water. If the w/c is lower than 0.4, some of the cement will always remain unhydrated but, in theory, all the originally mixing water–filled space could be filled with CSH. There is a misconception, often stated, that it takes only the amount of water in a 0.2 w/c paste to hydrate all of the cement. This is based on the fact that only 0.2 unit of water by mass chemically combines with cement during hydration. However, for a given volume of cement to hydrate, there must be an amount of originally mixing water–filled space equal to 1.2 times the volume of the cement. This is because the hydration product has about 30 percent pore space that must be present, and water must be available to fill it. If the amount of originally mixing water–filled space is less than that provided at a w/c of 0.4, not all of the cement can hydrate, even though only half of that water will go into chemical combination.

A lot of modern "high-performance" concrete made at w/c's well below 0.4 by mass will not, in fact, have all of the originally mixing water–filled space filled with hydration product. This is because the part of the mixing water that ends up in the gel pores undergoes a 10 percent reduction in volume because the pores are so small and the water is adsorbed. Philleo's 1991 discussion goes into the implications of the fact that additional water may enter while test specimens of very low w/c concrete are curing in the laboratory, but such externally available water will not get very far into larger masses of field concrete even if it is made available. It is worth noting that even though I am a well-known advocate of membrane curing for field concrete, I put in the American Concrete Institute (ACI) standard for curing concrete (ACI 308-81) Section 3.2.2 that the use of liquid membrane-curing compounds should not be approved "when the concrete has a water-cement ratio of 0.4 or less."

In these comments there may have been the implication that something is desirable about hydrating all the cement in a concrete mixture. If the w/c is higher than 0.4, then the more of the cement that hydrates, the larger the proportion of the originally water-filled space that gets filled, the higher the strength, and the lower the permeability. Therefore, if the concrete needs all the strength and reduced permeability that it can get, then the longer it is kept moist, the closer it will come to having all its cement hydrated and the greater its strength and impermeability will be. There are, however, at least two possibly undesirable consequences of a concrete's having all of its cement hydrated and becoming as strong as it can become. First, if there is no remaining unhydrated cement, then there can be no autogenous healing of microfractures as water enters and is available to react with unhydrated cement to accomplish the healing. Second, if the concrete is as strong as it can possibly become, it will have a higher modulus of elasticity, be more brittle, and crack at a lower strain level. Reduced strain capacity—both elastic strain

and creep strain—is not a desirable property in a lot of concrete. As Philleo put it,

> the desirable magnitude of creep is an issue on which practitioners have not agreed. Structural engineers find it a nuisance they could easily do without. . . . On the other hand, builders of unreinforced mass concrete structures find creep an indispensable property of concrete. . . . Creep redistributes stresses . . . permitting highly stressed regions to shed some of their stresses to low-stressed regions before cracking occurs. . . . [Mass concrete] structures could not survive if concrete behaved elastically. (*1*)

Those further interested in concrete should read Philleo (*1*,*2*).

CLASSES OF DETERIORATION

Very little concrete fails to provide the desired level of performance because its mechanical strength is intrinsically insufficient. Indeed, as noted earlier, one of the undesirable things that can happen to concrete is that, by getting too strong, it can also get too brittle and have an undesirably low strain capacity before fracturing. Consequently, the efforts to achieve the desired performance should be those that avoid the problems generally comprehended under the subject "durability."

I have spent a great deal of time over a good many years explaining to people that concrete has no property called durability. Any concrete, no matter how unsuitable for use in many environments, will be completely durable in some environment. I have argued that any concrete strong enough to resist the loads to which it will be subjected in service will also be durable in that service, regardless of all other considerations, if it is allowed to get dry and to stay dry. "Dry" in this context means that the evaporable water is allowed to and does escape and the internal relative humidity drops below 80 percent, under which conditions there are no longer any chemical reactions that can take place and there is no water that can freeze. Earthquakes and possibly fire could damage such concrete, of course, but generally speaking, the resistance to earthquakes comes under the heading "if it is strong enough" and the damage due to fire is much lower in concrete that is dry than in concrete that is not.

We may thus explore durability as it relates to concrete in transportation with the assumption that the concrete that we are talking about is being used in an environment in which rarely, if ever, are the structures allowed to get dry and stay dry. However, remember that if we have any such structures, we are in a fortunate position with respect to the steps we need to take to achieve satisfactory performance.

I suggest classifying the causes of deterioration of concrete into two categories. The first category includes those causes of damage in which the cause acts on the concrete, causes the damage, and then ceases to act usually for a very long time or forever. These causes include earthquakes, tornadoes, hurricanes, fire, and lightning strikes. Once a gasoline truck has burned up on a pavement, the damage done to that concrete by that fire is the damage that can be discovered by simply examining the affected structure. Any concrete that has not been damaged by that influence is not going to be damaged by that event subsequently. Therefore, from the standpoint of maintenance and repair, if what has been damaged is repaired, that which is undamaged will never be damaged by whatever brought about the need for the repair.

The second, more difficult class of deteriorative influences includes all of the mechanisms that, when recognized as having caused damage to some concrete in service, are of such a nature that the prudent conclusion is that much more of the concrete may be expected to be damaged unless it can be protected from the processes that caused the initial damage. In this class are those concretes that are unable to resist freezing and thawing or chemical attack (especially sulfate attack); those concretes that have been produced of materials that contained the seeds of their own destruction such as aggregates of inadequate volume stability, unsound cement, and unfortunate combinations of alkali-reactive aggregate and high-alkali cement or high-alkali solutions from the environment; and those unprotected reinforcing steel with inadequate cover over the steel and an excess of substances that promote corrosion in the environment. All such damage may be expected to be progressive unless there is a way to stop it. This line of reasoning yields the conclusion that a very important purpose of the investigation of damage, distress, deterioration, and failure is to have a clear appreciation of the causes. This is essential to establishing whether the causes were permitted to work because of a defective specification or the failure to follow a proper one, which is relevant to issues of liability. It is also essential to planning a proper repair or replacement strategy. And, as related to the present topic, it is essential to one's overall strategy in preparing proper specifications for future work.

The way to obtain satisfactory concrete is to know what to avoid and to take proper steps to avoid it. The art of knowing what to avoid means matching the intended environment of service with similar environments in which concrete has performed less well than desired and knowing what interrelationship of environmental stress and concrete deterioration produced that less-than-desired result. There is enough available knowledge, summarized perhaps best in the 1992 report of ACI Committee 201, that we need not to go back to square one (*3*). The ACI committee report takes up the problems of durability of concrete in chapters dealing with freezing and thawing; aggressive chemical exposure including sulfate attack, acid attack, and carbonation; abrasion; corrosion of embedded metals and other materials; and chemical reactions of aggregates. The report also includes two more chapters, which address the repair of concrete and the use of protective barrier systems to enhance concrete durability, respectively.

I will talk no further about repair practices, but I will say in passing that although protective barrier systems can function beneficially—especially if by some means one can cause some concrete to become dry and the barrier can be applied in such a manner as to cause the concrete to stay dry—then if the concrete is afflicted with a defect that would make it nondurable in service and it can be caused to become dry and stay dry, it may very well survive for a long time in that environment. However, most concretes that are vulnerable to damage in service have difficulty getting dry, and if they do dry, it is hard to keep them dry by sealing them because one cannot seal all six sides: top, bottom, front, back, left, and right. Some bridge decks appear to be the exception to this rule. In most other concrete structures in transportation, at least the bottom is in contact with moisture.

Let me now comment briefly on the several classes of phenomena potentially harmful to the durability of concrete as they are dealt with in the ACI 201 report.

Freezing and Thawing

I recently summarized in a paper what I thought I understood about the resistance of concrete to freezing and thawing (*4*). The content of this paper is not in conflict, I think, with what ACI Committee 201 says; however, I approach it from a slightly different point of view. I point out, rather obviously, that concrete will be immune to the effects of freezing for several reasons: (a) if it is not in an environment in which freezing and thawing take place so as to cause water in the concrete to freeze; (b) if, when freezing takes place, there are no pores in the concrete large enough to hold freezable water; (c) if any pores can hold freezable water, they are less than 91 percent full at the time of freezing; or (d) if pores that can hold freezable water are *more* than 91 percent full, the cement paste has a proper air-void system, sound aggregate, and moderate maturity. In the extensive work of Paul Klieger, moderate maturity was discovered to exist if the combination of w/c and cement hydration has proceeded so that the concrete has developed a compressive strength of about 30 MPa (4,000 psi) before it is allowed to freeze and thaw in a critically saturated state. Sound aggregate is the kind of aggregate that when used in concrete containing a proper air-void system in the paste, which is allowed to get moderately mature before freezing, gives frost-resistant concrete as can be measured in the laboratory using ASTM C666 Procedure A. A satisfactory air-void system in the paste is one that is characterized by having an air bubble not more than 0.2 mm (0.008 in.) from anywhere.

As far as I am aware, there is essentially no place in the world today where concrete is needed in transportation structures that is likely to be critically saturated when exposed to freezing and thawing for which sound aggregates cannot be obtained or the concrete be protected against freezing and thawing while critically saturated until it is moderately mature, and for which circumstances preclude using an appropriate amount of proper air-entraining admixture so as to produce concrete with a satisfactory air-void system. Some of us feared that we might be in a situation in which we could not produce concrete with a satisfactory air-void system using roller-compacted concrete, which is of considerable interest especially for paving in military reservations. However, recent work has made it clear that adequately frost-resistant concrete can be made even at the levels of harshness and dryness that characterize concrete suitable for roller compaction (*5*).

Aggressive Chemical Exposure

Sulfate Attack

The Corps of Engineers' requirements for taking account of sulfate in the environment say that if the level of water-soluble sulfate in soil or dissolved in fresh water expressed as SO_4 is less than 0.1 percent or 150 ppm, respectively, no precautions are necessary (*6*). If the amount of sulfate is between 0.1 and 0.2 percent in soil or 150 and 1,500 ppm in water, the attack is considered moderate and the appropriate precaution is to use Type II moderately sulfate-resisting cement in which the calculated C_3A content is 8 percent or less. If Type II cement is not economically available, an equivalent degree of sulfate resistance can usually be obtained by using either blended cement made with pozzolan or granulated blast-furnace slag or by adding a proper amount of ground slag or an effective pozzolan such as fly ash or silica fume. Finally, if the sulfate content is higher than the larger values just mentioned, the level of protection should be proportionately greater and will be achieved by using either Type V highly sulfate-resistant cement in which the C_3A content must be kept to 5 percent or less. If such cement is not economically available, a proper amount of an appropriate ground slag or pozzolan can be used.

It is interesting to note that much work has indicated that if the permeability of the concrete is reduced, either by adhering to a lower w/c or by adding ground slag, the amount of C_3A in the cement can be allowed to rise. The Corps of Engineers now permits up to 10 percent calculated C_3A if the w/c of the concrete is kept below 0.45 and the concrete is permanently submerged in seawater.

Another relevant recent development is a performance test that will properly evaluate the sulfate resistance of a cementitious material or blend of such materials. This is ASTM C1012, which involves fabricating mortar bars and storing them in water until they develop a specific degree of maturity and thereafter immersing them in a standard sulfate solution. The sulfate resistance of the cementitious material is regarded as adequate if the expansion of the mortar bars remains below 0.1 percent. This limit has been adopted in the new performance-based ASTM specification for blended hydraulic cements (ASTM C1157).

Acid Attack

Besides sulfate attack, other aggressive chemical exposures involve acid and CO_2. Concrete in transportation structures is not likely to be exposed to acid very often or very severely. If I were making this talk 10 or 15 years ago, I would warn against the hazards to concrete bridge piers that might result from the establishment of an industry upstream that released strong acids into the water, but clean water laws make this much less likely today. There are cases in which acid from coal mine drainage can cause rivers and streams to have very low pH, in which case it would be better if no transportation structure made out of concrete came into contact with the acid. The Corps of Engineers was asked once to build a dam where the so-called water in the reservoir was said to have a pH as low as 2.0, except after a heavy rain when it went up to 2.4. Nobody suggested making concrete that would be intrinsically resistant to this exposure; instead, we worked on developing an organic coating that would keep the acid from coming into contact with the concrete.

Carbonation

The effects of exposure to concrete of CO_2 in the atmosphere and the resulting carbonation of the concrete appear to be

the current scare phenomenon in concrete technology. People have noticed for a century or more that, after some years of exposure in the first few millimeters below the surface, the cement paste in hardened concrete typically contains no longer calcium hydroxide but calcium carbonate. It has been assumed, correctly, that this represents the reaction of CO_2 from the air with calcium hydroxide in the cement paste to produce calcium carbonate. The carbonation of the cement paste in concrete lowers the amount of calcium hydroxide that is available to replenish the aqueous phase of that concrete with calcium hydroxide in solution to maintain saturation and, hence, a pH of about 12.6—which is, of course, the normal and desirable circumstance from the standpoint of preserving embedded steel from corrosion. Much nonsense has been perpetrated largely by people who oppose the use of ground slag and pozzolans in concrete; they have argued that such use consumes some of the calcium hydroxide that would otherwise be present and is needed to keep up the pH and prevent corrosion of steel. The other argument has been that one ought to use pozzolans for converting the otherwise useless and to some extent undesirable calcium hydroxide—or, as they would call it, free lime—to beneficial CSH with the concomitant reduction in the amount of soluble calcium hydroxide that could go into solution, be carried to the surface through cracks, exit the cracks, and produce ugly efflorescence.

In my judgment, both of these arguments are without practical merit and have little theoretical justification. It would take a great deal of activity to produce an aqueous phase in concrete of even modest quality that was not a saturated solution of calcium hydroxide considering the great excess of calcium in portland cement beyond that needed to make CSH of all the silica in the cement plus all of the available pozzolanic silica at the normal ratios of cement to pozzolan in high-quality structural concrete as should be used in transportation structures. To avoid efflorescence, one should provide appropriate drains so that water does not pass through cracks in walls and bridges and deposit calcium hydroxide that later carbonates.

Abrasion

The third chapter of the ACI 201 report deals with abrasion. This subject is a very important one in transportation because probably more concrete in the world is subject to abrasion in transportation than in any other class of use. When concrete is less resistant to abrasion than desired, sometimes unsafe surface textures develop that create severe hazards because the pavement is nonresistant to skidding.

ASTM has developed several tests to evaluate the degree to which concrete is worn away by rubbing and friction; however, it is important to separate the things that are relevant to one class of structure from those relevant to another. The wearing away of the top surface layer of a very smooth industrial floor under vehicular or other traffic and the consequent production of dust that can harm manufacturing operations is quite different from the wearing away of the texture of a pavement surface. Similarly, the issue of the relative resistance to wear of the mortar portion of the concrete and the coarse aggregate portion becomes very important to skid resistance. It has been necessary and effective to use a special abrasion-resistant coarse aggregate so that if the surface mortar skin is removed by abrasion, the coarse aggregate will continue to protrude above the base level and provide a skid-resistant surface.

The ACI 201 recommendations suggest that almost all the good practices in concrete production benefit the improvement of abrasion resistance of the surface, especially practices that reduce segregation and the consequent development of a thicker-than-desired layer of mortar at the surface, avoiding bleeding that may cause the surface mortar to have a higher-than-intended w/c and avoiding finishing procedures that bring up more fines or take place at an undesirable time. Obviously, one cannot develop an abrasion-resistant concrete surface unless the concrete at that surface is allowed to develop its potential strength and, hence, abrasion resistance. Thus, a major factor in producing abrasion-resistant concrete is the quality of the curing.

Section 3.6 in the ACI 201 report deals specifically with wear on concrete resulting from tire chains and studded snow tires. It says that studded snow tires have caused widespread and serious damage even to high-quality concrete. It adds that "fortunately the use of studded snow tires has been declining for a number of years," and it specifically calls attention to *NCHRP Synthesis of Highway Practice 32* (*7*).

Corrosion of Metal

It is my guess that more concrete that has failed to provide satisfactory service for its intended service life because of premature deterioration from interacting with its environment, especially over the last couple of decades, has done so because the precautions taken to prevent corrosion of the reinforcing steel turned out to be inadequate. I have gone on record several times to the effect that all that is needed to prevent corrosion of the steel is to have a cover of high-quality concrete 50 mm (2 in.) thick over the steel and appropriate measures to control concrete cracking. This approach usually works with massive constructions such as bridge piers, dry docks, wharf structures, and off-shore structures. However, this has not been the case with highway bridge decks and superstructures and parking structures. People who design bridge decks, or at least who did in the past, often failed to provide decks thick enough that the required reinforcing steel could be put in place and still have 50 mm (2 in.) of good concrete over it. Thin, strong bridge decks are preferred because they have less deadweight and are more aesthetically pleasing. We need to take extra precautions to protect steel from corrosion if we must live with thin reinforced concrete structures in environments of high potential for materials corrosion; these include highway bridge decks that are deiced with chloride-based deicing chemicals and parking garages in which slush caught under vehicle fenders melts and runs out onto the floor as water with a rather high chloride concentration. We should not, however, in the process give up the effort to make the concrete that we do have concrete of high quality, low w/c, and proper curing. What we do is one or both of two things; some recent experiences have suggested that where the need for protection is great, it is prudent to

do both. These two measures are as follows: (a) use properly prepared, thermally bonded epoxy coatings on the reinforcing steel, and (b) use corrosion-reducing chemical admixtures such as calcium nitrite. I believe that in nearly all cases of serious risk of corrosion, either of these solutions by itself will be completely satisfactory if the potential benefits are realized. However, it has become apparent that there are structures whose owners believed that they were using properly protective epoxy-coated steel when, in fact, the steel put into the structure corroded very quickly. I have not heard recently of an owner who believed that he or she was protected by a chemical admixture and was not, but I am sure I will someday. Then one should consider the use of lightweight concrete with which, for the same deadweight, one can have greater cover over the steel. Alternatively is the option of using up to 30 percent less concrete to achieve a 25 percent reduction in deadweight by using stronger concrete, 60-MPa (8,700-psi) concrete, rather than 35-MPa (5,000-psi) concrete and external prestressing.

There has been much debate on the issue of how much chloride should be in the concrete at the time it is produced. We are aware now, of course, that in addition to the intentional use of calcium chloride as an accelerator to assist in producing early strength in concrete, there is chloride to some degree in other admixtures used for other purposes. Chloride is present in some cementitious materials, and chloride can be present in sea-dredged aggregates, as are used in several places, notably England and Japan, and in certain limestones that are used as concrete aggregate in the United States far from the seacoast. There is also chloride in some mixing water. If one is using epoxy-coated steel or calcium nitrite, it should not matter how much chloride is in the concrete as made. If neither of these precautions is taken, it might matter a lot.

The question of whether it is ever prudent to assume that none of the measures that I have mentioned will be satisfactory and to install cathodic protection for the steel at the time the structure is built is, I think, still undecided. This may be wise in some cases, but I expect that they are few and far between.

Chemical Reactions of Aggregates

Tom Stanton, of the California Department of Transportation (although they didn't call it that then), discovered alkali-silica reaction in 1940 (*8*,p.54ff). I went to work for the Concrete Laboratory at the Corps of Engineers in August 1941. Word of his discovery had already reached that laboratory, and one of the first bits of work I did was looking at "siliceous magnesian limestone," which was described as the offending ingredient of concrete that had deteriorated. At that point the Corps of Engineers was quite concerned because, to us, magnesian limestone meant dolomite, and dolomite was very widely used in Corps of Engineers structures. Our position had been that *most* limestones were satisfactory but substantially *all* dolomites were. It turned out that the siliceous magnesian limestone that caused the trouble in California is an almost unique rock that contains a lot of opaline chert. As far as I know, no other dolomite in the world contains enough opaline chert to cause trouble.

The Ninth International Conference on Alkali-Aggregate Reaction on Concrete took place in July 1992 in London in the Queen Elizabeth II Conference Center across the street from Westminster Abbey; several hundred people attended from essentially everywhere in the world. Aggregates that were not previously regarded as reactive are now shown to be reactive when used with cements of higher alkali content than they had been used with. Cements in many parts of the world are now of higher alkali content than they used to be, partly because more of them are made using raw materials containing relatively large amounts of alkali (such as, for example, all of the cement in Iceland for which all of the calcareous raw material is seashells dredged from the ocean) and also partly because of the capture of kiln dust and its insertion into the product. With regard to this last point, I am told that some farmers now must buy substantial amounts of potash fertilizer because cement plants upwind are catching the kiln dust that used to go out their stacks and putting it back into the cement, to the detriment of both the cement and the farmer.

Alkali-silica reaction involves a series of events. A reactive aggregate is one that contains silica, SiO_2, in a form that is capable of being dissolved by pH solutions substantially higher than the 12.6 pH that characterizes the saturated calcium hydroxide solution that is normal in concrete. Either the cement contains enough sodium or potassium so that the pH is raised when the cement hydrates and these ions go into solution, or the alkalies come in from the outside and raise the pH. In any event, the pore fluid in the concrete gets to be high enough in pH to dissolve the silica and produce an alkali-silica gel that has the property of taking up water, swelling, and expanding and disrupting the concrete.

If the circumstances are such that any problems that might be brought about by alkali from the environment can be ignored, then, in many cases, all that is necessary is to invoke the specification option for cement and require the use of low-alkali cement when reactive aggregate must be used. This requirement means that the cement will not be allowed to contain more than 0.60 percent alkalies calculated as the percentage Na_2O plus 0.658 times the percentage K_2O. If low-alkali cement is not available, equivalent protection can usually be provided by using an appropriate amount of an acceptable ground slag or pozzolan, the acceptability being based on tests by ASTM C441.

There is also an alkali-carbonate rock reaction that has been found in a number of highway structures, especially some in Illinois, Indiana, Iowa, Michigan, Missouri, New York, South Dakota, Tennessee, Virginia, and Wisconsin. Not all such reactions are deleterious. Sometimes the reaction simply takes place, and a small portion inward from the outer surface of an aggregate particle is altered so that when one slices through the concrete and acid-etches the sawed surface, the aggregate particle develops two levels of etching. Sometimes the interior is more acid-soluble than the rim, and sometimes it is less acid-soluble than the rim; in either case the fact that the rim is on crushed stone particle is evidence that a reaction took place in the concrete.

To avoid harmful alkali-carbonate-rock reactions, use nonreactive aggregate or figure out a combination with low-alkali cement. The ACI committee report recommends a value less than 0.60 percent Na_2O equivalent.

CONCLUSION

To obtain the performance that is desired of concrete in transportation, it is necessary to

1. Decide what sorts and levels of imperfections are tolerable and intolerable,
2. Understand what causes imperfections that are intolerable,
3. Evaluate the environment in which the concrete is to serve to recognize the presence of influences that must be resisted if the concrete is to perform as desired,
4. Prepare concrete specifications that require appropriate levels of relevant properties of concrete so that the concrete can resist the deteriorative influences it will encounter in service, and
5. Ascertain that both the contractor's quality control and the owner's quality assurance systems work to ensure that the concrete produced is as specified.

ACKNOWLEDGMENT

The author gratefully acknowledges permission from the Chief of Engineers to publish this paper.

REFERENCES

1. R. E. Philleo. Concrete Science and Reality. In *Materials Science of Concrete II* (J. Skalny and S. Mindess, eds.), American Ceramic Society, Westerville, Ohio, 1991, pp. 1–8.
2. R. E. Philleo. *NCHRP Synthesis of Highway Practice 129: Freezing and Thawing Resistance of High-Strength Concrete*. TRB, National Research Council, Washington, D.C., 1986.
3. Guide to Durable Concrete (ACI 201.2R-92) (Draft). *ACI Materials Journal*, Vol. 88, No. 5, Sept.–Oct. 1991, pp. 544–582 (to be published in *Manual of Concrete Practice*, American Concrete Institute, Detroit, Mich., 1993).
4. B. Mather. How To Make Concrete That Will Be Immune to the Effects of Freezing and Thawing. In *ACI SP-122: Paul Klieger Symposium on Performance of Concrete* (D. Whiting, ed.), American Concrete Institute, Detroit, Mich., 1990, pp. 1–18.
5. S. A. Ragan. The Use of Air Entrainment To Ensure the Frost Resistance of Roller-Compacted Concrete Pavements. In *ACI SP-126: Durability of Concrete*, American Concrete Institute, Detroit, Mich., 1991, pp. 115–130.
6. *Standard Practice for Concrete*. Engineer Manual 1110-2-2000. Office of the Chief of Engineers, U.S. Army Corps of Engineers, Washington, D.C., 1985.
7. L. D. Byrd. *NCHRP Synthesis of Highway Practice 32: Effects of Studded Tires*. TRB, National Research Council, Washington, D.C., 1975.
8. T. E. Stanton. Expansion of Concrete Through Reaction Between Cement and Aggregate. *Transactions*, ASCE, Vol. 107, 1940.

PART 2

Developments in Concrete Technology

Part 2
Foreword

The papers in Part 2 of this Record deal with various facets of concrete technology; they should be of interest to state and local construction, design, materials, and research engineers as well as contractors and material producers.

Emmons and Vaysburd propose a ranking system that would assist in the selection of materials for concrete repairs with a potentially lower risk of shrinkage stresses, cracking, and debonding. They conclude that there is an urgent need for developing performance criteria for the selection of compatible repair materials along with the selection or development of a reliable industrywide shrinkage test method. Schemmel and Leming discuss a Strategic Highway Research Program (SHRP) contract to investigate the use of high-performance concrete for rapid highway pavement repairs. They provide details regarding site locations, type of concrete used, the construction process, and the testing plan. They conclude with a discussion of lessons learned from the field trials.

Buch and Zollinger examine the effects of relative humidity on concrete pavement strength and behavior. From their preliminary investigation they suggest that a system of crack control may be based on the determination of the change in relative humidity. Kamel et al. discuss the performance of a silane-penetrating water-repellent material applied to three concrete mix types. Smutzer and Chang present the methodologies and the results after 3 years of a field study to evaluate the resistance of various generic concrete pavement sealers to chloride ion penetration. Salami et al. describe their investigation of the influence of three coarse-aggregate types on the relationship between compressive and tensile strength of a plain concrete. Salami and Zhao discuss the development and use of a constitutive model based on the theory of plasticity to characterize the stress-deformation behavior of three epoxy concrete materials.

Parameswaran et al. discuss their study on the behavior of slurry-infiltrated fibrous concrete (SIFCON) under different types of loading. Soroushian et al. describe their investigation of the effects of polypropylene fibers and construction operations on the plastic shrinkage cracking of concrete slabs. They found that polypropylene fibers, at low fiber volume fractions, substantially reduced the plastic shrinkage cracking in slab surfaces subjected to restrained plastic shrinkage movements. They also observed that slower screeding rates of the fresh concrete led to reduced plastic shrinkage cracking. Nanni et al. report on the results of an experimental project to determine the validity and repeatability of the plastic shrinkage test procedure under consideration by ASTM. The results of their efforts indicate that the proposed ASTM standard has merit.

Hammons and Neeley report on triaxial characterization tests conducted on high-strength portland cement concrete. The objective of the tests was to develop mechanical response data along selected stress and strain paths in multiaxial stress space. Leming et al. present and examine data obtained from the field installation of high performance concrete in North Carolina as a part of SHRP Contract C-205, Mechanical Properties of High Performance Concretes.

McVay et al. describe the laboratory testing performed to determine the cause for scaling on concrete aircraft parking ramps. The testing confirmed that the combination of spilled aircraft oils and downward-directed blasts from auxiliary power units are responsible for the scaling. Bayasi and Celik in their study found that silica fume is useful in improving the effectiveness of synthetic fiber as reinforcement in concrete and in dramatically reducing the permeability of fiber concrete. Mather discusses the use of chemical and mineral admixtures to prevent excessive expansion of concrete to alkali-silica reaction.

Grove et al. report on research to study the effectiveness of various techniques to enhance bond strength between a new portland cement concrete overlay and an existing asphalt cement concrete pavement surface.

Compatibility Considerations for Durable Concrete Repairs

P. H. EMMONS AND A. M. VAYSBURD

Concrete repair and rehabilitation will have an even more vital role in the future than it does now. Major reconstruction of our aging infrastructures can no longer be delayed. Critical to achieving long service life of repaired structures is the correct choice and use of materials. Evaluation of materials by research and testing falls far behind the development of new products. Regrettably, design professionals still do not fully understand such aspects of their medium as (a) the importance and meaning of compatibility between repair materials and existing substrate and (b) the considerable differences between the properties measured by existing standard methods and the properties of the same materials in situ. The designer and prospective user of materials are not equipped with performance criteria that provide a rational analytical tool for selecting the appropriate materials for a particular repair in a specific environment. Without such criteria, durable concrete repair is more of an art than a science. Compatibility, the most important factor determining the durability and structural effectiveness of concrete repairs, is defined and discussed; drying shrinkage, one of the decisive components of compatibility, is discussed in detail. A ranking system that would help in the selection of repair materials with a lower risk of shrinkage stresses, cracking, and debonding is proposed. In conclusion, there is an urgent need for development of performance criteria for the selection of compatible repair materials, along with the selection or development of a reliable industrywide shrinkage test method.

Many papers and reports during the past few years have described the condition of our nation's infrastructure. The rapid growth in construction of highways, bridges, and airports during the 1950s and 1960s has significantly slowed, and the rehabilitation, reconstruction, and repair of existing structures will consume a growing share of our efforts.

Concrete repair and restoration is considered the growth sector of the construction industry of the 1990s. It was recently estimated that nearly $50 billion will be needed to repair or restore currently deficient bridges in the United States. Repair of buildings, parking structures, and other concrete structures will substantially increase this figure.

Even though concrete repair is a growth industry, there is no great increase in the number of durable concrete repairs being performed. However, more people are devoted to concrete repair research and more contractors are dedicated to repair, rehabilitation, and reconstruction.

The quality and maintenance of our 21st-century infrastructure will depend on our ability to properly design, specify materials, and construct to ensure the long-term performance of repaired concrete structures. Most people concerned with long service life of concrete repairs simply use the rule of trying to determine what materials and proportions and construction practices had previously been used successfully in a comparable exposure. There is an attempt to duplicate—or at least simulate—those materials, without understanding in particular detail why these materials and methods yielded a durable repair.

Indeed, we do have successful repair projects where, to paraphrase the late Robert Philleo (*1*), reliance was placed on assumption, and assumption was based on intuition, available properties, and test results. Painful experience, however, has proved that knowledge is preferable to assumption.

The theories of durable repair have been derived, probably for as long as we have used concrete, from observations and through trial and error, with both good and bad results. Theoretically, we can predict the probability that a repair will withstand the complex forces and elements acting on it. Practically, we do not have enough reliable information to select correctly a repair system required to oppose the destructive stresses from volume changes and environment. Today, the field of concrete repair cannot give the complete answer to the engineer's problem and satisfy the main requirement of the task: to design a durable repair.

The phenomenal explosion of proprietary repair materials and systems has increased the complexity of material selection and the risk of failures. Evaluation by research and testing falls far short of the development of new products. Regrettably, design professionals still do not fully understand their medium. There is a lack of understanding of (a) the importance and meaning of compatibility between repair materials and existing substrate and (b) the considerable differences between the properties measured by current standard tests and the properties of the same materials in situ.

The designer and prospective user of materials are not equipped with a rational analytical tool for selecting the appropriate materials for a particular repair in a specified environment. This tool can be achieved by developing performance criteria for selection of repair materials. Without such criteria, durable concrete repair is more of an art than a science.

In any examination of the durability of concrete repairs, it is important to distinguish between two elements of durability: the selection of repair material and the production of a durable repair.

The topic of durability of concrete repair is too broad to be presented in a single paper. This paper, therefore, will be limited to reviewing one problem aspect of repair: compatibility. This paper is an attempt to characterize compatibility between repair materials and existing concrete and its relative contribution to durability.

Structural Preservation Systems, Inc., 3761 Commerce Drive, Suite 414, Baltimore, Md. 21227.

COMPATIBILITY OF REPAIR MATERIALS AND EXISTING CONCRETE

The term "compatibility" has become very popular in the field of concrete repairs. Then why do we not normally specify compatibility as the primary factor of concrete repair durability, other than because it is not traditional to do so? There are probably four reasons:

1. Lack of clear definition of compatibility;
2. Absence of performance criteria for selecting materials on the basis of compatibility;
3. Lack of reliable industrywide, easy-to-use test methods for evaluating different components of compatibility; and
4. Lack of correlation between laboratory test results and expected in situ performance.

Compatibility is always associated with the repair durability in general and with the load-carrying capacity of structural repairs. Durability and compatibility are defined in this paper as they relate to concrete repairs. Durability is the capability of a repaired structure or its components to maintain serviceability over a designed period of time in a specified environment. Compatibility may, in general, be defined as the balance of physical, chemical, and electrochemical properties and dimensions between repair material and existing substrate that ensures that the repair withstands all anticipated stresses induced by volume changes, chemical and electrochemical effects without distress, and deterioration over a designed period of time (Figure 1).

The compatibility of materials and sections is a complex subject with many facets. However, dimensional compatibility (the phenomenon of volume instability) is a major problem of concrete repair. Dimensional incompatibility impairs the durability and load-carrying capacity of structural repairs. In structural repairs, dimensional incompatibility may lead to an inability to carry the expected proportion of the load and would not necessarily affect durability.

Chemical compatibility properties include alkali content, C_3A content, and chloride content; electrochemical compatibility properties include electrical resistivity and pH. Failure to take into account each of these items may harm the durability of repairs.

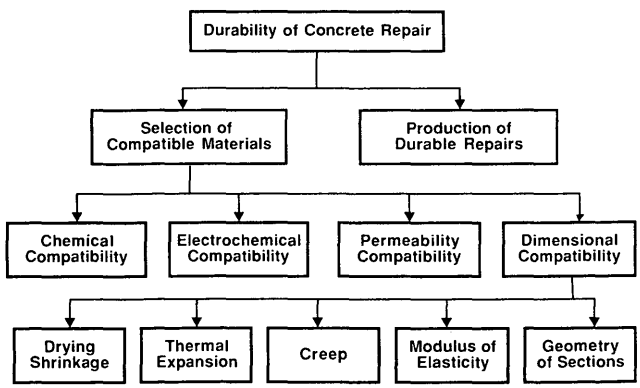

FIGURE 1 Factors affecting durability of concrete repair.

All aspects of chemical compatibility must be considered when selecting materials. For instance, when concrete being repaired includes potentially reactive aggregates, a repair material with low alkalinity must be specified.

For each reinforced concrete repair case, electrochemical compatibility must be considered and the electrochemical behavior of local (substrate) and potential (repair material) macrocell must be evaluated. For instance, in some cases, the repair material must be able, as in concrete, to passivate the steel at pH values of about 12.5 and to bind small amounts of chloride ions in the C_3A. Unfortunately, ignorance of electrochemical compatibility during attempts to repair deteriorated structures and prevent further corrosion has actually caused disastrous failures. For example, applying a surface repair to a portion of a potentially anodic area can increase the cathode/anode area ratio, accelerating the corrosion process. Protecting the cathodic area, where moisture and oxygen should be restricted, would be the proper solution. In another example, macrocells can be introduced inadvertently during the repair of a spalled area. The deteriorated concrete is removed from the spall or delamination and replaced with non-chloride-contaminated concrete. In many instances, the surrounding concrete is contaminated with chlorides. The result is a macrocell in which the rebar around the perimeter of the repair is the anode and the rebar in the repaired area provides a large cathode. A delamination occurs either adjacent to the repair or completely around it (*2*).

It is thought that extremely low permeability is very desirable for repair material, which is not true for all cases. This generally accepted concept can, in some cases, lead to a false sense of security and unsuitable materials incapable of providing lasting performance. Following is an example of unsuccessful use of a low-permeability repair material. The problem occurred where latex-modified shotcrete was used around the pier cap to repair initial damage from deicing salts; however, the top of the cap was not protected and the source of the salt and moisture penetration not eliminated. In this case, an even more severe attack on the reinforcement with subsequent steel corrosion and spalling can develop. Water with deicing salts on the bridge deck drips onto the pier cap, penetrates it, and is unable to escape. Without such a repair, continued deterioration could have been expected, but with the repair it was accelerated and intensified (*3*). The lesson from this example is that in some cases, the selection of low-permeability repair materials not compatible with existing concrete may lead to failure. It is important to note that a few through cracks in the repair, or its debonding, will drastically offset the benefit of having a repair material with very low permeability. In the cases discussed, repair materials with permeability compatible with the existing concrete should have been specified and used.

As was indicated earlier, compatibility is a prime factor related to durability of concrete repairs. Dimensional compatibility, as can be seen from the chart in Figure 1, is an element of fundamental importance.

DIMENSIONAL COMPATIBILITY

Material properties that influence dimensional compatibility include drying shrinkage, thermal expansion, modulus of elas-

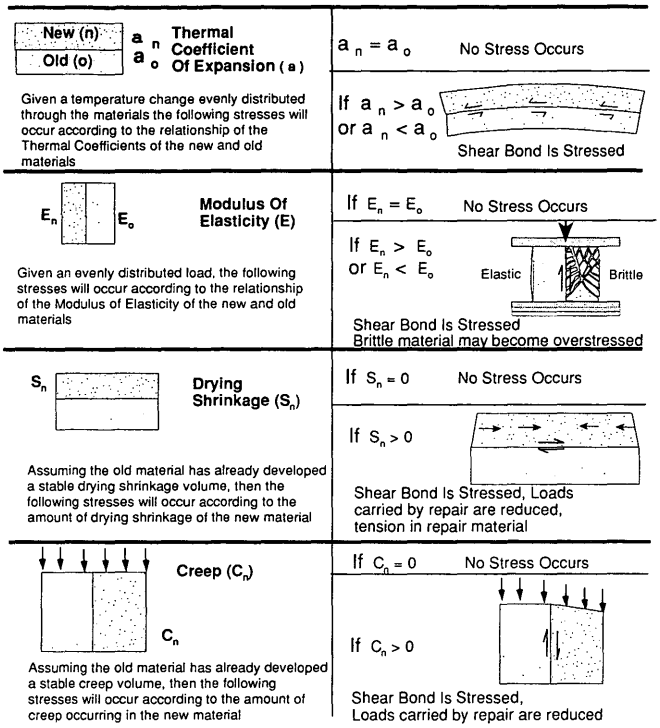

FIGURE 2 Volume change effects on repair.

ticity, and creep. Many materials change volume as they initially set, and practically all of them change volume with moisture and temperature changes. Tensile stresses are induced in one material, compressive stresses in the other; as a result, a substantial shear will occur at the interface. Identical stresses will result from the differential thermal shrinkage and moduli of elasticity (Figure 2) (*4*).

When polymer concretes are used for thick concrete repairs, often the result is distress caused by significant differences in the shrinkage and mechanical and physical properties of the two materials. For example, the flexural modulus of elasticity of an epoxy mortar is about 6.9×10^6 KPa (10^6 psi), and that of the base concrete is 3.1×10^7 KPa (4.5×10^6 psi). (*5*). If a repair with such an epoxy mortar is thick and continuous, tensile stresses induced by cycling of temperature will cause cracking. The volume change from the wetting and drying of the concrete can increase the stress.

Restrained contraction of repair materials—the restraint being provided through the bond to the existing concrete substrate—significantly increases the complexity of repair projects as compared with new construction. Volume changes cause contractions that often result in cracking and debonding of the repair section. Therefore, the specified repair materials must be dimensionally compatible with the existing concrete substrate to minimize the potential for cracking and delamination as a result of restrained contraction.

The stress states that develop at the subsequent bonds vary considerably depending on the type and use of the structure. For example, the bond on a bridge deck overlay may be subject to shear stress in conjunction with tensile or compressive stresses induced by shrinkage or thermal effects, in addition to compression and shear from service loads.

Table 1 indicates typical differences in some of the important short-term properties of repair materials (*6*). Differences in properties will always exist between the repair material and the substrate concrete, regardless of the material. Even by using concrete as a repair material, it is impossible to match all properties because at the time of the repair a large percentage of the ultimate shrinkage has already taken place. And do we need to match the properties of two materials in a composite structure? The temptation to seek parity of properties of the repair materials and base concrete is strong, but attempts to avoid mismatches founder on the definition of compatibility (*7*). The real requirements for durable and structurally adequate repairs are clearly spelled out in the definition of compatibility.

TABLE 1 Typical Short-Term Properties of Repair Materials

Property	Resin Mortar	Polymer modified cementitious mortar	Plain cementitious mortar
Compressive strength (MPa)[a]	50-100	30-60	20-50
Tensile strength (MPa)	10-15	5-10	2-5
Modulus of elasticity in compression (MPa)	(10-20) x 10^3	(15-25) x 10^3	(20-30) x 10^3
Coefficient of thermal expansion (mm/mm/ °C)[b]	25-30 x 10^{-6}	10-20 x 10^{-6}	10 x 10^{-6}
Water absorption (% by weight)	1-2	0.1 - 0.5	5-15
Maximum service temperature (°C)[c]	40-80	100-300	>300

[a] 1 MPa = 145.0326 psi
[b] mm/mm/°C = 0.56 in./in./°F
[c] °C = (°F-32)/1.8

Selecting repair materials on the basis of compatible thermal coefficients and moduli of elasticity is relatively simple because they are known quantities. Shrinkage, however, is not easy to deal with. Selecting repair materials on the basis of minimal shrinkage requires an understanding of the shrinkage processes. Volume changes accompany the loss of moisture from either fresh or hardened cementitious materials. The term "drying shrinkage" is generally used for hardened material. The term "plastic shrinkage" is used for fresh material since its response to loss of moisture is quite different. "Carbonation shrinkage," which occurs when hydrated cement reacts with carbon dioxide from the atmosphere, can be regarded as a special case of drying shrinkage. Shrinkage is only a cement paste property: any aggregates and reinforcing components in the material have a restraining effect on the volume changes.

Loss of water from fresh repairs, if not prevented, can cause cracking. The most common situation is surface cracking due to the evaporation of water from the surface. Suction of water from the repair by the substrate can also cause cracking or add to the effects of surface evaporation. When the water is removed from the cementitious paste by evaporation, a complex series of menisci is formed. These, in turn, generate negative capillary pressures, causing the volume of the paste to contract. The effects of plastic shrinkage are not uniform throughout the material and are restrained at the interface. Differential volume changes can also cause cracking under induced tensile stresses.

Plastic shrinkage cracking is most common on horizontal surfaces of repair, where rapid evaporation occurs. Its occurrence affects the integrity of the repair and reduces its durability. Plastic shrinkage may be aggravated by special environmental conditions such as a combination of high wind velocity, low relative humidity, high air temperature, and a high temperature of the repair material. The most effective way to control plastic shrinkage is to ensure that the surface of the repair is kept moist until it has been finished and curing has begun.

In our view, perhaps the most significant property with regard to dimensional compatibility is drying shrinkage. Shrinkage, as related to the cementitious and polymer-modified cementitious repair materials, is discussed not only because of its importance for compatibility, but also because it is the most ignored property in published research literature on repair materials.

Drying shrinkage of hardened material is a much more important and critical phenomenon than plastic shrinkage. It should be emphasized, however, that the fundamental processes underlying drying shrinkage are yet to be fully understood. About 70 percent of the ultimate drying shrinkage occurs in the first 30 days.

Tensile stresses begin to accumulate in the repair material when shrinkage begins. As shrinkage stresses accumulate, the repair material resists cracking until the stress exceeds the tensile capacity of the repair material (Figure 3). The phenomenon of repair distress is triggered by the stress concentrations at the interface—a region in which the probability of failure is higher than in the material itself.

The load-carrying capacity of the new repair material does not come into play when the repair material fails to fill the cavity as designed because of the effects of drying shrinkage.

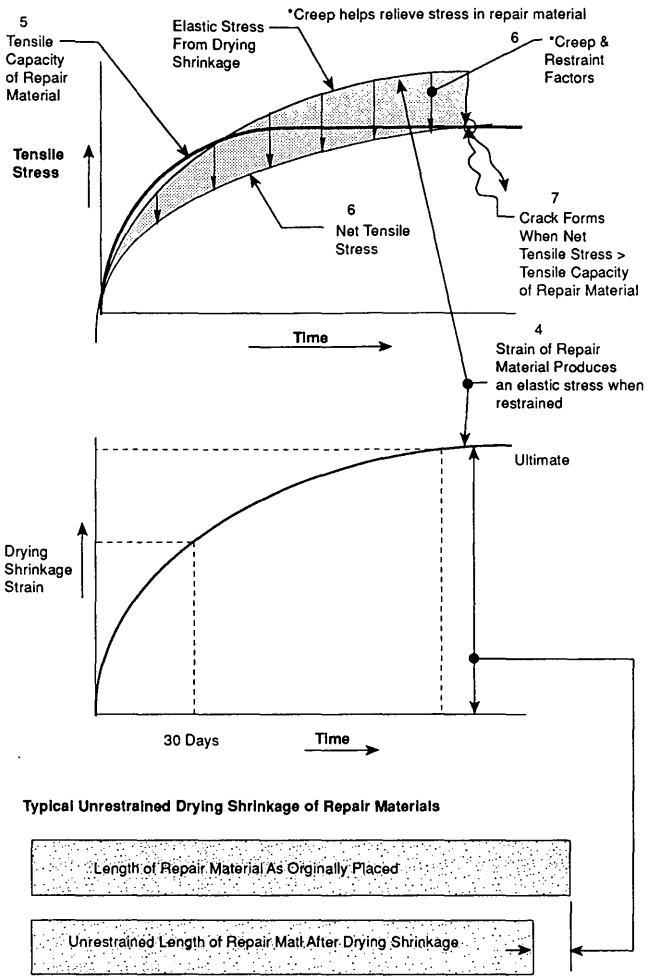

FIGURE 3 Drying shrinkage effects on repair.

Figure 4 shows the stress distribution around a new repair that does not carry its part of the load.

The effect of a repair under load is very important. The behavior of small surface repairs introduced to restore durability to the member is likely to be influenced considerably by the deformation of the surrounding steel and concrete. Here, the strain capacity of the repair material rather than its ability to carry stress is of prime importance. With larger structural repairs where a contribution to member stiffness is required, the repair material must possess properties that ensure not only that it stays in place to protect the steel but also that it is able to resist stress for the subsequent design life of the structure. In both contexts, the effect of repair under load is important (*6*).

The desirable shrinkage of repair material for satisfactory performance should be 0.00 percent. But what is the acceptable value of low shrinkage, and how do you select repair materials with low shrinkage? Parameters must be established to define shrinkage for repair materials.

In 1987 Alberta Transportation and Utilities conducted an evaluation program for concrete patching materials (*8*). In this study, 46 repair materials were evaluated for various properties, one of which was drying shrinkage. The ASTM C157 shrinkage test was used to determine individual values,

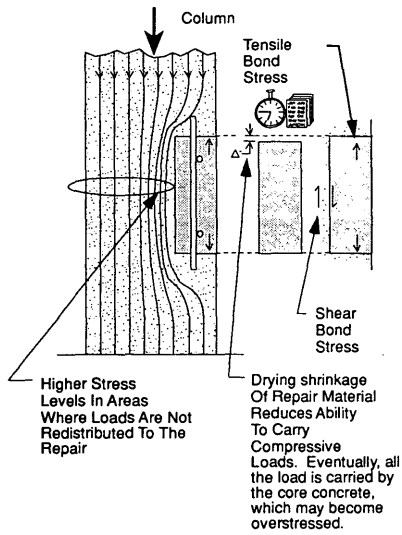

FIGURE 4 Stress distribution around the repair not participating in load sharing.

and all the tests were performed by one independent laboratory. Figure 5 presents a diagram of the results of the shrinkage testing sorted from the lowest shrinkage on the left to the highest shrinkage on the right.

By sorting the test results from low to high shrinkage, a cross section of the industry's repair materials was available for comparison. The study yielded a surprising result: the shrinkage of most of the repair materials far exceeded the shrinkage value of normal concrete: 0.05 percent at 30 days (*9*,p.2). The percentages of shrinkage do not sound large, but their effects are dramatic. Restrained shrinkage induces tensile stress. Most repair materials have a tensile capacity of 1.4 to 6.9 MPa (200 to 1,000 psi), depending on age and design. Shrinkage of 0.025 percent translates into 6.9 MPa (1,000 psi) tensile stress assuming an elastic modulus of 27 480 MPa (4,000,000 psi).

Today the industry cannot require the manufacturers of repair materials to meet a certain maximum shrinkage value because the basis for acceptable shrinkage value has not been established. ASTM C928-91 provides physical requirements for packaged cementitious concrete repair materials. This standard calls for shrinkage not to exceed 0.15 percent. According to the classification outlined in Figure 6, shrinkage of 0.15 percent is in the high range, being three times the shrinkage of normal concrete that is established as a benchmark in the classification. It is our opinion that repairs with such materials will be highly susceptible to excessive drying shrinkage stress, cracking, delamination, and failure.

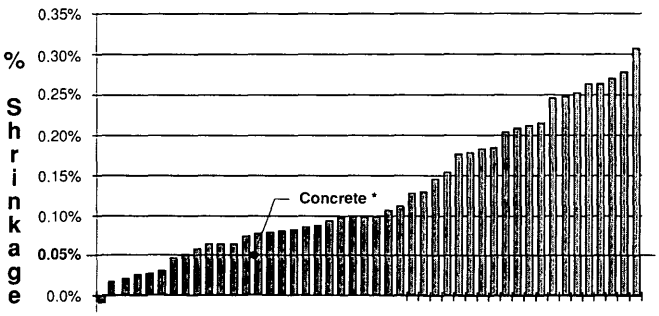

FIGURE 5 Repair material shrinkage test rests: ASTM C157 30- and 60-day results.

For purposes of this discussion, the presented classification materials are grouped into three basic categories of shrinkage:

- Low: less than 0.05 percent.
- Moderate: 0.05 through 0.10 percent
- High: more than 0.10 percent.

It is interesting that according to the classification, only 7 of the 46 repair materials tested (15 percent) can be labeled as low-shrinkage materials. It appears that many manufacturers of repair products are not designing for minimized shrinkage despite claiming that the materials are expansive, nonshrinking, or shrinkage-compensating.

A review of product data sheets indicates that compressive strengths of repair materials are unnecessarily high (Table 2). The excessive compressive strengths for some products may indicate excessive cement content. Although some products have a low water-cement ratio, they have significant shrinkage because shrinkage is proportional to both the cement content

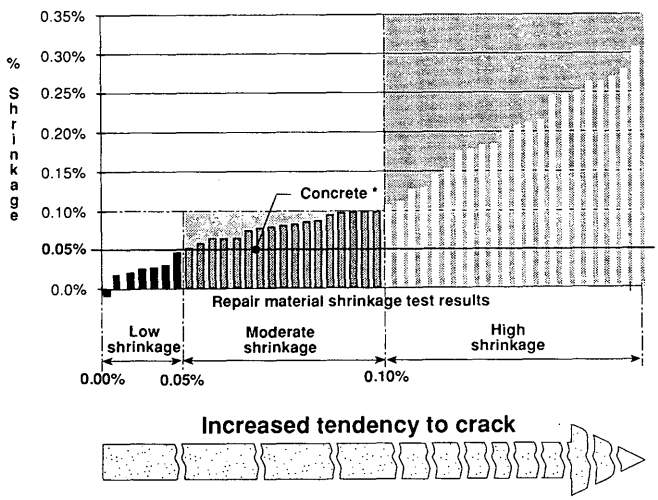

FIGURE 6 Classification of repair materials.

TABLE 2 Compressive Strength of Representative Surface Repair Materials

PRODUCT TYPE	COMPRESSIVE STRENGTH (28-DAY) MPa[a]
cast-in-place	48
trowel	41
cast-in-place	48
cast-in-place	76
trowel	47.9
cast-in-place	42
rapid set	58.6
shotcrete	76

and the total water content. Shrinkage is not eliminated or reduced by simply achieving a low water-cement ratio. Because of this, the typically high cement factors of repair materials are a disadvantage.

And what is the advantage of repairing the existing 24 MPa (3,500 psi) concrete of a deteriorated bridge pier with 48 MPa (7,000 psi) repair material? So that as the pier disintegrates with time, the patch will stay as a monument of the specifiers' incompetence?

METHODS OF TESTING

It was found that only limited properties are available from manufacturers' data sheets. Information about shrinkage is not even listed on some of them. To select materials for a particular application by comparing properties, and shrinkage in particular, the necessary data must be available.

Given a particular application, the relative merits of the materials available can be assessed objectively only if one standard method is used for testing. Manufacturers tend to use different tests and standards to evaluate the performance of their products. Many tests are modified; some are found to be deficient or to provide unrealistic results. It has become clear that test results must be examined critically to ensure their validity.

As a result of the arbitrary application of test methods, predicting the performance of many materials is uncertain. Our survey of material data sheets revealed that manufacturers used eight shrinkage test methods:

- CRD-C 621-82A
- ASTM C596
- ASTM C490
- ASTM C157
- ASTM C157 Dry
- ASTM C157 Modified
- Ring Modified
- DIN 52450

Variations in the techniques and conditions in each of these test methods—including restraint conditions, specimen dimensions, curing, temperature, time of initial readings, and test duration—make it impossible to interpret the comparative test results.

A study of the available test methods for properties that influence dimensional compatibility must be conducted to evaluate the existing repair methods, to identify their limitations, and, if necessary, to develop new test methods that will ensure that test results are reliable for predicting field performance of repair materials.

More research is needed on the long-term performance of repair materials in actual field conditions. The ultimate test of material durability is how it performs in the environment in which it has been placed. Laboratory tests should be used with extreme caution for predicting field performance of repair materials, because different scales of application and different environmental conditions may lead to damage by different mechanisms. Currently, no acceptable method exists for comparing the severity of different environments when different mechanisms may be responsible for damage. More research is needed to clarify compatibility of materials in various environments so that better comparisons can be made between the laboratory tests and expected field performance. This is especially important with the development of new materials that are significantly different from cementitious materials that have been used in the past to develop the current body of knowledge concerning the resistance of concrete to natural weathering. Finally, performance criteria and guide specifications for dimensionally compatible repair materials must be developed. There is a demonstrable need for such criteria to ensure dimensional compatibility and to provide durability for repair jobs.

CONCLUSIONS

1. As a prerequisite for concrete repair durability, clear understanding of compatibility between repair materials and the existing concrete is essential.
2. Drying shrinkage is one of the most important factors influencing dimensional compatibility. An investigation into the desirable shrinkage properties of various repair materials for satisfactory performance was undertaken. Materials are grouped into three basic classifications and shrinkage of concrete is taken as a benchmark.
3. Existing test methods and practices do not produce comparative shrinkage measurements due to variations in techniques and test conditions. The industry must choose or develop a test method that will ensure reliable test results for predicting the field performance of materials.
4. There is a need to integrate our knowledge and understanding of the compatibility of repair materials with existing concrete and to develop performance criteria to provide an engineer with the methodology of modeling for repair durability under various conditions of repair-environment interaction.
5. If the service life span expected on repaired structures is to be achieved, the construction of durable repairs is essential and it is vital for the engineer to apply engineering principles to the design and specification of repair materials just as it is done in designing structures and structural elements.

ACKNOWLEDGMENTS

The shrinkage classification presented is based on test results from an evaluation program carried out at the Research and Development Branch of Alberta Transportation and Utilities, Canada. The authors are grateful to Paul Carter for allowing them to use the results of the report.

REFERENCES

1. R. E. Philleo. A Need for In Situ Testing of Concrete. *Concrete International*, No. 9, Sept. 1979, pp. 43–44.
2. A. M. Vaysburd. Some Durability Considerations for Evaluation and Repair of Concrete Structures. *Proc., 2nd National Concrete Engineering Conference*, Chicago, Ill., 1992.
3. E. Schrader and R. Kaden. Durability of Shotcrete. *ACI SP-100: Katharine and Bryant Mather International Conference on Durability of Concrete*, Vol. 2, pp. 1071–1101.

4. P. H. Emmons. Selecting Concrete Repair Materials For Long-Term Durability Based on Available Test Data. *Proc., 2nd National Concrete Engineering Conference*, Chicago, Ill., 1992.
5. M. Schupack. Divorces and Ruptured Relations Between Epoxies and Concrete. *Concrete Construction*, No. 10, Oct. 1980, pp. 735–738.
6. G. Mays and W. Wilkenson. Polymer Repairs to Concrete: Their Influence on Structural Performance. *ACI SP-100: Katharine and Bryant Mather International Conference on Durability of Concrete*, Vol. 1, pp. 351–375.
7. D. R. Plum. The Behavior of Polymer Materials in Concrete Repair, and Factors Influencing Selection. *The Structural Engineer*, Sept. 1990, pp. 337–345.
8. *Alberta Concrete Patch Evaluation Program Report*. Report ABTR/RD/RR-87/05. Edmonton, Alberta, Canada, 1987.
9. Volume Change of Concrete. *Concrete Information*. Portland Cement Association, Skokie, Ill., Chapter 12 (revised).

Publication of this paper sponsored by Committee on Performance of Concrete.

Use of High-Performance Concrete for Rapid Highway Pavement Repairs: An Overview of Five Field Installations

JOHN J. SCHEMMEL AND MICHAEL L. LEMING

The Strategic Highway Research Program awarded a contract to investigate the use of high-performance concrete in highway pavements and bridge structures. One of the primary objectives of this research effort was "to provide recommendations and guidelines for using these concretes in highway applications." As a result, the research program included an examination of the field performance of high-performance concrete. Field test sections were constructed in Arkansas, Illinois, Nebraska, New York, and North Carolina. Except in North Carolina, the installations consisted of full-depth and lane-width patches. Traffic and environmental exposure conditions differ for all locations. Each batch of concrete brought to a site was tested for its fresh concrete properties. Specimens were cast for long-term testing too. The field installations will continue to be monitored for at least 18 months after construction. Details about site locations, the type of concrete used, the construction process, and the testing plan are provided, and the most important lessons learned from the field trials are discussed.

In March 1989, Strategic Highway Research Program (SHRP) Contract C-205 was awarded to investigate the mechanical properties of high-performance concrete (HPC) for highway applications. A consortium of three universities—North Carolina State University (NCSU), the University of Arkansas, and the University of Michigan—make up the research team. The 4-year research effort has focused on an investigation of three classes of HPC. These concretes are intended for use in pavements and bridge structures where durability and strength development are critical.

Within the context of the NCSU study, HPC is defined as any concrete that provides substantially improved resistance to environmental influences, extraordinary properties at early ages, or enhanced long-term mechanical properties. The primary objective of this research effort has been to evaluate the mechanical properties and field performance of the concretes developed for the project. Major tasks have included establishing the proportions for three different classes of concrete, performing laboratory tests to determine the properties of these concretes, and constructing field installations to investigate the production and in-service performance of the concrete.

This paper will focus only on the field installations and is intended to provide guidance to prospective users of HPC in highway applications. General information about the construction of the test sections is presented. Limited data are provided regarding the results of field tests.

J. J. Schemmel, Department of Civil Engineering, 4190 Bell Engineering Center, University of Arkansas, Fayetteville, Ark. 72701. M. L. Leming, Department of Civil Engineering, Box 7908, North Carolina State University, Raleigh, N.C. 27695.

PURPOSE OF FIELD INSTALLATIONS

One of the main tasks of the SHRP research effort was to determine how various field service conditions, such as traffic and climate, affect the behavior and properties of HPC. Actual field conditions often cannot accurately be simulated in the laboratory. Thus, to accomplish the stated task, several field test sections were constructed using HPC. The field installations also would provide an opportunity to determine if the HPC developed under controlled laboratory conditions could readily be produced and placed in the field. An important aspect of the SHRP study was that the production of HPC should be possible with locally available materials and methods.

DESCRIPTION OF FIELD INSTALLATIONS

Five separate field installations were constructed as part of this research. The installations are in Arkansas, Illinois, Nebraska, New York, and North Carolina. The candidate test sites were selected partly on the basis of their traffic and environmental exposure conditions. Variables considered in the selection process included expected traffic volume, percentage truck traffic, freeze-thaw potential, moisture potential, exposure to deicing agents, and site availability and convenience. A general description of the location, geometry, and exposure condition of the five sites follows.

New York

The first installation was constructed in June 1991. The site is located on I-88 about 80 km (50 mi) west of Albany near the town of Worcester. A single 18.5-m (61-ft) patch was placed in the passing lane of the eastbound highway. The patch is full depth and width, about 230 mm (9 in.) and 3.6 m (12 ft), respectively. Transverse joints are positioned every 6 m (20 ft). Insulation covered the entire patch until the morning after placement, when the patch was opened to traffic. The concrete is subject to a moderate level of traffic. The

climatic exposure can be described as wet with a hard freeze in the winter.

North Carolina

The second field installation was placed in July 1991. The site is an approach to a new bridge located in the southbound lanes of US-17 just east of Williamston. Williamston is 96.5 km (60 mi) east of Raleigh and about 40 km (25 mi) west of Albemarle Sound on the Atlantic Ocean. The North Carolina installation was more extensive than the other four sites. Plain concrete pavement totaling 55 m (180 ft) was placed in two adjacent lanes. The pavement was roughly 230 mm (9 in.) thick. A number of insulated and noninsulated sections were constructed. Two coarse aggregates and two high-range water reducers (HRWRs) were used. The inside lane was constructed at a slow rate to allow for the best control and time for adjustments to the concrete mixture. The outside lane was placed at a more typical construction rate. Traffic in the area of the installation is light. Exposure is that of a mild marine environment so there is limited potential for freeze-thaw cycles to occur. Little to no deicer salt application is expected.

Illinois, Arkansas, and Nebraska

The remaining three installations have many similarities in terms of their geometry and construction. However, their traffic and climatic exposures are quite different. The third installation is located on I-57 about 8 km (5 mi) north of Effingham, Illinois. This installation was constructed in October 1991. Two 14-m (45-ft) patches are located in the right lane of the northbound traffic. The fourth installation was placed in Arkansas on I-40 about 5 km (3 mi) west of Forrest City. Forrest City is about 48 km (30 mi) west of Memphis, Tennessee. Two 14-m (45-ft) plain concrete patches were constructed in the passing lane of the westbound traffic. The fifth installation is in the eastbound lane of US-20 about 8 km (5 mi) west of Osmond, Nebraska. Osmond is northwest of Norfolk. A 29-m (96-ft) section of plain concrete was placed in July 1992, representing two 14-m (48-ft) patches.

Full-depth and lane-width repairs were made at all three sites. The slabs ranged in thickness from 200 to 250 mm (8 to 10 in.). Lane widths were 3.5 m (12 ft) in Illinois and Arkansas and 3.3 m (11 ft) in Nebraska. Transverse joints were positioned at intervals of roughly 4.6 m (15 ft). The same basic concrete mixture was used for all three installations. One of the two patches was insulated for 4 to 6 hr after placement of the concrete, and the other patch was left uncovered. Only the Nebraska installation was opened to traffic on the day of placement. The other two sites were opened the next morning.

Traffic levels in Illinois and Arkansas can be classified as moderate. However, the Arkansas site has a high percentage of truck traffic. Traffic in Nebraska is very light, yet the pavement is subjected to occasional heavy loads because of the many farms nearby. Like New York, the Illinois installation can be described as wet with a hard freeze. The Arkansas site can be considered wet with freeze-thaw cycling. In Nebraska, the potential for freeze-thaw cycles is very high and deicing salts are likely to be used after each snowfall.

MIX PROPORTIONS AND CHARACTERISTICS

Three classes of HPC were developed in the NCSU study. These concretes have been designated VES (very early strength), HES (high early strength), and VHS (very high strength). There are two categories of the VES mixture. Performance criteria for these mixes are as follows:

1. Water-cement ratio ≤ 0.35
2. Durability factor ≥ 80 percent after 300 freeze-thaw cycles (ASTM C666, Method A)
3. VES: 14 MPa (2,030 psi) in 6 hr using portland cement, 17 MPa (2,465 psi) in 4 hr using pyrament blended cement; HES: 34 MPa (4,930 psi) in 24 hr; VHS: 69 MPa (10,014 psi) in 28 days.

All three concretes were formulated to achieve their desired performance using the fewest ingredients possible and the least amount of each. In addition, the concretes can be produced using locally available materials and placed using standard construction practices.

Each of the three categories of HPC was developed for specific applications. The primary use for the VES mix is in rapid patch repairs, for which strength development is more critical than cost. The HES mix was designed for use in construction and repair of bridge decks, for which durability, especially corrosion of the reinforcement, is a significant concern. The HES mix can also be used in pavement patching when cost is an important factor. The VHS mix was developed for use in bridge construction, girders and piers being the prime focus. The primary material used in the field installations was the HES mixture. As explained later, the VES mixes were examined indirectly. The VHS concrete was not evaluated in the field trials.

There were two reasons for using the HES mix for the field trials instead of the VES patching material, as originally intended. First, at the time that the field installations were to be constructed (except Nebraska), performance criteria, approved materials, and proportions for the VES concrete had not been made final. Changes in each of these areas led to delays in developing a satisfactory VES mix. Because the field installations had been scheduled for completion in the summer of the third project year, these delays effectively removed the VES mix from consideration.

Second, in laboratory testing it was found that the HES mix, when insulated, would frequently satisfy the performance criteria of the VES mix. It was believed that both the HES and VES mixes could, in effect, be tested in the field by constructing two patches with the HES mix. One patch would be insulated and the other, noninsulated. Thus, the VES mix would be simulated by the HES mix and the insulation. A secondary benefit of using the HES mix for the installations was that the material could be examined under circumstances that were more forgiving in terms of strength development. If the performance of the HES concrete (intended for use on bridge decks) turned out to be less than anticipated, lower strength in a pavement section would be less serious than the failure of a bridge deck.

The general HES mix design used for the field installations is presented in Table 1. Given is a broad range for the aggregate contents. The coarse-aggregate content can be de-

TABLE 1 HES Mix Proportions

Material	Dry Weight	
	(kg/m^3)	(lb/cy)
Cement	516	870
Water (1)	178	300
Coarse Aggregate	940 - 1020	1,580 - 1,720
Fine Aggregate	560 - 620	950 - 1,050
HRWR (Naphthalene)	6.1 L/m^3	18 oz/cwt
AEA (Vinsol Resin)	1.7 L/m^3	5 oz/cwt
Calcium Nitrite	20 L	4.0 gal

(1) Adjust for free aggregate moisture and water in Calcium Nitrite.

termined according to American Concrete Institute (ACI) guidelines for normal weight concrete (ACI 211.1-81). A fine-aggregate proportion adequate to produce the desired yield can then be determined. The proportions given in Table 1 are sufficient for both No. 57 and No. 67 nominal maximum-sized aggregate. The New York installation used an earlier version of this mix, but the general proportions were very similar to those in Table 1. In North Carolina, Illinois, and Arkansas the mixes used were based on Table 1 with adjustments only to the admixture dosages. When the Nebraska installation was constructed, it was decided to intentionally invert the coarse- and fine-aggregate quantities for the SHRP work. Conventional practice in the area of the installation calls for a 30 percent maximum coarse-aggregate fraction because of the potential for an alkali-aggregate reaction. Therefore, it was decided to impose the same restriction on the SHRP concrete since a prime objective of the field work was to determine if HPC could be produced using local materials and methods.

Several admixtures were used to produce the HES concrete, including an HRWR, an air-entraining agent (AEA), and a nonchloride set accelerator/corrosion inhibitor. An HRWR was chosen over a conventional water-reducing admixture, or combination of both, to minimize set retardation. So-called extended-life HRWRs were not used because they typically cause substantial increases in set times. Strength gain begins essentially at final set, so it was necessary to limit extension of the set time very closely in order to provide acceptable early age strengths. A calcium nitrite solution was used as the set accelerator/corrosion inhibitor. It must be added at the job site because workability is maintained for only about 15 min after addition in warm weather. The commercially available calcium nitrite solution used contained about 3.4 kg (7.5 lb) of water for each 3.8 L (1 gal) of product. This means that about 13.6 kg (30 lb) of water per 0.765 m^3 (1 yd^3) of concrete had to be held back during initial batching to maintain the intended water-cement ratio. The water-reducing admixture was added during initial batching to provide acceptable workability and, very importantly, entrained air content of these mixes with low water-cement ratios (no more than 0.35). Job-site addition of an HRWR to recover or enhance workability has been questioned when frost resistance is critical. Research by the Indiana Department of Transportation indicates problems with the frost resistance of concretes that have been redosed with an HRWR (*1*). The Arkansas research team is researching this issue.

CONSTRUCTION PROCESS

Construction of the patch sections in New York, Illinois, Arkansas, and Nebraska was similar in many respects. Figure 1 depicts a typical patch. A general discussion of the construction process is presented. When necessary, differences among the field sites will be highlighted. The North Carolina installation, being new pavement construction, will not be included in the following discussion. For more details on the North Carolina test installation, see the paper by Leming et al. in this Record.

The pavement that was to be replaced was removed by the lift-out method. Any subbase material disturbed during removal of the concrete was compacted using a hand-operated vibratory plate compactor. Sand was used in New York and Nebraska to return the subbase to the proper grade. Transverse joints are roughly spaced at 4.5-m (15-ft) intervals. Thus, a 14-m (45-ft) patch was separated into three sections of equal lengths. Joint spacing was 6 m (20 ft) in New York. Dowel bars were placed at all transverse joints and grouted into the existing concrete; all dowel bars were greased. New York and Illinois used welded wire mesh, placed on chairs, in constructing the patch. A bond breaker was placed along the longitudinal joint. The patches were also instrumented with thermocouples to monitor the temperature development in the slab.

The patch area was prepared on the morning of the placement in New York and Nebraska. The New York patch was small enough that all of the work could be completed in 1 day. In Nebraska, an overnight lane closure was not permitted because the highway has only two lanes.

Except in Illinois, where a central mixer was used, the concrete was dry-batched at a local ready-mix plant and transported to the job site. Each truck was charged with enough material to fill one 4.6- × 3.7-m (15- × 12-ft) section and cast the necessary test specimens. The basic batching sequence follows:

1. Wash out drum and discharge all water.
2. Add a fourth of total water and two-thirds of HRWR.

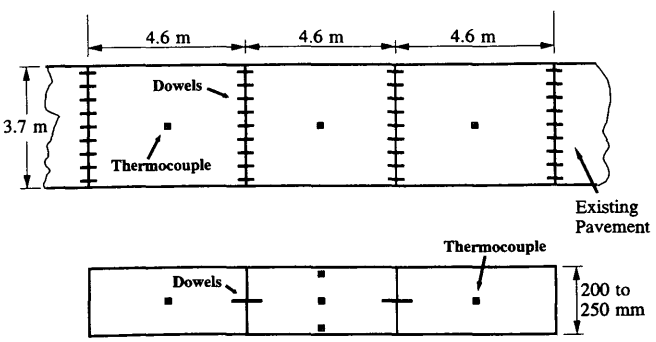

FIGURE 1 Typical field installation: *top*, plan view; *bottom*, cross section.

3. Add half of cement, coarse aggregate, and fine aggregate, and a third of AEA and mix while remaining material is weighed.
4. Add the other half of cement, coarse aggregate, and fine aggregate, and two-thirds of AEA.
5. Add three-fourths of total water less that held back for washing down the truck hopper.
6. Add the remaining third of HRWR.
7. Wash down hopper.
8. Mix for about 5 min.
9. Transport to site. (Drum at agitate speed.)
10. Add calcium nitrite.
11. Mix for 3 min.
12. Discharge concrete within 15 min.

Several points must be made with regard to batching the HES mixture, or any other HPC, in the field. First, the mix proportions given in Table 1 should be viewed as a first approximation for the mix. Differences in cement, aggregate, and admixture will most likely necessitate changes in the quantities and dosages of the constituent materials. Second, the order and split addition of the materials has been found necessary for three reasons. First, because of the dry nature of this mix, it is essential to add both water and HRWR to the drum of the truck. This will help to reduce the chance of head packing. Second, many batch plants do not have the capacity to weigh all of the required dry material at one time. Thus, batching can be done only by splitting the weights. Third, the effects of delayed addition of HRWR on the durability of this concrete had not been established when the installations were constructed.

Another critical point regarding the use of HPC in the field is the condition of the mixing trucks. Any truck likely to be used for a job involving HPC should be checked before any work is started. Inadequate mixing due to worn or coated blades will lead to dramatic problems as a result of nonuniformity of the concrete. Concrete that is not thoroughly mixed and uniform in consistency will be difficult to discharge, place, and finish.

Finally, all materials, except the calcium nitrite, were added at the batch plant. The calcium nitrite was added manually at the job site, which should not present any problems. In Nebraska this material was pumped into the mixing drum. At the other field sites the material was supplied in 210-L (55-gal) drums and was added manually using 19-L (5-gal) plastic buckets.

Once bathed and mixed, the concrete was placed, consolidated, finished, cured, and insulated according to the various state standards at each site. No special placement or finishing techniques were required or used. Two of the states used a vibrating screed as well as internal vibration, and the others used only internal vibration for consolidation. All states used a liquid curing compound. Insulation was placed on one of the two patches at each site except in New York, where the entire patch was covered. The type of insulating material used differed for each state. Forms of insulation included rigid foam, blankets, and asphalt-treated sheeting. Generally, the insulation remained on the one patch 4 to 6 hr after placement. Joints were sawed as soon as practical. All but the Nebraska installation were kept closed to traffic overnight as a precautionary measure; the Nebraska patch was opened the evening of the placement.

TESTING PLAN

Besides the evaluation of the ability to batch and place the HES concrete in the field, an extensive test program is continuing at each site. As with other aspects of the installations, the test program is essentially the same at each field site. The fresh concrete properties, internal temperature development, cylinder compressive strength, and core compressive strength are monitored at each site. Each site is visually inspected whenever specimens are retrieved or cores taken.

Each truckload of concrete brought to a site was sampled and tested for its fresh properties in accordance with AASHTO specifications and testing procedures. Slump, air content, unit weight, and as-placed concrete temperature were recorded. On the basis of experiences in the laboratory with the HES mix, an air content of 5 to 8 percent and a slump of greater than 51 mm (2 in.) was desired. In cool weather, a mix temperature of at least 27°C (80°F) was thought to be necessary for a sufficient rate of strength gain. Adjustments to the admixture dosages were made as necessary on the basis of the properties of the prior loads of concrete.

Each patch was instrumented with thermocouples in order to monitor temperature development. A short length of small-diameter PVC pipe was used to stabilize the position of the wires during placement of the concrete. All thermocouples were placed along the centerline of the patch. The outside sections of each patch had one thermocouple at mid-depth. The center section was instrumented with three thermocouples. One was placed about 25 mm (1 in.) from the top of the patch, one at mid-depth, and the third at about 25 mm (1 in.) above the subbase (Figure 1). Temperature readings were taken on a regular basis with a hand-held digital thermometer.

A large number of 100- × 200-mm (4- × 8-in.) compression cylinders were cast from each load of concrete. These cylinders were cast for both short- and long-term testing. The center section of each patch was identified as the representative section, and thus more specimens were cast from this concrete. The outside sections had cylinders cast for 1-, 7-, and 28-day testing. The center patch had additional cylinders cast for 6-, 12-, and 18-month tests. The insulated patch had still more specimens prepared. Cylinders were taken from the center section for testing at 4, 5, 6, and 7 hr after placement to study the rate of strength gain and early age properties of the mix.

The cylinders were cured for up to 1 day in a curing box constructed of extruded rigid foam insulation. The boxes provide a minimum of 50 mm (2 in.) of insulation around each specimen. The outside edge of the boxes are 150 mm (6 in.) thick. A thermocouple was placed in the cylinder in the center of the box. It has been found that the temperature history of this cylinder is very similar to that of the mid-depth thermocouple in the slab. Thus, it is believed that the cylinders are being cured in like manner to that of the slab. For the specimens taken from the insulated patch, a sheet of insulation is placed over the top of the curing box for as long as the slab is insulated. When the insulation was removed from the slab,

the specimens in the curing box were uncovered but remained in the box. After curing in their boxes for 24 hr (except those tested earlier), the cylinders were removed and buried along the side of the road. The cylinders were buried so that their top surfaces are exposed to the environment and remain in their plastic molds until tested. Highway department personnel retrieve and test the specimens according to an established schedule.

The patches are also being cored at 6, 12, and 18 months of age. Three cores are taken at each test date from the center section of each patch. One core is taken from each of the outside sections. The first coring is done between the wheelpaths to correlate the strength with the field-cured cylinders. Later cores are taken from the wheelpath to evaluate any damage that may have occurred over the past 6 months.

RESULTS

Figures 2 and 3 and the following in-text table present selected data from the various field sites; space limitations do not permit data from all the field sites to be presented. Figure 2 shows the early strength development of test cylinders at the Arkansas and Nebraska sites. The concrete at the Arkansas installation nearly doubled in strength over a 3-hr period. In Nebraska the concrete started out at a high level of strength, which then increased by one-third. However, 7 hr after placement, the compressive strength of the concrete was essentially the same at both sites. Figure 3 shows the long-term compressive strength development of the test specimens cast in Arkansas. The strength of the insulated concrete, on the basis of cylinder specimens, is greater for the ages tested than that of the noninsulated concrete for the Arkansas site. Although this is typical, it is not universally true. Furthermore, it is important to note that these results are based on specimens that received no moist curing after being removed from their molds at 24 hr or less. The difference between the cylinder strengths has declined from 30 percent at 1 day to 7 percent at 6 months. At 6 months the difference is approximately 5 MPa (700 psi).

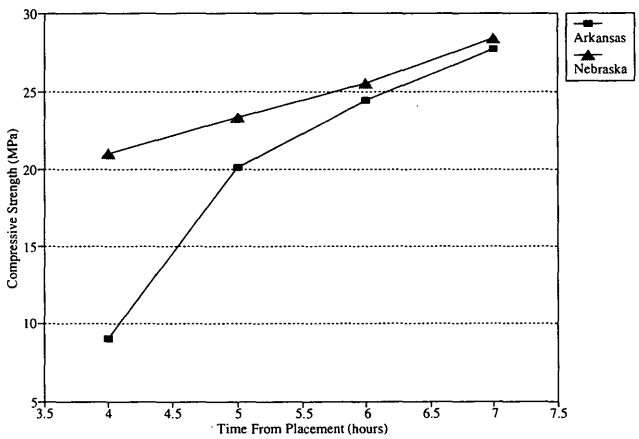

FIGURE 2 Early age compressive strength of insulated concrete.

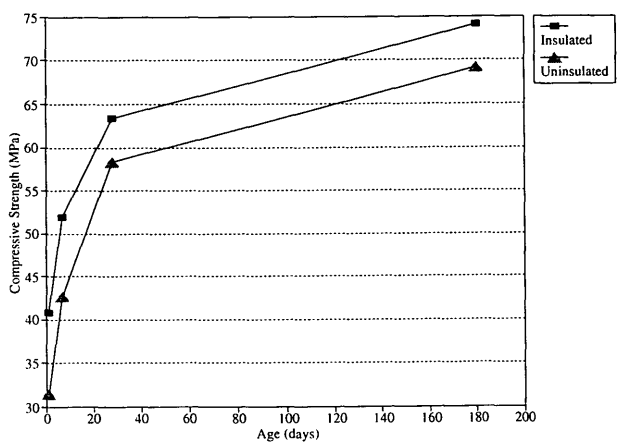

FIGURE 3 Long-term compressive strength.

The following table presents compressive strength data at 6 hr and at 1 day (1 MPa = 145 psi):

Site	*Insulated (6 hr) (MPa)*	*Noninsulated (1 day) (MPa)*
New York	10.3	No data
Illinois	10.8	34.5
Arkansas	24.4	31.4
Nebraska	23.3	30.8

These data were obtained from test cylinders cast from the second truck for both the insulated and noninsulated test sections at all sites but North Carolina. The table shows that the early strength of the insulated cylinders in Arkansas and Nebraska exceeded the minimum requirement of 14 MPa (2,000 psi) compressive strength in 6 hr for the VES mix. However, in these states, the noninsulated cylinders did not meet the requirement of 34 MPa (5,000 psi) in 1 day for the HES mix. The situation in New York and Illinois was reversed: the 1-day strength criterion of the HES mix was met, but the 6-hr strength criterion of the VES mix was not. It is important to note that the concrete should reach its target strength within the desired time frame and certainly before being loaded by traffic. The incremental rate of strength development up to this point, or the additional strength gained after this point, is not as important. Although the strength of this concrete at 28 days, and later, is much greater than that required for a pavement, it is an unavoidable side effect of requiring very high strengths at very early ages.

CONCLUDING REMARKS

After having placed HPC in the field on five occasions, much has been learned about the material and what it takes to produce and place it properly. To use this material successfully, certain aspects of the construction process require special attention. A brief discussion follows of what the authors believe to be a few of the more important lessons.

First, the calcium nitrite solution added at the job site must be thoroughly mixed into the concrete. This is critical even with central mix batching. Worn blades, fin buildup, or minimum drum rotation speed will hinder effective mixing. Chain-driven drums have proven susceptible to mixing problems with dry-batched HPC.

Because of the staged batching process, the low water-cement ratio, and limited mixing time available after addition of the calcium nitrite, it was found necessary to limit the size of the loads to no more than two-thirds of the truck's rated mixing capacity. This holds true for all truck mixers, even those in good operating condition. If adequate mixing is a problem, or if trucks in adequate condition (ASTM C94-90) are not available, it may be helpful to limit the load size to half the rated mixing capacity.

A preconstruction meeting should be held with the contractor; the concrete supplier, including the batch plant operator; and appropriate highway department personnel. Although important for any concrete construction, it is especially important when HPC is used. Topics to be discussed should include the mix proportions and needed materials; the batching sequence, including the site addition of calcium nitrite; travel time and route; placing, consolidation, and finishing procedures; the stiff and sticky nature of the mix; insulation; criteria for opening the patch to traffic; and field trial batching.

The batch plant should be made aware of the desire for tight control over water content. Excess water will harm the performance of the HPC more so than it will for conventional concrete. In addition, more care must be taken in the batching process to ensure that the correct materials are batched in the proper sequence. Drivers should be told that delays in transporting the concrete can cause serious problems. They must also understand that all wash water needs to be fully discharged before being charged with the HPC mixture and that the drum must be kept in constant rotation.

Contractor personnel should be informed of the stiff and sticky nature of the concrete. HPCs usually do not flow like the mixtures commonly used in patching, so more effort will probably be required to place the concrete. The mix will react well to vibration. However, a vibration should not be used to move the concrete to its final position, which may cause the mix to segregate. Usual finishing practice still applies to HPC, although the finishers may find the mix somewhat difficult to work. If possible, the finishers should have a chance to work with the mix during trial batching.

Enough laboratory and field trial batches should be produced to confirm the mix proportions, batching sequence, and workability of the mix. The basic proportions of the HPC mixture will have to be modified for the physical characteristics of the local aggregates and cement. It has been found that use of ACI's proportioning guidelines (ACI 211.1-81) for determining aggregate quantities will yield a satisfactory first approximation of the mix proportions. The brand, type, and time of addition of the admixtures will also affect the properties and performance of the concrete.

Laboratory batching of the constituent materials should be conducted as closely as possible to that expected in the field. Slump, air content, unit weight, and temperature of the fresh concrete should be determined. Several cylinders should be cast to evaluate the rate of strength gain and ultimate strength capacity. Curing of the cylinders should be as expected in the field. The mix proportions should be adjusted until the desired performance is achieved. At least one additional batch of a successful mix should be produced for confirmation.

After the mix has been adjusted in the laboratory, field trials should be conducted. Rarely does the mix not require further adjustments in the field to obtain the desired slump, air content, strength, and durability. The moisture content of the aggregate will play a significant role in adjusting the mix proportions. The best approach to the field trials is to produce a number of small batches to confirm the mix proportions and the time available to work the material. These batches can be used for patching, placed in temporary forms in the batch plant yard, or used as temporary working slabs on site. Between the preconstruction meeting and field trial batching, most potential problems can be addressed and remedied.

With small loads adequate mixing can be ensured, waste is minimal, a single patch can be filled by a single truck, and many trials can be conducted without excessive costs. If the concrete is used for patching, discontinuous patches are best. This will eliminate the potential for any cold joints due to construction delays. In addition, work can be stopped at just about any time. Only after the mixture has been successfully produced in field trials should any major construction be undertaken.

A final note on working with HPC in the field has to do with patience. The research team has found that a full day of production is typically required to bring all participants up to speed, and the learning curve costs during this first day can be appreciable. However, at field sites where multiple days of operation were possible, subsequent work went much more smoothly.

ACKNOWLEDGMENTS

This research is being conducted by North Carolina State University, the University of Arkansas, and the University of Michigan in cooperation with SHRP. SHRP is a unit of the National Research Council that was authorized by Section 128 of the Surface Transportation and Uniform Relocation Assistance Act of 1987.

REFERENCE

1. R. K. Smutzer and A. R. Zander. A Laboratory Evaluation of the Effects of Retempering Portland Cement Concrete with Water and a High-Range Water-Reducing Admixture. In *Transportation Research Record 1040*, TRB, National Research Council, Washington, D.C., 1985, pp. 34–39.

Publication of this paper sponsored by Committee on Performance of Concrete.

Preliminary Investigation on Effects of Moisture on Concrete Pavement Strength and Behavior

NEERAJ BUCH AND DAN G. ZOLLINGER

The effects of moisture on pavement concrete properties and behavior are reviewed. Drying of concrete is investigated in terms of Gibbs free energy. A nondestructive system was devised to measure the change in relative humidity with time. The relative humidity and temperature changes within the body of the specimen were measured using humidity and temperature sensors; these sensors were connected to a continuous data logging device. The humidity profile shows that drying in the surface layers is greater than in the interior concrete. Moisture content measurements indicate that the strength of concrete is dependent on the relative humidity. From the experimental results, it can be concluded that as concrete dries, the stress levels increase under varying restrained conditions. This observation may be useful to pavement engineers using certain assumptions in determining when to introduce a saw cut in a freshly constructed rigid pavement. Thus, on the basis of the determination of the change in relative humidity, a system of crack control may be devised.

From the viewpoint of engineering analysis and design of concrete pavements, it is desirable to control pavement cracking at joint locations and at desirable intervals in the pavement for decreasing the possibility of the formation of uncontrolled cracks. One of the most critical periods in the life of a concrete pavement is soon after placement of the concrete when the strength of the material is low in comparison with the development of tensile stress and subsequent cracking under hot weather concreting conditions. During this initial period, significant changes can occur in the relative humidity of the pavement surface (Figure 1); these changes may cause the shrinkage properties of the surface concrete to be very different from the concrete below the surface. The surface layer of concrete is referred to as the "skin" of the concrete pavement (*1*). The behavior of the skin can be of particular interest to the pavement engineer in terms of understanding the factors that influence the development of environmentally induced stress and cracking in concrete pavements. It may be suggested that the stress state of the skin concrete may be related to the moisture state or the relative humidity of the skin concrete and that, as a consequence, may provide an indication of saw-cut timing on the basis of comparisons of the concrete stress to the concrete tensile strength.

The concrete at the surface of the pavement may be thought of as having three skins: the cement skin (about 0.1 mm thick), the mortar skin (about 5 mm thick), and the concrete skin (about 30 mm thick). These skins are created by sedimentation and segregation as a result of gravity, compacting methods such as vibrating, and permeation and evaporation of water in and out of concrete (*1*). The skin effect leads to variations in cement, aggregate, and water content and in porosity over the surface layers and so affects durability, differential hygric and thermal shrinkage and swelling, and differential strength and deformability. As observed experimentally, the surface layers dry faster, causing the skin to be coarser and more porous. As a noted consequence, increased water sorption by cement and mortar skin together with an increased water-cement ratio may cause increased dilatation by freezing and thawing and especially by use of deicing salts. The increased porosity of the surface layers gives greater erosion and wear potential while aggressive components of air or chemical solutions may penetrate quicker in concrete and increase chemical reactions in the skin (*1*,*3*).

Recent literature review has revealed that the prediction of the history and distribution of pore humidity in concrete structures is a problem of major importance, as is the state of environmentally induced stress. By measuring the moisture state within a concrete structure, a realistic prediction can be made for creep, shrinkage, thermal dilatation, stress state, deflections, and crack formation (*3*). The pore humidity may affect not only the concrete state of stress but also the strength, thermal conductivity, and rate of hydration or maturing of

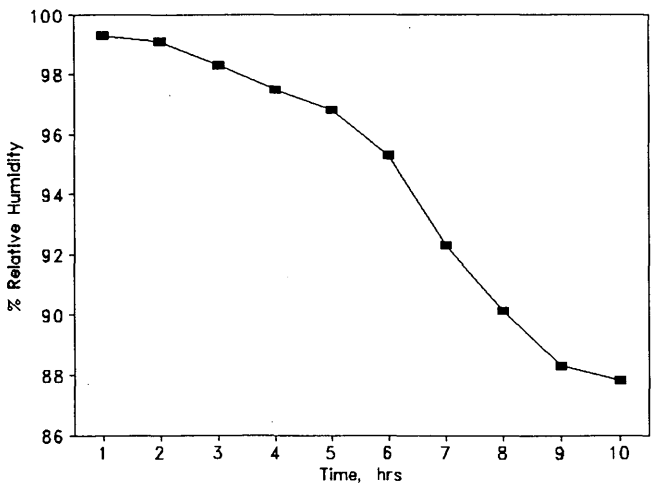

FIGURE 1 Change in relative humidity with time at pavement surface.

Texas Transportation Institute, Texas A&M University, College Station, Tex. 77843.

the concrete. As the drying process progresses, the moisture is lost with ever-increasing difficulty and the drying becomes much slower than an extrapolation of the initial drying curve; hence, diffusivity decreases with water content (*4*).

A pore water parameter related to the pore relative humidity of the concrete is the tensile stress of the pore water, sometimes called Gibbs free energy (*5*). To establish a relationship between a change in relative humidity (over time) and the change in modulus of rupture (MR) of the concrete, it is useful to introduce the concept of Gibbs free energy. To this end, an experiment was undertaken to measure the change in relative humidity within the body of concrete specimens subjected to a drying environment at different time intervals. The moisture data were then used in determining the Gibbs free energy and the change in the free energy as related to the state of stress in terms of MR. This information is useful for establishing a correlation between limiting changes in the pore relative humidity of the concrete and the state of stress with respect to the concrete strength at a certain time soon after concrete pavement placement.

EXPERIMENTAL PROGRAM

Test specimens used in this study consisted of beams 6 × 6 × 20 in. All specimens were cast using a water-cement ratio of 0.50. The nominal maximum coarse aggregate size was 1 in. The aggregate consisted of crushed limestone and river sand. Portland cement C150 (ASTM Type I), with no admixtures or air entraining agents, was used.

Material	*Design Weight* (lb/yd^3)
Cement (Type 1)	590
Fine aggregate (river sand)	1044
Coarse aggregate (limestone)	1841
Water	295

The concrete mix was designed in accordance with ACI 211.1-81 (revised 1985). Eight beam specimens were molded. PVC pipe sleeves of ½-in. diameter and 1- and 3-in. lengths were inserted in the fresh concrete below the surface of the concrete specimen to act as an encasement for the relative humidity sensors (Figures 2 and 3). The sleeves were provided

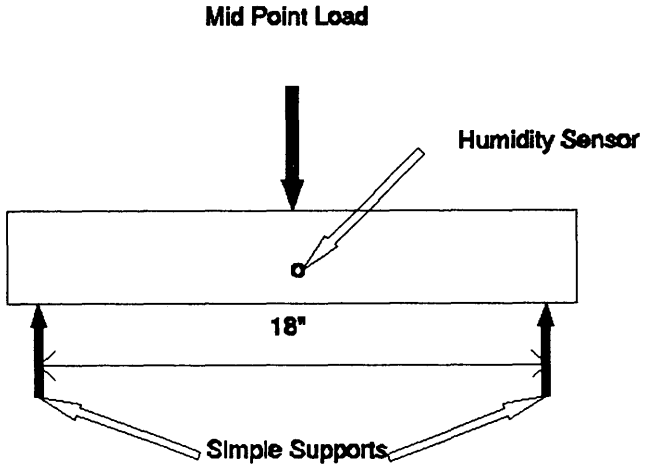

FIGURE 2 Stress measurement setup.

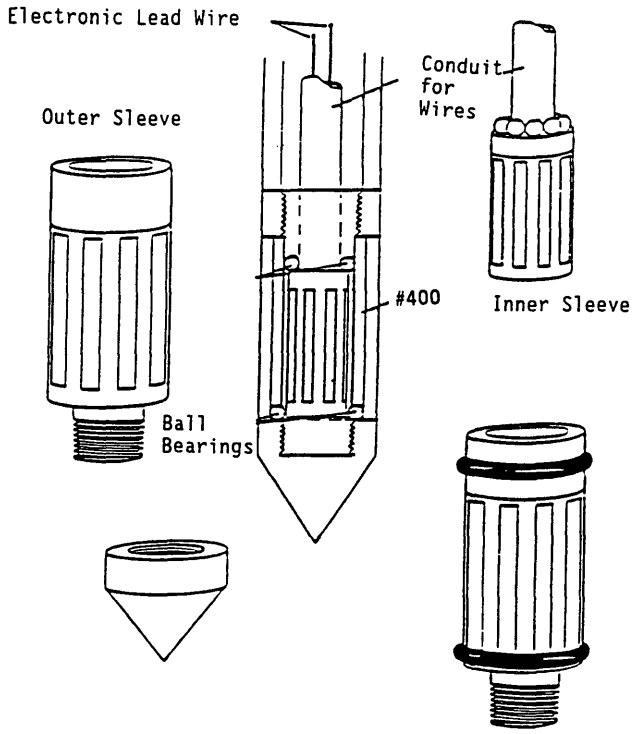

FIGURE 3 Configuration of relative humidity meter.

to prevent the sensor tips from making direct contact with the concrete. The relative humidity sensors were connected to a continuous recording data logger.

The data logger provided continuous information about the relative humidity and temperature in the concrete specimen at the specified depths. To prevent moisture loss through the PVC casing, the sensors were equipped with a rubber plug that fitted perfectly into the casing, providing an airtight seal. The entire assembly was then placed in an environment chamber (73°F, 95 percent relative humidity) for the duration of the experiment.

Measurements were made within the specimens at 3, 7, 14, 21, and 28 days. These measurements included recovery of the change in the relative humidity and temperature within the body of the concrete. This was achieved by downloading the information from the data logger to a personal computer and evaluating the data. Before the removal of the relative humidity sensors, the beam specimen was tested under single-point bending and subsequently determined both the load at failure and change in moisture. This procedure was repeated for all the specimens on the test days. To compute the Gibbs free energy, an accurate determination of moisture change is an essential parameter. Once all the data were collected and processed, the following relational plots were developed:

- Time versus change in relative humidity with time and depth of measurement
- Gibbs free energy versus relative humidity
- Change in Gibbs free energy versus modulus of rupture

This instrumentation can be placed in the field easily. In fact, experience has shown that a contractor's labor force can in-

stall the relative humidity meters with little supervision (Figure 4).

The second phase of the experiment consisted of testing beam specimens for strength at different dried stages. This experiment consisted of molding six beam specimens using the same mix design as in Phase 1 with identical beam dimensions. After molding, the beam specimens were transferred to a temperature-controlled water bath; the curing temperature was 73°F. The specimens were cured under identical conditions for 3 days. After the initial curing period, two beam specimens were tested immediately, and the other four specimens were allowed to air dry in the environment chamber. The remaining two pairs were tested after 2 and 4 hr of air drying, respectively. The results of the experiment are given in Table 1.

ANALYSIS AND DISCUSSION OF RESULTS

The results, as shown in Figure 5, reveal that relative humidity within the specimen body reduced with curing time such that the upper layers experienced a quicker loss of moisture than the interior of the concrete. The relative humidity is related to loss of moisture. This fact may be considered when designing the concrete cover for the reinforcing steel.

"The adsorbed molecules are much less susceptible to flow than capillary water because of the strong surface forces" (*4*). The change in the diffusivity may be explained in terms of a diffusion mechanism in that the size of the mean free path of water molecules in vapor is much greater than the size of the continuous pores in concrete, so that the probability of a vaporized water molecule passing through a narrow pore is reduced (*4*).

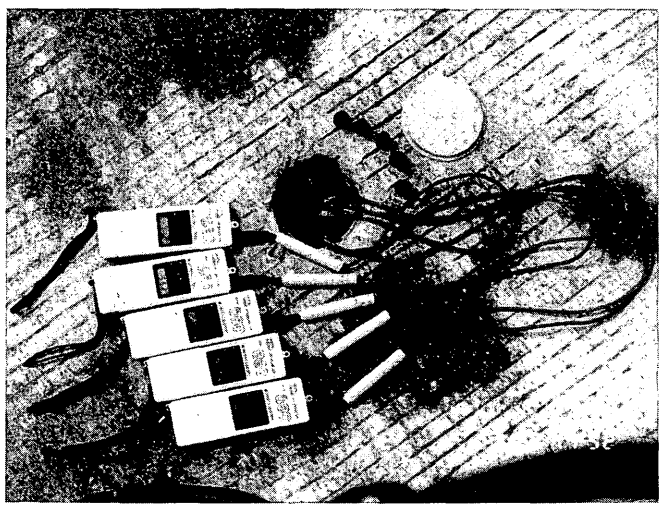

FIGURE 4 Photograph showing field placement of relative humidity meters.

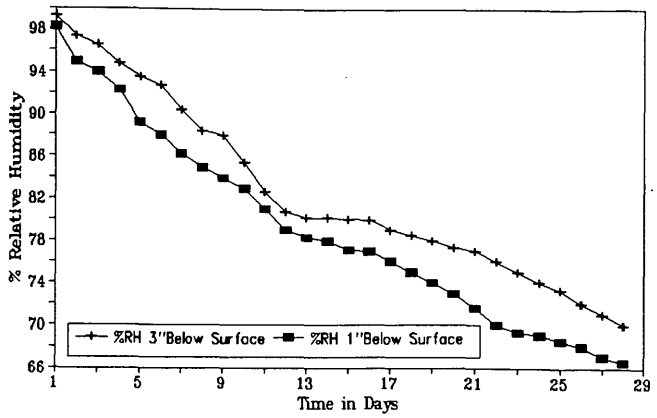

FIGURE 5 Reduction in relative humidity at different depths.

One of the parameters analyzed using the experimental data was the Gibbs free energy (Ψ):

$$\Psi = \frac{R \times T}{m \times g} \times \ln\left(\frac{H}{100}\right) \quad (1)$$

where

R = universal gas constant,
T = temperature in degree Kelvin,
m = gram-molecular weight of water,
g = gravitational constant, and
Ψ = Gibbs free energy.

Table 2 shows the variation in Gibbs free energy as calculated using Equation 1. Gibbs free energy is a negative quantity, such that as the specimens dry, relative humidity and free energy decreases. This relationship is clearly illustrated in Figure 6.

"For a given evaporable water content the system has a thermodynamic state that can be expressed as the thermodynamic equation of state, the determinants of which are pressure, temperature, and volume. With two of these parameters known, the third can be determined. . . . This thermodynamic state is true for any system, homogeneous or not" (*6*). Because the energy content of the system varies with the evaporable water content, it is essential to consider the evaporable water content when defining equilibrium conditions. The composition of the system under study may vary with change in evaporable water content; with each such change

TABLE 1 Effect of Curing Concrete Strength

Type of Curing	Load @ Failure, lbs	Modulus of Rupture,psi
Wet Cured, No Air Drying	1490	250
	1440	240
Wet Cured, Air Dried for 2 hr	1290	215
	1200	200
Wet Cured, Air Dried for 4 hr	1170	195
	1140	190

TABLE 2 Change in Gibbs Free Energy with Relative Humidity

Time in Days	% Relative Humidity	Gibbs Free Energy, psi
1	99.3	-137.6
3	96.5	-697.7
7	90.5	-1954.7
14	80.2	-4320.8
21	77.0	-5118.1
28	70.0	-6984.5

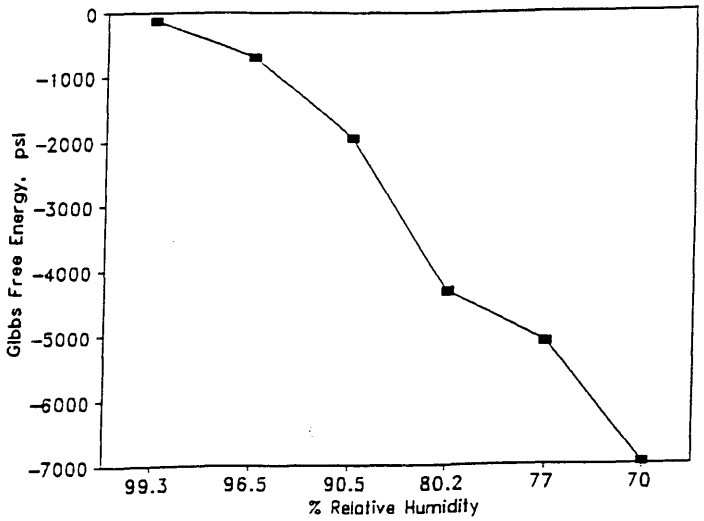

FIGURE 6 Change in Gibbs free energy with humidity.

of composition, there is a change of energy content. "If there are no changes in energy content with changing water content, the spontaneous phenomenon of shrinkage and swelling could not be detected, and within certain stress limits neither [could] creep" (*6*).

The beam specimens referred to previously were loaded using a single-point center load until failure. Before the modulus of rupture was determined, the relative humidity was recorded. At completion (at failure) of the testing, the relative humidity was measured once again (Figure 2). These humidity measurements were made directly under the load. This procedure was repeated for all the beam specimens tested at 3, 7, 14, 21, and 28 days. The intent of these measurements was to establish a relationship between the concrete stress state at failure and the Gibbs free energy.

The net change in Gibbs free energy is negative and varies with the level of stress (Table 2). On the basis of the theory of pure bending, one can derive the following relationship (using center-point loading):

$$M = PL/4$$
$$\sigma = Mc/I$$

where

c = $d/2$
I = $bd^3/12$

Assuming the tensile stress is distributed uniformly at failure,

$$M_{ult} = \sigma_t \times (bd/2) \times (d/2) = P_f L/4$$

Hence

$$MR = P_f L/bd^2$$

where

σ = bending stress (psi),
MR = modulus of rupture (psi),
P = load (lb),
I = moment of inertia (in.^{3}), and
c = distance of extreme fiber (in.).

$$\sigma_t = A \times \Delta\Psi \tag{3}$$

where A is -16.236 and $\Delta\Psi$ = change in Gibbs free energy.

From Equation 3 and the experimental relationship shown in Figure 7, the modulus of rupture ranges from -0.27 to -0.08 times the change in Gibbs free energy. On performing the t-test, it was determined that the slope of the regression line differs significantly from zero at an α of 5 percent.

Table 3 shows the change in the modulus of rupture for the three pairs of beam specimens tested at 7 days in flexure after being dried in air for different periods. The experimental results reveal that the specimens exposed to any degree of air drying showed corresponding lower strengths, even though the concrete mix design was identical and the initial curing conditions were the same. Apparently these results indicate

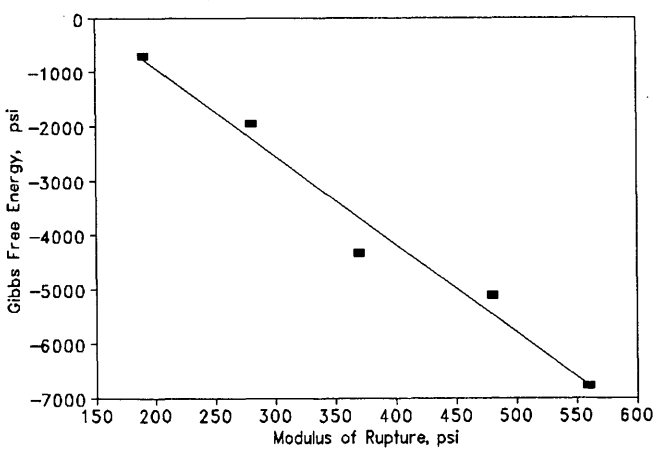

FIGURE 7 Change in MR as a function of Gibbs free energy: $y = 2329.04 - 16.235\,x$, $R^2 = .97$, standard error = 449.2258.

TABLE 3 Change in Beam Stress as a Function of Gibbs Free Energy

Time in Days	MR, psi	$\Delta\phi$, psi	MR/$\Delta\phi$
3	190	-698	-0.27
7	280	-1955	-0.14
14	370	-4321	-0.08
21	480	-5118	-0.11
28	560	-6984	-0.08

the dependence of concrete strength on the moisture state of the concrete. Because of the age of the beam specimens, it is unlikely that the decrease in strength is due to shrinkage-related cracks. However, it has been noted that if the drying is rapid, shrinkage cracks may develop in the transition zone and influence the flexural strength of the concrete specimen. The magnitude of the apparent loss of strength depends on the magnitude of moisture loss from the surface of the specimen (*7,8*). Therefore, it may be stated that the moisture in concrete may play two roles on the mechanical behavior of concrete: one that affects the strength, and one that affects the level of stress depending on how the Gibbs energy is developed in the pore water. These findings may be useful in developing a quality-control plan for saw cutting of concrete pavement, because concrete strength (and susceptibility to cracking) is affected by the moisture state of the concrete. It is recognized, however, that further research is warranted to investigate the effects of age (beyond those considered in this study), resaturation, and stresses in the elastic range on Gibbs energy.

Application to Jointed Concrete Pavements

As changes occur in the moisture state of concrete, a concrete pavement is subjected to volumetric changes similar in character to those produced by changes in temperature. These changes can lead to the development of gradients that contribute to subgrade friction and more particularly, curling- and warping-related stresses in the slab (Figure 8). Stress development at an early age in a concrete pavement system may be largely due to moisture-related behavioral characteristics in the concrete. The climatic conditions to which the pavements are exposed involve changes in precipitation and humidity. The instrumentation procedure described in this paper allows for the measurement of moisture variation in the pavement slab and provides an indication of stress induced thereby. Warping stresses, as suggested by Westergaard (*9*), depend on a structural parameter known as the radius of relative stiffness (ℓ, typical values range from 36 to 42 in.). The ℓ-value relates to the level of restraint as it varies from zero at the slab edge to a maximum value at a distance of 4.44ℓ from the edge in slabs of lengths (L) greater than 12ℓ (*10*), as illustrated in Figures 8 and 9. The varying level of restraint can be described in terms of the L/ℓ ratio. Figure 9 shows the variation in maximum stress (described in terms of the coefficient C) with varying levels of restraint. For slabs longer than 12ℓ, the maximum stress occurs at 4.44ℓ from the edge of the slab (*10*). Typically, cracks in the slab appear at these maximum stress locations, which suggests where joints should be saw cut in a jointed concrete pavement system. The restraint conditions under which Gibbs free energy was determined in the laboratory beam specimen described previously are directly applicable to the restraint conditions in concrete pavements at distances of 4.44ℓ or more from the free edge. The laboratory beam specimens were used to measure the change in Gibbs free energy from under fully restrained conditions, which allows the results to be applicable to the restrained portion of concrete pavements. The level of restraint in a concrete pavement is a function of curling stress coefficient (C) and Poisson's ratio (μ). Hence, the beam stresses obtained under the fully restrained conditions should be modified in order to obtain stresses in a concrete pavement.

Once the stress field in a concrete pavement is determined, the principles of fracture mechanics allow for the application of the stress field to the geometry of a concrete slab in the analysis of crack potential. The size effect law (SEL) considers for characterization of the stress intensity at the tip of a saw-cut notch in the pavement surface with respect to the slab thickness (*11*). Therefore, if the critical slab stresses at an early concrete age can be quantified, the nominal stress factor as involved in the SEL, illustrated in Figure 10, is based upon

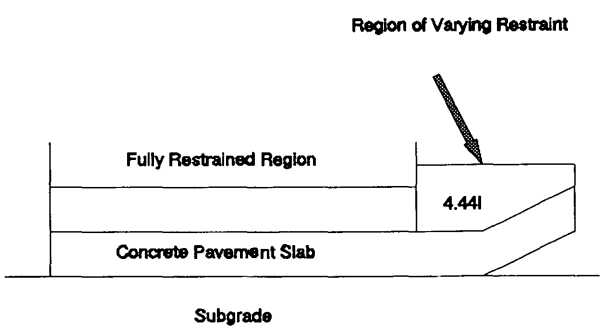

FIGURE 8 Concrete slab restraint conditions.

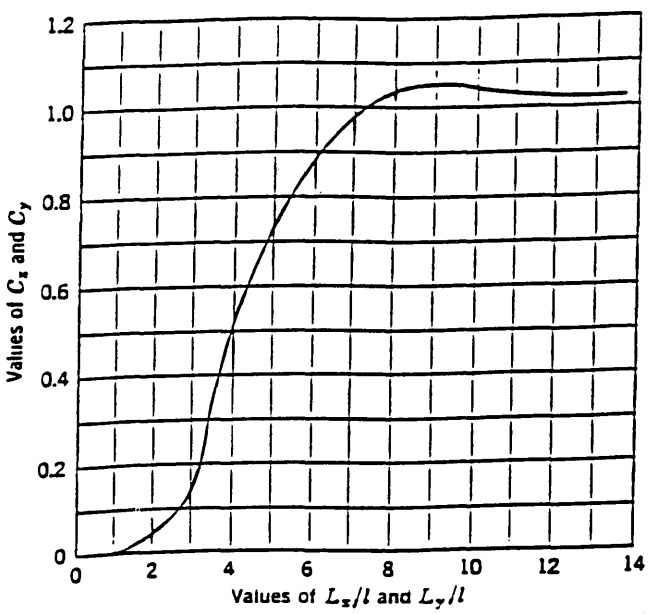

FIGURE 9 Curling stress coefficients (*10*).

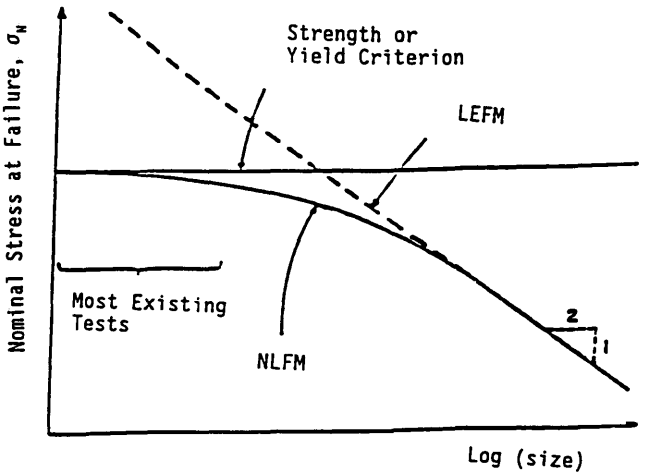

FIGURE 10 Size effects according to stress criterion (*3*).

the use of linear elastic fracture mechanics (LEFM) and therefore is useful in describing the stress and strength (fracture toughness) of concrete at the tip of the saw-cut notch in terms of the stress intensity factor (K_I).

The stress intensity factor for the opening mode fracture can be expressed as:

$$K_I = \sigma_N(\pi a)^{1/2} N(\omega) \quad (4)$$

where a is the crack length and $N(\omega)$ is a function of slab geometry, type of loading, and the ratio of the crack length to a specimen dimension ($\omega = a/d$). The term $N(\omega)$ is the nominal stress. The σ_N or MR as shown in Table 3 represents the stress field as it would occur in the fully restrained portions of the slab. The tensile stress will change vertically because of the change in moisture (consequently, it also results in a change in Gibbs free energy) and will also vary with respect to depth of cut. The development of the function $N(\omega)$ is found from finite element analysis and is elaborated elsewhere (*12*). The results of Equation 4 can be compared (over the first 12 hr after placement) to the fracture toughness of the material to ensure timely placement of saw cuts in a jointed concrete pavement. As far as the practitioner is concerned, given the relationship between saw-cut depth and stress intensity (*12*) and the early age strength of the material, the measurement and monitoring of the in situ relative humidity of the concrete in the pavement (particularly near the surface) as described in this paper offers a practical way to determine when saw-cut operations should begin.

CONCLUSIONS

The knowledge of the failure stress as it relates to the change in relative humidity can be important to determining when to saw cut a freshly constructed rigid pavement, in order to minimize random crack formation. This can be achieved by monitoring and interpreting measured relative humidity data from the pavement slab during construction.

The experimental investigation as reported in this paper reveals that the relative humidity measurements provide a convenient and direct indication of moisture level at the surface of a concrete pavement. The drying at the surface of a slab has a definite effect on the performance of the concrete pavement, especially the skin. The free energy concept is applicable in predicting tensile stresses and shrinkage potential in concrete, by measuring on-site relative humidity conditions near the slab surface. Even though further experimentation is required to investigate both stress and strength variations with moisture in concrete when subjected to different curing regimes, it is evident that a saturated beam specimen exhibits a higher flexural strength than a dry specimen. Thus, the moisture state in concrete should serve as a useful tool in the control of cracking of concrete pavement during construction operations.

ACKNOWLEDGMENTS

This research was carried out in the laboratory of the Texas Transportation Institute, Texas A&M University, College Station, Texas, and was supported by the Texas Department of Transportation.

REFERENCES

1. P. C. Kreijger. The Skin of Concrete—Composition and Properties. *Materials and Construction*, Vol. 17, No. 100, pp. 275–283.
2. L. J. Parrot. Moisture Profiles in Drying Concrete. *Advances in Cement Research*, Vol. 1, No. 3, July 1988, pp. 164–170.
3. Z. P. Bažant. Constitutive Equation for Concrete Creep and Shrinkage Based on Thermodynamics of Multiphase Systems. *Materials and Construction*, Vol. 3, No. 13, 1970, pp. 3–36.
4. Z. P. Bažant and L. J. Najjar. Nonlinear Water Diffusion in Non-Saturated Concrete. *Material and Structures*, Vol. 5, 1972, No. 25, pp. 3–20.
5. G. N. Lewis and M. Randall. *Thermodynamics*. McGraw-Hill Book Company, Inc., New York, N.Y., 1961.
6. T. C. Powers. The Thermodynamics of Volume Change and Creep. *Materials and Construction*, Vol. 1, No. 6, 1968, pp. 487–507.
7. S. Mindess and F. J. Young. *Concrete*. Prentice Hall, Englewood Cliffs, N.J., 1981.
8. A. M. Neville. *Properties of Concrete* (3rd ed.) Pittman Publishing, Aulander, N.C., 1975.
9. H. M. Westergaard. Analysis of Stresses in Concrete Pavements Due to Variations of Temperature. *HRB Proc.*, Vol. 6, 1926, pp. 201–215.
10. R. D. Bradbury. *Reinforced Concrete Pavements*. Wire Reinforcement Institute, Washington, D.C., 1938.
11. Z. P. Bažant. Size Effect in Blunt Fracture: Concrete, Rock, Metal. *Journal of Engineering Mechanics*, Vol. 110, No. 4, 1984, pp. 518–535.
12. D. G. Zollinger, T. Tang, and D. Xin. Sawcut Depth Requirements for Concrete Pavement based upon Fracture Mechanics Analysis. Presented at the 72nd Annual Meeting of the Transportation Research Board, Washington, D.C., 1993.

Publication of this paper sponsored by Committee on Performance of Concrete.

Silane Performance: Testing Procedures and Effect of Concrete Mix Design

AMR A. KAMEL, THOMAS D. BUSH JR., AND ARNULF P. HAGEN

The performance of a silane-penetrating water-repellent material applied to three concrete mix types was evaluated using alternative test procedures. One of the mix types was similar to standard reference concrete often used in laboratory testing. The other two mixes represented structural deck concrete and high-density overlay concrete, with correspondingly lower water-cement ratios and varying mix designs. Performance was evaluated with respect to depth of penetration, absorption, water vapor permeability, and chloride ingress. Test procedures and mix type were both found to affect the parameters used to evaluate the performance of the treated concretes. Results indicate the need to represent field conditions (such as mix design) to the extent possible in order to predict better field performance with laboratory tests.

The problems that arise from water and chloride-laden water intrusion into concrete bridge decks are often costly to repair. These problems range from scaling due to freeze-thaw cycles to corrosion of reinforcement and subsequent spalling of the concrete cover (*1*). The problems typically occur where the concrete bridge deck is exposed to freeze-thaw cycles and intermittent wetting, especially where deicing chemicals are used (*2*).

Over the past decade the use of silane to protect concrete bridge decks has grown in popularity because of its desirable performance characteristics, namely, reduction of chloride and water ingress, penetration into the concrete (which is useful on wearing surfaces and offers protection from the deteriorating effects of ultraviolet radiation), and unaffected skid resistance (*3*). However, the implementation of silane technology has been hindered by the lack of consensus concerning standardized testing procedures. This situation is costly to the various departments of transportation, in many cases because of uncertainties and concerns related to the effects of various commonly encountered field conditions often not considered in the testing procedures. Many current testing procedures use a standard laboratory reference concrete with a water-cement ratio (w/c) of approximately 0.50. However, structural concrete used for bridge decks usually has a somewhat lower w/c ratio, often about 0.45. Other mixes, such as high-density overlay concrete, may have even lower w/c's. Variations in mix design for concrete in the field may be significant, and the projected performance based on laboratory testing of a reference concrete mix type may vary greatly from the field where a different concrete type is used.

A. A. Kamel, Structural Engineering Associates, Inc., San Antonio, Tex. 78229. T. D. Bush, Department of Civil Engineering and Environmental Science, University of Oklahoma, Norman, Okla. 73019. A. P. Hagen, Department of Chemistry and Biochemistry, University of Oklahoma, Norman, Okla. 73019.

This study examines the effect of mix design on the performance of a silane water-repellent treatment material, with alternative testing procedures used to evaluate performance. Physical parameters studied in the tests include water absorption, chloride ingress, depth of penetration, and moisture vapor permeability (MVP). The effect of concrete moisture content at the time of application was also examined since the tests used different treatment conditions. Results of the first phase of a research project sponsored by the Oklahoma Department of Transportation (ODOT) are presented in this paper. It is anticipated that ODOT will use results to improve existing screening methods and to develop criteria to promote better field performance of penetrating water-repellent treatment materials.

SILANE WATER-REPELLENT MATERIAL

When silane is applied to the surface of concrete, the molecules are absorbed to the depth of penetration because of capillary suction forces (*4*). In the presence of moisture the hydrolysis process starts and produces silanol molecules, which are unstable and condense to form a SI-O bond with the silicate molecules in the concrete (*5*). The hydrocarbon group is in turn bonded to the silane molecules with a SI-C chemical bond. The hydrocarbon group is responsible for water and chloride repellency and lines the micropores of the concrete matrix, producing a hydrophobic layer by reducing the concrete surface tension (*3*).

The silane water-repellent treatment material used in the study was produced by the Chemistry Department of the University of Oklahoma to ensure the material's quality and reproducibility. The solution contained 40.3 percent (by weight) isobutyltrimethoxysilane in an isopropyl alcohol carrier, with a recommended application rate of 3.07 m^2/L (125 ft^2/gal). This rate was used for the research program.

EXPERIMENTAL PROGRAM

Concrete Mix Types

Three mix types were investigated and designated Types A, AA, and HD (high-density overlay). Specifications and properties for the mixes are shown in Table 1.

Test Procedures

Two basic test series were performed for each mix type: ODOT series tests and tests based on *NCHRP Report 244* Series II

TABLE 1 Specifications and Measured Properties of Mixes

Mix Type	A	AA	HD
W/C Ratio	0.49	0.44	0.33
Cement Factor (kg/m³)	335	390	490
Specified Slump (mm)	25-75	25-75	13-25
Specified Air Content (%)	5-7	5-7	5.5-7.5
Measured Slump* (mm)	50, 50	38, 25	13, 19
Measured Air Content* (%)	6.5,5.2	4.9,4.5	5.2,6.0
Maximum Size Aggregate† (mm)	13	13	13
Coarse Aggregate‡ (kg/m³)	950	950	964
Fine Aggregate‡ (kg/m³)	869	802	640
28 Day Compressive Strength (MPa)	39.3	46.2	56.5

(1 kg/m³ = 1.68 lb/cyd, 1 mm = 0.039 in, 1 MPa = 0.145 ksi)

* Values for each of two batches
† Maximum aggregate size used in laboratory concrete specimens
‡ Batch weights at saturated surface dry condition

(*6*). Brief descriptions of the tests performed for each series follow.

ODOT Series Tests

The ODOT series tests consisted of procedures to evaluate depth of penetration, MVP, absorption, and chloride ion intrusion. For all tests except chloride ion intrusion, test specimens were broom-finished blocks 200 × 200 × 50 mm (8 × 8 × 2 in.). The chloride ion intrusion test (salt ponding) used blocks 300 × 300 × 75 mm (12 × 12 × 3 in.).

- Depth of penetration—OHD-L34 (*7*): oven-dried specimens were treated and broken, and the depth of the hydrophobic layer was measured at multiple locations.
- MVP—OHD-L35 (*8*): specimens were treated after 48 hr of immersion in deionized water. The weight of water lost during oven drying was measured to provide an indication of the vapor transmissibility through the silane treatment.
- Absorption—ASTM C642–81: absorption through the top (unwaxed) specimen surface after 48-hr and 50-day immersion in water was measured for treated and untreated blocks.
- Chloride ion intrusion—AASHTO T259-80/T260-84: chloride contents were determined after 90-day ponding with a 3 percent NaCl solution. Powder samples were taken at depths of 1.6 to 13 mm (1/16 to ½ in.) and 13 to 25 mm (½ to 1 in.) using a rotary hammer. Chemical analysis was performed according to AASHTO T260, and results were reported as total chlorides absorbed (total chlorides minus total base chlorides in control specimens).

NCHRP Report 244 Series II Tests

The basic test procedure described in *NCHRP Report 244* (*6*), with slight modifications, was used for the major part of the study. Two variations of the procedure were also examined.

Treated and untreated cubes [100 mm (4 in.)] of each mix type were immersed in a 15 percent NaCl solution for 21 days and then air-dried for 21 days. Specimen preparation specifics included light sandblasting to remove surface laitance and 21 days of self-curing in plastic bags with a 5-day air-drying period before treatment. Weight recordings were performed every 3 days during the immersion and air-drying periods. Triads of cubes were used for each test group instead of pairs of cubes, as were used in the original NCHRP study. Chloride samples taken at the conclusion of the test procedure were obtained by rotary hammer drilling into three faces of the cube at two depth intervals, similar to the AASHTO T259/T260 procedures. This differs from the original NCHRP study, in which samples were obtained by crushing half of a cube to a fineness sufficient for chloride analysis.

Two variations of the procedure were carried out in parallel with the basic test procedure. In one variation, the cubes were not sandblasted before treatment. The second variation differed from the basic procedure in that the cubes were oven-dried, rather than air-dried, at the conclusion of the 21-day immersion period.

Other Depth-of-Penetration Tests

The moisture content of the concrete, among other factors, influences the depth of penetration of silane water-repellent treatment materials. The various tests performed used a wide range of moisture contents at treatment (from oven dry to saturated surface dry), so depth of penetration was measured for selected specimens (in addition to the primary purpose of the original test). Measurements were taken using absorption specimens, cubes, and MVP specimens. A pilot study was conducted to examine the effect of retreatment on specimens that initially exhibited negligible penetration. Previously untreated specimens from earlier tests were treated at random

moisture contents to examine the effect on penetration, and a controlled study was performed using Mix Type AA.

RESULTS AND DISCUSSION OF RESULTS

Test results are presented to give insight into the behavioral parameters of depth of penetration, water absorption, chloride ingress, and MVP. All results presented are averages of individual test specimens for each mix type.

Depth of Penetration

Primary depth of penetration results were obtained from the ODOT test, which is designed solely for that purpose. Additional results were obtained as described earlier. The depth of penetration and absorption tests specified treatment after oven drying (zero moisture content), whereas the MVP test used treatment at a nearly saturated surface dry state. The high moisture content of the MVP specimens resulted in negligible penetration depth for all mix types. To examine the feasibility of retreatment, the MVP specimens were oven-dried, and silane reapplied at full [(3.07 m^2/L (125 ft^2/gal)] and half [6.14 m^2/L (250 ft^2/gal)] coverage rates.

Results for all mix types are shown in Table 2. The depth of penetration was consistently higher for Mix Type HD, despite the low w/c of the mix. This could be due to the mix configuration and pore size. Mix Type A (w/c = 0.49) yielded higher depth-of-penetration values than Type AA (w/c = 0.44). Thus, results of these tests suggest that the w/c alone does not provide a relative indication of performance. Retreatment of specimens that originally had no measurable penetration led to significant improvement. Retreatment at full coverage rate resulted in penetration comparable to the other dry-treated specimens. It must be recognized that the retreated specimens were oven-dried before silane was reapplied and that the scope of this portion of the study was very limited.

Results of the preliminary study using surplus and originally untreated specimens treated at random moisture contents are shown in Figure 1. Because of various factors, the moisture contents could in some cases be determined only approximately; however, the results shown in Figure 1 indicate that concrete moisture content at the time of treatment can have a dramatic impact on the depth of penetration. Results of a controlled study for Mix Type AA are shown in Figure 2. Significant reductions in penetration occurred for moisture contents higher than about 1 percent.

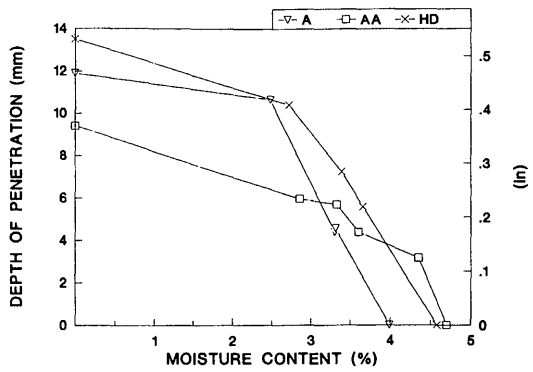

FIGURE 1 Influence of moisture content on penetration: preliminary study.

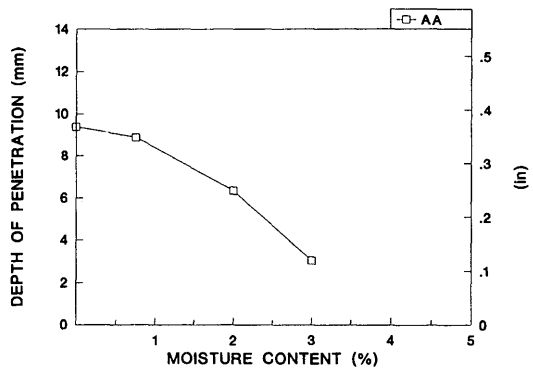

FIGURE 2 Influence of moisture content on penetration: controlled study.

Water Absorption

ODOT Series Test

Absorption results, obtained from tests following ASTM C642, are shown in Table 3. Mix Type A absorbed more water than Type AA, even though Type A had a higher depth of penetration. In general, the Type HD mix absorbed the least water. The percentage reduction in absorption due to treatment was higher for Type AA than the other two mixes. The percentage improvement due to treatment dropped after 50 days, reflecting the difference in absorption rates between untreated and treated specimens. For the untreated specimens, approxi-

TABLE 2 Depth of Penetration Results For Dry Application (mm)

Mix Type	Depth of Penetration Test	Absorption Specimens	MVP Specimens, 1/2 Rate Reapplied	MVP Specimens, Full Rate Reapplied
A	11.9	11.7	9.1	11.9
AA	9.4	8.6	8.4	11.9
HD	13.5	15.5	10.2	14.5

(1 mm = 0.039 in)

TABLE 3 Results of ODOT Series Absorption Tests

Mix Type	48 hr Absorption (%)			50 day Absorption (%)		
	Untreated	Treated	Improvement (%)	Untreated	Treated	Improvement (%)
A	4.28	0.55	87	5.25	2.20	58
AA	4.12	0.17	96	5.11	0.79	85
HD	3.98	0.36	91	4.68	0.77	84

mately 80 percent of the 50-day moisture gain was absorbed during the first 48 hr of soaking, whereas the treated specimens absorbed only 20 to 45 percent of the 50-day moisture gain during the first 48 hr.

NCHRP Report 244 Series II Test

Weight gained or lost was normalized with respect to the cube weight immediately before immersion, because dry weight of the untreated cube is not obtained from the test procedure. Approximate moisture contents at time of treatment, obtained from oven-dried cubes, were 3.3, 4.0, and 3.6 percent for Mix Types A, AA, and HD, respectively. Average weight gained or lost for each mix type is presented for untreated cubes in Figure 3 and for treated cubes in Figure 4. A statistical comparison (*t*-statistic) between means of the weight-gained curves (at selected times after immersion) confirmed that differences in behavior of the mixes were significant at the 5 percent level.

Mix Type AA gained more moisture than the other two mix types for treated and untreated specimens, although the difference was not great for the treated specimens. The rate of weight gain was also higher for the Type AA mix. Compared with the other two mix types, the treated and untreated Type HD specimens absorbed the least water on immersion.

The percentage improvements in absorption due to treatment (at 21-day immersion) do not compare directly to the values obtained from the ODOT series absorption tests, because the durations of immersion and moisture contents at the time of treatment are different for the two tests. And the cubes were immersed in a salt solution instead of water. The values, given in the following table, indicate that in general,

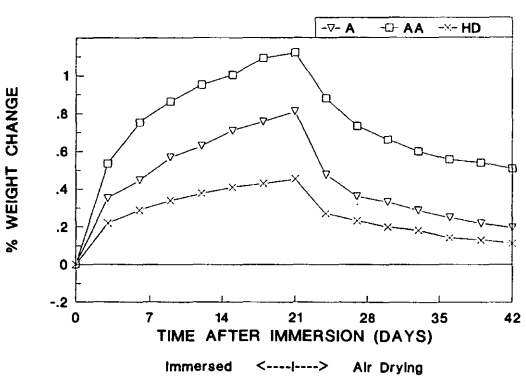

FIGURE 3 Weight gain or loss of untreated cubes (air-dried).

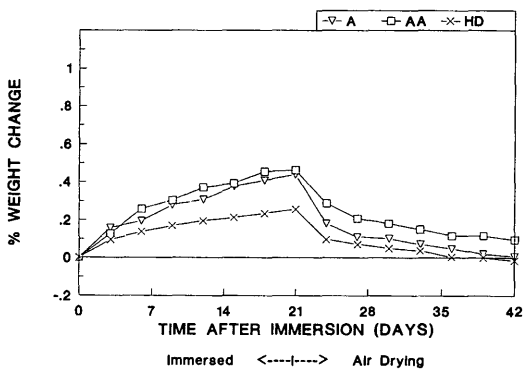

FIGURE 4 Weight gain or loss of treated cubes (air-dried).

the improvement in moisture repellency was greater when silane was applied to oven-dried specimens, as with the ODOT absorption tests (Table 3).

Mix Type	*Improvement (%)*
A	59.0
AA	47.5
HD	44.4

Cubes that were not sandblasted before immersion exhibited absorption characteristics similar to those of sandblasted cubes.

Moisture Vapor Permeability

For the ODOT series test, the depth of penetration was negligible because of the high specimen moisture content at the time of application. Moisture loss due to evaporation before the completion of treatment resulted in a large variation of results; this part of the testing program was deemed inconclusive. MVP behavior of the treated NCHRP 244 cubes can be seen in Figure 4 (air-dried cubes) and Figure 5 (oven-dried cubes). The absence of sandblasting had little effect on the vapor transmission characteristics of the specimens; those results are not presented here.

Treated air-dried cubes (Figure 4) lost much, if not all, of the weight absorbed during immersion by the end of the 21-day drying period. Mix Types A and HD lost 93 and 108 percent, respectively, of the water absorbed during immersion; Mix Type AA lost 75 percent of its absorbed water. The better vapor permeability characteristics of treated A and HD cubes were partially inherent in the mixes themselves. Untreated cubes reflected the same trend as treated cubes (Figure 3). The percentages of absorbed moisture lost on air drying were higher for the treated cubes than for the untreated cubes,

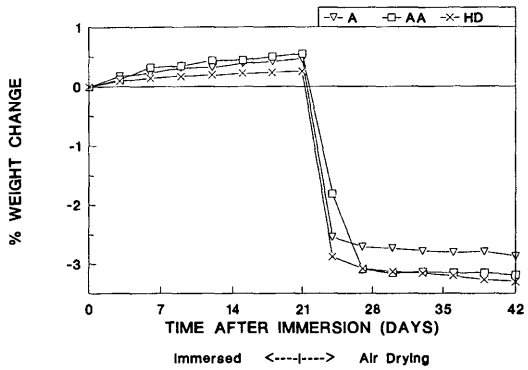

FIGURE 5 Weight gain or loss of treated cubes (oven-dried).

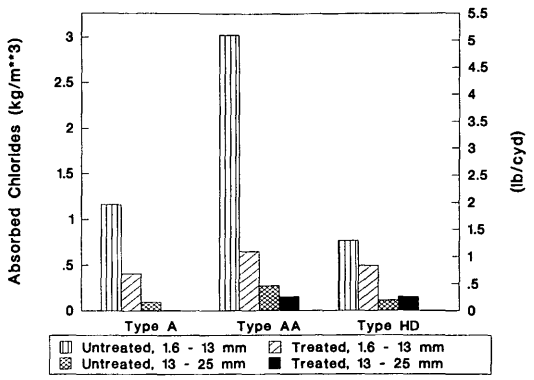

FIGURE 7 Absorbed chlorides, NCHRP 244 series test.

indicating that the vapor permeability characteristics of the mixes were largely unaffected by the silane. It must also be recognized that the specimens were immersed in salt water. It would be expected that not all of the weight gained during immersion would be lost upon drying, because some salt could remain in the concrete. The amount of actual moisture lost upon drying may be slightly higher than predicted by the test.

Curves for the oven-dried cubes are shown in Figure 5. As expected, the immersion branches of the curves are essentially identical to those of the air-dried cubes (Figure 4). The results reflect the different moisture contents of the mixes at the time of immersion. For example, Mix Types AA and HD exhibited the largest negative weight change upon oven drying, largely because of their higher moisture contents at time of immersion.

Absorbed Chlorides

Results for AASHTO salt ponding specimens and NCHRP cube specimens are shown in Figures 6 and 7, respectively. These figures contain means for the individual data. Because of the fairly large variability observed in the data, statistical comparisons were performed. Differences in means were tested using the *t*-statistic at the 5 percent level.

Considering differences between treated and untreated mixes for the AASHTO salt ponding tests (Figure 6), at the first depth the Type HD mix absorbed the least chlorides, and Types A and AA appear similar. These observations were verified statistically, except no difference was observed between Types HD and A. An unexplained larger variation in the data occurred for Type A, particularly for the untreated specimens, which contributed to this statistical observation. No statistical difference was observed between mixes at the second depth, for untreated or treated concrete.

Comparison between treated and untreated slabs (for a given mix) indicated that the difference for Types AA and HD was significant at the first depth. The absence of difference due to treatment for Mix Type A is again explained by the large variability in the data. No statistical difference was observed between treated and untreated concrete, regardless of mix, at the second depth.

Examining results from the NCHRP cubes (Figure 7), the untreated Mix Type AA absorbed considerably more chlorides at the first depth than did Types A and HD, which were statistically similar. No statistical difference was found between treated mixes at the first depth or between treated or untreated mixes at the second depth. Considering treated versus untreated cubes for a given mix, the only statistical difference observed was for Mix Type AA at the first depth.

Comparing the results from the AASHTO slabs to those of the NCHRP cubes yielded no statistically significant differences in absorbed chlorides for samples of the same mix, depth, and treatment. However, for both test procedures, the difference between chlorides measured at the first and second depths was significant for all mixes for a given treatment condition. The small measured chlorides at the second depth, regardless of treatment or mix, suggest that chloride absorption in the upper 13 mm (½ in.) may be a more useful indicator of performance using these tests. The observed variability in the chloride data also suggests that the cost of testing and importance of the results should be closely examined in selecting the number of specimens to be sampled.

Although variability in the data limited statistical conclusions, in all but one case (NCHRP test, HD mix, second depth), mean chlorides absorbed by treated mixes were lower than for corresponding untreated mixes. This trend was consistent and should not be ignored. The fact that treatment lowered chloride absorption is clear, despite statistical conclusions, although the degree of improvement is subject to debate. This dilemma results from the fact that observations

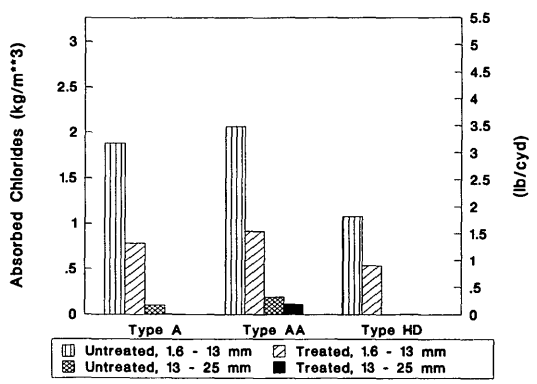

FIGURE 6 Absorbed chlorides, ODOT series test (AASHTO T259/T260).

concerning macrolevel behavior are being based on microlevel sampling. Large variability is commonly encountered in such cases. Similarly, the lack of statistical difference between treated and untreated mixes at the second depth should not be interpreted to mean that silanes do not reduce chlorides at depths below 13 mm (½ in.). Instead, it may indicate that the tests performed do not produce sufficient chloride levels at this depth to assess adequately the improvement due to treatment.

SUMMARY AND CONCLUSIONS

The performance of a silane-penetrating water-repellent material applied to three concrete mix types was evaluated using tests based on ODOT procedures and *NCHRP Report 244* Series II procedures. The three mixes were representative of standard reference concrete (Type A), structural concrete (Type AA), and high-density overlay concrete (Type HD).

1. Depth of penetration was good for all mixes when treatment was applied to dry (0 percent moisture) concrete. Significant reduction in penetration was observed with increasing moisture content at treatment.
2. From the results of statistical analyses, absorbed chlorides in the first 13 mm (½ in.) depth were significantly reduced by silane treatment for Mix Types AA and HD according to the AASHTO salt ponding test. However, the NCHRP cube tests indicated that only Mix Type AA was improved by treatment at this depth. Small amounts of absorbed chlorides were measured at the second depth for all mixes, regardless of treatment. Mean absorbed chlorides were consistently reduced by treatment for all mixes at both depths (with one minor exception). The variability in chloride data should be closely considered in selecting numbers of test samples, developing screening limits, and interpreting results.
3. The treated HD mix generally outperformed treated specimens of the other two mixes, exhibiting greater depth of penetration and lower water and chloride absorption. Improvement in performance resulting from silane treatment was usually not as great as for the other mixes; tests on untreated specimens indicated inherently better performance of the HD mix.
4. Performance of treated Mix Types A and AA was fairly similar, with some relative behavior affected by the test procedure used to obtain the physical parameter of interest. For treated NCHRP 244 cubes, Type A slightly outperformed Type AA with respect to absorption and vapor permeability, but they had similar absorbed chlorides. In the ODOT test series, Type A exhibited greater depth of penetration and similar chloride absorption but higher water absorption—despite its greater depth of penetration and contrary to the trend observed in the NCHRP 244 cube tests.
5. Performance of untreated Mix Types A and AA was similar for the ODOT test series. The NCHRP series suggested superior performance of untreated Type A over Type AA in terms of moisture gain and chloride absorption.
6. Results of the tests indicate that the interrelationship between performance characteristics of treated concretes is not straightforward. Use of a more "dense" mix (lower w/c and higher cement factor) did not necessarily reduce penetration or absorption, and smaller depth of penetration did not necessarily lead to higher absorption. There is a need for a more thorough understanding of the mechanisms responsible for performance.
7. Of the test procedures examined, the *NCHRP Report 244* Series II cube tests more closely represented field conditions, at least in terms of specimen moisture content at the time of silane application. Moisture content was shown to have a dramatic impact on depth of penetration; it is not known to what degree other performance characteristics are influenced by this variable. However, variability in test conditions exists since moisture content at the time of silane application is not controlled.
8. Results of this study point to the need to duplicate field conditions in the laboratory, to the extent possible, in order to better predict field performance of concrete treated with silane. Use of standard reference concrete for product screening purposes may be advantageous in comparing data from various testing agencies. However, silane performance of treated standard reference concrete may not predict field performance, because of the myriad variables introduced (of which mix type is but one).

ACKNOWLEDGMENTS

The support of this study by the Research Division of ODOT and by FHWA is gratefully acknowledged. The assistance of Phani Kalluri and other students, the technician, and staff of Fears Structural Engineering Laboratory is greatly appreciated. Chemical analyses were performed by Tisha Jones of the Chemistry Department at the University of Oklahoma; her assistance is gratefully acknowledged.

REFERENCES

1. *Durability of Concrete Bridge Decks: A Cooperative Study*. Final Report EB067.01E. State highway departments of California, Illinois, Kansas, Michigan, Minnesota, Missouri, New Jersey, Ohio, Texas, and Virginia; the Bureau of Public Roads; and Portland Cement Association, Skokie, Ill., 1970.
2. P. Carter. Sealing To Improve Durability of Bridge Infrastructure Concrete. *Concrete International*, Vol. 13, No. 7, July 1991, pp. 33–36.
3. E. McGettigan. Silicon Based Weatherproofing Materials. *Concrete International*, Vol. 14, No. 6, June 1992, pp. 52–56.
4. E. McGettigan. Application Mechanism of Silane Weatherproofers. *Concrete International*, Vol. 12, No. 10, Oct. 1990, pp. 66–68.
5. M. Smith. *Silane Chemical Protection of Bridge Decks*. Research and Development Division, Oklahoma Department of Transportation, Oklahoma City, Dec. 1986.
6. D. Pfiefer and M. Scali. *NCHRP Report 244: Concrete Sealers for Protection of Bridge Structures*. TRB, National Research Council, Washington, D.C., 1981.
7. *Test for Depth of Penetration of Concrete by Penetrating Water-Repellent Treatment Solutions*. OHD-L34. Oklahoma Department of Transportation, Oklahoma City (nd).
8. *Test for Moisture Vapor Permeability of Treated Concrete*. OHD-L35. Oklahoma Department of Transportation, Oklahoma City (nd).

Publication of this paper sponsored by Committee on Performance of Concrete.

Field Tests of Resistance to Chloride Ion Penetration on Sealed Concrete Pavement

RICHARD K. SMUTZER AND LUH-MAAN CHANG

The results and methodologies of a field study of portland cement concrete sealers on a traffic bearing surface in Indiana are presented. The study was to examine the resistance of chloride ion penetration on sealed concrete pavement. Various generic sealers were put on the surface of concrete pavement, then replicate samples were taken from the unsealed and sealed parts of the pavement. The content of chloride ions in the samples was analyzed and compared with the results of *NCHRP Report 244*. After 3 years of exposure, the test areas for some generic sealers continued to demonstrate better effectiveness than others in maintaining resistance to chloride ion penetration in concrete. Meanwhile, the field test results are significantly different from the laboratory test results in this study.

It has been well documented that deicing salts penetrate concrete and cause embedded reinforcing steel to corrode; moreover, the corrosion accumulates around the steel, causing cracks that allow the intrusion of even more damaging chloride ions. Thus, these cracks accelerate corrosion, induce spalling, and eventually shorten the service life of the concrete structure. Surface sealer has been applied to the concrete in attempts to minimize the damage caused by chloride ions from deiced salt (*1–3*). Although the use of sealers has met with varying degrees of success in the past, it is not uncommon for their use to result in premature failure of the highway concrete structure because of the corrosion caused by chloride ions.

The purpose of this paper is to present the results and methodologies of a field study on a traffic bearing surface. The study was to examine the resistance of chloride ion penetration on sealed concrete pavement. Various generic sealers were put on the surface of concrete pavement, and then replicate samples were taken from the sealed concrete pavement. The content of chloride ions in the samples was analyzed and compared with the reported laboratory tests.

After a detailed introduction of the field test methods and the presentation of their results, the differences between field and laboratory test results will be discussed. Finally, the conclusion and recommendation for future study will be made. The reader should be cautious: many methods have been developed to evaluate the performance of concrete sealers. Traditionally, most performance evaluations of concrete sealers are conducted in the laboratory. In a laboratory environment, not only can the variables be easily controlled, but the test processes can be accelerated. However, the laboratory test results do not always correlate with the results of the field tests or service tests; sometimes they are poor predicators of the long-term field performance (*4*). In this study the laboratory test procedure of *NCHRP Report 244* (*5*) is compared with the sealer's field performance on a traffic bearing surface.

R. K. Smutzer, Division of Materials and Tests, Indiana Department of Transportation, 120 South Shortridge Road, Indianapolis, Ind. 46219. L.-M. Chang, School of Civil Engineering, Purdue University, West Lafayette, Ind. 47907.

METHODOLOGY

Type of Sealers Evaluated

A field evaluation was authorized by the New Products Evaluation Committee of the Indiana Department of Transportation (INDOT) to appraise the field performance of seven portland cement concrete (PCC) sealers (*6*). These sealers are totally different types of brands of materials. On the basis of their generic content, they are named as the following (to facilitate the discussion, the abbreviations will be used to represent the individual type):

- Silane (Silane)
- Siloxane 1 (Silox 1)
- Siloxane 2 (Silox 2)
- Blend of siloxane and silane (Blend)
- Modified aluminum siloxane (Modified)
- Epoxy 1 (EPS 1)
- Epoxy 2 (EPS 2)

Location of Test Site

A concrete pavement contract was selected as the site for the field evaluation of these sealers. All seven of the PCC sealers are one-coat systems. A 5-gal sample of each PCC sealer was received from the product manufacturer for use in the evaluation. The test strip was in the southbound traffic lane from Station 274 + 60 to Station 277 + 00 along I-69, just north of the I-69 and SR-18 interchange, near Marion, Indiana. The average daily traffic along the test section is approximately 7,700.

Concrete Mix Design

The properties of the concrete and its materials are as follows:

- Cement: Louisville Type IA
- Cement content: 564 lb/yd^3
- Water: 170 lb/yd^3
- Fine aggregate: 1,281 lb/yd^3 (wet weight)

- Coarse aggregate: 1,819 lb/yd³ (wet weight) (1 in. topsize)
- Daravair R air entraining agent: 2.75 oz/100 lb
- Slump: 2.5 in.
- Net air content: 7.8 percent
- Unit weight: 141 lb/ft³
- Water-cement ratio: 0.40 to 0.44

(Conversion factors are 1 lb = 0.454 kg; 1 yd³ = 0.765 km³; 1 ft³ = 0.028 m³; 1 oz = 29.57 mL; 100 lb = 45.4 kg.) The batch weights reported for the fine and coarse aggregates are the wet weights. The water-cement ratio could not be located; tests usually range from 0.40 to 0.44 in Indiana.

Surface Preparation

The field work for preparing and sealing the pavement sections was conducted on June 4, 1987. The weather conditions were fairly clear and warm with temperatures near 26.7°C (about 85°F). Before the test areas were sealed, the PCC surface of the evaluation strip was sandblasted by the INDOT Gas City Maintenance Section to remove the curing compound (i.e., a Type II AASHTO M148 curing compound), surface dirt, and cement latency. The curing compound was applied at approximately 3.69 m²/L (150 ft²/gal), and the pavement concrete was allowed to cure more than 28 days before PCC sealers were applied. The pavement surface was then swept and blown clean.

Application of Sealers

The sealing was performed by the Special Studies Section. Table 1 is given for reference purposes. The concrete sealers were all applied to the test areas at a rate judged to be necessary for complete and uniform coverage of the tinned concrete surface. As indicated by Table 1, this was typically heavier than what would normally be recommended by the manufacturer. Three 22.32 m² (240 ft²) control areas (designated Controls 1, 2, and 3) were spaced along the test strip where no concrete sealer was applied. Two areas were delineated for the application of state-approved polysulfide type, epoxy penetrating sealers (EPSs).

These test areas (designated EPS 1 and EPS 2) were created to provide data from a known performer in sealing concrete. Figure 1 shows the locations and sizes of the various PCC sealer test and control areas. The various PCC sealers were applied as follows:

- Silane was poured across the 33.48 m² (360 ft²) test area. A thick-napped roller was used to squeegee and spread it uniformly over the test area. The sealer was applied at a rate of 2.46 m²/L (100 ft²/gal), which is somewhat heavier than the recommended rate, which is 3.07 m²/L (125 ft²/gal).
- Blend was poured across the 33.48 m³ (360 ft²) test area. A stiff-bristled broom was used to spread the material uniformly over the test area. Then the material was groomed further to work the material into the concrete surface. The

TABLE 1 PCC Sealer Application Information

Test Areas by Type of Sealer	Manufacturer's Recommended Surface Preparation	Manufacturer's Recommended Application Equipment	Manufacturer's Recommended Application Rate (ft^2/gal)	Test Area Application Rate (ft^2/gal)
SILANE	Sandblast or Waterblast	Spray, roller, or Bristly broom	125	100
SILOX 1	14 day (minimum) concrete cure & "clean" concrete surface	Low pressure sprayer, roller, brush, or broom	75-125	100
SILOX 2	Clean concrete surface with high pressure water and cleaners	Low pressure spray (preferred) or saturated brush or roller or "broom"	125	90
BLEND	Waterblast or Sandblast	Push broom (preferred) must broom into surface	100-125	100
MODIFIED	Waterblast or Sandblast	Push broom (preferred) must broom into surface	100-125	85
EPS I	Sandblast	Flood surface and spread with roller	90-110	90
EPSII	Sandblast	Flood surface and spread with roller	90-110	90

ft^2 = square feet = 0.093 meters squared; gal = gallons = 3.785 liters

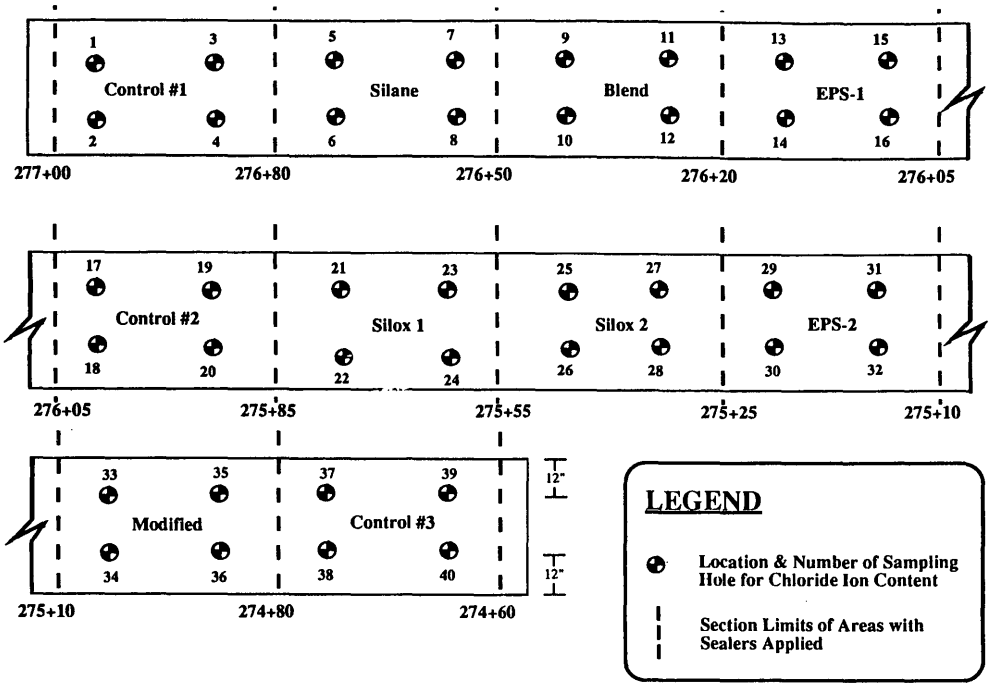

FIGURE 1 Plan view of field test site.

sealer was applied at a rate of 2.46 m^2/L (100 ft^2/gal), which is the heavier amount of the recommended range of 2.46 m^2/L (100 ft^2/gal) to 3.07 m^2/L (125 ft^2/gal).

- Modified was applied in the same manner as Blend. It was applied at a rate of 2.09 m^2/L (85 ft^2/gal), which is heavier than the recommended range of application rate, which is 2.46 m^2/L (100 ft^2/gal) to 3.07 m^2/L (125 ft^2/gal).
- EPS 1 and EPS 2 were applied on separate areas of the test strip. Each EPS was mixed after combining the resin and hardening components. Each EPS was applied by pouring the material across the 16.74 m^2 (180 ft^2) test area, then a thick-napped roller was used to squeegee and spread the sealer uniformly over the test area. Each EPS was applied at a rate of 2.21 m^2/L (90 ft^2/gal); the recommended rate was 2.21 m^2/L (90 ft^2/gal) to 2.70 m^2/L (110 ft^2/gal). Once applied, the EPSs were allowed to begin the set before sand veneer was spread over the surface to add skid resistance.
- Silox 1 was poured across the 33.48 m^2 (360 ft^2) test area. A thick-napped roller was then used to squeegee and spread the material uniformly over the test area. The sealer was applied at a rate of 2.46 m^2/L (100 ft^2/gal), which is the midpoint of the recommended range of application.
- Silox 2 was poured across the 33.48 m^2 (360 ft^2) test area. A thick-napped roller was then used to squeegee and spread the material uniformly over the test area. This sealer was applied at a rate of 2.21 m^2/L (90 ft^2/gal), which is heavier than the amount recommended by the manufacturer—3.07 m^2/L (125 ft^2/gal).

As mentioned, the test area surfaces were clean and dry before the sealers were applied. On June 3, 1987, the day before the sealer was conducted, it was a sunny day with clouds. The temperature was about 15°C (in the upper 60's Fahrenheit); the wind blew 16.1 km (10 mph). Traffic was not allowed on the pavement for at least 4 hr after the applications. Several photographs were taken to document these application activities; the photographs are on file at the INDOT Division of Materials and Tests.

Field Sampling and Chloride Ion Determination

The sealers were applied on June 4, 1987, and field samplings were conducted on May 25, 1988; October 4, 1989; and May 18, 1990: at 12, 24, and 36 months, respectively. Sampling holes were drilled at locations illustrated in Figure 1 for each test and control area. Samples for chloride ion content were obtained according to the method described in AASHTO T260, except that sampling tools were not washed before each sampling. A rotary hammer drill was used to advance the bit in the concrete. The pulverized cuttings or dust were obtained at 12.7-mm (0.5-in.) increments of bit penetration to a total depth of 3 in. The sampling procedure used several hammer drill bits with diameters of 31.75 mm (1.25 in.), 25.4 mm (1 in.), and 19.05 mm (0.75 in.). Each bit was used to obtain two samples from each hole, thus creating a stepped sampling hole, to prevent contamination of successively deeper samples. The samples obtained from each drill hole were submitted to INDOT Chemistry Laboratory for the determination of chloride ion content using an automated method duplicating ASTM C114. The chloride ion content and the depth of sample increments was established for each sampling location per year of exposure. Each sampling location is just outside the wheelpaths. They are approximately 25.4 mm (1 in.) from the outer edge of the pavement or center longitudinal joint, as shown in Figure 2. The results are presented in Table 2. Each value in Table 2 represents the mean of four sample data for each sealer.

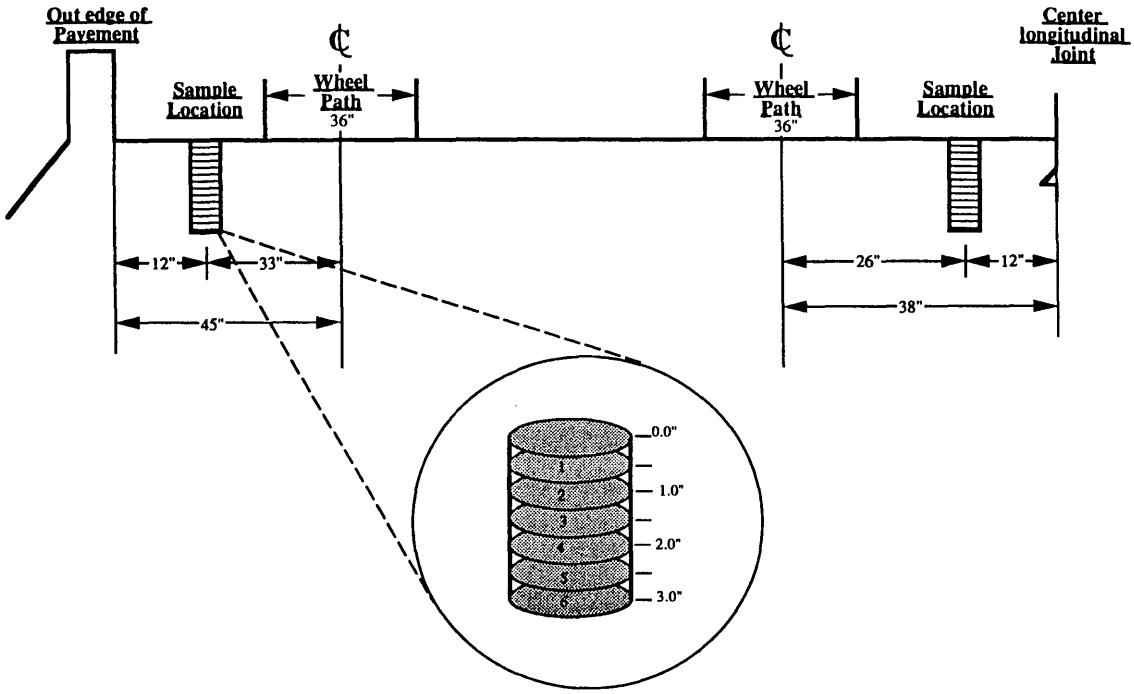

FIGURE 2 Typical wheelpath location on PCC pavement (1 in. = 25.4 m).

TABLE 2 Chloride Ion Content for Each Depth

Type of Sealer	Year 1						Year 2						Year 3					
Depth	1	2	3	4	5	6	1	2	3	4	5	6	1	2	3	4	5	6
Cont-1	5.31	2.81	1.57	1.98	1.50	1.61	7.43	7.12	2.92	1.89	1.58	1.74	11.00	9.52	4.18	2.30	1.57	1.61
Cont-2	5.30	3.45	2.40	1.85	1.49	1.93	8.69	7.44	3.05	1.70	1.90	2.20	10.20	8.69	4.07	2.03	1.58	1.94
Cont-3	5.56	3.28	2.05	1.72	2.02	1.71	7.15	7.11	3.51	2.11	1.71	1.84	8.88	8.01	3.60	2.24	1.78	1.63
Silox 1	1.99	2.27	1.94	1.55	1.55	1.72	3.97	4.90	3.21	2.29	1.73	1.60	4.75	5.74	2.86	2.01	1.69	1.91
Silox 2	2.51	2.31	1.77	1.91	2.04	1.63	4.85	5.84	3.24	2.27	1.70	1.69	5.45	6.40	2.55	1.60	1.65	1.46
Eps-1	2.69	2.19	1.56	1.70	1.50	1.67	4.15	3.79	2.35	1.87	1.69	1.58	5.00	4.02	2.75	1.93	1.75	1.45
Eps-2	3.14	2.63	2.14	2.01	1.39	1.28	5.13	3.85	2.92	2.48	1.75	2.53	5.33	4.18	2.21	1.66	1.55	1.76
Blend	2.59	2.10	2.14	1.57	1.99	1.73	5.80	6.36	2.63	1.75	1.59	1.72	6.67	7.88	3.83	2.21	1.78	1.59
Modified	3.58	2.57	1.55	2.26	1.83	1.59	6.46	6.58	3.10	2.29	1.92	2.03	7.15	8.58	3.82	2.07	1.77	1.55
Silane	1.69	1.90	1.61	1.64	1.49	1.73	2.31	2.82	2.13	2.33	1.90	1.68	2.88	3.46	2.27	2.01	1.47	1.75

1 pound = 0.454 kilograms, 1 cubic yard = 0.765 meters cubed

NOTE: Depth 1 = 0 to 12.7 mm (0 to 0.5 in.), Depth 2 = 12.7 to 25.4 mm (0.5 to 1.0 in.), Depth 3 = 25.4 to 38.1 mm (1.0 to 1.5 in.), Depth 4 = 38.1 to 50.8 mm (1.5 to 2.0 in.), Depth 5 = 50.8 to 63.7 mm (2.0 to 2.5 in.), and Depth 6 = 63.7 to 76.2 mm (2.5 to 3.0 in).

The surfaces of test and control areas were observed at the time of each sampling. After 3 years of exposure the first EPS test area had sealer still evident in the tinning. Most of the sealer appeared to be worn away on the surface. The second EPS had sealer still evident in the tinning and between wheelpaths. There were no significant signs of surface scaling or aggregate pop-outs in any test or control area along the evaluation strip.

Figures 3 through 7 illustrate the chronological sequence of the operation from blasting to applying the sealer and sampling. Both blasting and sealer application were done on the same day.

Data Analysis and Results

Table 2 shows the amount of chloride ion content found in samples from the various test holes. Each value represents the average annual value from four test holes of each test area. Six sample data were taken from each test hole. Because the study was only over 3 years, little chloride will penetrate below 50.8 mm (2 in.). Thus, the data analysis is based on the depths between 0 and 50.8 mm (0 to 2 in.).

Table 3 indicates the percentage of reduction of chloride ion due to the sealers applied to the surface of concrete test areas. For instance, the first-year value of 1.71 lb/yd^3 for

FIGURE 3 Sandblasting operation cleaning the concrete surface, removing the curing compound.

FIGURE 4 Applying sealers, flooding surface, uniformly distributing with roller.

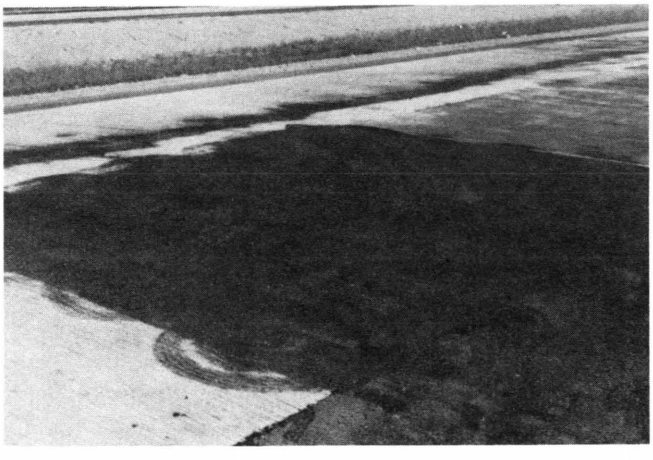

FIGURE 5 Epoxy sealer applied and sanded.

FIGURE 6 Finishing after all sealers applied in traffic lane.

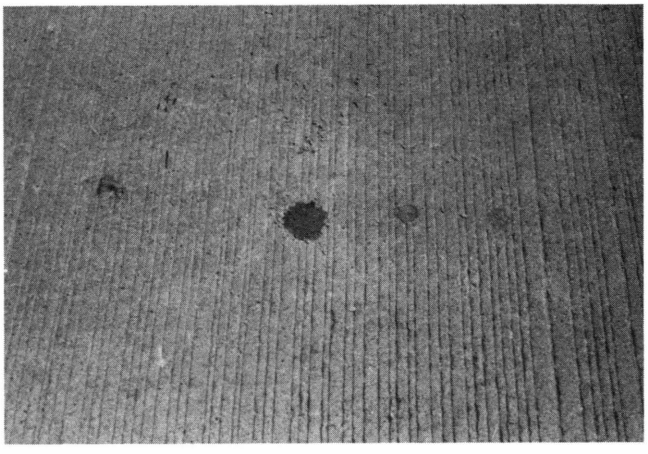

FIGURE 7 Close look at Location 30 after 3 years of sampling.

Silane is derived from Table 2. The average value of four depths, which represents depths from 0 to 50.8 mm (0 to 2 in.), is obtained by the calculation [(1.69 + 1.90 + 1.61 + 1.64)/4 = 1.71]. The corresponding reduction is obtained by comparing the average value of the Silane test area with the average value of the nearby controlled test areas, Sections 1 and 2. The reduction for the first year is 44.5 per cent [(3.08 − 1.71)/3.08 = 44.5 percent]. The percentage reduction for most treated test areas is increased each year. The last column contains the 3-year average. Silane has the comparatively highest reduction, and Modified has the lowest.

Figures 8 and 9 are the graphic representation of Table 3. The data shown in Table 4 are the reductions for the depth between 0 and 63.7 mm (0 to 1.5 in.) only. The reason for examining this layer is to attempt to compare the results with the results of *NCHRP Report 244* (*5*). In the report, the penetration of chloride ions in the concrete slabs subject to southern accelerated weathering exposure was examined between 6.35 and 31.75 mm (0.25 and 1.25 in.) below the concrete surface. The results in Table 4 are similar to the results in Table 3: the Silane test area has the highest percentage

TABLE 3 Present Reduction of Chloride Ion Penetration Between the Depth from 0.0 to 2.0 in. (Depths 1 to 4)

Type of Sealer	Year 1			Year 2			Year 3			Three Years		
	Avg.	SD	% Red	Avg.	SD	% Red	Avg.	SD	% Red	Avg.	SD	% Red
Silox 1	1.94	0.74	39.4%	3.59	1.09	29.5%	3.84	2.28	35.6%	3.12	1.76	34.2%
Silox 2	2.12	0.37	33.8%	4.05	1.45	20.4%	4.00	2.10	32.9%	3.39	1.73	28.6%
Eps-1	2.04	0.69	33.8%	3.04	1.27	39.6%	3.42	1.75	47.4%	2.83	1.47	41.8%
Eps-2	2.48	0.57	22.5%	3.59	1.14	29.5%	3.34	1.54	44.0%	3.14	1.25	34.0%
Blend	2.10	0.54	31.8%	4.13	2.03	17.9%	5.15	2.69	20.8%	3.79	2.34	22.1%
Modified	2.49	0.84	22.2%	4.60	2.07	9.6%	5.40	2.68	9.4%	4.16	2.36	12.4%
Silane	1.71	0.25	44.5%	2.40	0.78	52.3%	2.65	1.05	59.2%	2.25	0.87	53.7%
(C1+C2)/2	3.08	1.48		5.03	2.82		6.50	3.61		4.87	3.12	
(C2+C3)/3	3.20	1.49		5.09	2.68		5.96	3.25		4.75	2.83	

1 inch = 25.4 millimeters Avg.: Average SD: Standard Deviation Red.: Reduction

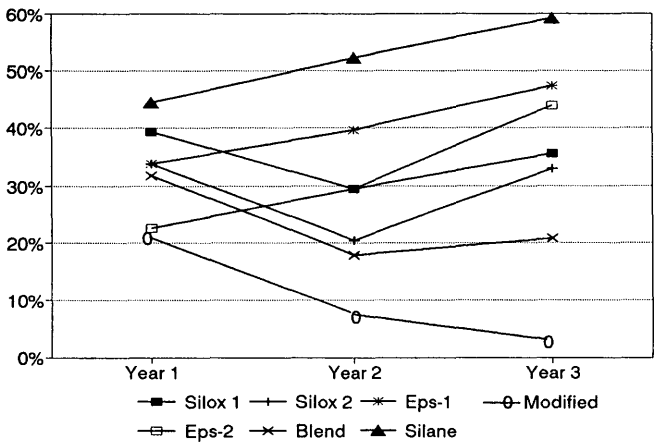

FIGURE 8 Yearly change of percentage of reduction.

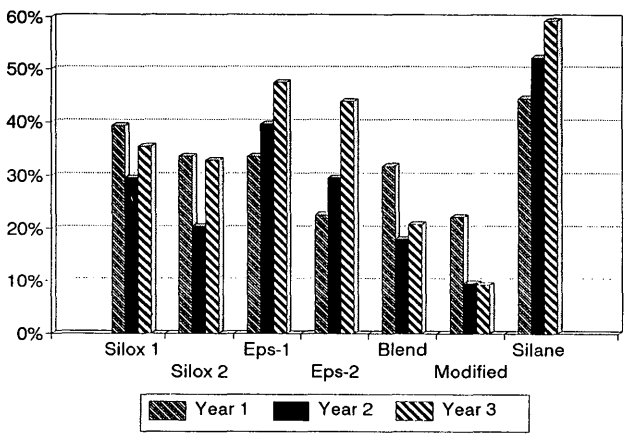

FIGURE 9 Comparison of percentage reduction for 3 years.

TABLE 4 Present Reduction of Chloride Ion Penetration Between the Depth from 0.0 to 1.5 in. (Depths 1 to 3)

Type of Sealer	Year 1			Year 2			Year 3			Three Years		
	Avg.	SD	% Red	Avg.	SD	% Red	Avg.	SD	% Red	Avg.	SD	% Red
Silox 1	2.07	0.61	43.6%	4.03	0.94	34.6%	4.44	2.42	38.6%	3.51	1.32	38.2%
Silox 2	2.20	0.42	40.2%	4.64	1.23	24.6%	4.80	1.89	33.7%	3.88	1.18	31.8%
Eps-1	2.15	1.03	38.1%	3.43	1.30	43.8%	3.92	1.83	50.6%	3.17	1.39	45.8%
Eps-2	2.64	0.56	28.2%	3.96	1.05	35.7%	3.90	1.42	46.1%	3.50	1.01	38.5%
Blend	2.28	0.52	34.4%	4.93	1.77	19.3%	6.12	2.48	22.9%	4.44	1.59	23.9%
Modified	2.56	0.93	30.2%	5.37	1.86	12.8%	6.51	2.23	10.0%	4.81	1.67	15.3%
Silane	1.73	0.22	50.1%	2.41	0.86	60.5%	2.86	1.12	64.0%	2.33	0.73	60.0%
(C1+C2)/2	3.47	1.57		6.11	2.54		7.94	3.12		5.84	2.41	
(C2+C3)/2	3.67	1.49		6.16	2.34		7.24	2.86		5.69	2.23	

1 inch = 25.4 millimeters Avg.: Average SD: Standard Deviation Red.: Reduction

reduction, and the Blend test area has the lowest. Moreover, both the Blend and Modified test areas display a diminishing percentage reduction.

Table 5 exhibits the average yearly value of chloride ion content for both intervals from 0 to 50.4 mm (0 to 2 in.) and from 0 mm to 38.1 mm (0 to 1.5 in.).

An analysis of variances was performed to examine the differences among the exposures. The results demonstrate that they are significantly different at a 99.9 percent confidence level. Year 3 has more chloride ion penetration than Year 2, and Year 2 has more than Year 1. It is logical that the longer the exposure is, the more chloride ions penetrate.

Student-Newman-Keuls grouping was conducted to test the differences among the means of various test areas. The results in Table 6 indicate that all the means of control test areas are not significantly different. They can be considered as an identical group at a 99.9 percent confidence level. Blend and Modified test areas are separate groups; Silox 1, EPS 2, and Silox 2 are a group; EPS 2, Silox 2, and EPS 1 are another group; and Silane is a totally different group.

The INDOT test is similar to the test reported in *NCHRP Report 244* except that it is a field test rather than a laboratory test. Although the INDOT testing did not precisely follow the manufacturers' recommended application rate, the INDOT testing used a more conservative measure to ensure a better sealing effect by generally applying the sealer at a lower square-feet-per-gallon rate.

Table 7 summarizes the application information. EPS 1 and EPS 2 were not tested per *NCHRP Report 244*. The results

TABLE 5 Comparison of Yearly Chloride Ion Content Between the Depth 0.0 to 2.0 in. and Depth 0.0 to 1.5 in.

	0.0" - 2.0"		0.0" - 1.5"	
Year	Avg.	SD	Avg.	SD
1	2.42	1.10	2.62	1.18
2	4.04	2.10	4.69	2.03
3	4.65	2.88	5.53	2.81

1 inch = 25.4 millimeters
Avg.: Average SD: Standard Deviation

TABLE 6 Results from Grouping Test (for 0.0 to 2.0 in., or Depths 1 to 4)

Type of Sealer	Mean	SD	Student-Newman-Keuls (SNK) Grouping
Cont-1	4.83	3.21	A
Cont-2	4.90	3.09	A
Cont-3	4.60	2.62	A
Modified	4.16	2.39	B
Blend	3.79	2.36	C
Silox 2	3.39	1.76	D
Silox 1	3.15	1.75	D E
Eps-2	3.14	1.26	D E
Eps-1	2.38	1.49	E
Silane	2.25	0.88	F

1 inch = 25.4 millimeters SD: Standard Deviation

TABLE 7 Comparison of Sealer Performances on Basis of Laboratory and Field Evaluations

Test Area	Laboratory Performance NCHRP No. 244, Series IV, SCE	INDOT Field Performance Based on 0" to 1 1/2" Sampling Interval (Similar to NCHRP No. 244, Series IV Criteria)		
		1-Year	2-Year	3-Year
SILANE	98.4%, 125 ft^2/gal.	50.1%	60.5%	64.0%
SILOX 2	92% to 93%,125 ft^2/gal	40.2%	24.6%	33.7%
BLEND	96% 125, ft^2/gal.	34.4%	19.3%	22.9%
MODIFIED	98.7%, 100 ft^2/gal.	30.2%	12.8%	10%
SILOX 1	89.30%, 100 $ft^{2/gal.}$	43.6%	34.6%	38.6%

1 ft^2 = 1 square feet = 0.093 meters squared
1 gal = 1 gallon = 3.785 liters
1" = 1 inch = 25.4 millimeter

in Table 7 indicate that the results from a field test could be significantly different from the results from a laboratory test. The laboratory results are not always applicable to the field, as the results from both test areas of Blend and Modified can verify. Both Blend and Modified sealers resisted chloride ion penetration very well under the reported laboratory atmosphere, achieving up to 96 and 98 percent reductions, respectively. However, the field tests for both demonstrated that their sealing effectiveness to reduce the chloride ion penetration diminishes under field conditions: they are on the 22.9 and 10 percent levels after 3 years of natural field exposure. It also appears that the severity of chloride ion penetration that resulted from laboratory testing is much greater than the 3 years of natural exposure.

The laboratory setup for accelerated weathering—which included acid, salt water, pounding, thermal heat, ultraviolet exposure, and drying (southern climate exposure)—appears to be much more severe than natural exposure from this study.

CONCLUSIONS

The following conclusions are based on the data presented in this report:

1. After 1 year of exposure, most of the test areas demonstrated effectiveness in resisting chloride ion penetration into the concrete. Silane and Silox 1 test areas demonstrated the highest effectiveness. The EPS 2 test area was not as effective as the other test areas, nor was the Modified test area.
2. After 2 years of exposure, the test area for Silane demonstrated the best effectiveness in maintaining resistance to chloride ion penetration in the concrete. The remaining sealer test areas demonstrated varying degrees of loss in effectiveness. Test areas for Blend and Modified had the most dramatic loss. The test areas sealed with Modified and Silox 2 did not perform as well as those areas sealed with the EPSs.
3. After 3 years of exposure, the test area for Silane continued to demonstrate the best effectiveness in maintaining resistance to chloride ion penetration in concrete. Both test areas for the EPSs demonstrated similar satisfactory effectiveness in reducing chloride ion penetration. Test area EPS 2 indicated a marked improvement from 2 to 3 years of exposure.

   The test areas sealed with Silox 1 and 2 demonstrated similar effectiveness after 3 years of exposure. The Silox test areas were not as effective as the test areas sealed with the EPSs. These sealers' test areas also indicated an improvement in effectiveness from 2 to 3 years of exposure.

   The test areas sealed with Blend and Modified demonstrated comparative effectiveness in reducing chloride ion penetration after 3 years of exposure, which was significantly below the effectiveness of EPSs.
4. The field test results are significantly different from the laboratory test results in this study. The laboratory test results cannot always be applied to the field. A measure should be developed to ensure that the results of laboratory tests are applicable to real-world situations.

REFERENCES

1. L. M. Chang. Laboratory Evaluation of Generic Concrete Sealer and Coating Systems. In *Transportation Research Record 1335*, TRB, National Research Council, Washington, D.C., 1992, pp. 1–27.
2. L. M. Chang and P. S. Garner. *An Investigation of Surface Coating on Exposed Concrete*. Report JHRP-8915. School of Civil Engineering, Purdue University, West Lafayette, Ind., May 1989, pp. 1–3.
3. C. Ozyildirim and W. Halstead. Resistance to Chloride Ion Penetration of Concretes Containing Fly Ash, Silica Fume, or Slag. In *ACI SP-108: Permeability of Concrete*, American Concrete Institute, Detroit, Mich., 1988, pp. 35–45.
4. B. R. Appleman. Performance Standards for Low VOC Coatings. *Journal of Protective Coatings and Linings*, Vol. 7, No. 11, Nov. 1990, pp. 106–114.
5. D. W. Pfeifer and M. J. Scali. *NCHRP Report 244: Concrete Sealers for Protection of Bridge Structures*. TRB, National Research Council, Washington, D.C., Dec. 1981, pp. 113–133.
6. A. R. Zamber. *Field Evaluation of Portland Cement Concrete Sealers*. Division of Materials and Tests, Indiana Department of Transportation, Indianapolis, Jan. 1991.

Publication of this paper sponsored by Committee on Performance of Concrete.

Coarse-Aggregate Effect on Mechanical Properties of Plain Concrete

M. REZA SALAMI, GARY SPRING, AND SHILONG ZHAO

The influence of three coarse-aggregate types on the relationships between compressive and tensile (split tensile and modulus of rupture) strengths of a plain concrete was investigated. It was found that, in some cases, aggregate type has significant effects on these strength relationships. The mineralogical differences in the aggregate types are considered to be responsible for this behavior. The commonly accepted 0.5 power relationship between compressive strength and tensile strength was found to be applicable neither for all aggregate types nor at different ages. From the available experimental data for modulus of rupture and splitting tensile strengths of concrete, alternative relationships between the tensile and compressive strengths were calibrated and are presented. Finally, a previous study of the effect of three coarse aggregates on the coefficient of linear thermal expansion and water-cement ratio was discussed and enhanced using graphic representations of the relationships. The correlation between the experimental results and analytical predictions provides a simple approach for developing tensile strength models for plain concrete using three types of aggregate. Tables of results and figures supporting these observations and conclusions are included.

It is generally assumed that concrete performance is governed mostly by its compression capabilities, but tensile strength (which directly influences cracking at prestress release) and shear capacity are important with respect to the appearance and durability of concrete structural members. It has been accepted by concrete researchers and the American Concrete Institute (ACI) that a 0.5 power relationship exists between the tensile strength and the compressive strength of concrete. Investigations have been conducted into the applicability of this 0.5 power relationship to medium-strength concrete (*1*). Several relations have been proposed for the tensile strength prediction from the compressive strength, but the effect of aggregate type on the prediction has not previously been clearly established. Chapter 18 of the ACI Building Code (ACI 318-83) represents the relationship between concrete tensile strength f_t and compressive strength by the relation

$$f_t = 6[f_c']^{0.5} \quad (1)$$

Ahmad and Shah reported that tensile strength of concrete with compressive strength between 6 and 12 ksi does not conform to the conventional ACI formulation (*1*). Therefore, they proposed an alternative relation for concrete compressive strength up to 12 ksi as

$$f_t = 4.34[f_c']^{0.55} \quad (2)$$

Department of Civil Engineering, North Carolina A&T State University, Greensboro, N.C. 27411.

ACI Committee 363 proposed another relation in the form of

$$f_t = 7.4[f_c']^{0.5} \quad (3)$$

as an upper bound (*2*).

Gardner and Poon suggested that splitting tensile strength is not necessarily proportional to the 0.5 power of compressive strength (*3*). They found that the tensile strength is proportional to the 0.8 power of the cylinder strength. A thorough review of literature related to this subject is presented by Oluokun (*4*).

As stated, none of the several relationships proposed for predicting tensile strength from compressive strength has clearly established the effect of aggregate type on their predictions. The conventional wisdom has been that for conventional concrete (less than 5.81 ksi), the properties of coarse aggregate seldom become strength-limiting because conventional concrete mixtures typically correspond to water-cement ratios (w/c's) of 0.4 to 0.7. Within this w/c range, the weakest components in concrete are the hardened cement paste and the transition zone between cement paste and coarse aggregate, rather than the coarse aggregate itself (*5*). Similarly, in designing conventional concrete mixtures, the mineralogy of coarse aggregate is rarely a matter of concern unless the aggregate contains some constituents that could have a deleterious effect on durability. For example, the presence of a reactive silica mineral such as opal in an aggregate can be harmful to concrete when the aggregate is used in combination with a portland cement containing more than 0.6 percent alkalies (Na_2O equivalent).

Given the lack of information in the published literature on the influence of coarse-aggregate characteristics, especially mineralogy, on the mechanical behavior of medium-strength concrete mixtures, the objectives of this paper are as follows:

- To investigate the effects of three coarse aggregates on the relationships between the compressive strength and the splitting tensile strength and moduli of rupture of a medium-strength concrete mixture;
- To calibrate a set of prediction models for the splitting tensile strength and moduli of rupture of concrete, as a function of its cylindrical compressive strength, f_c'; and
- To enhance discussions by Alungbe et al. (*6*) about the effects on linear thermal expansion of concrete due to aggregate type, curing time, saturation condition, and water-cement ratio.

PRESENTATION AND DISCUSSION OF TEST RESULTS

Test data reported by Alungbe et al. (*6*) were used to study the following tensile strength (a property that affects both resistance to cracking at prestress release and shear capacity) relationships as they pertain to aggregate type, and to derive associated prediction models. The test results and predicted models are shown in figures and tables as indicated:

1. Normalized tensile strength of concrete versus compressive strength: Equation 4 (Figures 1 and 2; Table 1), and
2. Normalized modulus of rupture versus compressive strength: Equation 5 (Figures 3 and 4; Table 2).

It should be noted that Equations 4 and 5 were normalized primarily to provide unitless constants. This normalization has no effect on the power values of the models (e.g., 0.5 in the ACI relationship).

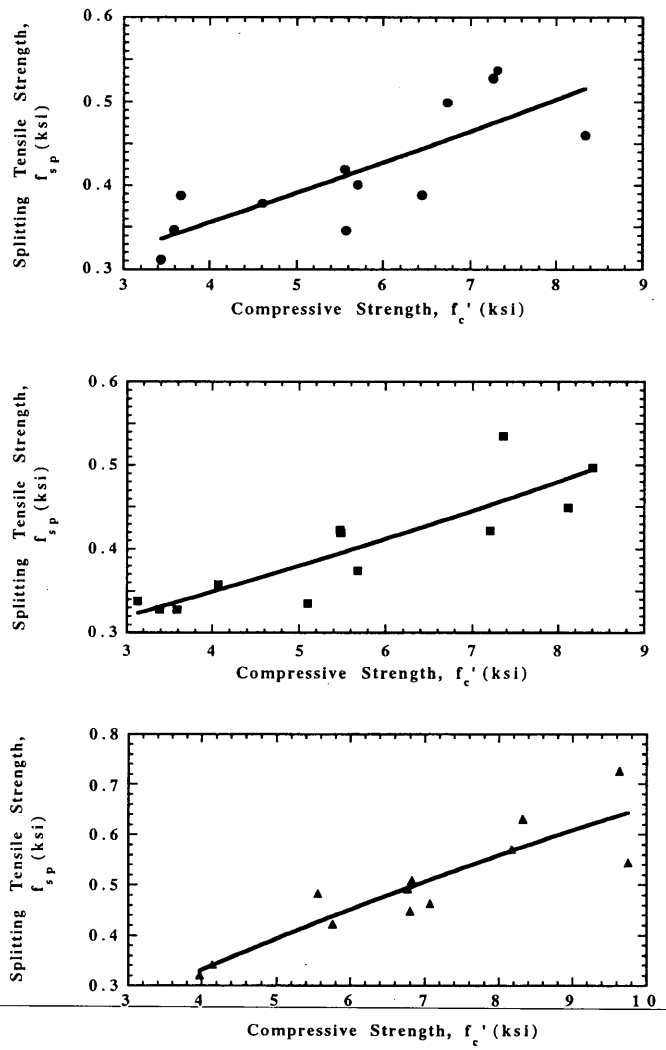

FIGURE 1 Plots of splitting tensile strength versus compressive strength for PL (*top*), RG (*middle*), and DL (*bottom*), Ruplicates 1 and 2 at 28 and 90 days.

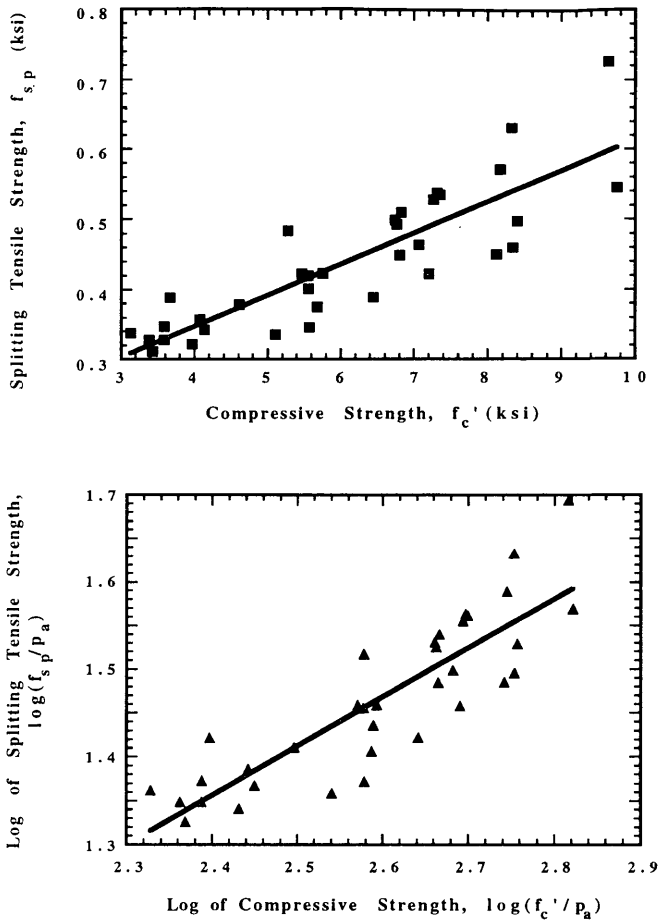

FIGURE 2 Plots of splitting tensile strength versus compressive strength (*top*) and log of splitting tensile strength versus log of compressive strength (*bottom*), for all data.

TABLE 1 Values of Parameters α_{sp} and β_{sp} from Proposed Expression of Splitting Tensile Strength for Three Types of Concrete Material

		28 days	90 days	28 & 90 days
Porous Limestone	R^2	0.56	0.63	0.59
	Mean α	0.535	0.401	0.462
	α 95% CI	0.23 to 0.85	0.20 to 0.60	0.30 to 0.63
	Mean β	1.1846	2.592	1.812
River Gravel	R^2	0.62	0.87	0.82
	Mean α	0.435	0.42	0.523
	α 95% CI	0.21 to 0.66	0.31 to 0.53	0.42 to 0.63
	Mean β	2.1	2.246	2.33
Dense Limestone	R^2	0.82	0.81	0.81
	Mean α	0.751	0.715	0.719
	α 95% CI	0.52 to 0.98	0.49 to 0.95	0.57 to 0.87
	Mean β	0.342	0.408	0.407
Combination of all three	R^2	0.7	0.75	0.72
	Mean α	0.586	0.547	0.56
	α 95% CI	0.46 to 0.72	0.44 to 0.65	0.48 to 0.64
	Mean β	0.157	0.162	0.161

For each of three aggregate types—namely, porous limestone (PL), river gravel (RG), and dense limestone (DL)—a set of tensile and compressive tests was conducted at three different w/c's at 28 and 90 days. In the original tests, as described by Alungbe et al. (*6*), two replicates of three speci-

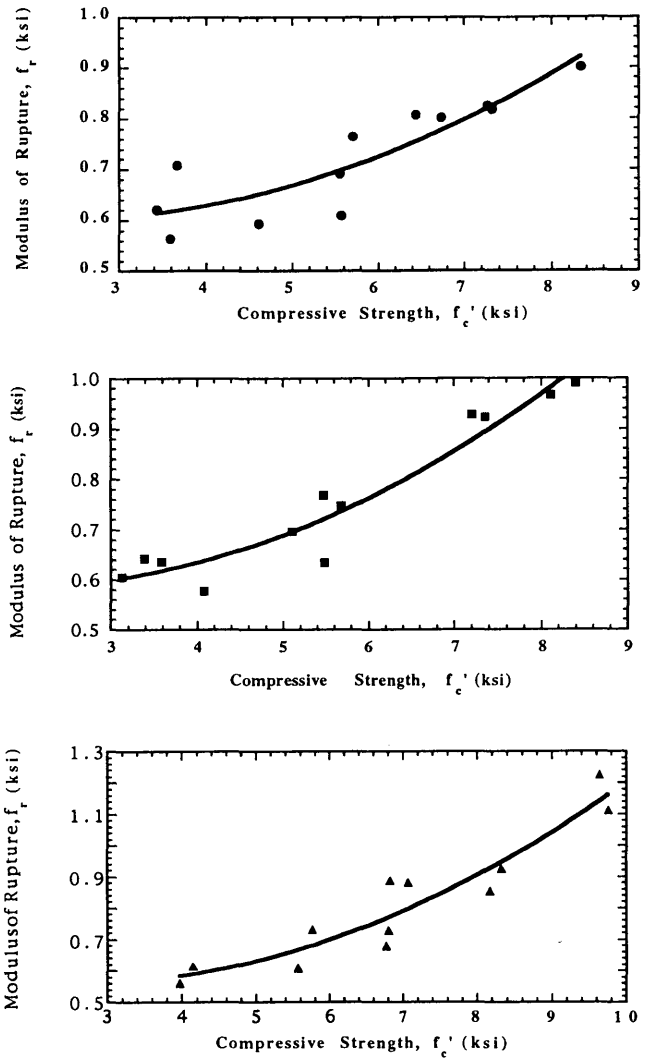

FIGURE 3 Plots of modulus of rupture versus compressive strength for PL (*top*), RG (*middle*), and DL (*bottom*), Ruplicates 1 and 2 at 28 and 90 days.

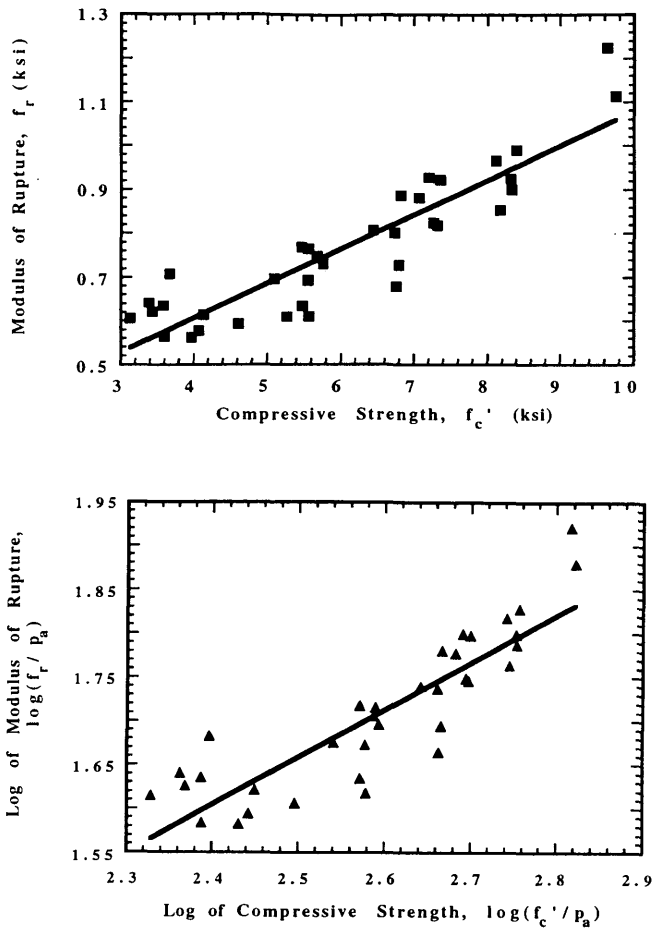

FIGURE 4 Plots of modulus of rupture versus compressive strength (*top*) and log of modulus of rupture versus log of compressive strength (*bottom*), for all data.

mens each for each material were conducted. Among the sets of three specimens, one consistently appeared to be an outlier. Thus, the best two specimens from each replicate were used in this study to derive the relationships presented in Tables 1 and 2. The raw data shown in Figures 1 and 3 for each aggregate, along with previous studies [e.g., Salami (*7–9*)], suggest the use of a logarithmic formulation as shown in Figures 2 and 4.

Splitting Tensile Strength

Equation 4 was used as the functional form for the model and was calibrated using simple linear regression for three types of concrete using different coarse aggregates and for different curing times. Regression results are presented in Table 1:

$$f_{sp} = -\beta_{sp} p_a \left\{\frac{f_c'}{p_a}\right\}^{\alpha_{sp}} \quad (4)$$

TABLE 2 Values of Parameters α_{sp} and β_{sp} from Proposed Expression of Moduli of Rupture for Three Types of Concrete Material

		28 days	90 days	28 & 90 days
Porous Limestone	R^2	0.37	0.95	0.66
	Mean α	0.271	0.602	0.422
	α 95% CI	0.05 to 0.49	0.51 to 0.70	0.29 to 0.55
	Mean β	10.03	1.351	4.01
River Gravel	R^2	0.71	0.92	0.73
	Mean α	0.455	0.603	0.423
	α 95% CI	0.26 to 0.65	0.49 to 0.72	0.30 to 0.63
	Mean β	3.488	1.452	2.24
Dense Limestone	R^2	0.85	0.96	0.82
	Mean α	0.644	0.778	0.76
	α 95% CI	0.46 to 0.81	0.67 to 0.88	0.61 to 0.91
	Mean β	0.975	0.503	0.521
Combination of all three	R^2	0.56	0.91	0.75
	Mean α	0.388	0.676	0.54
	α 95% CI	0.27 to 0.50	0.60 to 0.75	0.47 to 0.62
	Mean β	0.372	0.233	0.291

where β_{sp} and α_{sp} are the model parameters and p_a is atmospheric pressure in the same units as those of f_{sp} and f_c'.

The model, in all cases, demonstrates good statistics: α is statistically significant from zero at very high levels (i.e., *t*-values ranging from 5 to 100), and adjusted R^2- and *F*-values

are generally very high. For the PL, RG, and combined materials, α is not significantly different, at the 95 percent level of confidence, from the ACI suggested value of 0.5, although β-values are quite different: none turns out to be anywhere near previously reported values of greater than 4. The DL material, however, exhibits α-values in line with those proposed by Gardner and Poon (*3*). It is interesting to note that time does not appear to affect the relationship or its parameter estimates, except with respect to the confidence that one may reasonably place in the models. In general, the strength of the model's statistics increases with time. Adjusted R^2-, F-, and t-values all increase dramatically from 28- to 90-day data.

Beam Flexural Tensile Strength, f_r

Equation 5 was used as the functional form for the model and was also calibrated using simple linear regression for three types of concrete using different coarse aggregates and for different curing times. Regression results are presented in Table 2:

$$f_r = -\beta_r p_a \left\{\frac{f_c'}{p_a}\right\}^{\alpha_r} \quad (5)$$

Again, the model, in all cases, exhibits good statistics: α is statistically significant from zero at very high levels (t-values from 5 to 100), and adjusted R^2- and F-values are generally very high. For models calibrated using 28-day data, aggregate type does not affect α-values: none is significantly different from the ACI 0.5 value. At 90 days, however, all values are significantly greater than 0.5. Additionally, as with the split tensile strength models, the 90-day model statistics are stronger. Adjusted R^2-values increase to greater than 0.9, and t- and F-statistics again increase dramatically. There is, however, no apparent effect on the parameter values due to aggregate type. All α-value ranges have substantial overlap, indicating little (if any) effects of aggregate type on modulus of rupture predictions.

Coefficient of Thermal Expansion

Alungbe et al. performed a factor analysis using analysis of variance techniques on the effects of w/c, aggregate type, curing time, and saturation condition on linear thermal expansion. Figure 5 supports their conclusions about influence of aggregate type and saturation condition on thermal expansion. However, the figures also indicate that data are insufficient to make meaningful quantitative conclusions regarding the influence of w/c on the expansion variable. For each aggregate type there are only three data points (corresponding to the three w/c values). Although variation may be measured among three data points, statistical inferences appear dubious. It appears that more experimental work should be done in this regard.

CONCLUSIONS

This paper, using sets of uniaxial compressive and tensile tests performed on plain concrete for three aggregate types, examines the effects of aggregate type on the strength behavior of plain concrete. The results of these tests were used to calibrate a tensile strength prediction model of plain concrete on the basis of uniaxial compressive loading. Model parameters are presented in Tables 1 and 2. The following conclusions can be made from those results:

1. The relationships between splitting tensile strength and compressive strength of medium-strength concrete were shown to be influenced by choice of aggregate.
2. The splitting tensile strength of the DL aggregate concrete material and the moduli of rupture for all three aggregate types at 90 days were found not to be proportional to the 0.5 power of the compressive strength.
3. Tensile strength prediction relations (Equations 4 and 5) different from—and, given the results of this study, more accurate than—the ACI relation were formulated.

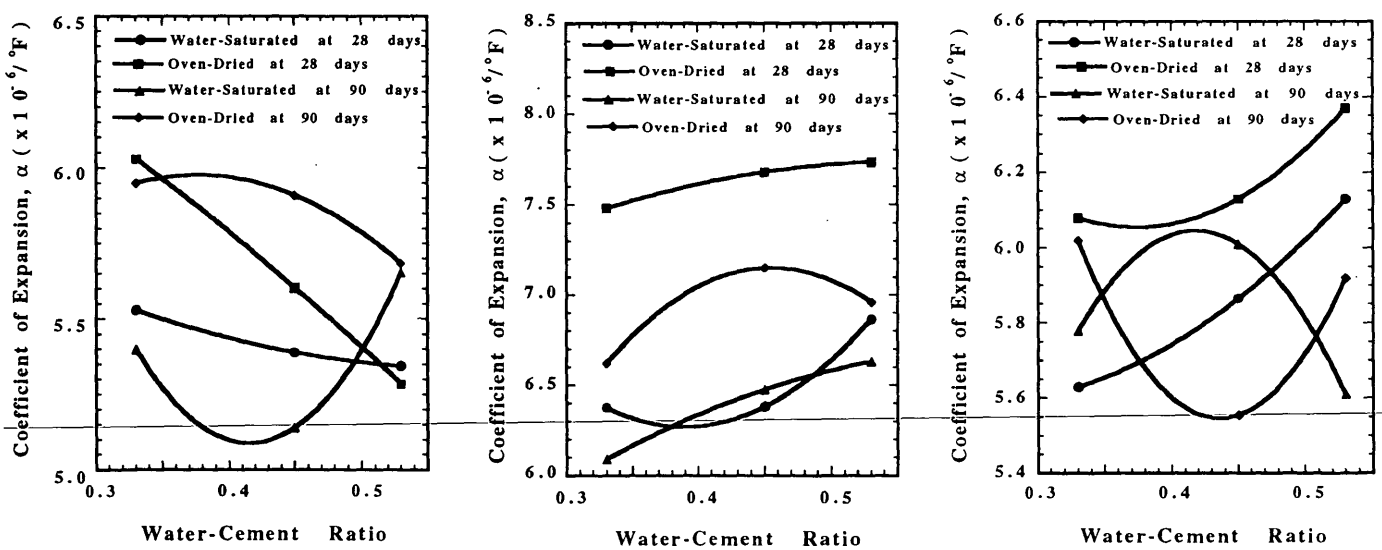

FIGURE 5 Plots of w/c versus coefficient of expansion for PL (*left*), RG (*middle*), and DL (*right*).

ACKNOWLEDGMENTS

The authors appreciate the support of the Department of Civil Engineering at the North Carolina A&T State University. This work was partially supported by a grant from the North Carolina Board of Science and Technology.

REFERENCES

1. S. H. Ahmad and S. P. Shah. Structural Properties of High Strength Concrete and Its Implications for Precast Prestressed Concrete. *PCI Journal*, Vol. 30, No. 6, Nov.–Dec. 1985, pp. 92–119.
2. ACI Committee 363. State-of-the-Art Report on High Strength Concrete. *ACI Journal*, Vol. 81, No. 4, July–Aug. 1984, pp. 364–411.
3. N. J. Gardner and S. M. Poon. Time and Temeprature Effects on Tensile, Bond, and Compressive Strengths. *ACI Journal*, Vol. 73, No. 7, July 1976, pp. 405–409.
4. F. A. Oluokun. *Investigation of Physical Properties of Concrete at Early Ages*. Ph.D. dissertation. University of Tennessee, Knoxville, May 1989, pp. 16–59.
5. P. K. Metha. *Concrete: Structure, Properties, and Materials*. Prentice-Hall, Inc., Englewood Cliffs, N.J., 1986, pp. 36–40.
6. G. D. Alungbe, T. Mang, and D. G. Bloomquist. The Effects of Aggregate, Water-Cement Ratio, and Curing on the Coefficient of Linear Thermal Expansion of Concrete. In *Transportation Research Record 1335*, TRB, National Research Council, Washington, D.C., Jan. 1992.
7. M. R. Salami. Analytical Expressions for Uniaxial Tensile Strength of Concrete in Terms of Uniaxial Compression Strength. In *Transportation Research Record 1335*, TRB, National Research Council, Washington, D.C., Jan. 1992.
8. M. R. Salami. *Constitutive Modelling of Concrete and Rocks Under Multiaxial Compressive Loading*. Ph.D. dissertation. Department of Civil Engineering and Engineering Mechanics, University of Arizona, Tucson, June 1986.
9. M. R. Salami and C. S. Desai. A Constitutive Model for Plain Concrete. *Proc., 2nd International Conference on Constitutive Laws for Engineering Materials: Theory and Application*. Tucson, Ariz., Vol. I, Jan. 1987, pp. 447–455.

APPENDIX A

Notation

The following symbols are used in this paper:

f_t = direct tensile strength
f_c' = uniaxial cylindrical compressive strength
f_{sp}', f_r = beam flexural and split cylinder tensile strengths
α_r, β_r = dimensionless constants for moduli of rupture
α_{sp}, β_{sp} = dimensionless constants splitting tensile strength
$\alpha_{o\text{-}d}$, $\alpha_{w\text{-}s}$ = coefficient of linear expansions (oven-dry) and (water-saturated)
p_a = atmospheric pressure
R^2 = proportion of variation explained by the model
Adj R^2 = R^2 reduced as penalty for adding a variable
t = number of standard deviations the coefficient lies from a value of zero
F = measure of overall explanatory power of the model

Publication of this paper sponsored by Committee on Mechanical Properties of Concrete

Three-Dimensional Constitutive and Failure Modeling of Polymer Concrete Materials

M. REZA SALAMI AND SHILONG ZHAO

A constitutive model based on the theory of plasticity is proposed and used to characterize the stress-deformation behavior of three epoxy concrete materials. It allows for factors such as stress hardening, volume changes, stress paths, temperature, cohesive and tensile strengths, and variation of yield behavior with mean pressure. It is applied to characterize behavior of three epoxy concrete materials. The constants for the model are determined from a series of available laboratory tests. The model is verified with respect to observed laboratory responses. Overall, the proposed model is found to be suitable to characterize the behavior of these three epoxy concrete materials.

Polymer concrete materials have been widely used in the rehabilitation of transportation structures (i.e., bridges and pavement overlays), building structures, and other patching applications. Polymer mortars have been used in construction applications, particularly as structural adhesive for bonding precast units of segmental construction (*1*). It is expected that polymer concrete materials will become more widely used over the next 25 years (*2*,p.413). In transportation engineering, for example, polymer concrete materials have been used in several full-depth bridge deck construction and rehabilitation projects.

Short-term static strengths of polymer mortars are known to be higher than those for portland cement concrete. Severe repeated loading and freeze-thaw exposure are two critical damaging factors for structural materials. The knowledge of degradation resistance of polymer mortars is important for the consideration of the durability of the material.

The literature surveyed regarding polymer concrete, failure criteria, and damage laws leads to some general conclusions (*1*,*2*). First, polymer mortars are in their early stages of development and characterization as a structural material. Second, when a model is developed for a new material, the initial model is simple with minimal parameters. Third, the material constants must be determined in the laboratory to make use of the model.

STRENGTH, FAILURE, AND CONSTITUTIVE MODELS FOR EPOXY POLYMER CONCRETE

Because polymer concrete materials are used in construction, a fundamental failure and constitutive model is needed for predicting material behavior. The present research is undertaken as a first step toward developing a fundamental failure and constitutive model for epoxy polymer concrete, as well as for providing benchmark data on the strength and failure characteristics of material specimens for future work. The failure model will be developed on the basis of a failure function. This model will predict the changes in constitutive properties and resistance values in aggressive environments.

Since previous work has shown that temperature can affect the strength properties (*3*), temperature was selected as the primary testing variable for investigating ultimate compressive and split tensile strength. A model relating strength to temperature and loading rate had been proposed by Kelsey and Biswas (*4*) and was compared with experimental data.

The proposed model for epoxy concrete materials is developed on the basis of previous models conducted by Salami (*5*). These models have been successfully applied to concrete, soil, and rock materials.

Constitutive Model

Theoretical development of the hierarchical model approach and application to soil, rock, and concrete behavior is given by Salami (*5*), Desai and Faruque (*6*), Desai et al. (*7*), and Desai and Salami (*8*,*9*). Application of the model for geological materials, including comprehensive modeling and verifications for various geological materials is discussed by Salami (*5*). The hierarchical concept provides a framework for systematically developing models with progressively complex responses: isotropic associative hardening, isotropic nonassociative hardening, anisotropic hardening, and strain softening. As a result, it can be sufficiently simplified in terms of material constants determined from laboratory tests and applications. A brief description of the model is presented in the following.

A compact and specialized form, F, of the general polynomial representation, by Salami (*5*) and Desai and Faruque (*6*) is adopted herein to describe both the continuous yielding and ultimate yield behavior; it is given by

$$F = \{J_{2D} - F_b F_s\}_T \quad (1)$$

where

J_{2D} = second invariant of deviatoric stress tensor, S_{ij}, of the total stress tensor σ_{ij};

Department of Civil Engineering, North Carolina A&T State University, Greensboro, N.C. 27411.

F_b = basic function; and
F_s = shape function.

The function F is a continuous function in the stress space with the final curve representing the ultimate behavior. In expanded form, Equation 1 is written as

$$F(J_1,J_{2D},J_{3D}) = \left\{J_{2D} - \left(\frac{-\alpha}{\alpha_0^{n-2}}J_1^n + \gamma J_1^2\right)(1 - \beta S_r)^m\right\}_T = 0 \quad (2)$$

where

$J_1 = \sigma_1 + \sigma_2 + \sigma_3$, the first invariant of σ_{ij};
S_r = stress ratio = $(J_{3D})^{1/3}/(J_{2D})^{1/2}$, which can also be the lode angle;
J_{3D} = third invariant of S_{ij};
α, n, γ, β = response functions;
T = temperature;
α_0 = 1 stress unit; and
m = $-\frac{1}{2}$ response function.

As a simplification, γ and m are assumed to be constants, whereas β is expressed as a function of mean pressure, J_1, to account for the observed yield behavior of geological materials (*5,7–9*). This constitutive model is developed to represent a wide range of materials.

From Equation 2, a new constitutive model is proposed to describe both failure and yielding of the polymer concrete materials. The model agrees with the experimental evidence regarding the shapes of yield surfaces on various planes. Moreover, both ultimate failure and yielding are defined by a single yield surface.

For the ultimate criterion given by Equation 2 to apply to concrete, polymer concrete, and rocks, the cohesion and tensile strength sustained by concrete, polymer concrete, and rocks must be included. This is done by translating the principal stress space along the hydrostatic axis by the addition of a constant stress $R = ap_a$ added to the normal stresses. The modified function is given by Salami (*5*) as

$$\{J_{2D}^* - (-\alpha J_1^{*n} + \gamma J_1^{*2})(1 - \beta S_r)^{-1/2}\}_T = 0 \quad (3)$$

where

$$J_1^* = \sigma_{11}^* + \sigma_{22}^* + \sigma_{33}^* \quad (4a)$$

$$J_{2D}^* = \tfrac{1}{6}[(\sigma_{11}^* - \sigma_{22}^*)^2 + (\sigma_{22}^* - \sigma_{33}^*)^2 + (\sigma_{11}^* - \sigma_{33}^*)^2] + \sigma_{12}^{*2} + \sigma_{23}^{*2} + \sigma_{13}^{*2} \quad (4b)$$

$$J_3^* = \tfrac{1}{3}\sigma_{ij}^*\sigma_{mn}^*\sigma_{ni}^* = \tfrac{1}{3}(\sigma_{11}^{*3} + \sigma_{22}^{*3} + \sigma_{33}^{*3}) \quad (4c)$$

$$J_{3D}^* = J_3^* - \tfrac{2}{3}J_1^*J_{2D}^* - \tfrac{1}{27}J_3^{*3} \quad (5)$$

The corresponding normal stresses σ_{11}^*, σ_{22}^*, and σ_{33}^* in Equations 4 and 5 at ultimate (failure) state are expressed as

$$\sigma_{11}^* = \sigma_{11} + R \quad (6a)$$

$$\sigma_{22}^* = \sigma_{22} + R \quad (6b)$$

$$\sigma_{33}^* = \sigma_{33} + R \quad (6c)$$

$$R = ap_a \quad (7)$$

where a is a dimensionless number and p_a is the atmospheric pressure. For cohesionless materials such as sand and gravel, $R = 0$, and the function at ultimate in Equation 3 reduces to that in Equation 2.

Growth Function, α

The response function α is the growth or evolution function. In this study, however, α will be made a function of a single parameter, ξ:

$$\xi = \int(d\varepsilon_{ij}^p\, d\varepsilon_{ij}^p)^{1/2} \quad (8)$$

where ξ is the trajectory of plastic strain in a nine-dimensional Euclidean space formed by the components of the incremental plastic strain tensor. With the definition of ξ, we can now define α in the form

$$\alpha = \frac{\alpha_1}{\xi^{\eta_1}} \quad (9)$$

where α_1 and η_1 are the material constants associated with plastic stress hardening.

Elastic-Plastic Constitutive Relations

The principles of continuity and consistency in Drucker's postulate (*10,11*) enable one to decompose an incremental strain tensor into elastic part and plastic part (assuming small strain) as

$$d\varepsilon_{ij} = d\varepsilon_{ij}^e + d\varepsilon_{ij}^p \quad (10)$$

where the superscripts e and p refer to elastic and plastic, respectively. The stress-elastic strain relationship can be written in the form

$$d\sigma_{ij} = C_{ijkl}\, d\varepsilon_{kl}^e \quad (11)$$

where C_{ijkl} is the elastic constitutive relation tensor and $d\varepsilon_{kl}^e$ is elastic part of the total incremental strain $d\varepsilon_{kl}$. Substituting for $d\varepsilon_{kl}^e$ in this equation gives

$$d\sigma_{ij} = C_{ijkl}(d\varepsilon_{kl} - d\varepsilon_{kl}^p) \quad (12)$$

In general, the yield function may be written as

$$F = F(\sigma_{ij}, d\varepsilon_{ij}^p) \leq 0 \quad (13)$$

with equality during yielding and negative during unloading. With the assumption of the normality principle and associated flow rule, the increment of plastic strain must be normal to the yield surface; hence,

$$d\varepsilon_{ij}^{p} = \lambda \frac{\delta F}{\delta \sigma_{ij}} \tag{14}$$

where λ is the unknown hardening parameter giving the magnitude of the plastic strain increments, with the direction governed by the normality rule. The stress-elastic strain relationship can be written in final form (*5,10,11*) as

$$d\sigma_{ij} = \left\{ C_{ijkl} - \frac{C_{rskl} \dfrac{\delta F}{\delta \sigma_{kl}} \dfrac{\delta F}{\delta \sigma_{ij}} C_{ijkl}}{\dfrac{\delta F}{\delta \sigma_{ij}} C_{ijkl} \dfrac{\delta F}{\delta \sigma_{kl}} - \dfrac{\delta F}{\delta \varepsilon_{ij}^{p}} \dfrac{\delta F}{\delta \sigma_{ij}}} \right\} d\varepsilon_{kl} \tag{15}$$

or

$$d\sigma_{ij} = \{C_{ijkl}^{e} - C_{ijkl}^{p}\}\, d\varepsilon_{kl} \tag{16}$$

This can be rewritten as

$$d\sigma_{ij} = \{C_{ijkl}^{e-p}\}\, d\varepsilon_{kl} \tag{17}$$

where $\{C_{ijkl}^{e-p}\}$ is known as the elasto-plastic constitutive tensor.

DETERMINATION OF MATERIAL CONSTANTS

General

The proposed model has a number of material constants including the Young's modulus (E); Poisson's ratio (ν); shear modulus (G); and bulk modulus (K). Determination of such constants for any material requires a comprehensive series of laboratory tests with number of loading, unloading, and reloading cycles as shown in Figure 1.

Three polymer concrete materials (epoxy types) were considered to obtain the material constants associated with the proposed constitutive model. These are (a) a low-modulus epoxy, (b) a medium-modulus epoxy, and (c) a high-modulus epoxy. Its application to these materials that were tested by Kelsey (*12*) is presented.

Procedures for Determining Material Constants

Ten material constants are associated with the proposed model as described in Equation 3. These constants can be classified into four categories:

1. Elastic constants: E, ν or G, K
2. Constants for hardening yielding: R, n, β_0, β_1, γ
3. Constants for hardening: a_1, η_1
4. Temperature: T

Elastic Constants

There are two elastic constants for an isotropic material: Young's modulus and Poisson's ratio. Figure 1 shows a typical stress-strain response curve. It may be noted that bulk modulus and shear modulus may also be used. It will be assumed that unloading and reloading is elastic. Thus E and ν can be found from the slope of the unloading-reloading curves. The slope of the unloading-reloading of the mean pressure–versus–volumetric strain curve is shown in Figure 2. [Volumetric strain is given by $\varepsilon_v = \varepsilon_1 + \varepsilon_2 + \varepsilon_3$, and mean pressure, by $p = \frac{1}{3}(\sigma_1 + \sigma_2 + \sigma_3)$.] This gives the bulk modulus (K) where K is related to E and ν through the following equation:

$$K = \frac{E}{3(1 - 2\nu)} \tag{18}$$

To obtain E and ν explicitly, a second equation is needed. To determine appropriate values for shear modulus plots of octahedral shear stress versus octahedral shear strain are used. The slope of the unloading-reloading of the τ_{oct}-versus-γ_{oct} curve represents a value equal to twice the shear modulus as

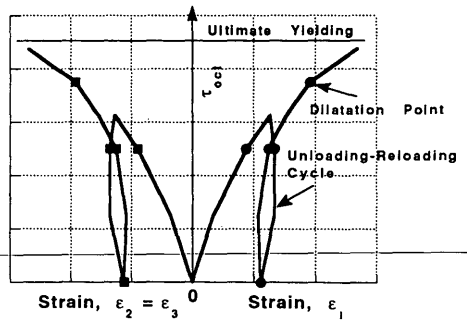

FIGURE 1 Typical stress-strain response curves.

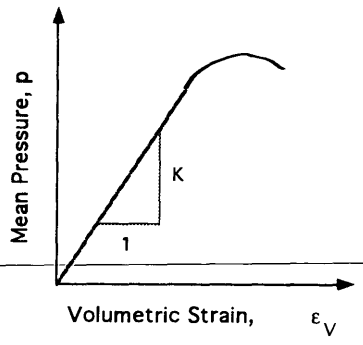

FIGURE 2 Volumetric strain versus mean pressure.

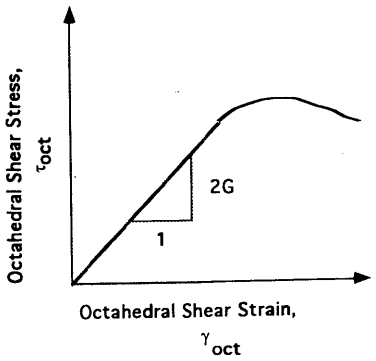

FIGURE 3 Octahedral shear strain versus octahedral shear stress.

shown in Figure 3. [Octahedral shear strain is given by $\gamma_{oct} = {}^1/_3\sqrt{(\varepsilon_1 - \varepsilon_2)^2 + (\varepsilon_2 - \varepsilon_3)^2 + (\varepsilon_3 - \varepsilon_1)^2}$, and octahedral shear stress, by $\tau_{oct} = {}^1/_3\sqrt{(\sigma_1 - \sigma_2)^2 + (\sigma_2 - \sigma_3)^2 + (\sigma_3 - \sigma_1)^2}$]. From these plots a weighted average value of shear modulus (G) was determined. G is related to E and ν through the following equation:

$$G = \frac{E}{2(1 + \nu)} \tag{19}$$

Using Equations 18 and 19, E and ν can be obtained explicitly.

Response Function, n

The value of n can be determined at the state of stress (in the experiment) at which the dilatation occurs—that is, volume change is zero (*5*); n can be determined as:

$$S = \left(1 - \frac{2}{n}\right) \tag{20}$$

where

$$\left[\frac{\left(\frac{\tau_{oct}^2}{J_1^2}\right) \text{ dilation}}{\left(\frac{\tau_{oct}^2}{J_1^2}\right) \text{ ultimate}}\right] = S \tag{21}$$

The n-value obtained from different stress paths (for different initial confining pressures) will, in general, be different. Thus, an average value of n will be calculated. Here, n is assumed to be 7.

Effect of Tensile Strength, R

If the uniaxial tensile strength, f_t, is not determined experimentally, Salami (*5*) gives an approximate formula relating f_t to the unconfined compression strength, f_c', through the following formula:

$$f_t = \left\{p\, p_a \left(\frac{f_c'}{p_a}\right)^q\right\}_T \tag{22}$$

where

p, q = dimensionless numbers,
T = temperature, and
p_a = atmospheric pressure in same units as those of f_t and f_c'.

Values of p and q have been determined, as described by Salami (*5*), for these three epoxy polymer concrete materials for various temperatures, and their values are given in Table 1. Once f_t is known, the value of R can be computed. R was found to be in the following range as

$$1.003\, f_t \le R \le 1.014\, f_t \tag{23}$$

With the estimated value of R, the resulting stresses in Equation 6 are calculated and then substituted into the expression of the stress invariants given in Equations 4 and 5.

Determination of β_0 and β_1

Consider the yield condition at ultimate failure at which $\alpha \rightarrow 0$. Then Equation 2 reduces to

$$J_{2D} - (\gamma J_1^2)(1 - \beta S_r)^{-1/2} = 0 \tag{24}$$

β is derived from Equation 24 by Salami (*5*) as:

$$\beta = \left[\frac{(J_{2D}^2)_{TC} - (J_{2D}^2)_{TE}}{(Sr\, J_{2D}^2)_{TC} - (Sr\, J_{2D}^2)_{TE}}\right] \tag{25}$$

It is evident from Equation 25 that β can be determined for a pair of tests (TC and TE) or (CTC and RTE) if the stresses at ultimate failure are known. Also from the following equation

$$\beta = \beta_0\, e^{-\beta_1 J_1} \tag{26}$$

taking natural log on both sides of Equation 26, one obtains

$$\ln(-\beta) = \ln(-\beta_0) - \beta_1 J_1 \tag{27}$$

Equation 27 represents a straight line when plotted in $\ln(-\beta) - J_1$ space as shown in Figure 4. Then β_0 and β_1 are obtained from the intersection and slope of the straight line, respectively.

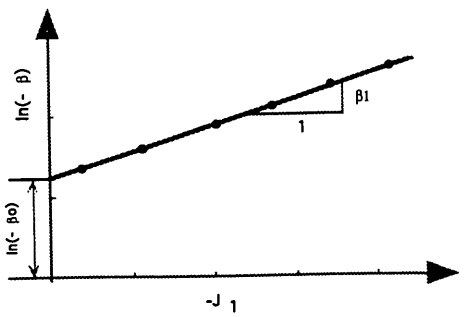

FIGURE 4 Schematic plot to determine material constants β_0 and β_1.

Determination of γ

The value of γ can be determined (*5*) as

$$\gamma = \frac{[J_{2D}\,(1 - \beta S_r)^{1/2}]}{J_1^2} \tag{28}$$

Since β is known, γ can be determined for any test if the stresses at ultimate failure are known; γ also can be found graphically from Equation 28 as shown in Figure 5.

Determination of a_1 and η_1

The growth function, Equation 9, after taking natural log of both sides can be written as

$$\eta_1 \ln(\xi) + \ln(\alpha) = \ln(a_1) \tag{29}$$

Equation 29 can now be used to determine η_1 and a_1. A typical plot is shown in Figure 6.

Material Constants for Three Epoxy Polymer Concrete Materials

Kelsey describes the epoxy polymer concrete materials and presents the test results (*12*). Figures 7 through 9 show stress-strain responses of three epoxy polymer concrete materials for various temperatures. These tests are used to obtain the material constants associated with the proposed model for three epoxy polymer concrete materials.

Values of p and q also were determined for these materials at various temperatures and are given in Table 1. The material constants for these three epoxy polymer concrete materials were obtained by previous procedures.

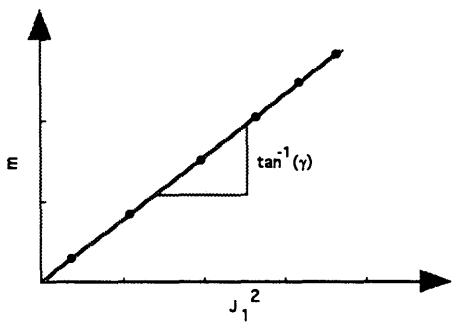

FIGURE 5 Schematic plot to determine material constant γ.

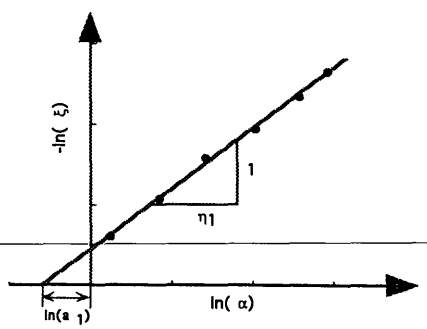

FIGURE 6 Schematic plot to determine material constants a_1 and η_1.

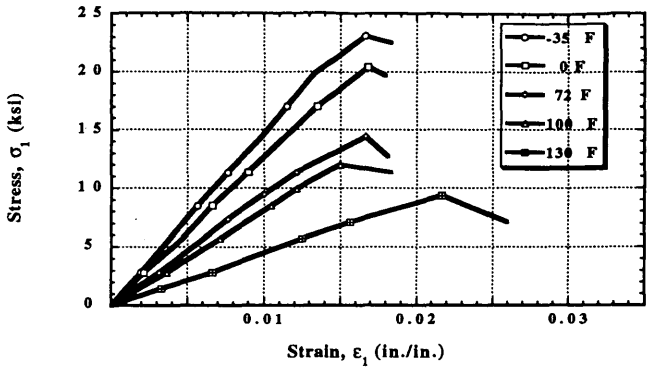

FIGURE 7 Plot of stress versus strain at different temperatures for high-modulus material (AEX1539).

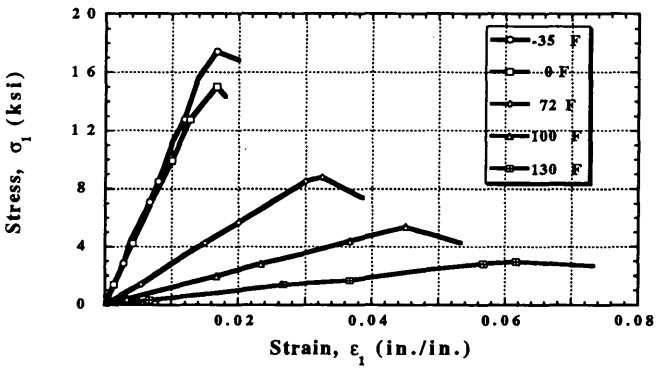

FIGURE 8 Plot of stress versus strain at different temperatures for medium-modulus material (AEX3070).

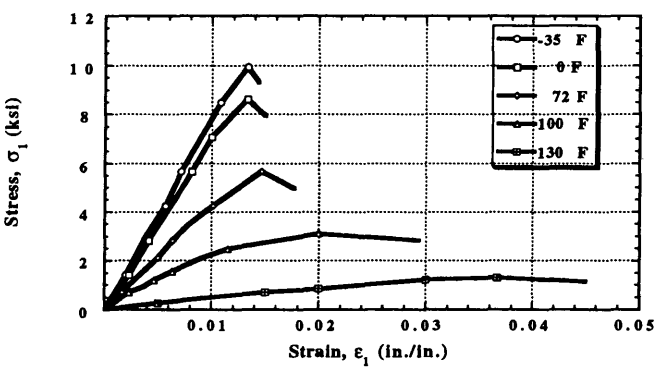

FIGURE 9 Plot of stress versus strain at different temperatures for low-modulus material (FLEXOLITH).

TABLE 1 Values of Parameters p and q from Developed Model for Various Temperatures for Three Epoxy Polymer Concrete Materials.

Temperature (°F)	p	q
0	1.6520	0.6509
32	1.5157	0.6720
72	1.5849	0.6745
100	1.4757	0.6813
130	1.9293	0.6593
160	0.3532	0.9400

CONCLUSIONS

A general yet simplified failure and constitutive model is proposed and used to model the behavior of polymer concrete materials as affected by complex factors such as state of stress, stress path, temperature, and volume change. The model allows for continuously yielding and stress hardening, ultimate (failure) yield, and cohesive and tensile strength components. The test results are used to derive material constants. The model is verified with respect to laboratory test data used for finding the constants. The model is found to provide satisfactory predictions for the observed behavior of the epoxy polymer concrete materials. It is also found to provide similar predictions for other concrete and rocks such as westerly granite, Durham dolomite, and sandstone (*5*). The proposed model provides a simple alternative approach for developing constitutive models for epoxy polymer concrete materials.

For the purpose of including reasonable values of tensile strengths in the failure criterion and constitutive model (for frictional materials with effective cohesion), it may be necessary to include the uniaxial tensile strength in the parameter determination. Simple expressions for evaluating the uniaxial tensile strengths for various temperatures on the basis of the uniaxial compressive strength are given. Some sets of uniaxial compressive and tensile tests for various temperatures were performed by Kelsey on three epoxy polymer concrete materials (*12*). The purpose of these tests was to acquire some understanding of the strength behavior of epoxy polymer concrete subjected to compressive and tensile load histories with various temperatures, and the results of these tests were used to calibrate the proposed tensile strength model for predicting the tensile strength of these epoxy polymer concrete materials based on the experimental uniaxial compressive loading.

The proposed tensile strength model has two material constants. Laboratory tests were used to determine these two material constants.

REFERENCES

1. M. Biswas. Precast Bridge Deck Design Systems. *ACI Journal*, Vol. 31, No. 40, 1986.
2. W. O. Nutt and B. Staynes. The Next Twenty-Five Years. *Proc., 5th International Congress of Polymers in Concrete*, Brighton, England, 1987.
3. M. Biswas, O. Ghattas, and H. Vladmirou. Fatigue and Freeze-Thaw Resistance of Epoxy Mortar. In *Transportation Research Record 1041*, TRB, National Research Council, Washington, D.C., 1985.
4. R. G. Kelsey and M. Biswas. Static and Repeated Load Tests of Polymer Mortar Materials. In *Transportation Research Record 1113*, TRB, National Research Council, Washington, D.C., 1988.
5. M. R. Salami. *Constitutive Modelling of Concrete and Rocks Under Multiaxial Compressive Loading*. Doctoral dissertation. Department of Civil Engineering and Engineering Mechanics, University of Arizona, Tucson, 1986.
6. C. S. Desai and M. O. Faruque. A Constitutive Model for Geological Materials. *Journal of the Engineering Mechanics Division*, ASCE, Vol. 110, No. 9, Sept. 1984, pp. 1391–1408.
7. C. S. Desai, G. N. Frantziskonis, and S. Somasundram. Constitutive Modelling for Geological Materials. *Proc., 5th International Conference on Numerical Methods in Geomechanics*, Nagoyo, Japan, April 1985.
8. C. S. Desai and M. R. Salami. Constitutive Model Including Testing for Soft Rock. *International Journal of Rock Mechanics and Mineral Science*, Vol. 24, No. 5, Oct. 1987, pp. 299–307.
9. C. S. Desai and M. R. Salami. A Constitutive Model for Rocks. *International Journal of the Geotechnical Engineering Division*, ASCE, Vol. 113, No. 5, May 1987, pp. 407–423.
10. D. C. Drucker. A More Fundamental Approach to Plastic Stress-Strain Relations. *Proc., 1st U.S. National Congress on Applied Mechanics*, Chicago, Ill., 1951, pp. 487–491.
11. D. C. Drucker and W. Prager. Soil Mechanics and Plastic Analysis of Limit Design. *Quarterly of Applied Mathematics*, Vol. 10, No. 2, 1952.
12. R. G. Kelsey. *Failure Theory for Epoxy Mortar Materials*. Doctoral dissertation. Department of Civil and Environmental Engineering, Duke University, Durham, N.C., 1988.

Publication of this paper sponsored by Committee on Mechanical Properties of Concrete.

Studies on Slurry-Infiltrated Fibrous Concrete (SIFCON)

V. S. PARAMESWARAN, T. S. KRISHNAMOORTHY, K. BALASUBRAMANIAN, AND SANTHI GANGADAR

Slurry-infiltrated fibrous concrete (SIFCON) can be considered as a special type of fiber concrete with high fiber content. The matrix usually consists of cement slurry or flowing mortar. SIFCON has excellent potential for application in areas where high ductility and resistance to impact are needed. Only very limited information is available about its behavior under different types of loading. Tests on 20-mm-thick SIFCON specimens were carried out in the Structural Engineering Research Center (SERC), Madras, India, to study their behavior in flexure and under subjection to abrasion and impact loads. Toughness characteristics of SIFCON were also evaluated by testing another set of specimens 100 × 100 × 500 mm per ASTM C1018. Both strength and deformation characteristics of the specimens were studied. The results obtained from these tests were compared with those carried out on companion plain mortar and conventional fiber-reinforced mortar (FRM) specimens. The investigations confirm the superior characteristics of SIFCON as compared with plain and normal FRM. Major conclusions drawn from the investigations are presented.

Slurry-infiltrated fibrous concrete or mortar (SIFCON) is a relatively new material that can be considered as a special type of fiber-reinforced concrete (FRC). In two aspects, however—namely, fiber content and the method of production—SIFCON is different from normal FRC. The fiber content of FRC generally varies from 1 to 3 percent by volume, but the fiber content of SIFCON varies between 5 and 20 percent. Again, the matrix of SIFCON consists of cement paste or flowing cement mortar as opposed to regular concrete used in FRC. These make the production of SIFCON far different from FRC. Unlike FRC, for which the fibers are added to the wet or dry concrete mix, SIFCON is prepared by infiltrating cement slurry into a bed of fibers preplaced and packed tightly in the molds.

SIFCON has been used successfully for refractory applications (*1*), pavement overlays (*2*), and structures subjected to blast (*3*) and dynamic loading. Because of its highly ductile behavior and far superior impact resistance, the composite has excellent potential for structural applications in which accidental or abnormal loads such as blasts are encountered during service. However, the composite was developed only recently, and only limited data are available on its behavior under different types of loading (*4,5*). Therefore, investigations were undertaken at the Structural Engineering Research Center, Madras, India, to study the relative behavior of SIFCON when subjected to flexure, abrasion, and impact loads. The toughness characteristics of the materials were also investigated. The results of the investigations carried out on a large number of test specimens cast using plain mortar, fiber-reinforced mortar (FRM), and SIFCON are presented.

Structural Engineering Research Center, CSIR Campus, Taramani, Madras-600 113, India.

DETAILS OF TEST SPECIMENS

Materials Used

The materials used in casting the test specimens consisted of portland cement, fine river sand, straight steel fibers, and a high-range water-reducing admixture called CONPLAST-430 (*6*). The cement conformed to Bureau of Indian Standards (IS) 269-1976. The sand was sieved through a 1.18-mm sieve to segregate the coarser particles. Straight round steel fibers of 0.4-mm diameter and a tensile strength of 1000 MPa were used.

Mix Proportions and Casting of Test Specimens

Flexure, Abrasion, and Impact Tests

Details of mix proportions used for making the test specimens intended for flexure, abrasion, and impact tests are given in Table 1. The SIFCON test specimens were cut from previously cast SIFCON slabs of 400 × 400 × 20 mm. The slabs themselves were cast using a wooden mold. A hand-operated steel roller was employed to compact the fibers inside the mold. Cement mortar slurry obtained from an electrically operated mortar mixing machine was poured uniformly over the preplaced fibers in the mold. The slurry consisted of cement and fine sand (passing through a 1.18-mm sieve) mixed in the proportion of 1:1 by weight. Compaction by table vibrator was used to ensure complete penetration of the slurry into the fiber pack. Twenty-four hours after casting, the slabs were demolded and cured in water for 28 days.

FRM and plain mortar test specimens were also prepared in a similar manner from the respective slabs of 400 × 400 × 20 mm.

The dimensions of the test specimens cut from the slabs (with the help of a concrete cutting machine) and used for flexure, abrasion, and impact tests were 400 × 100 × 20 mm, 70 × 70 × 20 mm, and 180 × 180 × 20 mm, respectively. Plain mortar cube specimens 70 × 70 × 70 mm were also cast to ascertain the compressive strength of the mortar used.

TABLE 1 Details of Mix Proportions and Dimensions of Test Specimens Used for Flexure, Impact, and Abrasion Tests

Specimen identification	Category of specimens	Cube compressive strength of slurry (MPa)	Fibre by volume (%)	Aspect ratio	Water-cement ratio	Superplasticiser by weight of cement (%)
P	Plain mortar	54.8	-	-	0.30	0.5
F1	FRM	56.0	1	75	0.35	0.5
F2	FRM	56.0	2	75	0.30	1.0
F3	FRM	80.0	3	75	0.32	2.0
F4	FRM	80.0	4	75	0.32	2.0
S1	SIFCON	60.0	6	75	0.38	2.0
S2	SIFCON	62.0	8	75	0.38	1.0
S3	SIFCON	58.5	6	100	0.35	2.0
S4	SIFCON	58.0	8	100	0.32	2.0

(dash) Not Applicable

The two parameters varied in these tests were fiber volume and aspect ratio. Whereas fiber volumes were varied from 1 to 4 percent in casting the FRM specimens, two volume percentages—6 and 8 percent—were used in making the SIFCON specimens. Aspect ratios 75 and 100 were used for SIFCON specimens, and a constant aspect ratio of 75 was maintained for FRM specimens.

Toughness Tests

Table 2 gives the details of the four mix proportions used for casting the SIFCON test specimens. The specimens were flexural prisms 100 × 100 × 500 mm. The prisms were cast using standard steel molds.

Three techniques were used for incorporating the steel fibers in the matrix. In the first case, the fibers were prepacked in the molds and the slurry was allowed to infiltrate the pack, assisted by proper compaction by means of a table vibrator (single-layer technique, designated as SL series). The second technique involved initial placing and packing of the fibers in the mold only up to one-third depth, followed by infiltration of the slurry up to this level. The contents in the mold were then vibrated. The process was repeated until the entire mold was filled and compacted (three-layer technique, designated as TL series). The third technique consisted of filling the mold up to one-third depth by the slurry, implanting the fibers into it immediately thereafter, vibrating the contents, and repeating the process until the mold was full (immersion technique, designated as I series).

The specimens were demolded 24 hr after casting and cured in water for 28 days.

For all the test specimens, the fiber volume and the aspect ratio were kept constant at 8 and 75 percent, respectively. The slurry used for infiltration consisted of portland cement and sand (passing through 1.18-mm sieve) mixed in the proportion of either 1:1 or 1:1.5 by weight (Table 2). Fly ash equal to 20 percent by weight of cement was used in some of the mixes to study its influence on the workability of the mix. The water-cement ratio was kept constant at 0.375, and the percentage by weight of CONPLAST-430 was varied from 1 to 5 percent.

Cylinders 50 mm in diameter and 75 mm high were also made out of SIFCON mixes using the same casting technique as adopted for the test specimens to ascertain the compressive strength of SIFCON. Plain mortar cubes 70 × 70 × 70 mm were also cast in each series to ascertain the cube compressive strength of the mortar used.

TEST PROGRAM

Flexure Test

Static flexure tests were carried out on SIFCON, FRM, and plain mortar test specimens using a universal testing machine with a capacity of 400 kN. The specimens were simply supported over an effective span of 360 mm and tested under constant bending moment over the middle-third portion. The specimens were subjected to a monotonically increasing load until failure. A dial gauge was used to measure the deflections at the midspan section.

Abrasion Test

As explained earlier, the abrasion test was carried out on 70- × 70- × 20-mm test specimens in accordance with IS 1237-1980 and using a standard abrasion testing machine. The specimens were first oven-dried at 100°C for 24 hr and then weighed to an accuracy of 0.001 N (0.1 g). Each specimen was then clamped on top of the disk in the machine and was loaded at its center by a weight of 300 N. Aluminum powder was used as the abrasive agent. After completing 22 revolutions, the rotation of the disk was stopped. The dust resulting from the abrasion of the specimen and the spillover of the aluminum powder was removed. Fresh powder in quantities of 0.2 N (20 g) was then added. After 110 revolutions, the

TABLE 2 Details of Mix Proportions Used for Casting SIFCON Specimens for Evaluation of Toughness Index

Designation of series and number	Mix proportion cement: sand (by weight)	Flyash content by weight of cement (%)	Super-plasticiser by weight of cement (%)	Average strength of SIFCON cubes* (MPa)	Average strength of SIFCON cylinders (MPa)	Average strength of plain mortar cubes (MPa)
**SL-A	***1:1	-	2	112.2	71.6	41.3
SL-B	1:1.5	-	3	22.0	-	39.8
SL-C	1:1	20	4	97.9	70.3	36.0
SL-D	1:1.5	20	5	25.7	-	34.1
TL-A	1:1	-	2	122.6	78.0	40.0
TL-B	1:1.5	-	3	74.4	-	36.0
TL-C	1:1	20	3	99.3	66.5	38.0
TL-D	1:1.5	20	5	119.5	-	26.5
I-A	1:1	-	1	80.8	88.4	42.6
I-B	1:1.5	-	2.5	96.2	89.0	34.4
I-C	1:1	20	3	93.3	97.6	43.4
I-D	1:1.5	20	5	129.3	107.0	26.5
P-A	1:1	-	1	65.0	29.1	35.8
P-B	1:1.5	-	3	63.7	29.0	37.0
P-C	1:1	20	3	59.2	26.6	29.2
P-D	1:1.5	20	5	37.7	25.6	30.0

Notes: * Cubes cut from tested flexural beams

** Each series consisted of three specimens. Values shown here are the average of results obtained for these three numbers.

*** For all the series, the water-cement ratio was kept constant at 0.375 and the percentage volume of steel fibres was kept constant at 8%. The aspect ratio of the fibres was kept as 75 in all cases.

(dash) Not Applicable/Unavailable

specimen was turned about its vertical axis through an angle of 90 degrees, and the test was continued until 220 revolutions were completed. The surface was cleaned, and the specimen was weighed. The test was continued in the same manner until 1,100 revolutions were completed. The loss due to abrasion (abrasion index) was calculated as the difference between the initial weight of the specimen and its weight after a fixed number of revolutions with respect to its initial weight (in this case, 220, 660, and 1,100 revolutions).

Impact Test

The impact test was carried out using the test rig shown in Figure 1. The specimen was placed in the bottom tub and clamped. The weight of drop was 50 N, and the drop height alone was varied from 250 to 1000 mm. Metallic pellets pasted at the bottom surface of the specimen in two mutually perpendicular directions helped to measure the residual strains using a Pfender strain measuring gauge, after the specimen had undergone a prescribed number of drops. For FRM specimens, the test was conducted by dropping the weight from a height of 250, 500, and 750 mm. One specimen was tested in each series. The drop height for SIFCON specimens was kept at 500, 750, and 1000 mm. The dropping of the weight was continued until the failure of the specimen, indicated by excessive cracking at its bottom surface or the formation of an indentation 20 mm in diameter (equal to the diameter of striker) on its top surface. The number of drops it took to cause one of these types of damage was recorded in each test.

Test for Toughness Index

Tests for evaluating the toughness index were conducted on SIFCON flexural specimens only. The toughness index was calculated using the methods prescribed in ASTM C1018 and Japan Concrete Institute (JCI) SF4.

The ASTM procedure involves determining the amount of energy required to deflect the beam to a specified multiple of the first-crack deflection, with the multiple based on functional (e.g., serviceability) considerations. The toughness indexes I_5, I_{10}, and I_{30} are calculated as ratios of the area of the

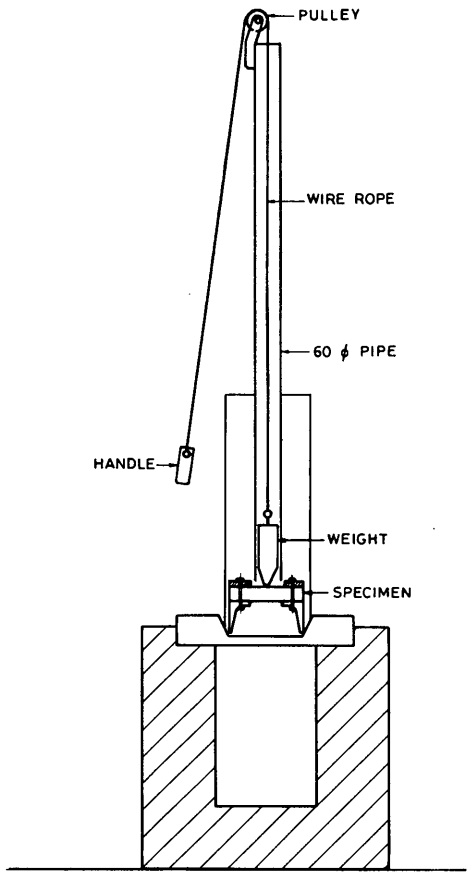

FIGURE 1 Impact test setup.

load-deflection curve measured up to deflections of 3, 5.5, and 15.5 times the first-crack deflection, divided by the area of the load-deflection curve up to the first-crack deflection (first-crack toughness), respectively.

In the JCI method, toughness is defined in absolute terms as the energy required to deflect a beam to a midpoint deflection of $\frac{1}{150}$ of its span.

The tests were carried out using a universal testing machine with a capacity of 400 kN. A two-point loading system was used in which the specimen was simply supported over an effective span of 300 mm. The point loads were applied 100 mm from each support. A dial gauge having a least count of 0.01 mm and mounted on a specially fabricated steel frame was used for accurate measurement of deflection.

The testing machine was operated in such a manner that the deflection of the specimen at midspan increased at a rate of 0.05 to 0.10 mm/min as specified in IS 269-1976. Deflection measurements were recorded at various stages of loading until failure of the specimen. The cylinder compressive strengths of SIFCON mixes and the cube strengths of plain mortars were obtained by carrying out tests on the respective specimens using the universal testing machine.

Cubes 100 × 100 × 100 mm were also cut from the tested flexural test specimens with the help of a concrete cutting machine; they were subsequently tested for ascertaining the compressive strength of SIFCON mixes.

ANALYSIS OF TEST RESULTS

Flexure Test

The results of the flexural tests are given in Table 3. The load-deflection behavior for the FRM and SIFCON specimens is illustrated in Figures 2 and 3, respectively (*7*).

In Table 3, the hypothetical ultimate flexural strength computed by assuming an uncracked section is tabulated for different test specimens. This strength is taken as an index for comparing the relative performance of the specimens under flexural loading (*8*). It may be seen from Table 3 that SIFCON specimens reinforced with fibers having an aspect ratio of 75 behaved better than those having an aspect ratio of 100. This is true for both the fiber volume percentages (6 and 8 percent). It is also seen that in FRM specimens, there is an increase in the hypothetical flexural strength with the increase in fiber content up to 3 percent. Beyond this, the flexural strength remains almost the same. However, for SIFCON specimens, the improvement in flexural strength is phenomenal as compared with FRM specimens. The improvement is also more

TABLE 3 Results of Flexure Tests

Specimen identification (aspect ratio given in bracket)	Cube compressive strength of the slurry (MPa)	Thickness (mm)	Failure load (kN)	Hypothetical ultimate flexural strength (MPa)**
P	54.8	22	0.9	6.7
F1(75)	56.0	21	1.4	11.4
F2(75)	56.0	21	2.3	18.5
F3(75)	80.0	21	2.4	19.5
F4(75)	80.0	21	2.4	19.5
S1(75)	60.0	20	3.6	32.4
S2(75)	62.0	23	6.0	40.8
S3(100)	58.5	25	5.0	28.8
S4(100)	58.0	25	6.4	36.8

** assuming an uncracked section

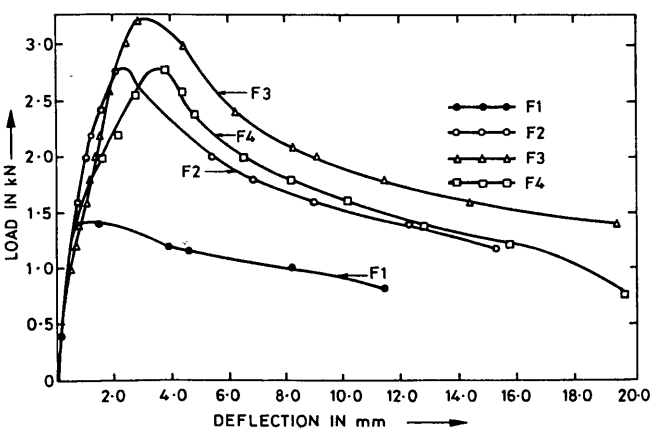

FIGURE 2 Load-deflection curve for Specimens F1, F2, F3, and F4.

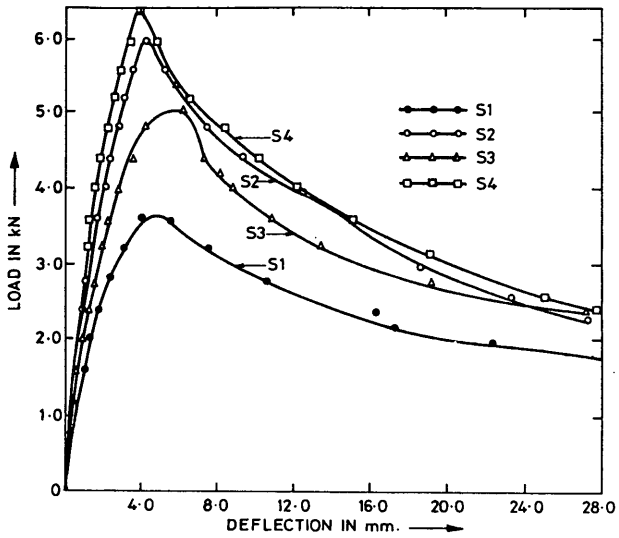

FIGURE 3 Load-deflection curve for Specimens S1, S2, S3, and S4.

with a higher percentage of fiber content. An increase in flexural strength of about 500 percent is shown by SIFCON specimens with 8 percent fiber volume over companion plain mortar specimens. The increase is about 100 percent over normal FRM specimens. From Figures 2 and 3, it is seen that SIFCON specimens exhibit greater ductility, fewer cracks, and less spalling of concrete during the tests than FRM specimens.

It may also be of interest that the ultimate flexural strengths obtained from the current tests are in the range of 35 to 41 MPa, as reported by earlier investigators (*1*).

Abrasion Test

The results obtained from the abrasion tests are given in Table 4. It is clear that SIFCON specimens containing 8 percent fiber content exhibit greater abrasion resistance than other types of specimens. The degree of abrasion, even though high in the initial stages of revolution of the disk (because the outer mortar surface of the specimens wore out faster) is still much lower than plain and FRM specimens.

TABLE 4 Results of Abrasion Tests

Specimen identification	Abrasion index percentage after number of revolutions *		
	220**	660**	1100**
P	10.2	39.0	66.0
F1	9.3	25.3	40.5
F2	8.36	20.6	31.83
F3	6.73	16.25	29.00
F4	6.16	14.00	26.00
S1	4.63	13.10	20.96
S2	4.11	12.26	18.60

*Abrasion index = (weight loss/initial weight of specimen) X 100

**Average of three specimens

Impact Test

The results of the impact tests are given in Table 5. The plain mortar specimen failed even after a single dropping of the weight from a height of 250 mm. Adding fibers to plain mortar greatly improves its impact resistance. More the fiber content, the resistance to impact is higher even for FRM specimens. The results also clearly establish the superiority of SIFCON specimens under impact load over FRM specimens. Here again, the resistance is more pronounced with increasing fiber content. An interesting feature is that SIFCON specimens reinforced with fibers having an aspect ratio of 100 exhibit greater impact resistance than those reinforced with fibers having an aspect ratio of 75. In the flexural tests, however, a reverse phenomenon was noticed, if one goes by the comparison of the respective values of the hypothetical ultimate flexural strength.

The extent of damage in SIFCON specimens during tests was also less than that of FRM specimens.

Test for Toughness Index

The values of the toughness indexes I_5, I_{10}, and I_{30} and the toughness energy of the SIFCON specimens cast using the three techniques described earlier are given in Table 6. The toughness index for plain concrete being equal to unity, because all plain mortar beams failed immediately after first crack, the superior toughness characteristics exhibited by SIFCON are quite evident from the values given in the table. The SL-C, TL-C, and I-D beams gave a higher toughness index, indicating thereby that mixes with a 20 percent fly ash content improve the toughness characteristics. It is also observed that the toughness index is not much dependent on

TABLE 5 Results of Impact Tests

Specimen identification	No. of drops the specimen withstood before failure			
Weight of drop (N)	50	50	50	50
Height of drop (mm)	250	500	750	1000
Impact energy (N mm X 10^3)	12.5	25.0	37.5	50.0
P	1	-	-	-
F1	120	20	10	-
F2	314	33	18	-
F3	600	43	23	-
F4	1000	72	40	-
S1	-	240	43	10
S2	-	625	112	33
S3	-	300	47	20
S4	-	750	130	100

(dash) Unavailable

TABLE 6 Results of Tests for Toughness Index of SIFCON Specimens

Specimen identification*	I_5	I_{10}	I_{30}	I_{10}/I_5	I_{30}/I_{10}	Toughness energy by JCI Method (N mm)
SL-A	6.37	16.25	51.52	2.55	3.17	163540
SL-B	6.43	14.8	45.68	2.3	3.09	100300
SL-C	6.35	16.3	52.99	2.57	3.25	164150
SL-D	6.28	15.13	48.17	2.41	3.18	91250
TL-A	6.9	17.53	60.7	2.54	3.46	168090
TL-B	6.65	16.22	53.32	2.44	3.29	166730
TL-C	6.35	17.52	66.67	2.76	3.81	229600
TL-D	6.98	17.83	66.36	2.55	3.72	180340
I-A	5.89	14.19	46.53	2.41	3.28	134670
I-B	6.55	16.08	54.09	2.45	3.36	177050
I-C	5.86	14.32	47.16	2.44	3.29	144580
I-D	6.78	17.4	65.92	2.57	3.78	227820

*Values shown are the average of results obtained from three specimens

Note: For plain mortar prisms (P-A to P-D), the index is unity.

the method of placing the fibers in the form. From the results obtained by earlier investigators (ASTM C1018; *9*), it is concluded that the toughness index of SIFCON is far greater than FRC or FRM. The average I_{30} index for SIFCON observed from the current tests is about 55, while the range observed for FRC and reported in IS 1237-1980 and JCI SF4 is only 6 to 40.

CONCLUSIONS

The following conclusions are drawn from the investigations presented here:

1. SIFCON specimens with 8 percent fiber content showed a fivefold increase in (hypothetical) ultimate flexural strength over companion plain mortar specimens and a twofold increase over normal FRM specimens with 2 to 4 percent fiber content. Fibers with an aspect ratio of 75 were found to contribute more to the hypothetical ultimate flexural strength of SIFCON than those with an aspect ratio of 100. Higher fiber percentages also gave higher ultimate flexural strength for the same aspect ratio.
2. SIFCON specimens exhibited greater ductility and greater resistance to cracking and spalling of concrete than normal FRM specimens.
3. Whereas the abrasion resistance generally improved to a great extent with the addition of fibers, even for FRM specimens, the improvement was phenomenal for SIFCON. This result suggests that SIFCON is ideally suited for applications demanding a high degree of wear and abrasion resistance.
4. The extent of damage in SIFCON due to impact load was found to be far less when compared to plain mortar and normal FRM, confirming thereby the superior impact resistance of SIFCON.
5. The toughness indexes for SIFCON specimens were found to be significantly higher than plain mortar specimens. The values of I_{30} as well as the ratios I_{10}/I_5 and I_{30}/I_{10} given in Table 6 indicate that the behavior of SIFCON is akin to an ideal elasto-plastic material. The range for I_{30} values was observed to be 45 to 60, which is far greater than the range observed for FRC by earlier investigators, namely, 6 to 40.
6. The three techniques used for incorporating fibers in the mortar slurry proved effective during the casting of the SIFCON specimens, but there was not much difference in the toughness indexes obtained from tests on identical SIFCON specimens that were cast differently using any of the three techniques. However, the three-layer and immersion techniques were found to be easier and simpler in actual practice than the single-layer technique.
7. A fiber content of 8 percent was found to be suitable for making SIFCON specimens using the mix proportions reported in the paper from the point of view of workability and strength (flexure, impact, abrasion, and toughness).

ACKNOWLEDGMENTS

The authors wish to express their appreciation for the assistance and cooperation rendered by the technical staff of the Concrete Composites Laboratory, SERC, Madras, India. This paper is being published with the kind permission of the director, SERC, Madras.

REFERENCES

1. D. R. Lankard and D. H. Lease. Highly Reinforced Precast Monolithic Refractories. *American Ceramic Society Bulletin*, Vol. 61, No. 7, July 1982, pp. 728–732.
2. V. S. Parameswaran, T. S. Krishnamoorthy, and K. Balasubramanian. Development of High Fiber Volume Composite Overlay

for Heavy Traffic Loads. Presented at the National Seminar on Airfield Pavements, Feb. 1990, New Delhi, India.
3. D. R. Lankard. Slurry Infiltrated Fibre Concrete (SIFCON). *Concrete International*, Dec. 1984, pp. 44–47.
4. D. R. Lankard and J. K. Newell. Preparation of High Reinforced Steel Fibre Reinforced Concrete Composites. *ACI SP-81: Fiber-Reinforced Concrete—International Symposium*, American Concrete Institute, Detroit, Mich., 1984, pp. 287–306.
5. P. Balaguru. Behaviour of Slurry Infiltrated Fibre Concrete (SIFCON). *Proc., International Symposium on Fibre Reinforced Concrete*, Dec. 1987, Madras, India, pp. 7.25–7.36.
6. *Product Summary Guide: Fosroc Construction Chemicals*. Fosroc Chemicals Limited, Bangalore, India, 1991.
7. V. S. Parameswaran, T. S. Krishnamoorthy, and K. Balasubramanian. Behaviour of High Volume Fibre Cement Mortar in Flexure. *Cement and Concrete Composites*, Vol. 12, 1990, pp. 293–301.
8. P. Balaguru and J. Kendzulak. Mechanical Properties of Slurry Infiltrated Fibre Concrete (SIFCON). *ACI SP-105: Fiber Reinforced Concrete Properties and Applications*, American Concrete Institute, Detroit, Mich., 1987, pp. 247–268.
9. V. Ramakrishnan, G. Y. Wu, and G. Hosalli. Flexural Behavior and Toughness of Fiber Reinforced Concretes. In *Transportation Research Record 1226*, TRB, National Research Council, Washington, D.C., 1989, pp. 69–77.

Publication of this paper sponsored by Committee on Mechanical Properties of Concrete

Plastic Shrinkage Cracking of Polypropylene Fiber–Reinforced Concrete Slabs

PARVIZ SOROUSHIAN, FAIZ MIRZA, AND ABDULRAHMAN ALHOZAIMY

The effects of polypropylene fibers and construction operations on the plastic shrinkage cracking of concrete slabs were investigated. Statistical methods of experimental design and analysis were used to derive statistically reliable conclusions. Polypropylene fibers, at relatively low fiber volume fractions, were observed to reduce substantially the total area and maximum crack width of slab surfaces subjected to restrained plastic shrinkage movements. The rate of screeding of the fresh concrete surface was also a critical factor (particularly in plain concrete). Slower screeding rates led to reduced plastic shrinkage cracking.

When concrete surfaces dry at early ages, plastic shrinkage cracks form before the concrete hardens. The surface dries when the rate of water loss from the surface exceeds the rate at which the bleed water is made available to the surface. Polypropylene fibers have become popular in recent years for the reinforcement of concrete materials, mainly because of their effectiveness in reducing cracking at early ages under the effects of restrained plastic shrinkage.

Reducing the rate of evaporation is the conventional approach to the control of plastic shrinkage cracks during the construction of concrete slabs in dry conditions. It is likely, however, that under given evaporation conditions, the extent and severity of plastic shrinkage cracking may be increased by certain construction practices, particularly those relating to the finishing operations (screeding rate and direction, bull-floating, floating, and troweling).

The thrust of this investigation was to produce a comprehensive set of experimental data, on the basis of the practice of concrete slab construction, in order to derive statistically reliable conclusions about the effects of low-volume fractions of collated fibrillated polypropylene fibers on the plastic shrinkage cracking of concrete slabs finished by different construction methods. The work was motivated by the limited test data reported on the plastic shrinkage cracking of concrete materials. The available test data generally deal with fine-aggregate mortars that, because of size effects, may behave differently from coarse-aggregate concrete materials.

BACKGROUND

Unrestrained (free) shrinkage is rarely found in typical concrete structures. Restraints are always present, either internal or external, because of support conditions and reinforcement or nonuniform drying. These restraints induce tensile stresses that approach the tensile strength of concrete and cause cracking.

Plastic shrinkage cracks occur during the first few hours after casting the concrete while the material is still in a semi-fluid or plastic state. The study of plastic shrinkage cracking is complicated because the material properties that determine whether such cracks will form are time-dependent and change rapidly during the first few hours. To develop reliable means of preventing this type of damage to the concrete, it is desirable to know the physical or chemical origins of plastic shrinkage. Because plastic shrinkage takes place within the first few hours after placing the concrete, it can be shown that chemical shrinkage does not contribute to plastic shrinkage to a significant extent. One common observation, which is recorded in nearly all of the relevant papers, is that plastic shrinkage–induced cracks are created as soon as the surface of the fresh concrete dries. In other words, plastic shrinkage is likely to occur when the rate of evaporation exceeds the rate at which the bleeding water rises to the surface (*1*). It is also believed that plastic shrinkage cracking occurs at the exposed surfaces of freshly placed concrete because of the consolidation of the concrete mass. This leads to open water channels that produce tensile stress in surface tears and cracks that destroy surface integrity and impair durability.

The use of polypropylene fibers at low fiber volume fractions improves several aspects of the production and application of fiber-reinforced concrete, including shrinkage and crack control, impact resistance, and toughness characteristics. Many parameters govern the performance of polypropylene fiber–reinforced concrete subjected to restrained shrinkage. These include the potential extent of shrinkage, the degree of restraint, time-dependent tensile properties of concrete, and fiber-to-matrix interfacial bond characteristics (*2–4*).

When plastic shrinkage forces are applied to concrete in the presence of polypropylene fibers, the fibers resist early shrinkage cracking and increase the stability of concrete at the initial and early set stages, causing the material to be less susceptible to settlement cracking and to adverse vibration effects at the same time.

There is currently no standardized procedure for quantifying the effects of polypropylene fibers or any other synthetic fibers on plastic or drying shrinkage cracking.

It has been found that the quantity of surface bleed water is significantly reduced by the addition of polypropylene fi-

Department of Civil and Environmental Engineering, Michigan State University, East Lansing, Mich. 48824.

bers. It is suggested that fibers cause a reduction in consolidation and thus reduce the formation of damaging capillary bleed channels and cause an increase in intergranular pressure in the plastic concrete (*5*).

Although unrestrained shrinkage tests do provide some information about the shrinkage characteristics of fiber-reinforced cement composites, results of these tests may not provide any useful information on how composites respond to shrinkage-induced stresses in restrained conditions when shrinkage strains translate into tensile stresses in concrete. After cracking, polypropylene fibers are believed to transfer the tensile stresses across cracks and to arrest or interrupt crack tip extensions so that many fine (hairline) cracks occur instead of few larger cracks (*4–6*).

The leveling operation after placing the concrete into forms, known as striking off or screeding, has been found to be a critical factor in plastic shrinkage cracking (*6*). Thus the effects of the rate and direction of screeding and the effects of the finishing operations on plastic shrinkage cracking were investigated.

EXPERIMENTAL PROGRAM

Plastic shrinkage cracking of polypropylene fiber–reinforced concrete was investigated experimentally. Three variables were considered, each at two levels, to assess their effects on plastic shrinkage cracking of concrete. The three variables and their corresponding levels are given:

Variable	*Level 1*	*Level 2*
Fiber volume fraction	0.0%	0.1%
Screeding speed	3 m/min (2.74 ft/min)	12 m/min (10.97 ft/min)
Screeding direction	Long side	Short side

A 2-×-2-×-2 factorial combination of the variables was considered; the screeding direction was eventually used as a blocking variable to form a randomized block design of experiments. Because screeding direction has only a secondary effect of changing the direction of cracking (as observed in this investigation), it was selected as a blocking variable in order to enhance the sensitivity of the statistical analysis. The statistical analysis method (factorial analysis of variance of randomized block design with screeding direction as the blocking factor) allows for determining the level of confidence in each of the conclusions derived on the basis of the test results.

Materials

The basic concrete mix constituents were cement, coarse aggregate, fine aggregate, and water. A brief description of all the materials used in this research is given in the following:

- *Portland cement*: Type I portland cement (ASTM C150-89) was used; the specific gravity was 3.15 and fineness (percentage retained on #325 sieve) was 10.7.
- *Coarse aggregate*: Crushed limestone with maximum aggregate size of 13 mm (0.5 in.) was used; its gradation met the ASTM C33 requirements. The specific gravity of coarse aggregate was 2.55, and its absorption capacity was 1.0 percent.
- *Fine aggregate*: Natural sand with fineness modulus of 3.0 was used in this research; its gradation met the ASTM C33 requirements. The specific gravity of fine aggregate was 2.50, and its absorption capacity was 3.5 percent.
- *Polypropylene fibers*: Collated fibrillated polypropylene fibers were used in this research. Some of the physical properties of these fibers are:
  - Tensile strength = 628 to 760 MPa (80 to 110 ksi)
  - Young's modulus = 3.5 GPa (500 ksi)
  - Specific gravity = 0.9
  - Melting point = 160 to 170°C (320 to 340°F)
  - Ignition point = 590°C (1,100°F)

The fibers also exhibit low thermal conductivity, low electrical conductivity, and high acid and salt resistance.

The mix proportions for all panels for cement:coarse aggregate:fine aggregate:water were 1:2.5:2.0:0.47. The cement content was 386 kg/m^3 (650 lb/yd^3). This mixture produced a slump of 100 to 125 mm (4 to 5 in.). The designated water-cement ratio was selected to produce plastic shrinkage cracking in the specific (relatively moderate) conditions of this investigation [temperature of 24 to 27°C (75 to 80°F), humidity of 50 ± 5 percent, and wind speed of 12.8 km/hr (8 mph)].

Construction

All mixtures were mixed in a conventional rotary drum concrete mixer with a capacity of 0.04 m^3 (1.41 ft^3). The mixing procedure for the concrete mixture followed ASTM C192-90. The mixer was first loaded with the coarse aggregate and a portion of the mixing water. After the mixer was started, the fine aggregate, cement, and rest of the water were added and mixed for 3 min. This was followed by 3 min of rest and 2 min of final mixing. For fibrous mixtures, the fibers were added after all other mix ingredients were. Fresh concrete mixtures were tested for bleeding (ASTM 232) and set time (ASTM 403). All the panels were cast immediately after mixing, and the tests were conducted after the adopted restrained plastic shrinkage test procedure prescribed in the following section.

Plastic Shrinkage Cracking Test Procedure

The test procedure proposed by Kraii (*7*) and refined by Shaeles and Hover (*6*) was used for evaluating the effects of polypropylene fibers on plastic shrinkage cracking of concrete.

Two 533- × 838-mm (21- × 33-in.) slabs 38 mm (1.5 in.) thick (one plain and the other fibrous concrete) were cast side by side and exposed to identical finishing processes and environmental conditions (temperature, humidity, and wind velocity). A vertical partition was used between the two panels to prevent nonuniformities arising from interference effects between the two fans and slabs. To monitor the weight of water lost from concrete during the test, two cylinders 152 mm (6 in.) across and 64 mm (2.5 in.) high filled with concrete were placed adjacent to the panels and weighed during the test. Open pans of water were similarly placed and weighed to monitor the rate of evaporation from a free water surface (see Figure 1). The fans were started 25 min after the addition of water to the mixer for all test slabs in order to have identical

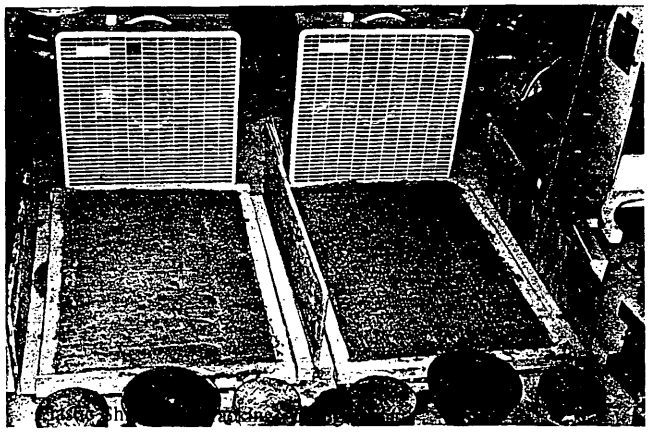

FIGURE 1 Plastic shrinkage cracking test arrangement.

conditions. The temperature, relative humidity, and wind velocity were measured during tests on each pair of panels.

Procedures for placing and finishing the concrete slabs were performed according to those described by Kosmatka and Panarese (*8*). The finishing procedures used in this project are summarized in the following:

1. Screeding (strike off): Screeding of the slab surface was done immediately after the concrete was poured into the forms using a wood straight edge that was moved across the concrete surface with a sawing motion and advanced forward a short distance with each movement.
2. Bullfloat or Darby: Immediately after screeding, an aluminum bullfloat was applied to eliminate high and low spots and embed large aggregate particles. Bullfloat application was completed before bleed water accumulated on the surface of the slab.

TEST RESULTS AND DISCUSSION OF RESULTS

The formation of plastic shrinkage cracks was visually determined. Generally, the cracks began to form within 40 to 120 min after the fans were started. The fan was stopped after 5 hr. Subsequently, the crack widths and lengths were measured using optical lenses. Total crack area was calculated by multiplying the width of each crack by its length. Characterizing the cracks by their total area instead of their total length helps to account for the fact that some cracks are simply hairlines and others are much wider.

The rate of evaporation from concrete surfaces was found to range from 0.25 to 3.18 kg/m^2/hr (0.05 to 0.65 lb/ft^2/hr), whereas the rate of free water evaporation was almost twice that amount. The times of setting for plain and polypropylene fiber–reinforced concretes are shown in Figure 2. The initial and final setting times were decreased by 9 and 27 percent, respectively, with the addition of polypropylene fibers. This reduction is expected to reduce the period of exposure of fresh concrete (before setting) to the dry environment; the drying period is responsible for plastic shrinkage cracking. The amount of bleed water for plain and fiber concretes is shown in Figure 3. The addition of polypropylene fibers caused an 18 percent decrease in the amount of bleed water of concrete; the fibers could be reducing the settlement of heavier mix constituents (e.g., aggregates), thereby reducing the upward movement (and bleeding) of concrete.

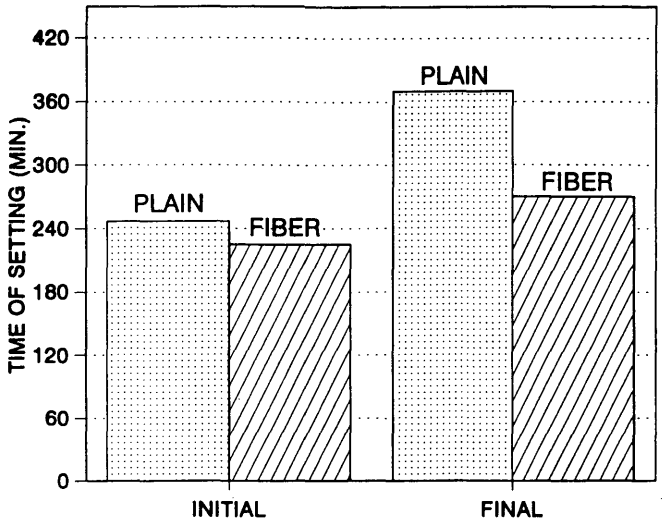

FIGURE 2 Time of setting for plain and fiber concretes.

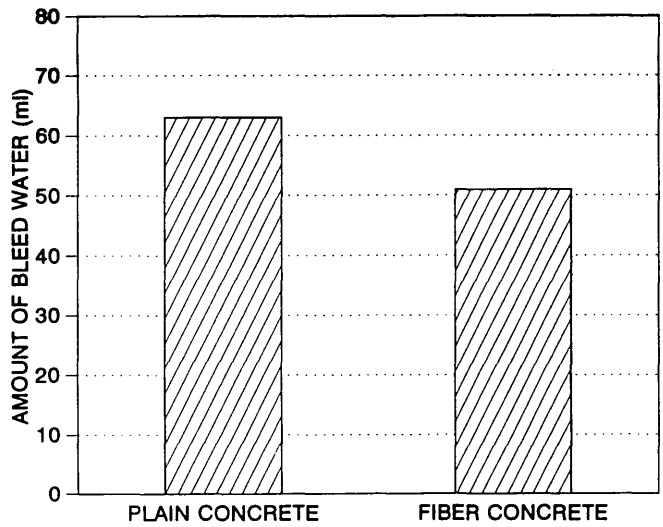

FIGURE 3 Bleeding test results.

EFFECTS OF CONSTRUCTION OPERATIONS

The average values of the total crack areas and maximum crack widths are shown in Figures 4 and 5, respectively. The average values are obtained from two test results (with two screeding directions). Because of the relatively large range of the total crack area measurements, resulting from negligible crack widths of polypropylene fiber–reinforced panels, transformation of test results was necessary to perform a reliable statistical analysis of the total plastic shrinkage crack areas. Square root transformation was found to be suitable for the total crack area measurements. Randomized block analysis of variance of the transformed data revealed that fiber volume

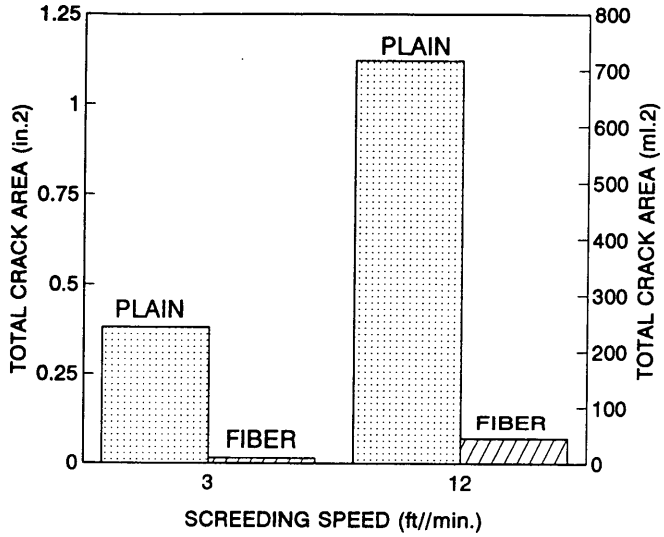

FIGURE 4 Effects of construction operations and fiber volume fraction on total plastic shrinkage crack area.

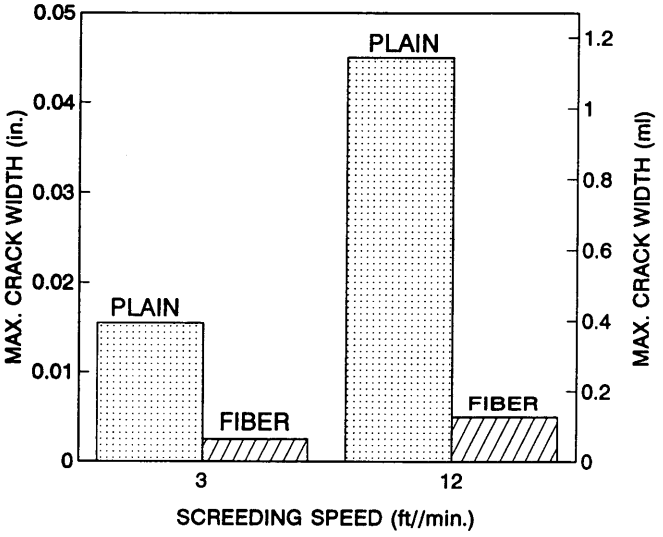

FIGURE 5 Effects of construction operations and fiber volume fraction on maximum plastic shrinkage crack width.

fraction and screeding speed had significant effects on the plastic shrinkage cracking area and maximum crack width at 99 and 95 percent levels of confidence, respectively. There appeared to be significant interaction between construction operations (screeding speed) and polypropylene fibers in influencing the total area of plastic shrinkage cracks. However, screeding speed had not statistically significant interaction with fibers in causing the maximum crack width.

Multiple comparisons of the test data indicated that in all cases the total plastic shrinkage cracking area in fiber concrete was significantly less than that in plain concrete. In fiber concrete, slow rate of screeding significantly reduced the total plastic shrinkage crack area of concrete panels.

The plastic shrinkage cracks were hairline cracks in polypropylene fiber–reinforced panels, so the multiple comparisons of the maximum crack width test results revealed that maximum crack widths were statistically comparable in all cases in the presence of fibers (irrespective of the screeding speed). Multiple comparison of the maximum crack width measurements in plain concrete panels confirmed that slower screeding led to narrower maximum crack widths when no fibers were present.

Polypropylene fibers reduced the total plastic shrinkage crack area by 95 percent at high screeding speed. Fibers eliminated any detectable plastic shrinkage cracks at low screeding speed.

SUMMARY AND CONCLUSIONS

The effects of collated fibrillated polypropylene fibers, at 0.1 percent fiber volume fraction, and construction operations on plastic shrinkage cracking of concrete were investigated experimentally. Statistical analysis of the data was performed to confirm the validity of the following conclusions at a 95 percent (or higher) level of confidence:

1. Polypropylene fibers significantly reduce the total plastic shrinkage crack area and maximum crack width at 0.1 percent fiber volume fraction.
2. The construction operations (screeding rate) affect the total plastic shrinkage crack area in both plain and fibrous concretes.
3. Because polypropylene fiber–reinforced concrete is characterized by fine plastic shrinkage cracks, the maximum crack width was not influenced by any of the construction operations (screeding rate) in fibrous concrete. On the other hand, the maximum plastic shrinkage crack widths of polypropylene fiber–reinforced concrete decreased significantly when compared with plain concrete. In plain concrete, higher screeding rates led to a statistically significant increase in the maximum crack width.

ACKNOWLEDGMENTS

The authors are thankful to the Research Excellence Fund of the state of Michigan and the Composite Materials and Structures Center of Michigan State University for supporting this project. The polypropylene fibers used in this investigation were provided by Fibermesh Company. All these contributions are gratefully acknowledged. Umm Al-Qura University sponsored the second author and King Saud University sponsored the third author during this research project.

REFERENCES

1. F. H. Wittman. On the Action of Capillary Pressure in Fresh Concrete. *Cement and Concrete Research*, Vol. 6, No. 1, Jan. 1976, pp. 49–56.
2. P. A. Dahl. Influence of Fiber Reinforcement on Plastic Shrinkage Cracking. *Proc., International Conference on Recent Development on Fiber Reinforced Cement and Concrete*, Cardiff, Wales, Sept. 1989, pp. 435–441.

3. S. Goldfein. *Plastic Fibrous Reinforcement for Portland Cement*. Technical Report 1757-TR. U.S. Army Engineer Research and Development Laboratories, Fort Belvoir, Va., Oct. 1963.
4. M. Grzybowski and S. P. Shah. Shrinkage Cracking of Fiber Reinforced Concrete. *ACI Materials Journal*, Vol. 87, No. 2, 1990, pp. 138–148.
5. R. F. Zollo, J. Allter, and G. B. Bouchacourt. Plastic and Drying Shrinkage in Concrete Containing Collated Fibrillated Polypropylene Fibers. *Proc., RILEM 3rd International Symposium on Development in Fiber Reinforced Cement and Concrete*, Sheffield, England, Vol. 1, July 1986.
6. C. A. Shales and K. C. Hover. Influence of Mix-Proportions and Construction Operations on Plastic Shrinkage Cracking in Thin Slabs. *ACI Materials Journal*, Vol. 85, No. 6, 1988, pp. 495–504.
7. P. P. Kraii. A Proposed Test to Determine the Cracking Potential Due to Drying Shrinkage of Concrete. *Concrete Construction*, Vol. 30, Sept. 1985, pp. 775–778.
8. S. H. Kosmatka and W. C. Panarese. *Design and Control of Concrete Mixtures*. Portland Cement Association, Skokie, Ill., 1986.

Publication of this paper sponsored by Committee on Mechanical Properties of Concrete.

Plastic Shrinkage Cracking of Restrained Fiber-Reinforced Concrete

ANTONIO NANNI, DENNIS A. LUDWIG, AND MICHAEL T. MCGILLIS

It is well established that the low-volume addition of fibers (synthetic or steel) to concrete can significantly reduce cracking due to plastic shrinkage. However, as of today, there is no consensus standard test method available to measure this effect. A test procedure is under scrutiny at ASTM. In this procedure, the surface cracks of a plain concrete panel are compared with those of a fiber-reinforced concrete panel under conditions of severe and controlled moisture loss. The results of an experimental project aiming to determine the validity and repeatability of the test procedure on plastic shrinkage under consideration by ASTM are reported. For this purpose, various fiber types (i.e., synthetics and steel), in different configurations (i.e., monofilament, fibrillated, deformed) and of various lengths, were used with the same concrete matrix. The results show that the proposed ASTM standard has merit. Its major drawback is that specimen performance characterization is based exclusively on crack width.

Volume changes of fresh concrete are due to water absorption and evaporation, sedimentation and segregation, cement hydration, and thermal changes. In addition to the mixture constituents and proportions, volume changes are influenced by the surrounding environment (i.e., temperature, humidity, and wind speed). Plastic shrinkage cracking occurs in the superficial layer of fresh concrete within a few hours after placement. The principal cause of this type of cracking is an excessively rapid evaporation of water from the concrete surface, such that it exceeds the rate at which bleeding water rises to the surface (*1*,*2*). The formation of plastic shrinkage cracking takes place when internal stress is higher than the tensile strength of concrete. Internal stress is closely related to the capillary pressure of the pore water within the fresh concrete (*1*). Plastic shrinkage cracking occurs most often in slabs and pavement construction exposed to hot and dry weather. Construction operations (screeding and finishing) have a very significant effect on plastic shrinkage cracking (*3*). Cracking can be avoided with the proper concrete mixture design and the proper construction and curing procedure.

In recent years, the use of fibers, particularly of the synthetic type, has become common to minimize plastic and early drying shrinkage cracking in slab-on-grade construction. From here, the need has emerged for a testing procedure that would quantify the beneficial effects of fiber addition and could help in selecting the most appropriate fiber parameters (i.e., fiber type, length, volume percentage) for a specific concrete matrix subjected to specific environmental conditions. Several test methods have been proposed (*4*–*6*). In 1985, Kraai mentioned in the introduction to his paper that a testing procedure was under consideration by ASTM (*4*). But 7 years later, no standard test has been approved. A task group within ASTM Subcommittee C09.03.04 has arrived at the fifth draft of a proposed method for evaluating plastic shrinkage cracking of restrained fiber-reinforced concrete (FRC). No data have been published in the literature on the performance of this proposed test method other than a summary diagram presented by Berke et al. (*6*). The diagram shows only the average crack area for nine mixtures using the same fiber type at three different lengths and three different volumes. The salient feature of the test procedure being considered is in the specimen configuration (see Figure 1). In this case, the restraining effect of a perimeter wire mesh as proposed by Kraai (*4*) is substituted with three stress risers. Shrinkage cracking is expected to initiate at the central riser, where the specimen thickness is reduced from 100 mm (4 in.) to 38 mm (1.5 in.). The experimental results obtained by Berke et al. (*6*) with this specimen are very similar to those obtained by Kraai and presented by Vondran and Webster (*7*). Significant shrinkage cracking reduction was obtained when using fibers in the concrete matrix.

The objective of this research project was to evaluate independently the validity and reliability of the proposed ASTM procedure by obtaining several experimental results on plain concrete and FRC mixtures.

TEST PROGRAM

Materials

The concrete matrix used for the entire project had the following proportions: portland cement Type I, 335 kg/m^3; water, 208 kg/m^3; coarse aggregate (20 mm maximum size), 1037 kg/m^3; fine aggregate, 814 kg/m^3. This mixture had a very high cement content and a very high water-cement ratio, and it did not contain any chemical or mineral admixtures. The slump was 180 mm (7 in.), the unit weight was 2286 kg/m^3 (3,853 lb/yd^3), and the air content was 0.9 percent. The 28-day compressive strength was 24.7 MPa (3,590 psi) with a standard deviation of 2.5 MPa (361 psi) for 15 specimens.

The fibers used in the testing program are described in Table 1; their sources are not identified. Two types of steel fibers were used from two different manufacturers. Three mixtures (B, C, and D) contained steel fibers (straight and deformed) at the low dosage of 0.62 percent by weight (corresponding to 25 lb/yd^3). The remaining nine FRC mixtures were made with synthetic fibers of two base materials and different configurations (monofilament and fibrillated). The

Department of Architectural Engineering, Pennsylvania State University, 104 Engineering Unit A, University Park, Pa. 16802.

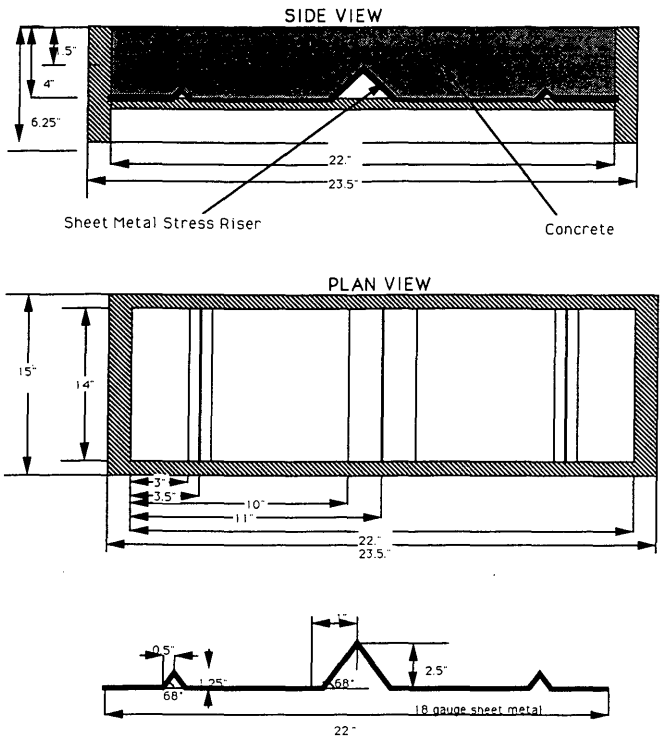

FIGURE 1 Specimen geometry and configuration (ASTM proposed standard) (not to scale).

TABLE 1 Specimen Key

MIXTURE	FIBER-MANUFACTURER	VOLUME (%)	CHARACTERISTICS
A	Plain Matrix	--	--
B	Steel-I	0.19	Straight
C	Steel-II	0.19	Deformed
D	Steel-I	0.19	Deformed
E	Synthetic-I	0.05	Monofilament
F	Synthetic-I	0.05	Monofilament
G	Synthetic-I	0.05	Monofilament
H	Synthetic-II	0.10	Fibrillated
I	Synthetic-II	0.10	Fibrillated
J	Synthetic-II	0.10	Fibrillated
K	Synthetic-II	0.10	Fibrillated
L	Synthetic-II	0.10	Fibrillated
M	Synthetic-II	0.07	Monofil

first type was used in different lengths and at the same dosage in three mixtures (E, F, and G). The second type was used in six mixtures (H, I, J, K, L, and M) with different lengths and at different dosages.

Fabrication and Testing Procedures

Each testing day 0.16 m^3 (5.5 ft^3) of concrete was batched. First, gravel and sand stored in sealed containers were placed into the mixer. While the aggregates were being weighed, the specimen molds were lightly oiled for bond breaking and preventing water absorption along the wooden sides of the molds. At the same time, predetermined amounts of fibers were prepared. After the aggregates were placed in the mixer, the mixer was turned on and half of the mixing water was added. Following a 3-min premixing, portland cement and, afterward, the rest of the mixing water were added. The concrete was then left to mix for another 5 min. A known amount of concrete was then discharged from the mixer. Part of this amount was used for the plain matrix specimen, compression cylinders, and fresh concrete tests (slump and air content). At this point, the selected fiber type was added to the concrete remaining in the mixer and mixed for an additional 3 min. This amount of FRC was sufficient for two identical specimens. After discharging the first FRC batch, the mixer was reloaded with an equal amount of plain matrix and the second fiber type was added for two more FRC specimens.

Five molds were filled with concrete and vibrated on a vibratory table for 12 sec and then screeded, floated, and weighed. The specimens were moved to an environmentally controlled room to be placed into individual air ducts. The room was equipped with a thermostat and a dehumidifier. At the start of each day, the room temperature was kept at approximately 38°C (100°F) and the relative humidity between 25 and 30 percent. Water pans were filled and weighed and then placed in each duct on a weighing scale positioned beside the specimen (so that the evaporation from the specimen would not interfere with the evaporation from the pan, and vice versa). The fans were turned on, pushing air across the specimens. Initial readings were taken (air and concrete temperature, humidity, and wind speed). Subsequent readings were taken every 30 min for 3 hr (for a total of seven readings). At the completion of the 3 hr period, the fans were turned off, a final water pan weight reading was taken, and the specimens were removed from the ducts. The specimens were then weighed and the length and width of cracks were measured. The width of each crack was measured with a crack scale at approximately every inch along its length. The crack length was determined by placing a string along the crack and then measuring the length of the string. The average width and the length were multiplied to compute the area of one crack. This procedure was repeated for each crack, and the total crack area was calculated by summing up individual values. After all measurements were taken, the specimens were disposed of.

With respect to the proposed ASTM test procedure, some comments that could lead to future improvements are offered:

- The procedure for filling the mold should be clearly spelled out. To the operator, it is natural to place scoops of concrete to the left and right of the central stress riser and then distribute the material over the entire mold. If this is done, the number of fibers crossing the riser may not be representative of the nominal fiber volume in the mixture.
- The water pan should be placed beside the specimen rather than behind it. The water pan placed on the scale in the wind stream can wobble and spill easily. If the pan is filled according to the proposed standard, the water will blow out of the pan.
- The specimens are large and unwieldy even for two people.

DISCUSSION OF RESULTS

Environmental Conditions

The proposed test procedure does not specify the environmental conditions in terms of temperature and relative hu-

midity, but it specifies a minimum air flow velocity of 4.5 m/sec (10 mph). Any combination of these three parameters is suitable, provided that the evaporation rate in the water pan is at least 980 g/m²/hr (0.2 lb/ft²/hr). To satisfy this requirement, it was attempted to maintain environmental conditions inside the duct as close as possible to 35°C (95°F), 40 percent relative humidity, and a wind speed of 5.2 m/sec (11.5 mph). The crack area of plain matrix specimens can be plotted as a function of the average temperature, relative humidity, and wind speed recorded during the 3-hr test. In this case, it appears that matrix cracking is insensitive to environmental conditions within the ranges experienced during this project. Even the combination of the three independent variables in one single parameter (directly proportional to temperature and wind speed and inversely proportional to relative humidity) has no effect on cracking area. It is therefore concluded that, as long as the evaporation rate in the water pan remains close to the prescribed value of 98 g/m²/hr, no significant effect on cracking is expected due to slight changes in environmental conditions.

The first shrinkage crack in all specimens was visible at the fifth (120 min) or sixth (150 min) interval reading. No significant difference in cracking time between plain matrix and FRC was observed. The average concrete temperature at the beginning of the test was 21.9°C (71.4°F) with a standard deviation of 1.1°C (1.9°F). After 3 hr, at the end of the test the average concrete temperature had climbed to 30.8°C (87.4°F) with a standard deviation of 2.9°C (5.2°F). The average room temperature and relative humidity over a 3-hr period were 36.8°C (98.2°F) and 38 percent.

Evaporation from Specimens

The addition of fibers to concrete has been reported to decrease the amount of water bleeding (*7*). The weight loss of all specimens was measured at the end of the 3-hr test. The crack area of all specimens can be plotted as a function of the weight loss (i.e., evaporated water). In this case, the trend of the data points would indicate that the higher the moisture loss, the higher the crack area. In addition, data points relative to the unreinforced matrix tend to cluster at the upper-right side of the diagram corresponding to higher values of evaporation and cracking. It can be concluded that, in general, water evaporation in FRC is less (and with less cracking) than for the respective plain matrix.

Plain Concrete and FRC Cracking

All specimens (plain matrix and FRC) cracked during the performance of the test. Given the specimen geometry and configuration, once a crack started over the central stress riser, it usually extended over the full width of the specimen and, obviously, could grow no further. The parameter that characterizes the performance of different samples becomes, therefore, the width of the crack. This is demonstrated by the two diagrams in Figure 2. In this diagram, the crack area is plotted as a function of the crack width for all specimens. The crack width given here represents the average value of all measurements for each sample. The first observation is that average crack width varied widely between 0.1 and 1 mm (one order of magnitude between maximum and minimum values), whereas the total length of cracks was about 380 mm (15 in.) (the width of the specimen was 356 mm, or 14 in.). The second observation is that the data points relative to the matrix concentrate at the higher values of the abscissa (wider cracks). It is concluded that for the specimen size and configuration of the proposed test method, the paramount characterization parameter is crack width.

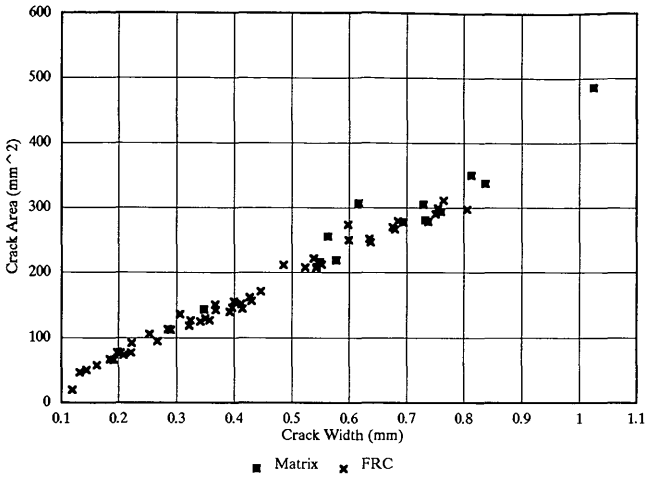

FIGURE 2 Crack area versus crack width (all specimens).

Evaluation of Proposed ASTM Standard

The average crack area of each FRC mixture (four samples), expressed as a percentage of the companion plain matrix specimen, is shown in Figure 3. In this diagram, the sample standard deviation is also plotted above and below the average value. From this figure, it is observed that with the exception of FRC Mixture F, the shrinkage cracking area of any FRC

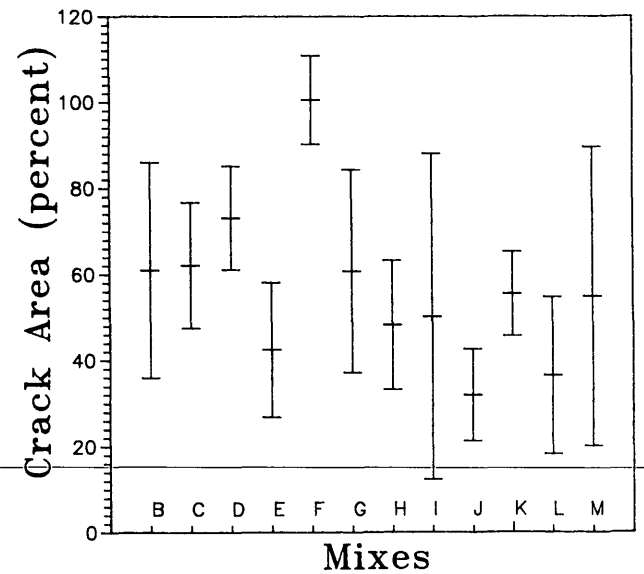

FIGURE 3 Average crack area (and standard deviation) for each FRC mixture relative to respective plain matrix.

is lower than that of the companion matrix. The variability is rather high but may be attributed to the nature of the parameter under study (shrinkage cracking) rather than the procedure itself.

Looking at the results from a practical end, assume that this project was intended to identify the most suitable fiber types to reinforce a given matrix. Would the proposed test method have helped? The answer is probably yes. The engineer could set an acceptability threshold (say, 50 percent shrinkage crack area reduction), consider all fiber types with better performance, and use this information with other parameters (e.g., cost, workability, etc.) to select the most desirable product. What is missing is the verification of the test results in terms of field performance. For this, only time and more work can provide the answer.

CONCLUSIONS

The objective of this work was to generate experimental data with a proposed ASTM standard test method meant to evaluate the ability of fibers to control plastic shrinkage cracking. The authors have concluded that the proposed method has merit and is not irremediably flawed. The major concern is in the fact that, because of the specimen configuration, crack width becomes the primary parameter to characterize the shrinkage cracking potential of different specimens. Rather than continuing an endless discussion, it is probably in the best interest of the public and the fiber industry to adopt a standard test method for the evaluation of plastic shrinkage cracking. The method can then be reevaluated after a fixed period.

ACKNOWLEDGMENTS

Financial contributions and materials were provided by steel and synthetic fiber manufacturers.

REFERENCES

1. F. H. Wittmann. On the Action of Capillary Pressure in Fresh Concrete. *Cement and Concrete Research*, Vol. 6, No. 1, Jan. 1976, pp. 49–56.
2. J. Van Dijk and V. R. Boardman. Plastic Shrinkage Cracking of Concrete. *Proc., RILEM International Symposium on Concrete and Reinforced Concrete in Hot Countries*, Haifa, Israel, 1971, pp. 225–239.
3. C. A. Shaeles and K. C. Hover. Influence of Mix Proportions and Construction Operations on Plastic Shrinkage Cracking in Thin Slabs. *ACI Materials Journal*, Vol. 85, No. 6, Nov.–Dec. 1988, pp. 495–504.
4. P. P. Kraai. A Proposed Test To Determine the Cracking Potential Due to Drying Shrinkage of Concrete. *Concrete Construction*, Vol. 30, No. 9, Sept. 1985, pp. 775–778.
5. I. Padron and R. F. Zollo. Effect of Synthetic Fibers on Volume Stability and Cracking of Portland Cement Concrete and Mortar. *ACI Materials Journal*, Vol. 87, No. 4, July–Aug. 1990, pp. 327–332.
6. N. S. Berke, M. P. Dallaire, S. A. Valle, and I. Callander. The Use of Collated and Fibrillated Polypropylene Fibers in Concrete. American Concrete Institute, Detroit, Mich. (in press).
7. G. L. Vondran and T. Webster. The Relationship of Polypropylene Fiber Reinforced Concrete to Permeability. *ACI SP-108: Permeability of Concrete* (D. Whiting and A. Walitt, eds.), American Concrete Institute, Detroit, Mich., 1988, pp. 85–97.

Publication of this paper sponsored by Committee on Mechanical Properties of Concrete.

Triaxial Characterization of High-Strength Portland Cement Concrete

MICHAEL I. HAMMONS AND BILLY D. NEELEY

Triaxial characterization tests were conducted on a high-strength portland cement concrete proportioned from readily available materials. The objective was to develop mechanical response data for this high-strength concrete along selected stress and strain paths in multiaxial stress space. The concrete chosen for testing had a water-cement ratio of 0.23 and an unconfined compressive strength at 56 days of 105 MPa. The triaxial test specimens were 50-mm nominal diameter right circular cylinders. All tests were performed in a 276-MPa-capacity cylindrical triaxial cell in conjunction with a 1340 kN-capacity servohydraulic materials testing system. Confining pressure was generated by an external 600-MPa-capacity, air-driven hydraulic pumping system. Active measurements attempted for each test included vertical and horizontal strain, testing machine displacement, axial load, and confining pressure. Triaxial shear tests were conducted at confining pressures of 50, 100, 150, and 200 MPa, and uniaxial strain tests were conducted to a principal stress difference of 350 MPa. These stress-strain data were plotted, and a failure envelope was developed. The test data show that high-strength portland cement concrete is capable of large plastic strains and ductile flow under states of high confinement. The material exhibited strain-softening behavior at the 50-MPa level; thus, it appears that the brittle-ductile transition for the material lies between the 50- and 100-MPa confining stress levels. At confining stresses of 100 MPa and greater, the material behavior is characterized by a strain-hardening ductile behavior to axial strains of 10 percent or greater.

Recent advances in concrete technology have made possible the development and placement of high-strength concrete for civil and military applications. The Concrete Technology Division of the Structures Laboratory at the U.S. Army Engineer Waterways Experiment Station has been developing concretes and binder systems, design procedures, and construction technology to enhance the survivability of hardened facilities (*1–4*). This paper documents the characterization of a high-strength portland cement (HSPC) concrete for use in projectile penetration studies involving various high-strength target materials (*5,6*). With increasing confinement, the strength and ductility of concrete increases dramatically. HSPC concrete should offer better penetration resistance than conventional-strength concretes because of enhanced mechanical properties.

The objective of this research was to develop mechanical response data along selected stress and strain paths in multiaxial stress space. This data will be used by analytical modelers as input into constitutive models for material response calculations.

Concrete Technology Division, Structures Laboratory, U.S. Army Engineer Waterways Experiment Station, 3909 Halls Ferry Road, Vicksburg, Miss. 39190.

A series of triaxial shear and uniaxial strain tests were conducted in a cylindrical triaxial cell to characterize the mechanical response of the material. Triaxial shear tests were conducted on these two mixtures at confining pressures of 50, 100, 150, and 200 MPa, and uniaxial strain tests were conducted to a principal stress difference of 350 MPa. These stress-strain data were plotted, and a failure envelope was developed.

CONCRETE MIXTURE

The project requirements called for an HSPC concrete having as high an unconfined compressive strength as convenient using available materials. The concrete mixture selected for characterization, designated PP/HSPC-1 is described in Table 1. This mixture had a water-cement ratio of 0.23 and an unconfined compressive strength at 56 days age of 105 MPa. Other fresh and hardened properties of the mixture are given in Table 2.

TEST DEVICES AND PROCEDURES

Specimen Preparation

The concrete was batched in the laboratory. Three 0.15- × 0.15- × 0.9-m prisms were cast using extended external mechanical vibration on a vibrating table. The concrete was vibrated until no air was observed coming to the top or until the mixture began to bleed. This technique produced concrete from which cores could be taken that would be expected to be adequately free of large voids. The prisms were cured for 56 days in a moist curing room.

The triaxial test specimens were 50-mm nominal diameter right circular cylinders cored from the prisms. Each core was brushed with a stiff wire brush to expose surface voids. The voids were then filled with gypsum cement to minimize the possibility of membrane puncture during testing.

The sides of the specimens were required to be smooth and free of any abrupt irregularities. The departure from perpendicularity was required to be less than 0.25 degrees. The straightness of the sides was determined by a dial gauge. Measurements were made at each end and at the quarter points on four axes 90 degrees apart. Planeness of the specimen ends was required to be within 0.025 mm. This requirement was checked by making four equally distributed measurements on each of the specimens with a dial gauge. An average diameter and length were computed for each speci-

TABLE 1 Concrete Mixture Proportions, Saturated Surface Dry Conditions: PP/HSPC-1

Item	Proportions, kg/m³
Type I portland cement	1,517
Silica fume	202
Class F fly ash	337
9.5-mm limestone coarse aggregate	2,321
Limestone fine aggregate	1,866
Water	472
High-range water-reducing admixture (powder)	32.9
Air-detraining agent (powder)	3.0

TABLE 2 Fresh and Hardened Properties: PP/HSPC-1

Property	Value
Slump, mm	200
Unit Weight, kg/m³	2,365
Air Content, percent	3.5
Compressive Strength, MPa	
7 days	85
28 days	96
56 days	105
Direct Tensile Strength, MPa	
56 days	5.4
Tensile Elastic Modulus*, MPa	
56 days	44,000
Tensile Strain at Failure, millionths, 56 days	135

*Test method described by Hammons et al.[6].

men, and these values were used as the pretest dimensions of the specimens.

All specimens were air-dried in the laboratory for a sufficient amount of time to equilibrate with the laboratory environment; therefore, all specimens were essentially free of pore water. The specimens were prepared for testing by placing hardened steel-bearing blocks on each end and encasing the specimen in an impermeable membrane. A 60-durometer neoprene tubing was then placed over the specimen and bearing blocks to serve as a flexible membrane. The membrane was secured at each end with hose clamps.

Triaxial Test Device and Procedure

Triaxial properties of concrete are determined generally from two types of test devices: cylindrical triaxial cells and truly triaxial (cubical) cells. This paper is concerned with cylindrical triaxial tests only. In the cylindrical triaxial test device, an axisymmetric stress state exists with two of the three principal stresses being necessarily equal. For this research all tests were performed in a 276-MPa-capacity cylindrical triaxial cell in conjunction with a 1340- kN-capacity servohydraulic materials testing system. This cell accepts a maximum specimen length of approximately 90 mm. Up to four channels of instrumentation can exit the pressure vessel through Fusite fittings in the base.

Confining pressure was generated by an external 600-MPa-capacity, air-driven hydraulic pumping system. The pumping system was connected through high-pressure tubing to a pressure port in the devices. A pharmaceutical-grade mineral oil was used as the confining medium. The loading ram was driven by the servocontrolled hydraulic materials testing system.

After the specimen was placed in the triaxial cell, the assembly was placed under the materials testing system. The confining pressure was increased by means of the pumping system and regulated by hand-operated valves. The universal testing machine provided the axial stress, and the confining pressure was maintained with the hydraulic pump and valve. The test proceeded in a stepwise manner along the prescribed stress or strain path.

After each test was completed, the test device was removed from the testing machine and disassembled. The specimen was recovered, and any anomalies were noted.

Instrumentation

Active measurements attempted for each test included vertical and horizontal strain, testing machine displacement, axial load, and confining pressure. Four foil-strain gauges were applied to each specimen at mid-height. Two vertical gauges were placed diametrically opposite, and two horizontal gauges were placed diametrically opposite on a diameter 90 degrees from the vertical gauges. The two gauges in each orientation were wired in series, and signal conditioners were set to average the data.

The testing machine crosshead displacement was assured by means of a linear motion potentiometer mounted directly on the testing machine. Axial stresses were measured by the load cell on the universal testing machine (corrected for friction on the piston seals) and confining stresses by a pressure transducer in the hydraulic loading system.

All data were recorded on Hewlett Packard Series 200 or 300 computers controlling digital data acquisition hardware. All voltage measurements were preconditioned and amplified using Wheatstone bridge conditioners.

CHARACTERIZATION TEST RESULTS

Project requirements dictated that the mechanical response of the concrete mixtures be characterized along two types of multiaxial paths: triaxial shear and uniaxial strain. Boundary conditions for these tests are described in the following.

Triaxial shear is defined as a stress state described by the following stress tensor, σ:

$$\sigma = \begin{pmatrix} \sigma_{11} & 0 & 0 \\ 0 & \sigma_{33} & 0 \\ 0 & 0 & \sigma_{33} \end{pmatrix}$$

where σ_{11} is the stress in the direction of the axis of the cylinder (herein referred to as "axial stress") and σ_{33} is the confining stress. Because of the boundary conditions of the cylindrical triaxial device, two of the three principal stresses are necessarily equal; therefore, confining stress = $\sigma_{22} = \sigma_{33}$.

The triaxial shear tests were conducted by increasing all three principal stresses isotropically until the desired level of confining stress was obtained. Subsequently, the confining stress was maintained while the axial stress was increased until the test was halted. The criteria for halting a test were as follows:

- Attaining a total axial strain of 10 percent, or
- Reaching ultimate axial stress capacity.

During the course of the triaxial shear tests, considerable barreling of the test specimens occurred at large strains. The axial stress in each test was calculated as the axial load divided by the current cross-sectional area. This definition of axial stress may not be consistent with large deformation theory. Also, as bulging occurs, a component of confining stress becomes directed vertically, causing a stress distribution that becomes quite complex.

A uniaxial strain test is defined by the boundary condition

$$\varepsilon = \begin{pmatrix} \varepsilon_{11} & 0 & 0 \\ 0 & 0 & 0 \\ 0 & 0 & 0 \end{pmatrix}$$

where ε is the engineering strain tensor and ε_{11} is the engineering strain along the axis of the cylinder. These boundary conditions are maintained by manipulating the confining stresses to force $\varepsilon_{22} = \varepsilon_{33} = 0$ as ε_{11} varies.

Triaxial shear tests for the two concretes were conducted at confining stress levels of 50, 100, 150, and 200 MPa, and two uniaxial strain tests were conducted on each mixture. Selected data plots are given in the text of this paper.

Test Results

Table 3 gives a summary of the maximum stress levels obtained during each test. Also reported in the table are maximum values of principal stress difference (PSD), defined as

$$\text{PSD} = \sigma_{11} - \sigma_{33}$$

and mean normal stress (MNS), defined as

$$\text{MNS} = \frac{\sigma_{11} + 2\sigma_{33}}{3}$$

The MNS is a measure of the hydrostatic component of the applied stress, whereas the PSD is a measure of the shear component of the applied stress state. For the cylindrical triaxial test boundary conditions, volumetric strain is calculated as

$$\varepsilon_v = \frac{\Delta V}{V} = \varepsilon_{11} + 2\varepsilon_{33}$$

Principal strain difference is calculated as

$$P\varepsilon D = \varepsilon_{11} - \varepsilon_{33}$$

Composite plots of test data from the triaxial shear tests are shown in Figures 1, 2, and 3. Figure 1 shows the stress paths for the triaxial shear tests. This plot indicates the increase in shear capacity of the concrete as the hydrostatic stress increases. The PSD at the 200-MPa confining stress level is approximately twice that observed at the 50-MPa confining stress level. Figure 2 shows the stress-strain response of the concrete during the triaxial shear phase of the tests. These data show the ductile nature of the response of HSPC concrete under states of high confining stress. The volumetric response of the material (Figure 3) is characterized by volumetric compaction during the hydrostatic compression portion and dur-

TABLE 3 Results of Characterization Tests: PP/HSPC-1

Test Name	Test Type	Length (mm)	Diameter (mm)	Length-Diameter Ratio	Maximum Radial Stress, $\sigma_{33\ max}$ (MPa)	Maximum Axial Stress, $\sigma_{11\ max}$ (MPa)	Maximum Axial Strain, $\varepsilon_{11\ max}$, at $\sigma_{11\ max}$ (%)	PSD at $\sigma_{11\ max}$ (MPa)	MNS at $\sigma_{11\ max}$ (MPa)
CTC75-1	Triaxial Shear	88.9	53.6	1.66	50	257	1.5	207	121
CTC145-1	Triaxial Shear	88.5	51.0	1.73	100	408	10.0	308	203
CTC21-2	Triaxial Shear	88.5	53.6	1.65	150	540	10.0	390	274
CTC30-1	Triaxial Shear	88.9	53.6	1.66	200	631	10.0	431	346
UX-1	Uniaxial Strain	88.5	51.0	1.73	236	499	2.0	263	324
UX-2	Uniaxial Strain	88.9	53.6	1.66	235	493	2.4	258	321

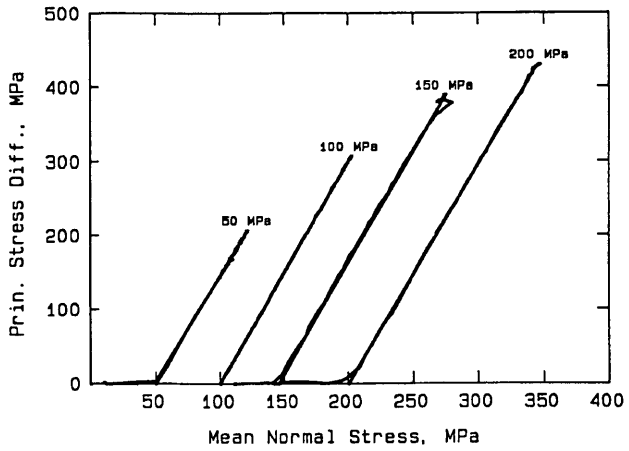

FIGURE 1 Triaxial shear test results, principal stress difference versus mean normal stress, PP/HSPC-1.

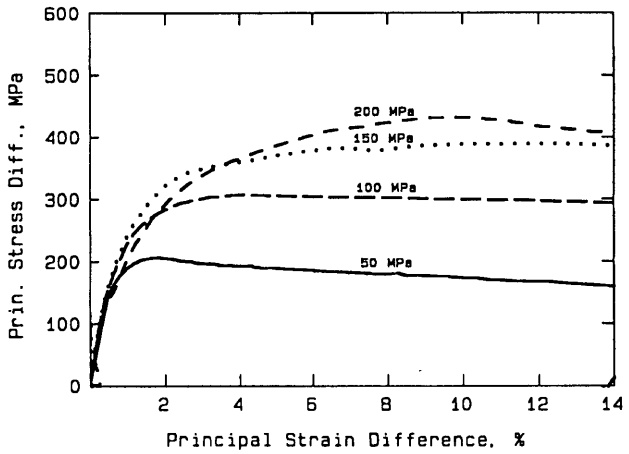

FIGURE 2 Triaxial shear test results, principal stress difference versus principal strain difference, PP/HSPC-1.

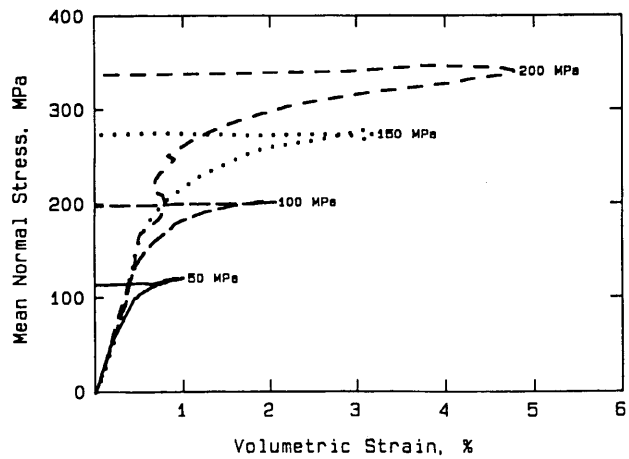

FIGURE 3 Triaxial shear test results, mean normal stress versus volumetric strain, PP/HSPC-1.

ing the initial stages of the triaxial shear loading. However, as can be seen in the Figure 3, for each confining stress level, a certain point is reached beyond which shear dilatancy initiates abruptly.

In Figures 4 and 5, composite data from the uniaxial strain tests have been plotted. From these data it can be observed that slope of the MNS versus ε_v curve is essentially bilinear, with the initial slope being stiffer than the final slope.

Analysis

Several salient features of the response of HSPC concrete to multiaxial stress states can be observed from these data. The overall multiaxial response of HSPC concrete is not significantly different from that of normal-strength concretes. HSPC concrete is typically considered to be a brittle material. However, these test data show that HSPC concrete is capable of

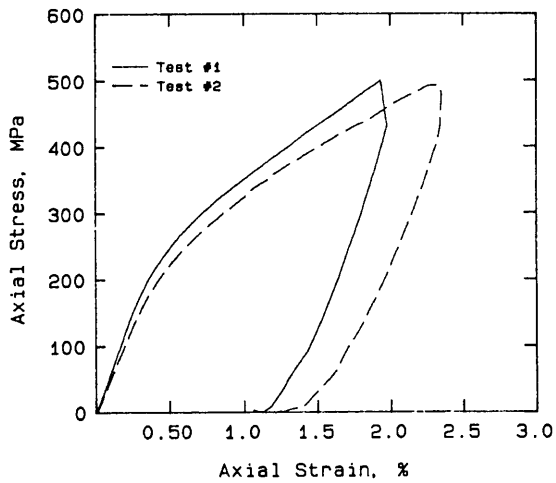

FIGURE 4 Uniaxial strain test results, axial stress versus axial strain, PP/HSPC-1.

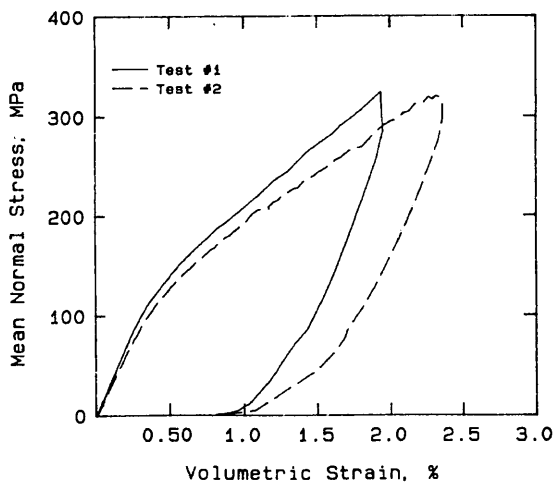

FIGURE 5 Uniaxial strain test results, mean normal stress versus volumetric strain, PP/HSPC-1.

large plastic strains and ductile flow under states of high confinement. The material exhibits strain-softening ductile behavior at the 50-MPa level. At confining stresses of 100 MPa and greater, the material behavior is characterized by a strain-hardening ductile behavior to axial strains of 10 percent or greater. The volumetric response under states of triaxial shear is characterized by shear compaction up to a point of minimum volume, followed by rapid onset of shear dilatancy. The uniaxial strain response is similar to that of normal-strength concretes.

In Figure 6 failure data obtained in the triaxial shear tests up to 200-MPa confining pressure have been used to construct an interpreted failure surface in the PSD-MNS plane. The unconfined compressive strength of the mixture is also included as a point in the plot. These data are essential to the development and verification of constitutive models for predicting the multiaxial response of HSPC concrete.

Recent advances in constitutive model development for concrete have included plasticity-based models, continuous damage models, endochronic models, and others. Factors to be considered in the choice of a constitutive model for HSPC concrete include the abilities to predict

- Strain-softening ductile behavior,
- Strain-hardening ductile behavior, and
- Shear dilatancy.

As tabulated in Table 3, the length-to-diameter ratios (L/D) for the test specimens were in the range of 1.65 to 1.73. Ideally, these ratios should be approximately 2 or greater. The effect of the low L/D ratio on the outcome of the tests cannot be quantified.

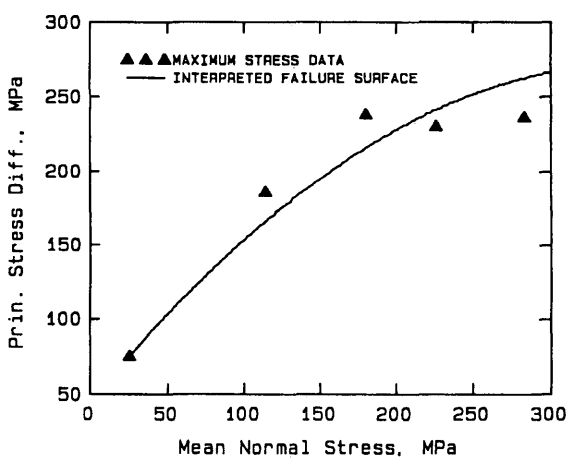

FIGURE 6 Triaxial shear test failure data and interpreted failure surface.

CONCLUSIONS

Multiaxial response characterization tests were conducted on an HSPC concrete mixture with a water-cement ratio of 0.23 and an unconfined compressive strength of 105 MPa at 56 days of age. The concrete mixture proportions were selected from readily available materials. The triaxial response tests were conducted along triaxial shear and uniaxial strain paths. Triaxial shear tests were conducted at confining stresses of 50, 100, 150, and 200 MPa. Stress-strain response data as well as failure data were obtained in the tests. The test results show that HSPC concrete, usually considered to be a brittle material, is capable of large plastic strains and ductile flow under states of high confinement. To capture the essential features of the multiaxial response of HSPC concrete, a constitutive model should be capable of predicting strain-softening ductile response, strain-hardening ductile response, and shear dilatancy.

ACKNOWLEDGMENTS

The tests described and the resulting data presented herein, unless otherwise noted, were obtained from research conducted under the Hardened Structures Research Program of the U.S. Army Corps of Engineers by the Waterways Experiment Station. Permission was granted by the Chief of Engineers to publish this information.

REFERENCES

1. K. L. Saucier. *High-Strength Concrete Past, Present, and Future.* Miscellaneous Paper SL-79-12. U.S. Army Engineer Waterways Experiment Station, Vicksburg, Miss., May 1979.
2. K. L. Saucier, W. O. Tynes, and E. F. Smith. *High Compressive Strength Concrete, Report 3, Summary Report.* Miscellaneous Paper 6-520. U.S. Army Engineer Waterways Experiment Station, Vicksburg, Miss., March 1984.
3. A. A. Bombich and A. D. Magoun. *Optimization of High-Strength Concrete Mixture Proportions for the ANMCC Improvement Project.* Miscellaneous Paper SL-82-12. U.S. Army Engineer Waterways Experiment Station, Vicksburg, Miss., Aug. 1982.
4. K. L. Saucier. *High-Strength Concrete for Peacekeeper Facilities.* Miscellaneous Paper SL-84-3. U.S. Army Engineer Waterways Experiment Station, Vicksburg, Miss., March 1984.
5. B. D. Neeley, M. I. Hammons, and D. M. Smith. *The Development and Characterization of Conventional-Strength and High-Strength Concrete Mixtures for Projectile Penetration Studies.* Technical Report SL-91-15. U.S. Army Engineer Waterways Experiment Station, Vicksburg, Miss., Aug. 1991.
6. M. I. Hammons, B. D. Neeley, and D. M. Smith. *The Development and Characterization of Fiber-Reinforced and Slag-Binder Concrete Mixtures for Projectile Penetration Studies.* Technical Report SL-92-16. U.S. Army Engineer Waterways Experiment Station, Vicksburg, Miss., June 1992.

Publication of this paper sponsored by Committee on Mechanical Properties of Concrete.

High-Performance Concrete: North Carolina Field Installation Results

MICHAEL L. LEMING, JOHN J. SCHEMMEL, PAUL ZIA, AND SHUAIB H. AHMAD

A Strategic Highway Research Program contract included five installations in five states. The objectives of the field installations were to confirm the ability to produce and place certain high-performance concretes and to achieve desired strength-time targets under realistic conditions, with several sources of raw materials. Data obtained from the most extensive field trials, conducted in North Carolina, are presented and examined.

High-performance concrete (HPC) may be defined as concrete with enhanced durability and strength-time performance. Field testing of an HPC was conducted as part of a Strategic Highway Research Program (SHRP) contract in Arkansas, Illinois, Nebraska, New York, and North Carolina. The most extensive field trials occurred in North Carolina; this report examines those results.

OBJECTIVE AND SCOPE

The primary objective of the North Carolina field installation was to

1. Verify the ability to reproduce HPC under realistic field conditions,
2. Verify lab results for strength-time data, and
3. Identify potential problems not encountered in the lab.

Both insulated and noninsulated sections were investigated. Two types of coarse aggregate and two types of high-range water reducer (HRWR) were used. In addition, sections were constructed at both a deliberate rate and under more typical construction rates.

SITE DESCRIPTION

A two-lane experimental approach slab, approximately 55 m (180 ft) long, to a bridge was placed using HPC. The bridge was under construction on US-17, over the Roanoke River in northeastern North Carolina just north of Williamston. Weather during this period was very hot and humid. Daytime temperatures ranged from the low 20s to the mid-30s in degrees Celsius (mid-70s to mid-90s Fahrenheit).

M. L. Leming, P. Zia, S. H. Ahmad, Department of Civil Engineering, North Carolina State University, Box 7908, Raleigh, N.C. 27695. J. J. Schemmel, Department of Civil Engineering, 4190 Bell Engineering Center, University of Arkansas, Fayetteville, Ark. 72701.

The concrete pavements was unreinforced, jointed at intervals of 4.6 m (15 ft) and doweled at the end of each day's placement with a maximum of 36.6 m (120 ft) between doweled sections. The concrete was placed on an asphalt base course. Depth of the pavement was a minimum of 23 m (9 in.).

Three 18.3-m (60-ft) sections were placed in the passing lane at a rate that allowed more extensive testing. The fourth section was the driving lane. Using typical placement rates, all 54.9 m (180 ft) were placed in 1 day (see Figure 1).

MATERIALS

Nominal batch weights of HPC used in this project are as follows:

- Cement: 516 kg/m^3 (870 lb/yd^3)
- Added water: 160 kg/m^3 (270 lb/yd^3)
- DCI: 20 L/m^3 (4 gal/yd^3)
- Total water: 178 kg/m^3 (300 lb/yd^3) [total water includes that contributed by DCI, air entraining agent (AEA), and HRWR]
- AEA: dosage as necessary, but as high as 0.9 L/m^3 (2.5 oz/cwt) was required.
- HRWR: up to 8.1 L/m^3 (24 oz/cwt) of naphthalene HRWR or 8.8 L/m^3 (28 oz/cwt) melamine HRWR; much higher dosages tended to produce unacceptable strengths at 6 hr due to excessive retardation.
- Coarse aggregate quantities (saturated surface dry): about 1020 kg/m^3 (1,720 lb/yd^3) for the crushed granite and 970 kg/m^3 (1,640 lb/yd^3) for the marine marl; sand quantities were adjusted as necessary to provide a yield of 1 m^3 (27.0 ft^3/yd^3) at minimum air content.

Type III portland cement was used, with a 5500-blaine fineness and slightly more than 0.6 percent alkalies as sodium oxide.

A 30 percent solution of calcium nitrite, $Ca(NO_2)_2$, tradenamed Darex Corrosion Inhibitor™ (DCI), produced by W.R. Grace, was used in all the HPC. DCI is typically used to reduce the corrosion rate of reinforcing steel, but it is also a powerful set accelerator. It was therefore selected as a nonchloride accelerate that would also improve long-term durability of reinforced structures such as bridge decks.

DCI could not be added at the time of batching because of rapid slump loss. Mixtures containing a retarder were not used

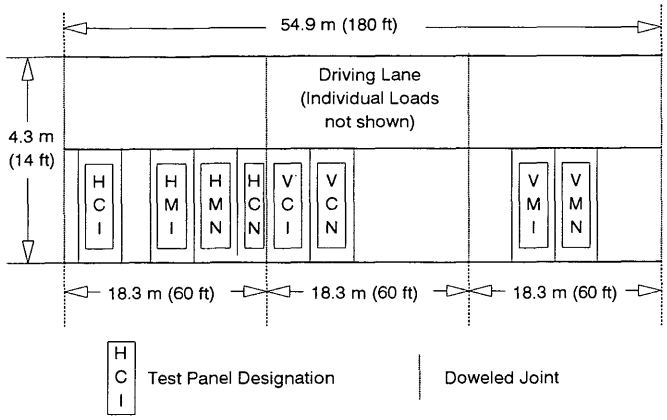

FIGURE 1 SHRP C-205 field installation layout, North Carolina.

because they retarded early strength development. DCI contains a substantial amount of water that must be withheld during batching.

The concrete contained either a naphthalene-based HRWR produced by W.R. Grace or a melamine-based HRWR produced by Cormix. The only other admixture used was Micro-Air, an AEA manufactured by Master Builders, Inc.

Either crushed granite or marine marl coarse aggregate meeting ASTM C33 #57 specifications was used. Virtually all the aggregate passed the 25-mm (1 in.) sieve. The crushed granite was a hard, angular aggregate of low absorption (0.4 percent). The specific gravity, saturated surface dry (SSD) was 2.64. The marine marl was a cubical to subangular, relatively porous, high-absorption (typically over 4.5 percent, but variable) shell limestone. The specific gravity, SSD of the marl was typically 2.48. Fine aggregate was the same in all mixes.

Test panels were designated by three letters. The first letter indicated the type of HRWR: H for naphthalene-based or V for melamine-based HRWR. The second letter indicated the type of aggregate: C for crushed granite or M for marine marl. The third letter designated whether the slab was insulated: I for insulated or N for noninsulated.

PRODUCTION, PLACEMENT, CURING, AND SAWING

The ready-mixed-concrete supplier operated a small dry-batch plant in Williamston. The plant did not have automated moisture control. The lack of automated moisture control and the sensitivity of the mix to variations in water created difficulty in maintaining the desired level of quality control. Because of scale capacity, batches were weighed out in two equal halves. Because of this, and adding the HRWR by hand, batching time was generally just under 10 min.

Field trial batches of 1.5 to 2.5 m^3 (2 or 3 yd^3) were conducted to fine-tune the mix for the raw materials used and to permit crews and supervisors to practice handling techniques. Strength levels were confirmed.

The trial batches went reasonably well, but early loads indicated difficulty in mixing, and subsequent batch sizes were reduced. Batch sizes were typically half the rated mixing capacity of the truck.

The specific batch sequence used for the North Carolina installation was to first load one-third of the batch water and two-thirds of the HRWR into the truck. Then, with the drum rotating at mix speed, approximately a third of both the fine and the coarse aggregate were added. Then the cement was ribboned in with the remaining aggregate. All of the AEA, the remaining water, and HRWR were then added. Typically 10 to 20 L (3 to 5 gal) of batch water, depending on the batch size, was held back for washing down the hopper during plant mixing. After mixing for a minimum of 70 revolutions at the plant, the mix was checked, at least visually, and sent to the job site.

The batch plant was close to the job site, and travel time was between 5 and 10 min. The DCI was added by hand and mixed, and the load was discharged. The concrete was placed by a bridge deck machine on rails, followed by hand floating and a burlap drag. The surface was tined as soon as possible and immediately covered with curing compound.

On sections to be insulated, plastic sheets were spread on the surface once it was tack-free. A sheet of rigid-foam building insulation 25 mm (1 in.) thick was then placed on the slab with weights to hold it down. Insulation was removed at the end of 6 hr.

Significantly, no cracking due to plastic shrinkage was noted on any of the slabs. Although the high humidity certainly contributed to this, other factors were important. First, everyone was anxious to get the surface finished and curing compound applied as soon as possible. The contractor would frequently mist the area, which was beneficial since these were nonbleeding mixes. Furthermore, the mixes were probably gaining strength faster than they were losing moisture; shrinkage-induced stresses were less than the strength of the concrete.

Premature cracking due to delayed sawing was a problem in two cases, though, for which sawing was delayed until the following day. In both cases, the slab had either cracked already or cracks ran out ahead of the saw blade. HPC may be more prone to cracks resulting from delayed sawing because of volume changes of the concrete at very early ages as it undergoes significant temperature changes. Interestingly, crack spacing was approximately 4½ m (15 ft).

Four test panels were placed during the first day, all containing naphthalene HRWR. Two panels were insulated, and two remained uncovered. One of the insulated panels was placed using crushed granite (HCI) and the other using marine marl (HMI), as were the noninsulated panels (HCN and HMN). Sections were completed with concrete of the same type as being tested.

Two test panels were placed in the next section. The concrete placed here contained crushed granite and melamine HRWR. One panel was insulated (VCI) and the other panel was not (VCN). Two test panels were also placed in the third section, which contained concrete produced using marine marl and melamine HRWR. Again, one panel was insulated (VMI) and the other panel was not (VMN).

The driving lane, placed in 1 day, contained both crushed granite and marine marl. Only routine testing was conducted on these mixes, since the primary purpose was to examine the effects of routine production rates on variability of the concrete as delivered.

TESTING PLAN

Slump and air content using the pressure method were determined for each batch. Cylinders 100 × 200 mm (4 × 8 in.) were fabricated for each panel for testing at 6 hr, 1 day, 7 days, 28 days, 6 months, and 1 year, using plastic molds with tightly fitting lids.

Where the concrete was to be insulated, the cylinders were also initially insulated by being placed in specially constructed "cubes" made by gluing layers of closed-cell, rigid-foam building insulation together and sawing out holes for the cylinders (in their molds). A fully loaded cube could be lifted by two individuals.

Beams 100 × 100 × 400 mm (4 × 4 × 16 in.) were cast in some cases; however, test results were extremely variable and beam data provided little useful information.

A number of Type-T copper-constantan thermocouples were placed in the pavement and in some cylinders to monitor temperatures.

Cylinders were transported to the North Carolina Department of Transportation testing laboratory, close by in Williamston, either just before testing at 6 hr for insulated cylinders or at about 20 hr for all other cylinders. All insulated cylinders were removed from the insulating cubes at 6 hr, regardless of age at testing. Cylinders were stored outside the laboratory until tested. The cylinders remained in the plastic molds, after the lids had been removed at 1 day. The cylinders were thus exposed to conditions that were very similar to those of the pavement.

Rapid chloride permeabilities (RCPs) were determined in accordance with AASHTO T277 from specimens cut from the top of cores removed from the slab. Duplicate cores were used to obtain specimens for determination of RCP, as opposed to two slices from the same core.

TEST RESULTS AND DISCUSSION OF RESULTS

A synopsis of data for all test panels is given in Tables 1 and 2. Nominal water-cement ratios for all mixes were between 0.33 and 0.35. All results are the average of two specimens. The 28-day core results are not shown because they were accidentally taken at the wrong locations.

Seventeen batches of concrete were produced during the 3 days of slow construction rate placement. Slumps ranged from 45 mm (1¾ in.) to 150 mm (6 in.); 70 mm (2¾ in.) was the average. Air contents during this period ranged from 4.2 to 9.2 percent, with an average of 6 percent.

Sixteen batches were produced in the long section placement. All concrete placed there was to be noninsulated, and somewhat higher dosages of HRWR were used to increase the slump. Slumps during this phase of construction ranged from 50 mm (2 in.) to 240 mm (9½) in., with a 130-mm (5-in.) average. Air contents ranged from 4.4 to 10.3 percent, with an average of 7 percent.

Air contents and slumps were generally within desired limits; but variability in slump and air during the long placement was higher than that during the shorter, slower placements. Although this variability may be related to some reduction in the level of batch to batch control, much of it, along with generally higher values of slump and air, may be due to holding trucks for a shorter time for testing and adjustment.

Two strength-time criteria—14 MPa (2,000 psi) at 6 hr and 34 MPa (5,000 psi) at 24 hr—were investigated. Strengths of insulated panels met the 6-hr target in all but one case. Strengths of noninsulated panels were also relatively high. This is almost certainly due to the high ambient temperatures at the time of placement. Two mixes, VMI and VMN, did not meet the required strength at 6 hr. These mixes contained a very large quantity of HRWR, which caused retardation of the mix and low early strengths, although strengths at 1 day were comparable to the other mixes.

Strengths at 1 day did not all meet the criteria for 24-hr strength but were fairly close. Average 1-day cylinder strength for the test panels was greater than 34 MPa (5,000 psi), however. Average 28-day cylinder strength was about 50 MPa (7,300 psi).

Crushed granite mixes had higher strengths than did mixes produced with marine marl. Additionally, mixes

TABLE 1 Concrete Batch Properties, SHRP C-205 Field Data Synopsis, Williamston, N.C.

ID	HCI	HMI	HMN	HCN	VCI	VCN	VMI	VMN
Batch (m^3)	4.6	4.6	3.1	3.1	3.1	4.6	4.6	4.6
Batch (yd^3)	6	6	4	4	4	6	6	6
Slump (mm)	90	55	55	150	75	90	75	45
Slump (in)	3 ½	2 ¼	2 ¼	6	3	3 ½	3	1 ¾
Air (%)	6.1	5.5	6.8	4.9	6.2	5.7	8	6.4
Cylinder Temp (°C)								
placed	33	32	33	32	32	31	32	35
max	na	61	60	57	na	na	na	na
Slab Temp								
placed	32	34	34	na	32	33	34	35
max	na	67	52	na	59	57	na	na

"na": data not acquired; °F = (1.8 × °C) + 32

TABLE 2 Compressive Strengths and RCP, SHRP C-205 Field Data Synopsis, Williamston, N.C.

ID	HCI	HMI	HMN	HCN	VCI	VCN	VMI	VMN
Cylinder Strength (MPa)*								
6 hrs	16.0	22.5	15.2	12.3	14.9	9.2	2.9	2.6
1 day	36.4	42.0	33.4	31.5	35.6	36.5	33.2	32.4
28 days	52.4	53.0	50.4	53.5	48.3	50.7	42.1	45.3
6 mo	61.8	63.3	57.0	63.6	58.2	63.6	50.1	52.5
12 mo	65.3	64.3	55.2	65.8	61.4	63.6	49.3	52.9
18 mo	70.4	62.2	59.2	70.7	65.5	67.2	51.0	54.9
Cylinder Strength (selected) (psi)*								
6 hrs	2320	3260	2200	1780	2160	1340	420	380
1 day	5280	6090	4850	4570	5170	5290	4820	4700
28 days	7600	7680	7310	7760	7000	7360	6100	6570
18 mo	10,210	9020	8580	10,250	9510	9750	7400	7960
Core Values at 12 months								
fc (MPa)	60.3	51.5	47.5	66.9	61.4	62.6	45.6	55.4
fc (psi)	8750	7470	6890	9700	8910	9080	6620	8030
RCP (c)*	1650	3160	1150	2000	1510	1030	2260	1810

* *Compressive strength from 100 mm x 200 mm (4"x8") cylinders, cores 100 mm (4") diameter; RCP: rapid chloride permeability (coulombs), all values are the average of two specimens.*

with naphthalene HRWR tended to outperform mixes with melamine HRWR at later ages, as expected. HPC continued to gain strength with time, under typical field exposure conditions.

RCP results indicate that the concrete is only moderately permeable to chlorides, although results are generally low. These results should be viewed with caution, however, because the presence of any soluble salt, such as calcium nitrite, can increase the measured value by reducing the resistivity of pore solution in the concrete. The concrete is therefore probably less permeable than RCP data indicate. There is no clear pattern to RCP values on the basis of the type of insulation, aggregate, or HRWR.

CONCLUSIONS AND RECOMMENDATIONS

A thorough briefing of all participants before any construction and adequate full-size trial batches to adjust mix proportions and give the participants practice in handling the concrete is essential.

Stricter-than-usual control of aggregate moisture is required because of the increased sensitivity of HPC to water content.

Mixing capability of trucks is critical, particularly in a dry-batch operation. Volume of HPC batched should exceed neither two-thirds of the rated mixing capacity of a ready-mixed-concrete truck nor, in many cases, half of the rated mixing capacity.

No apparent problem was found with plastic shrinkage cracking of these pavements; however, sawing of concrete must occur as early as practicable.

Using insulation, it is possible to attain compressive strengths of 14 MPa (2,000 psi) within 6 hr under typical summer working conditions in North Carolina, using HPC. One-day strengths of 34 MPa (5,000 psi) were attained in all cases with 6 hr of insulation, but without insulation, strengths were frequently 1.5 to 2 MPa (200 to 300 psi) below the 34-MPa (5,000-psi) criteria.

HPC continues to gain strength with time, under typical field exposure conditions and without exposure to continuous moist curing.

ACKNOWLEDGMENTS

The authors gratefully acknowledge the support provided by SHRP, a unit of the National Research Council authorized by Section 128 of the Surface Transportation and Uniform Relocation Assistance Act of 1987. The authors also appreciate the contributions of the general contractor, the ready-mixed-concrete supplier, and the raw materials suppliers, without whose whole-hearted cooperation these investigations would have been impossible. In particular, the cooperation and patience of the North Carolina Department of Transportation are deeply appreciated.

Publication of this paper is sponsored by Committee on Mechanical Properties of Concrete.

Damage to Aircraft Parking Ramps from Jet Oils and Auxiliary Power Units

MICHAEL C. MCVAY, CHARLES W. MANZIONE, AND JAMES G. MURPHY

The precise cause for concrete damage observed in the vicinity of parked B-1 and F/A-18 aircraft has been determined. The combination of downward-directed auxiliary power unit (APU) blast and spilled aircraft oils are responsible for the scaling observed at these sites. Laboratory tests confirmed that ester-based lubricating oils and hydraulic fluids are chemically reacting with the hydroxyl component from the calcium hydroxide or the calcium silicate hydrate in the concrete and destroying the bond. The cyclic heating of the pavement by the APU greatly accelerates the reaction and facilitates the mixing and refluxing of aircraft fluids with the aqueous calcium hydroxide present. Laboratory techniques are demonstrated that duplicate the chemical reactions occurring in the field and allow for quick and accurate assessment of new materials before field testing. In addition, hydrolysis of lubricating oils and hydraulic fluids was replicated in a controlled laboratory experiment within 5 weeks, eroding a 10-cm (4-in.) concrete slab that was kept partially submerged in water.

Jet exhaust damage to concrete is not new, and it manifests itself in more than one form. For two decades, the F-4 aircraft eroded engine run-up pavements around the world. Today, the vectored thrust of the next generation of Harrier aircraft can spall a durable concrete surface in seconds. However, direct blast from the main engines of jet aircraft is not the only cause of surface damage. During the 1980s, the United States Air Force, Navy, and Marine Corps began to experience concrete scaling that was quite different from past erosion and spalling. This more recent damage, which is found on B-1 and F/A-18 parking aprons, is evident in parking areas on which auxiliary power units (APUs) impinge upon oil-soaked surfaces. This research has uncovered evidence that decisively separates the causes of concrete damage under vectored thrust from that related to aircraft APUs.

APUs

APUs were developed to provide aircraft generation support without having to use cumbersome ground equipment or run the main engines. They provide power for all electrical and hydraulic systems when the aircraft is parked and they can be used to start the main engines.

APUs are small turbojet engines with jet pipe exhaust temperatures of approximately 550°C (1,000°F) and exit velocities of about 135 m/sec (440 ft/sec). The exhausts of the B-1 and F/A-18 come out the bottom of the aircraft approximately 1.5 m (60 in.) and 1.0 m (40 in.) above the pavement, respectively, with angles of incidence of 45 degrees to the ground plane. Navy reports show the single exposure of an APU to be as long as 45 min, but 5 min is typical (*1*). APUs on the B-1, however, commonly run for 1 hr or more. Both the Navy and the Air Force have reported surface temperatures above 175°C (350°F) with exhaust velocities of more than 62 m/sec (203 ft/sec) at the pavement surface during APU operations. The location of the APU on an aircraft is normally one of the last design considerations. However, pavement damage and the potential for foreign object damage to jet engines have given more attention to APU placement on future aircraft.

M. C. McVay, Department of Civil Engineering, University of Florida, Gainesville, Fla. 32611. C. W. Manzione and J. G. Murphy, Air Force Civil Engineering Laboratory, Tyndall Air Force Base, Fla. 32403.

SURFACE SCALING UNDER APUs

Each F/A-18 and B-1 aircraft is assigned a parking space on the apron, from which it seldom deviates. Aircraft maintenance is performed on the aircraft while it is sitting on the parking ramp. The scaling is found in areas of APU blast impingement where large amounts of spilled lubricants, hydraulic fluids, and jet fuels have been either vented by the aircraft or spilled during routine maintenance.

In the past, the Navy often rearranged aircraft parking layouts to reduce the potential for foreign object damage to the aircraft. And the Navy and Air Force have experimented with heat-resistant diabase aggregate, refractory concrete, and surface coatings (*2*). All have resulted in less than a year of service life. Steel plates bolted to the pavement at impingement locations are being used successfully by the Navy and the Air Force. After 4 years of service, the plates have prevented concrete scaling; however, they pose several operational safety problems and are considered to be only a temporary solution.

OBJECTIVE AND SCOPE OF WORK

The objective of this research is to identify the source of scaling under aircraft and propose a solution. Investigators from the Operability and Repair Branch of the Air Force Civil Engineering Support Agency (AFCESA) traveled from Tyndall Air Force Base near Panama City, Florida, to several bases to see the damage and collect concrete samples. Subsequent laboratory work concentrated on (a) reproducing the field damage under controlled conditions, (b) performing chemical analysis on field samples to assess the material alteration and its significance, (c) developing a laboratory test that can screen potential repair materials before field testing,

and (d) offering recommendations to mitigate or eliminate this type of concrete damage.

FIELD INVESTIGATION

Researchers visited Cecil Field (F/A-18), Beaufort Marine Corps Air Station (F/A-18), and McConnell Air Force Base (B-1) in June and July 1991 to survey the damage and collect samples. The damaged concrete pavements at Cecil were made from granite, diabase, or soft limerock coarse aggregate, depending on the location on the airfield, and quartz sand. The Beaufort aprons were of granite or tough limestone aggregate and quartz sand. The McConnell concrete contained limestone aggregate. Inspection revealed that the zone of damage was confined to the APU impingement area in the presence of large spills of hydraulic fluid and lubricating oils.

Figure 1 is typical of the scaled concrete surface; the steel plate in the foreground is one of scores placed at Cecil Field to temporarily prevent further damage. Figure 2 is a close-up of a scaled piece of concrete that was easily flipped with fingertips. Initially, because of large amounts of exposed aggregate, it appeared the concrete aprons were delaminating at the paste-aggregate interface (Figure 3). However, the size of the scale and the entrapment of aggregate in scalings such as this suggested that the problem was not related to surface finishing. Full-depth cores 15 cm (6 in.) in diameter and 38 cm (15 in.) long were taken from the damaged areas; these cores revealed lubricant penetration from 1 to 2 cm (0.40 to 0.75 in.). Cores taken outside the zone of APU impingement, but within the fluid spill area, showed no surface damage and less oil penetration.

FIGURE 1 Concrete damage related to APU.

FIGURE 2 Scaling typical in older pavements.

LABORATORY RESULTS

Slab Testing

Work was initiated at AFCESA to reproduce the field damage under controlled laboratory conditions. This entailed cyclic heating of two 1-year-old concrete slabs that were 0.92 m (3 ft) in diameter and 10 cm (4 in.) thick. Concrete aggregates were crushed limestone and silica sand. The heat source was a radiant heater with a 15.2-cm (6-in.) ceramic core controlled by a thermocouple attached to the center of the heated area. The heater cycled temperatures on the concrete surface to 162°C (350°F) for up to 2 hr, allowing at least 1 hr of cooling time between cycles. Two or three cycles per day, excluding weekends, were completed. One slab was continuously coated with hydraulic and lubricating fluids, and the other was not treated with oils. Both slabs were kept submerged in water throughout the 25-day period, except for the top 2.5 cm (1 in.), to simulate availability of water in the field.

Initially, fines appeared on the surface of the slab treated with the hydraulic and lubricating fluids. After 5 weeks of cyclic heating, 10-mm (⅜-in.) aggregate started breaking loose from the surface. The damage was more like surface erosion than the scaling found in the field. There was no erosion observed in the slab that was not exposed to oils.

Chemical Investigative Tools Used

Because the scalings from the specimens were friable and rancid-smelling, they were considered to have been chemi-

FIGURE 3 Delamination of concrete below carbonated surface.

cally altered. These scalings were different from the spalled concrete resulting from jet blast, which is stronger and exhibits no material alteration.

Consequently, a chemical study of the damaged concrete was initiated at both AFCESA and the Materials Directorate of Wright Laboratory (*3*). This entailed gas chromatography/mass spectroscopy (GC/MS) and scanning electron microscopy (SEM) with energy dispersive analysis X-ray at AFCESA; and GC/MS, infrared spectral analysis (IR), and X-ray diffraction (XRD) at Wright Laboratory. It was conjectured that the esters in lubricating oils (MIL-L-7808 and MIL-L-23699) and hydraulic fluids (MIL-H-83282) could have been hydrolyzing. Of the two major constituents of the spilled fluids—hydrocarbons and esters—only esters have been known to be detrimental to concrete (*4*).

Hydrolysis of Oils

Esters, which are chemically combined acids and alcohols, will break down (hydrolyze) when heated in an aqueous acid or base solution (*5*). Discussions with Hatco, a major manufacturer of raw materials in lube oils and hydraulic fluids, reveal that lubricating oils are composed of 90 to 95 percent ester blends and that hydraulic fluids are 30 to 40 percent esters.

If the oils or hydraulic fluids were undergoing hydrolysis, it would have to be of an alkaline variety, since the pH of concrete may be as high as 12. This is due to the strong base calcium hydroxide [$CA(OH)_2$, pH = 12.4], which exists in both solution and crystal form in hardened portland cement concrete (*6*,p.867). Large and extensive crystals have been reported in young concrete in which 25 percent of the paste is calcium hydroxide (*7*). This is also true in very old cement paste (*8*). It has been reported that, for some aggregate types, calcium hydroxide provides both the bond as well as the load transfer mechanism between the aggregate and the cement mortar (calcium silicate hydrate) (*9*).

The reaction (*5*),

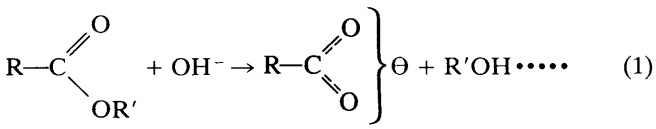

(1)

ester hydroxide salt alcohol

under alkaline conditions, produces the salt of the carboxylic acid and liberates the alcohol. In this reaction, the calcium hydroxide provides the (OH^-) anion, and the calcium (Ca^{2+}) cation is used in the formation of the acid salt. Believing this reaction to have caused the scaling observed, researchers set out to identify the products found on the scalings.

Identifying Reaction Products in Field Samples

At AFCESA, samples of the damaged concrete were crushed and mixed with an aqueous solution of sodium chloride and filtered. (Calcium salts of the fatty acids are slightly soluble in water, a polar medium, and insoluble in hexane, a nonpolar solvent; whereas acids are soluble in hexane but not in water). The filtered wash was then split into two portions with one portion being mixed with hexane, which was subsequently extracted and injected into the GC/MS. This ensured that the aqueous sodium chloride wash did not contain any hydraulic fluids or lubricating oils. The second portion of the sodium chloride wash was mixed with concentrated hydrochloric acid, which would convert any salts present into their fatty (carboxylic) acid counterparts. Hexane was added, the whole mixture was shaken, and the hexane was extracted and injected into the GC/MS. Comparing the resulting mass spectra to library values revealed the presence of hexanoic, octanoic, and nonanoic acids, components of esters found in turboshaft oil. It was then deduced that the salts that produced these acids were residua from spilled turboshaft oil.

Using IR spectrum, Wright Materials Laboratory found that the lubricating oils and hydraulic fluids were absent in the surface scalings but that limestone was very much evident. It was thought that the oils that had penetrated the scaled surface had broken down in presence of the calcium hydroxide.

Wright Materials Laboratory used water alone for its GC/MS extraction. Comparing the mass spectra to library values revealed that the salts had been converted into hexanoic, octanoic, and decanoic acids, when mixed with concentrated hydrochloric acid. All of these acids are straight-chain fatty acids found in the esters of turboshaft oil (MIL-L-7808 or MIL-L-23699). Presence of these calcium salts in the damaged concrete proved that hydrolysis of the lubricants had occurred.

Carbonization in Field Concrete

XRD spectrometry of both sides of the scaled concrete specimens at Wright Laboratory revealed the presence of quartz and calcium carbonate, but not of calcium hydroxide. It appeared that the calcium hydroxide had been converted to limestone by the carbon dioxide made available as a by-product of burned hydrocarbons in the jet exhaust. As shown earlier in Figure 2, some of these scalings had aggregate embedded in them.

To confirm the carbonization of the old surface, a core from an undamaged area was cut into 6-mm (0.25-in.) slices that were treated with a solution of phenolphthalein and alcohol. If the solution contacts a base with a pH greater than 9, it will turn violet. The surface of the top slice did not change color, indicating that complete carbonation had occurred; however, its bottom and both sides of all the other slices turned almost completely violet, indicating the presence of the calcium hydroxide. SEM investigation of the bottom of the top slice revealed calcium hydroxide's classical hexagonal platelets (*10*), validating the phenolphthalein's indication of the presence of calcium hydroxide.

Treating the bottom of the scalings from the damaged area with phenolphthalein caused a few vague violet patches, but many clear areas; none of the exposed aggregate surfaces was violet. All of the hydroxyl ion had been consumed.

In short, IR and GC/MS showed that ester hydrolysis was occurring; XRD showed that calcium hydroxide had been depleted; and the SEM and phenolphthalein solution con-

firmed that calcium hydroxide had been consumed in the damaged concrete.

FAILURE MECHANISM

Role of Temperature and Carbonization

Heat from the APU plays a significant role in the damage process by accelerating the chemical reaction that ultimately leads to scaling of the concrete. A rule of thumb for any chemical reaction is that the reaction rate doubles for every increase in temperature of 10°C (18°F) (*5*).

An inspection of concrete eroded by spilled vegetable oils at neighborhood fast-food stores (Figure 4) indicated that hydrolysis of fatty oils by the hydroxyl ion does not have to have heat to occur. However, as seen in Figures 2 and 3, the older pavements investigated during this study were scaling instead of eroding. This scaling always appeared to originate from weakened planes beneath the surface layer of concrete. As stated earlier, IR and phenolphthalein tests showed that the calcium hydroxide on the surface of these old pavements had already been depleted through contact with carbon dioxide to form a thin layer of calcium carbonate that did not react with spilled oils under the aircraft.

FIGURE 4 Hydrolysis of vegetable oils by newer pavement.

Thermal Cycling Enables the Process

To explain how the oils established contact with the calcium hydroxide just below the surface of the concrete, the following was observed from the field cores, but has not been verified. With the application of heat, the free moisture in the top 6 to 13 mm (0.25 to 0.50 in.) on the concrete is driven out. After the heat is removed and the pavement begins to cool, lubricating oils and hydraulic fluids on the surface as well as free moisture from within the concrete are sucked into the upper layers of the pavement. Rock or concrete with a liquid saturation of 0.2 percent or less has been reported to have suction pressures on the order of 10 MPa (1,450 psi) (*11*). When the APU is again fired up, the penetrating heat reaches the calcium hydroxide in solution, it hydrolyzes the esters in the absorbed fluids, liberating alcohol and forming calcium salts of the carboxylic (fatty) acids. For extensive heat durations (tens of minutes) and surface temperatures exceeding 100°C (212°F), the liquid moisture is converted to steam, expelling the oils, and the salts of the fatty acids are precipitated out in solid form. Upon cooling, the process repeats itself, and new oils are sucked in from top and water from below.

Role of Calcium Hydroxide

The hydroxyl ion is being consumed in each cycle. It is thought that calcium hydroxide provides one source of base for the

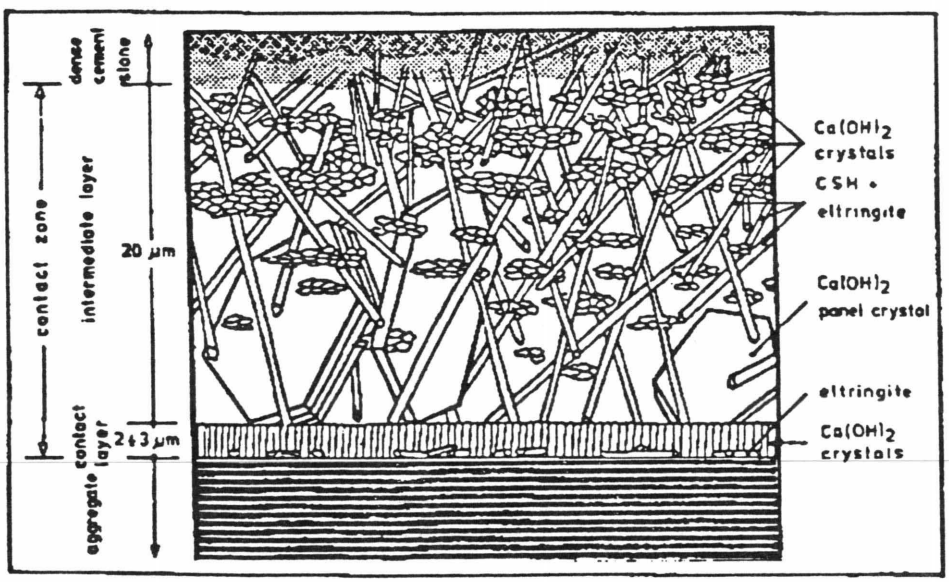

FIGURE 5 Model of paste-aggregate interface (*9*).

hydrolysis, to form the alcohol and the calcium salt of the fatty acid. The salts are soft, slightly soluble, and white (unless they have a red tinge from dye in hydraulic fluid). These salts replace the calcium hydroxide crystals. Damage may take months to become evident because of the low solubility of calcium hydroxide in water, limiting its availability for reaction.

Figure 5 illustrates the contact between the cement mortar (calcium silicate hydrate) and the aggregate in an early stage of the hydration process (*9*). With time and increased hydration the intermediate layer is overlapped by more of the panel-shaped calcium hydroxide crystals and the cement mortar. Zimbelmann states that the load transfer between the cement mortar and the aggregate is provided mainly by the large hexagonal platelets of calcium hydroxide (*9*). Both the contact layer around the aggregate and the large platelets of calcium hydroxide are probably being consumed in the hydrolysis process.

The hydroxyl ion can also come from the hydrated silicate and aluminate phases of the cement. Here, the calcium silicate hydrate cement decalcifies and converts to a highly porous form of silica.

Onset of Scaling

Eventually, as the available hydroxide is depleted, thermal differential stresses and aircraft loads will exceed the strength of the weakened mortar-aggregate bonds and cause planar failure or scaling 6 to 13 cm (0.25 to 0.50 in.) thick.

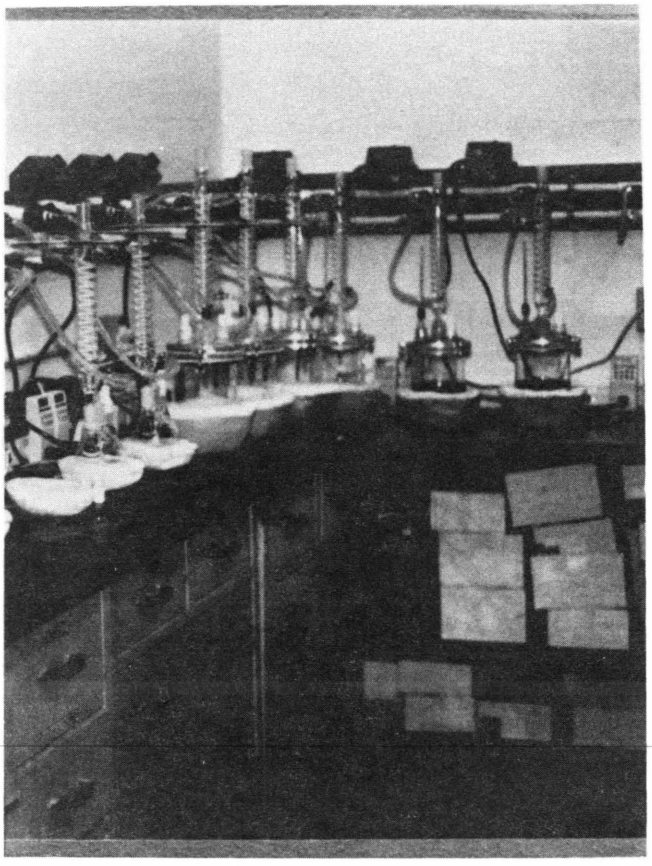

FIGURE 6 Laboratory setup to replicate field damage.

FINDING REPLACEMENT MATERIALS

After establishing that hydrolysis was leading to scaling, the search for a solution focused on finding materials that would either delay or stop the reaction. Since scaling takes months to materialize in the field, a laboratory testing scheme was developed that could replicate and accelerate field conditions.

Laboratory Setup

The laboratory setup included the use of Erlenmeyer flasks (for crushed material) and kettles (for solid pieces) that could simulate (in reaction vessels) the mixing and refluxing of oils and water that takes place in the field at elevated temperatures (Figure 6). Up to 24 vessels could be used simultaneously; each vessel could independently test a different material at controlled temperatures. After the material hydrolyzed, the

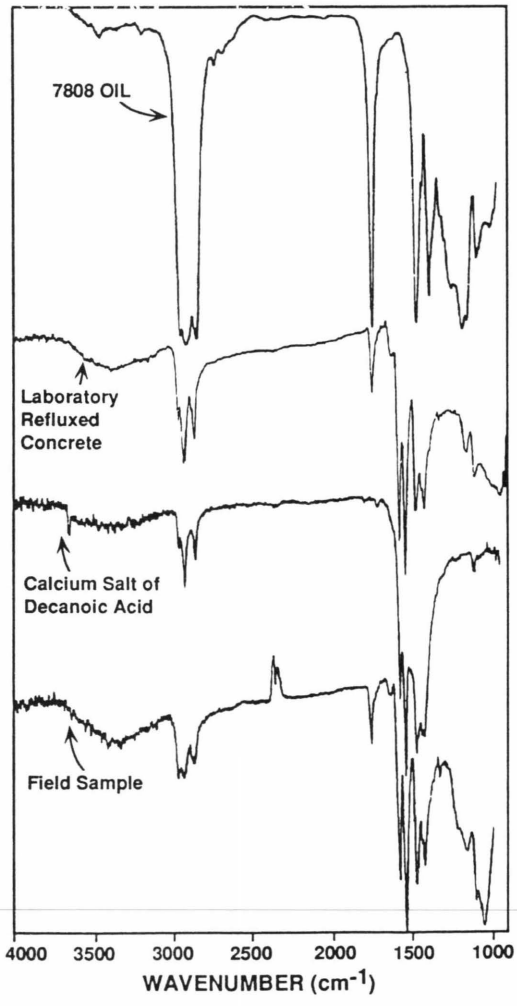

FIGURE 7 FTIR spectra for laboratory and field samples.

products formed were identified using Fourier transform infrared (FTIR) analysis. Next, cylinders 2.5 cm (1 in.) across and 5.1 cm (2 in.) high were tested. The cylinders were either sliced and run through the FTIR using a contact sampler or used for unconfined compressive strength tests.

Initial Tests

Tests initially compared field scalings with laboratory concrete made from finely crushed quartz aggregate and a water-cement ratio of 0.5. The vessel contained 10 percent concrete, 20 percent oil, and 70 percent water by volume. After five 24-hr days of refluxing, FTIR analysis of the hydrolyzed products formed are shown in Figure 7. The characteristic peak of calcium hydroxide shown in the laboratory sample was absent in the field scalings, indicating that it had been consumed by carbonation or ester hydrolysis. In addition, the acid spectra from both the laboratory and filed samples matched. The lab sample shows approximately twice as much transmittance as the field sample, indicating twice the number of salts. This verified that the experimental technique was performing as designed. Therefore, any material could be quickly and accurately assessed for ester hydrolysis.

Screening Replacement Materials

A number of materials ranging from lower to neutral pH binders were evaluated in the laboratory. Table 1 identifies the pH of the refluxed liquids after 3 days and indicates if any fatty acid salts were generated. Four replacement materials did not hydrolyze: three acid-base cements and a Furan polymer. Generally, an 18 percent loss in strength occurred for all specimens that salted. On the basis of this laboratory screening, all three acid-base cements have been placed at both B-1 and F/A-18 locations and are undergoing evaluation.

CONCLUSIONS

Concrete damage to B-1 and F/A-18 parking aprons in the vicinity of APU impingement is caused by the chemical reaction (hydrolysis) between spilled lubricating and hydraulic oils and the hydroxyl ion in the cement. Cyclic heating from the APU makes it possible for the oils to penetrate the concrete accelerating the hydrolysis process, which transforms the calcium around the aggregate and in the paste into salts of fatty acids, destroying the paste-aggregate bond. Evidence shows that the degree to which the concrete is damaged depends on the ability of the oils to penetrate. Therefore, it is believed that more permeable concretes incur more damage. Because of the carbonation of the surface of older pavements, oils must penetrate deeper to cause damage.

It is inferred that any hydraulic concrete system, whether acid or base, will hydrolyze and scale if jet oils are allowed to penetrate. The simplest solution to this problem is to keep all the lubricating and hydraulic oils off the pavement, especially in the vicinity of heat impingement. APU temperatures are not high enough, by themselves, to damage concrete. If oils cannot be kept off the pavement, the heat should not be allowed to impinge onto the spill areas since heat facilitates and accelerates the hydrolysis process. The use of steel plates appears to be working at Dyess Air Force Base and Cecil Field because the pavement is shielded from this heat.

Finally, the cement binder might be replaced by a neutral (or close to neutral) material with a pH between 6 and 8, such as a polymer concrete, phosphatic concrete, or ceramic. Several candidate materials in this category have already passed

TABLE 1 Change in pH of Replacement Materials

Sample	Before	After	Salt Generated
OPC	12.3	8.0	Yes
Magnesium Phosphate	8.7	8.1	No
Alumina Phosphate	5.6	5.2	No
Phoscrete (Magnesium & Alum.)	8.0	8.3	No
Furfuryl Alcohol	4.3	4.3	No
High Carbon OPC	12.2	11.2	Yes
10% Polyvinyl Alcohol Modified OPC	12.0	9.4	Yes
Calcium Sulfate	12.0	7.8	Yes
Room Curable Ceramic	11.0	8.5	Yes

NOTE: OPC = ordinary portland cement.

laboratory screening tests, have been placed in the field, and are undergoing evaluation.

ACKNOWLEDGMENTS

This research was funded by the AFCESA at Tyndall Air Force Base, Florida, and the Air Force Office of Scientific Research. The authors appreciate the assistance of Lee Smithson, director of the Materials Integrity Branch of Wright Laboratory, Wright Patterson Air Force Base, Ohio.

REFERENCES

1. M. L. Houck. *F-18 Auxiliary Power Unit Exhaust Gas Footprint Evaluation Test*. Final Report NAPC-LR-90-18. Naval Air Propulsion Center, Trenton, N.J., 1990.
2. G. Y. Wu. *Protective Coatings for F/A-18 Airfield Pavement*. Technical Memorandum 53-88-15, Program Y1316-001-04-030. Naval Civil Engineering Laboratory, Port Hueneme, Calif., 1988.
3. M. C. McVay, L. D. Smithson, and C. W. Manzione. *Chemical Damage to Airfield Concrete Aprons from Heat and Oils*. American Concrete Institute, Detroit, Mich., 1992.
4. F. M. Lea and C. H. Desch. *The Chemistry of Cement and Concrete*. Edward Arnold Publishers, London, England, 1956.
5. R. T. Morrison and R. N. Boyd. *Organic Chemistry*. Allyn and Bacon Publishers, Boston, Mass., 1977, Chapter 20.
6. W. H. Nebergall, F. C. Schmidt, and H. F. Holtzclaw. *College Chemistry*. D. C. Heath and Company Publishers, Lexington, Mass., 1972.
7. S. H. Kosmatka and W. C. Panarese. *Control of Concrete Mixtures*. Portland Cement Association, Skokie, Ill., 1988.
8. D. L. Rayment. The Electron Microprobe Analysis of the C-S-H Phases in a 136-Year-Old Cement Paste. *International Journal of Cement and Concrete Research*, Vol. 16, No. 3, 1986, pp. 341–344.
9. R. Zimbelmann. A Contribution to the Problem of Cement-Aggregate Bond. *International Journal of Cement and Concrete Research*, Vol. 15, No. 5, 1985, pp. 801–808.
10. D. Walsh, M. A. Otooni, M. E. Taylor, and M. J. Marcinkowski. Study of Portland Cement Fracture Surfaces by Scanning Electron Microscopy Techniques, *Journal of Materials Science*, Vol. 9, No. 3, 1974, pp. 423–429.
11. C. Doughty and K. Pruess. A Similarity Solution for Two-Phase Fluid and Heat Flow near High-Level Nuclear Waste Packages Emplaced in Porous Media. *International Journal of Heat and Mass Transfer*, Vol. 33, No. 6, 1990, pp. 1205–1222.

Publication of this paper sponsored by Committee on Mechanical Properties of Concrete

Application of Silica Fume in Synthetic Fiber–Reinforced Concrete

ZIAD BAYASI AND TAHIR CELIK

The effect of silica fume on the properties of synthetic fiber–reinforced concrete was assessed. Two fiber types were used: fibrillated polypropylene fibers and polyethylene-terphalate polyester fibers. Various fiber volume fractions were examined. Fiber volumes ranged from 0 to 0.6 percent, and fiber length was 12 mm (½ in.). Silica fume was used as partial replacement of portland cement on an equal-mass basis at 0, 5, 10, and 25 percent. The fresh mixtures were tested for slump, inverted slump cone time, and air content. The hardened concrete material was tested for compressive and flexural behaviors as well as impact resistance. Rapid chloride permeability was also measured. The purpose of the experimental investigation was to assess the suitability of synthetic-fiber silica-fume concrete for application in bridge-deck overlays and other applications for which the mechanical properties and permeability are important. The results indicate that silica fume is useful in improving the effectiveness of fiber reinforcement of concrete and reducing its permeability.

Silica fume is a by-product in the manufacture of silicon and ferrosilicon alloys. It is composed of fine particles with high silica (SiO_2) content (average particle size of the order of 0.1 micron = 4×10^{-6} in.). The use of silica fume in concrete as an admixture is common (*1*). Silica fume reacts with hydrated lime existing in cement paste, and calcium silicate hydrate is obtained. Calcium silicate hydrate contributes to the improvement of concrete properties, including strength, impermeability, and durability (*1*).

Various types of synthetic fiber are used for concrete reinforcement. They reduce shrinkage and cracking and enhance impact resistance and toughness (*2*). Silica fume has been found to have beneficial effects on the performance of steel fiber concrete (*3,4*). It was found that silica fume helped to enhance the interfacial bond between fibers and cement paste. As a result, the reinforcement effect of fibers in concrete was improved (Figure 1). The use of silica fume as a part of binder in concrete significantly reduces workability, air content, and permeability, but it increases compressive and flexural strengths (*1–3,5*). Optimum addition of silica fume reduces bleeding of concrete—a reduction that prevents early moisture loss from freshly placed concrete, which in turn reduces plastic shrinkage cracking.

The fineness and high pozzolanic reactivity of silica fume contribute to the enhancement of the density and adhesion capacity of cement paste, especially with other additives including fibers (*1–3,5*). Enhanced bonding between fibers and the cement matrix contributes to the strength and ductility of steel fiber–reinforced silica-fume concrete. One type of fiber commonly used is polypropylene fiber. Compared with unmodified concrete, concrete reinforced with polypropylene fiber has significantly less bleeding, less segregation, and lower plastic shrinkage cracking. Furthermore, polypropylene fiber–reinforced concrete shows increases in flexural fatigue strength and impact resistance, and it has shown reduced drying shrinkage cracking (*2,6*).

Polyester fibers have also been used to reinforcement concrete. Increases in flexural strength, toughness, and impact resistance were among the benefits of such reinforcement.

EXPERIMENTAL

Materials

Mix Type A: Monofilament Polyester Fiber–Reinforced Concrete

Type II portland cement was used for Mix A; coarse aggregate was pea stone with a maximum size of 9 mm (⅜ in.). The

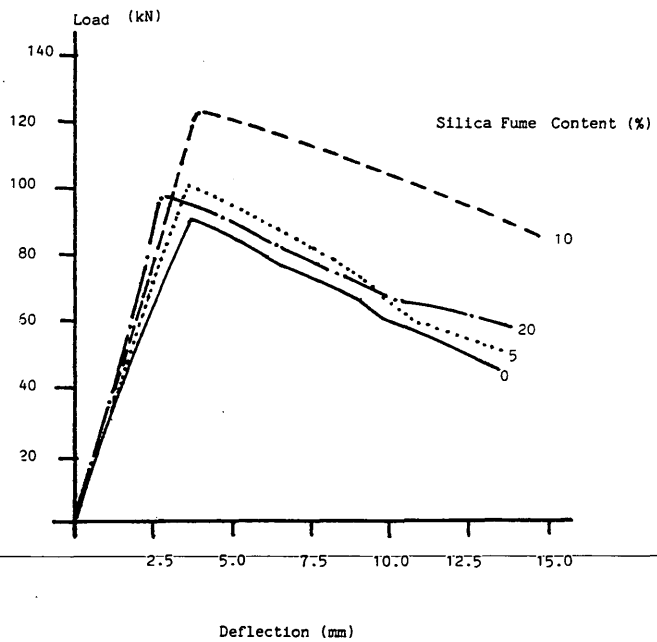

FIGURE 1 Flexural load-deflection relationships of silica-fume concrete.

Z. Bayasi, Department of Civil Engineering, San Diego State University, San Diego, Calif. 92182. T. Celik, Department of Civil Engineering, San Diego State University, San Diego, Calif. 92182; current affiliation: Department of Civil Engineering, Eastern Mediterranean University, Famagusta MERSIN-10, Turkey.

fine aggregate was sand with a modulus of 3.8. A naphthalene formaldehyde sulfonate–based superplasticizer was used; this superplasticizer has been found to be compatible with silica fume and maintains its effectiveness over a long period (*7*).

Polyethylene-terphalate (PET) polyester fibers with the following characteristics were commercially available (*8*):

- Diameter = 50 microns (0.002 in.)
- Specific gravity = 1.3
- Tensile strength = 380 MPa (55 ksi)
- Elastic modulus = 1.9×10^4 MPa (2,800 ksi)
- Fiber length = 12.5 mm (0.5 in.)

The chemical composition of the commercially available silica fume is given in Table 1; the physical properties are as follows (*9*):

- Specific gravity = 2.3
- Bulk density = 225 kg/m^3 (14 lb/ft^3)
- Specific surface = 200 000 cm^2/g (14×10^6 in.^{2}/lb)
- Average particle size = 0.14 microns (4×10^{-5} in.)
- Particles smaller than 45 microns (0.018 in.) = 99.5 percent

Mix proportionings were performed by the mass batching method. Silica fume was used as a partial replacement of cement on an equal-mass basis. For all the mixes in this series, the ratio of aggregate (fine and coarse) to binder (cement and

TABLE 1 Chemical Composition of Silica Fume

Chemical Compound	Percentage of Total Mass
SiO_2	96.5
C	1.40
Fe_2O_3	0.15
MgO	0.20
Al_2O_3	0.15
K_2O	0.04
Na_2O	0.20

TABLE 2 Mix Design Program

Mix No.	Designation	Fiber Volume %	Silica Fume /Binder (%)	Mix Type
1	Standard 1	0.0	0.0	A
2	Series	0.15	0.0	A
3	No. 1	0.35	0.0	A
4		0.60	0.0	A
5	Series	0.00	5	A
6	No. 2	0.15	5	A
7		0.35	5	A
8		0.60	5	A
9	Series	0.15	10	A
10	No. 3	0.35	10	A
11		0.60	10	A
12	Series	0.15	25	A
13	No.4	0.35	25	A
14		0.60	25	A
15	Standard 2	0.00	0.0	B
16	Series	0.10	0.0	B
17	No.5	0.30	0.0	B
18		0.50	0.0	B
19	Series	0.00	5	B
20	No. 6	0.10	5	B
21		0.30	5	B
22		0.50	5	B
23	Series	0.00	10	B
24	No. 7	0.10	10	B
25		0.30	10	B
26		0.50	10	B

Note: Mix Type A contains more filament polyester fibers while Mix Type B contains fibrillated polypropylene fibers.

silica fume) was 3.0, and the ratio of sand to gravel was 1.0. This proportioning results in a binder content of 520 kg/m^3 (870 lb/yd^3). The water-binder ratio was 0.45. The amount of superplasticizer was 1.0 percent of the binder by mass. Volume percentages of fiber ranged from 0.0 to 0.60 percent of the total volume.

Mix Type B: Fibrillated Polypropylene Fiber Concrete

The aggregates in Mix B were natural river sand and gravel with a maximum size of 9 mm (⅜ in.). Type I portland cement was used, as were fibrillated polypropylene fibers with the following characteristics (*10*):

- Specific gravity = 0.91
- Tensile strength = 550 to 760 MPa (80 to 110 ksi)
- Elastic modulus = 3500 MPa (500 ksi)
- Fiber length = 12.5 mm (½ in.)
- Melting point = 160°C (320°F)

The mix proportioning technique was also based on mass batching. Silica fume was considered as a partial replacement of cement on an equal-mass basis. In these mixes, the ratio of aggregate (fine and coarse) to binder was 4.0, and of water to binder, 0.41; this resulted in a binder content of 430 kg/m^3 (720 lb/yd^3). The amount of superplasticizer used was 1.0 percent of the binder by mass. The sand-gravel ratio was 1.0. Fiber concrete ranged from 0.0 to 0.50 percent as a volume percentage.

The variations in both Type A and B mixes are given in Table 2; Type A consisted of four series, and Type B had three series.

TABLE 3 Fresh Mix Results

Mix No.	Slump (mm)	Inverted Slump Cone Time (S)	Air Content %
1	250	*	1.0
2	190	9	1.8
3	125	17	3.0
4	45	13	1.7
5	200	*	2.5
6	190	9	2.2
7	125	12	3.0
8	40	13	2.7
9	125	10	2.5
10	50	22	2.7
11	25	24	1.5
12	0	21	3.4
13	0	36	3.2
14	0	55	3.2
15	215	*	2.0
16	235	*	1.5
17	200	*	2.5
18	190	14	4.5
19	200	*	3.0
20	235	*	4.0
21	175	*	4.2
22	50	13	6.0
23	165	*	3.0
24	165	6	3.8
25	65	12	5.2
26	50	14	6.0

* Fresh mixtures flows freely through the inverted cone. Therefore test not applicable.
25.4mm - 1in

Mixing and Testing

A conventional rotary-drum mixer was used to produce the concretes. The workability of the freshly mixed concretes was assessed using the slump and inverted slump methods (*11*). Air content was measured using the pressure method according to ASTM C231. The following specimens were cast and tested for each series:

1. Three prismatic flexural specimens 100 × 100 × 350 mm (6 × 6 × 16 in.) for four-point (⅓ point) flexural load-deflection behavior test over a span of 300 mm (12 in.) according to ASTM C78 and C1018. Load and load-point deflection were measured using a servocontrolled loading machine and two displacement transducers.
2. Two cylindrical specimens 150 × 300 mm (6 × 12 in.) for the compressive stress-strain test using a compressometer (ASTM C39 and C469).
3. Three cylindrical specimens 150 mm (6 in.) in diameter and 62 mm (2.5 in.) in height for the impact strength testing as reported by the American Concrete Institute (*11*).
4. Two cylindrical specimens 100 × 200 mm (4 × 8 in.) for the rapid chloride permeability test according to AASHTO T277.

Curing was under 22°C (77°F) and 100 percent relative humidity for 7 days and under ambient conditions until the testing age of 28 days.

DISCUSSION OF RESULTS

Fresh Mix

The properties of the freshly mixed concrete are given in Table 3. It can be concluded that the use of plastic fibers

TABLE 4 Impact Results

Mix No.	Mix Type	First Crack Strength (No. of blows)	Ultimate Strength (No. of blows)
1	A	16	22
2	A	46	58
3	A	70	90
4	A	87	120
5	A	28	33
6	A	117	129
7	A	75	101
8	A	59	87
9	A	95	121
10	A	73	106
11	A	68	97
12	A	37	59
13	A	66	70
14	A	19	31
15	B	10	14
16	B	17	28
17	B	47	60
18	B	50	71
19	B	9	15
20	B	92	110
21	B	101	112
22	B	144	160
23	B	10	20
24	B	50	66
25	B	65	82
26	B	69	87

decreases the workability of concrete as indicated by the results of the slump and inverted slump cone tests. Polyester fibers appear to have no significant effect on air content. However, polypropylene fibers appear to increase the air content significantly. Silica fume appears to reduce the workability of concrete, as shown by the decrease in slump and the increase of inverted slump cone time.

Impact Resistance

Impact test results are listed in Table 4. It can be seen that plastic fibers in both types of mixes significantly enhance the impact resistance of concrete. Furthermore, adding silica fume at 5 and 10 percent increases the impact resistance even more. It is postulated that this increase is attributed to the improvement in fiber dispersion and in bond between fibers and concrete caused by silica fume. The data indicated that a silica-fume content of 5 percent is optimal for impact resistance. It can also be postulated that the adverse effects on workability, caused by high contents of silica fume or fibers, resulted in the reduction in the impact resistance of the material.

Permeability

Table 5 gives the data obtained from permeability testing. The data indicate that adding synthetic fibers to plain or silica-fume concrete increases the permeability. However, with an increasing silica fume–binder ratio (25 percent for Mix A and 10 percent for Mix B), the effects of fiber on permeability are reversed. The result is that adding fiber to concrete with a high content of silica fume can be beneficial for impermeability. It is thought that this reversal occurred via the improved fiber dispersion caused by the stickiness and cohesiveness of concretes with high silica-fume contents. This advantageous effect of silica fume diminishes as fiber content increases and consolidation becomes a difficulty.

TABLE 5 Permeability Results

Mix No.	Mix Type	Permeability (couloumbs)
1	A	5961
2	A	8384
3	A	6596
4	A	5743
5	A	1692
6	A	2960
7	A	3228
8	A	3962
9	A	978
10	A	768
11	A	1317
12	A	1144
13	A	278
14	A	329
15	B	3162
16	B	6770
17	B	4510
18	B	6796
19	B	1723
20	B	1167
21	B	1160
22	B	1904
23	B	841
24	B	752
25	B	737
26	B	493

Compressive Behavior

Table 6 gives the obtained compressive properties of both types of mix. The compressive toughness index is defined as the total compressive energy absorption (area under the stress-strain curve) divided by the pre-peak energy absorption (area under the stress-strain curve up to the peak stress).

The effects of various contents of polyester fibers and polypropylene fibers on the compressive stress-strain relationships of concrete are shown in Figures 2 and 3, respectively. Each curve represents the average test of three test specimens. Within-batch variations were less than 5 percent.

From Table 6 and Figures 2 and 3, it can be concluded that both polyester and polypropylene fibers improve the compressive toughness of concrete. The polyester fibers appear to cause a slight increase in the compressive strength of concrete, but polypropylene fibers appear to have no significant effect on compressive strength. Furthermore, both types of fiber appear to increase the strain at peak compressive stress.

Figures 4 and 5 illustrate the relationships of compressive strength with silica-fume content for plastic fiber concrete with various fiber volumes. From Figure 4, it can be concluded that silica fume at 5 to 10 percent increases the compressive strength of polyester fiber concrete; at 25 percent, however, no increase is observed, which is attributed to inadequate workability. Optimum silica-fume content appears to be 5 or 10 percent, and optimum fiber content appears to be 0.35 percent. Figure 5 shows that silica fume caused an increase in the compressive strength of polypropylene fiber–reinforced concrete. Optimum silica-fume and fiber contents are as shown in Figure 5: 5 percent and 0.30 percent, respectively.

Flexural Behavior

Figures 6 and 7 present the effects of polyester and polypropylene fiber volume fractions on the flexural load-deflection

TABLE 6 Compression Characteristics

Mix No.	Compressive Strength (MPa)	Compressive Strain at Failure (0.001)	Compressive Toughness Index	Mix Type
1	38.5	16	2.1	A
2	43.5	24	2.1	A
3	41.5	24	2.2	A
4	43.5	33	2.8	A
5	50.5	22	1.5	A
6	51.0	27	2.0	A
7	52.0	32	2.1	A
8	44.0	30	2.2	A
9	49.0	22	2.4	A
10	50.5	26	2.9	A
11	50.0	30	3.3	A
12	43.0	29	2.8	A
13	39.5	21	2.8	A
14	45.0	31	3.3	A
15	39.5	16	1.2	B
16	42.0	19	1.3	B
17	41.0	22	2.0	B
18	38.5	32	1.4	B
19	41.5	21	1.3	B
20	46.5	17	1.8	B
21	50.5	30	1.5	B
22	45.0	32	1.6	B
23	40.0	23	1.4	B
24	45.0	26	1.4	B
25	45.5	29	1.6	B
26	45.5	30	1.5	B

1ksi = 6.89 MPa

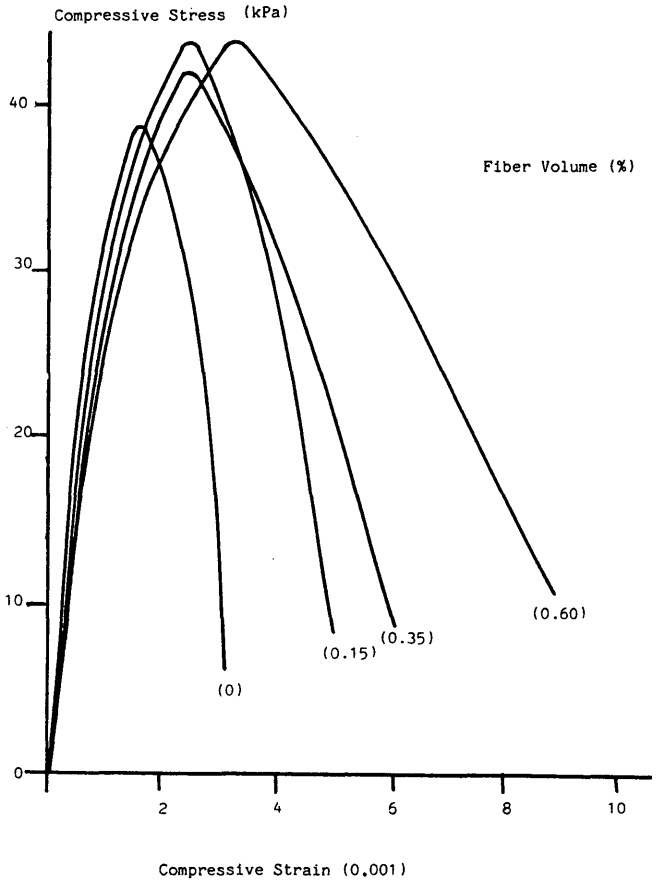

FIGURE 2 Compressive stress-strain behavior of polyester fiber concrete.

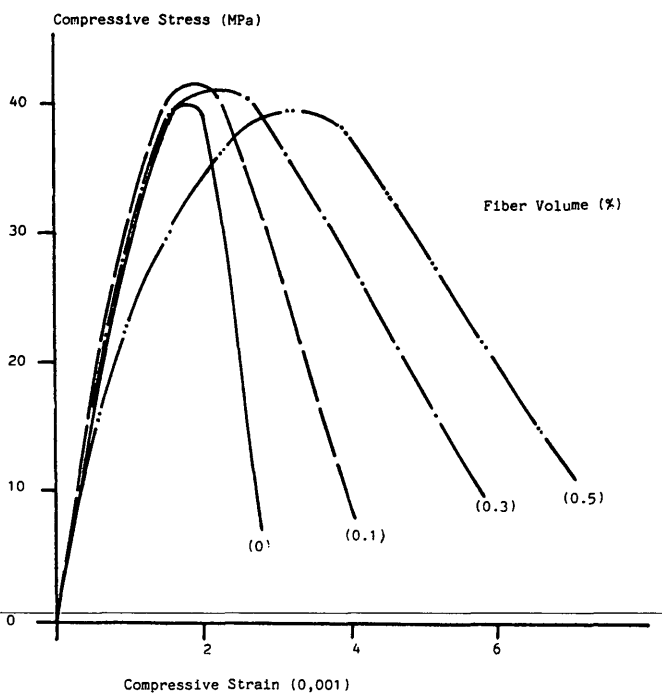

FIGURE 3 Compressive stress-strain behavior of polypropylene fiber concrete.

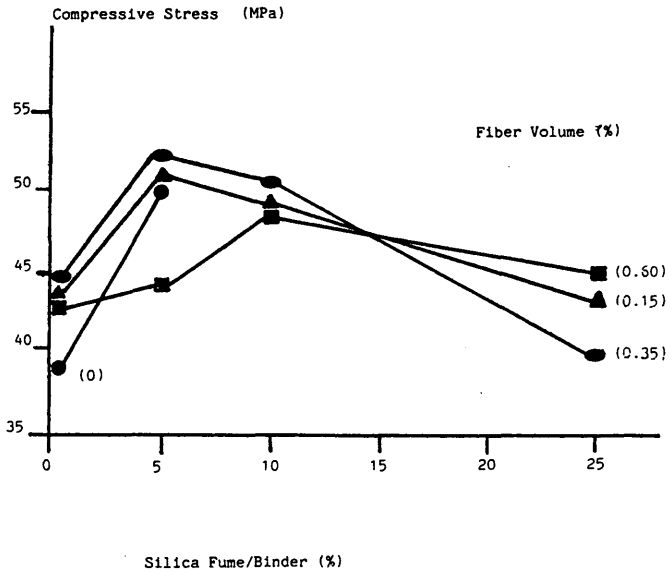

FIGURE 4 Compressive strength of polyester fiber concrete.

FIGURE 5 Compressive strength of polypropylene fiber concrete.

behavior of fiber-reinforced concrete. Each curve is the average of testing on three specimens. Within-batch variations were less than 10 percent. The characteristic flexural properties are listed in Table 7. Ultimate strength is defined as the maximum elastic flexural stress; post-peak strength, as the elastic flexural stress sustained by the specimen in the range beyond the peak load (which remains to some extent constant); and the toughness index, as $I_{5.5}$, according to ASTM C1018.

From Table 7 and Figures 6 and 7, it can be concluded that both polyester fibers and polypropylene fibers affect the flexural strength of concrete. Fibers significantly enhance the ductility of concrete, illustrated by changes in post-peak resistance and flexural toughness. This effect generally continues

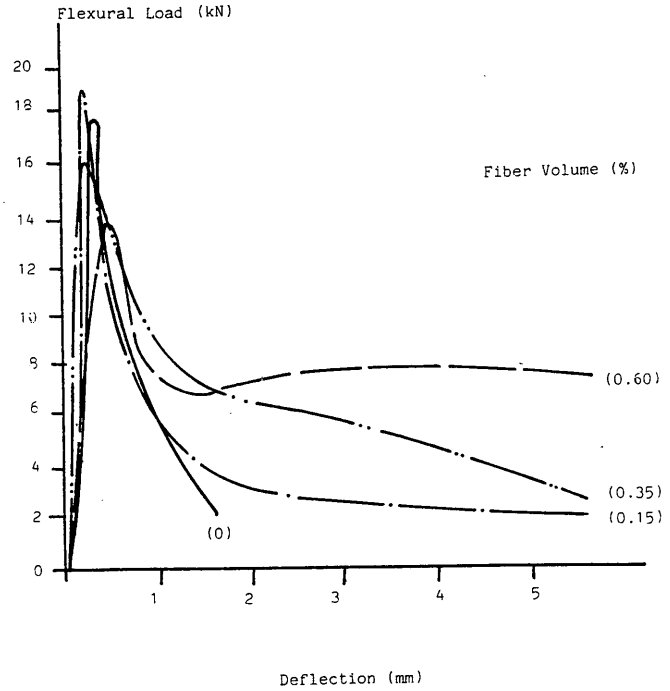

FIGURE 6 Flexural behavior of polyester fiber concrete.

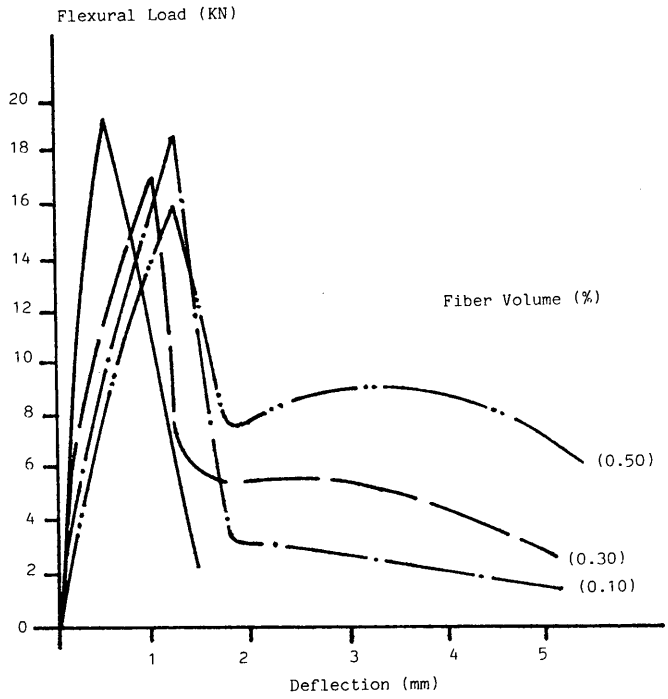

FIGURE 7 Flexural behavior of polypropylene fiber concrete.

TABLE 7 Flexural Characteristics

Mix No.	Ultimate Strength (kPa)	Post-Peak Strength (kPa)	Toughness Index	Mix Type
1	4510	-	2.5	A
2	5510	950	3.9	A
3	4650	1800	4.2	A
4	4270	2090	4.9	A
5	4605	-	2.6	A
6	4415	760	4.2	A
7	4750	1710	4.6	A
8	4270	1950	4.6	A
9	5220	1570	5.3	A
10	4130	2280	5.0	A
11	4510	2470	4.6	A
12	4840	1425	5.0	A
13	4370	1805	4.9	A
14	4035	2330	4.9	A
15	5600	-	1.5	B
16	5175	670	3.1	B
17	5220	1500	4.2	B
18	4415	2060	4.3	B
19	5840	-	1.7	B
20	4370	610	3.0	B
21	4795	1350	4.3	B
22	4795	1990	4.8	B
23	5935	-	1.8	B
24	4320	740	3.5	B
25	4415	1490	4.3	B
26	5030	2430	4.4	B

- Not applicable
1ksi = 6.89 MPa

to increase with increases in fiber volume fraction. Silica fume also appears to have a slight effect on increasing the ductility of fiber concrete. Figures 8 and 9 illustrate the effect of fibers and silica fume in post-peak resistance of concrete.

CONCLUSIONS

From the results of this investigation, the following can be concluded:

1. Both polyester and polypropylene fibers reduce the workability by increasing inverted slump cone time and decreasing slump. This effect is more obvious at higher contents of fibers (0.3 percent or more).
2. There is an increase in the air content of polypropylene fiber–reinforced fresh concrete, especially at a fiber content of 0.5 percent. However, there is an inconsistent effect of polyester fiber on the air content of fresh concrete.
3. Silica fume generally increases inverted slump cone time and decreases slump, which indicates adverse effects on workability.
4. Both types of fiber improve the impact resistance of concrete dramatically.
5. Optimum improvements of impact resistance for polyester fibers occur at a fiber volume of 0.15 percent and a silica-fume content of 5 percent. On the other hand, optimum improvements of impact resistance for polypropylene fibers were observed at 0.50 percent of fiber content and 5 percent of silica-fume content.
6. Fibers have a relatively small favorable effect on compressive strength. Both fibers slightly improve compressive behavior of concrete by enhancing toughness.
7. Use of silica fume enhances the compressive strength and toughness of fiber concrete with an optimum content of 5 to 10 percent.

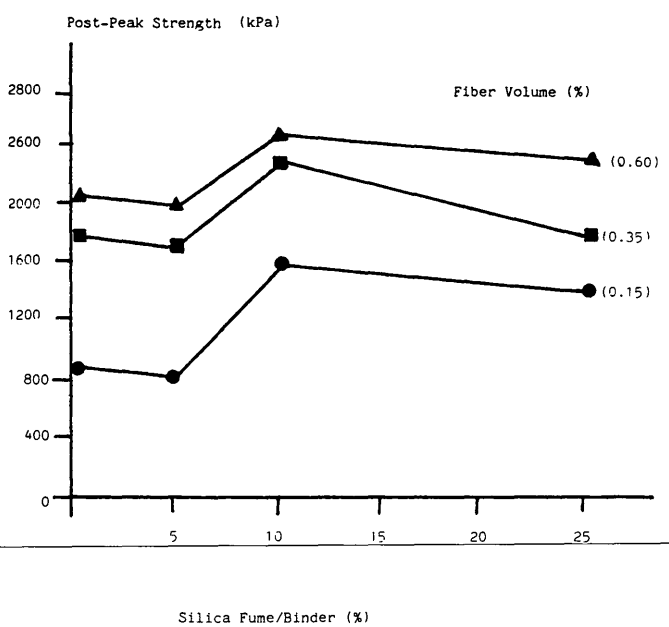

FIGURE 8 Post-peak flexural strength of polyester fiber concrete.

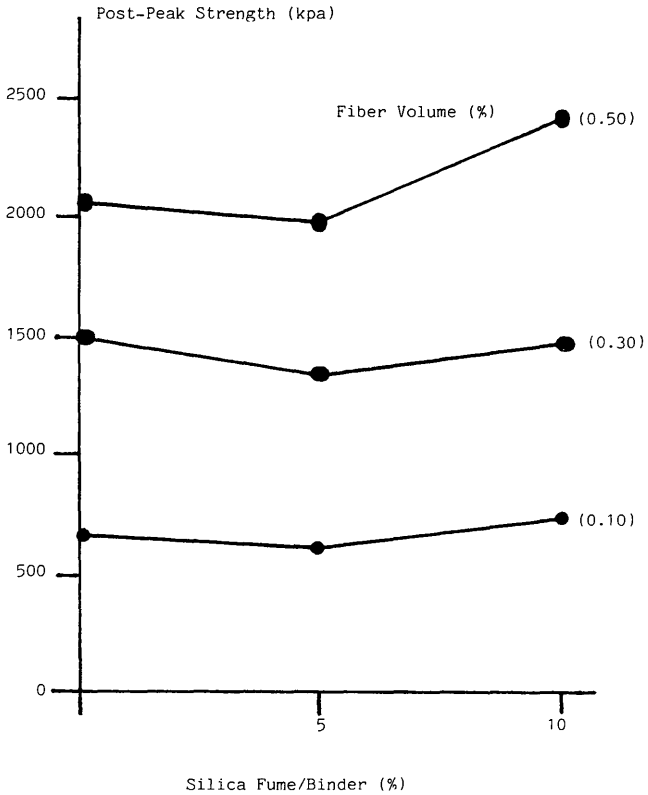

FIGURE 9 Post-peak flexural strength of polypropylene fiber concrete.

8. Polyester fibers and polypropylene fibers have an inconsistent effect on the flexural strength but significantly increase the flexural toughness and post-peak resistance of concrete. These improvements continue as fiber volume increases, except in ultimate strength, for which it starts to decrease beyond fiber volume of 0.35 percent.
9. Silica fume slightly enhances flexural toughness and post-peak strength of plastic fiber concretes.
10. Synthetic fiber–reinforced silica-fume concrete compared with plain concrete shows increases in impermeability, toughness, post-peak flexural strength, and impact resistance. These improvements indicate that such concrete is an alternative for use in pavements, overlays, slabs, grades, and other such applications.

ACKNOWLEDGMENTS

The authors would like to thank the Hoechst Celanese Company, which provided the financial support for this research project. The authors also thank Elkem Materials Company and W. R. Grace & Company for their material contribution for this research investigation.

REFERENCES

1. ACI Committee 226. Silica Fume in Concrete. *ACI Materials Journal*, Vol. 86, No. 2, March–April 1987, pp. 158–166.
2. Z. Bayasi, G. Peterson, and T. Ahn. Mechanical Properties and Durability of Plastic Fiber Reinforced Cement and Concrete.

Proc., Symposium on Advancements in Concrete Materials, Bradley University, Peoria, Ill., 1989, pp. 3.1–3.17.
3. Z. Bayasi and P. Soroushian. Optimum Use of Pozzolonic Materials in Steel Fiber Reinforced Concrete. In *Transportation Research Record 1226*, TRB, National Research Council, Washington, D.C., 1989, pp. 25–30.
4. V. Ramakrishran and V. Srinvasan. Silica Fume in Fiber Reinforced Concrete. *Indian Concrete Journal*, Vol. 56, No. 12, Dec. 1982, pp. 326–334.
5. Z. Bayasi, R. Fuesle, M. Taylor, and H. Helenck. *Silica Fume Effects on the Permeability and Microstructure on Concrete*. Research Report. Bradley University, Peoria, Ill., 1990.
6. A. Naaman, S. Shah, and J. Throne. Some Developments in Polypropylene Fibers for Concrete. In *ACI SP-81: Fiber Reinforced Concrete International Symposium*, American Concrete Institute, Detroit, Mich., 1984, pp. 375–385.
7. M. Buil, P. Witier, F. Delarrard, M. Detres, and A. Paillere. Physical Mechanism of the Action of the Naphthalene Sulfonate Based Superplasticizers on Silica Fume Concrete. In *ACI SP-91: Fly Ash, Silica Fume, Slag and Natural Pozzolans in Concrete*, Vol. 2, American Concrete Institute, Detroit, Mich., 1986, pp. 959–971.
8. *PET Polyester Fibers*. Information brochure. Hoechst Celanese Company.
9. *Microsilica-Typical Analysis*. Product information sheets. Elkem Materials, 1990.
10. *Technical Bulletin on Polypropylene Fibers*. Grace Construction Products, 1990.
11. ACI Committee 544. Measurement of the Properties of Fiber Reinforced Concrete. *ACI Materials Journal*, Vol. 85, No. 6, Nov.–Dec. 1988, pp. 583–593.

Publication of this paper sponsored by Committee on Mechanical Properties of Concrete.

Use of Admixtures to Prevent Excessive Expansion of Concrete Due to Alkali-Silica Reaction

BRYANT MATHER

In the reports of the American Concrete Institute Committee 212 on Admixtures, beginning in 1954, reference was made to the use of admixtures, both chemical and mineral, to prevent excessive expansion of concrete caused by the alkali-silica reaction. Work on this topic began at least as far back as 1947. Few data on the use of admixtures for this purpose in field concrete are known to have been published. Laboratory test results suggest that mineral admixtures are effective in smaller and smaller amounts as the silica content, silica solubility, and fineness increase. Ground granulated iron blast-furnace slag, a hydraulic cement (often incorrectly called a mineral admixture), is highly effective when used to make up 60 percent or more of the cementitious medium. Its effectiveness probably derives from its ability to reduce the permeability of concrete to 1/10 to 1/100 that of concrete of equal strength made using portland cement alone. Similar effects may occur when mineral admixtures are used. The use of chemical admixtures based on soluble salts of lithium has been referred to in the literature for many years and was reexamined in detail by Stark in 1992 in the recent Strategic Highway Research Program project on alkali-silica reaction. It may be technically feasible, but it may not be cost-effective.

To discuss the role of admixtures in preventing excessive expansion of concrete due to alkali-silica reaction, it is first necessary to define some terms and review some of the mechanisms involved in alkali-silica reactions. American Concrete Institute (ACI) 116R-90 defines an admixture as "a material other than water, aggregates, hydraulic cement, and fiber reinforcement, used as an ingredient of concrete or mortar, and added to the batch immediately before or during its mixing." Ground granulated iron blast-furnace slab (ggbfs) is a hydraulic cement, so it is not, by definition, an admixture.

ACI 116R-90 defines alkali-silica reaction as "the reaction between the alkalies (sodium and potassium) in portland cement and certain siliceous rocks or minerals, such as opaline chert, strained quartz, and acidic volcanic glass, present in some aggregates; the products of the reaction may cause abnormal expansion and cracking of concrete in service."

It is not the alkalies that cause the thermodynamically metastable silica to gelatinize, but the high pH of the aqueous phase of the concrete that is created by the association of hydroxide ions with sodium and potassium ions in the solution. This association comes about after the chloride or sulfate or other ions with which the sodium and potassium were associated (before going into solution) have precipitated out in relatively insoluble hydration products such as calcium sulfoaluminate or calcium chloroaluminate.

Structures Laboratory, U.S. Army Engineer Waterways Experiment Station, 3909 Halls Ferry Road, Vicksburg, Miss. 39180.

BACKGROUND

The occurrence of alkali-silica reaction was first reported by Stanton (*1*). However, when ACI Committee 212 on Admixtures published its first report (*2*), the only paper by Stanton that was cited was his 1938 paper on attack by sea water and "alkali" soils (*3*). Although the word "alkali" is used, it is clear that he means sulfate attack. He does report that "durability of a cement can be increased . . . by intergrinding a siliceous admixture [sic] with the cement clinker; even a clinker relatively high in C_3A" (*3*,p.443). This conclusion was based on experiments using portland-pozzolan cements as well as portland cements of differing calculated C_3A content. Some of his cements contained the pozzolan, ground calcined Monterey shale. His fifth conclusion is as follows: "A non-durable standard cement can be made more durable by the use of a good siliceous admixture." The same conclusion could be restated with no change at the end of this paper.

It is worth noting that the paper immediately following the 1944 report of ACI Committee 212 is Tremper's paper "The Effect of Alkalies in Portland Cement on the Durability of Concrete" (*4*).

By 1954, when Committee 212 released its second report (*5*), there were two relevant categories—pozzolans, and . . . alkali-aggregate expansion inhibitors"—and one stated objective of the use of admixtures was "control of alkali-aggregate expansion." In the latter section, it is stated: "certain . . . pozzolans are capable of reducing the expansion caused by high-alkali cements . . . used . . . with reactive siliceous aggregates." The report says that effective pozzolans are those containing "amorphous" siliceous or siliceous and aluminous substances such as opal, certain volcanic glasses, diatomaceous earths, calcined clays, and fly ash. It is also noted that McCoy and Caldwell found lithium salts to be effective (*6*).

RECENT STATUS

The third report was published in 1963 (*7*). Section 8 included a section on the use of finely divided mineral admixtures for reducing expansion caused by alkali-aggregate reaction, and Section 11 discussed chemical admixtures to reduce alkali-

aggregate reaction. In the former it noted that Hanna was the first to recommend using pozzolan to prevent expansion due to alkali-aggregate reaction (*8*). The committee then noted that "there have been only a few instances in which an admixture has been used in concrete containing known reactive aggregates and a known high-alkali cement and the pozzolan relied on to prevent the expected excessive expansion. Performance data on these projects are not available to the committee." I wrote these words. Originally, instead of "only a few" I wrote "no," but I was told that there were "a few." I still have no citations of performance data on them or any others. At the Ninth International Conference on Alkali-Aggregate Reaction in Concrete in 1992, I listened with some care for reports of such cases. There may have been one, as I will discuss later (*9*). There was a report (*10*) that an aggregate now known to be reactive and a cement now known to be high alkali had been used together in more than one construction, at least one of which also contained a pozzolan—the use of which was in no way intended to control expansion by alkali-aggregate reaction, but it had nevertheless done so, not surprisingly. So long as low-alkali cement is not much more expensive per unit quantity than cement not required to be low alkali, there is little or no incentive to establish that there is a more cost-effective method of dealing with alkali-aggregate reaction expansion involving the use of pozzolan or ggbfs.

DANGER OF USING TOO LITTLE POZZOLAN

In the 1963 report a caution was sounded:

> Certain materials when finely divided and of high opal content (e.g., certain diatomaceous earths and opaline cherts) will prevent expansions when used in amounts of less than 15 percent by weight of the cement. In proportions of 10 percent or less by weight of the cement, certain pozzolans may increase expansion of concrete containing reactive aggregate and high-alkali cement, presumably because interaction of a portion of the cement alkalies with the pozzolan produces a ratio of reactive silica to the available alkalies which more closely approaches the pessimum for formation of expansive alkali-silica gel.

No reference was given. This problem has received little reported attention since 1963, but it has remained to worry people.

Helmuth said,

> If the quantity of reactive aggregate is very large or if the specific surface is very high, the available alkalies are distributed in low concentration over the reactive surfaces and the expansion rate is very low. If there is very little reactive aggregate or aggregate surface for reaction of alkali, the rate of expansion is also reduced. At a certain proportion, dependent on aggregate type and fineness, the expansion will be at a maximum; this is referred to as the "pessimum" proportion. Maximum expansion may occur with small proportions of highly reactive material. This is the reason for the 15% lower limit of pozzolan content of ASTM Type P and IP cements and for the six tests for alkali reactivity of pozzolans in Type I (PM) [pozzolan-modified] cements in ASTM C595 (See Table 1.3) (*11*).

ASTM C595-89 provides in Section 10.1.13 ["Mortar Expansion of Pozzolan for Use in Pozzolan-Modified Portland Cement Types I (PM) and I (PM)–A"] that

> using the pozzolan and the clinker or cement that are to be used together in the production of the blended cement, prepare pozzolan-modified portland cements containing 2.5, 5, 7.5, 10, 12.5, and 15 weight [sic] % of the pozzolan. These blends shall be tested in accordance with Test Method C 227 using a sand judged to be a nonreactive by the mortar bar test in Test Method C 227. The expansion of the mortar bars shall be measured at 91 days and all the six blends shall meet the expansion requirement of Table 3.

The requirement of Table 3 is "mortar bar expansion at 91 days, max, % 0.05."

Popovics says that expansion can be prevent by replacing "a portion of the cement with certain fine powdered materials containing reactive silica, such as pozzolan, in the quantity of 20 g of reactive silica for each gram of alkali in excess of 0.5% of the weight of cement (Powers & Steinour, 1955 [*12*]; Mehta & Polivka, 1976 [*13*])," but "note that inadequate amounts of reactive silica would increase, rather than reduce, the expansion" (*14*,p.217). Vivian reported that the maximum expansion of mortar bars with amounts of opaline rock ranging from 0.02 to 40.0 percent took place when the amount was 5 percent, that is, about 60,000 particles per bar (versus 240 at 0.02 percent or 480,000 at 40.0 percent (*15*).

ACI 226.3R-87 makes no mention of possible harm resulting from use of too little fly ash but emphasizes throughout the discussion of effects of fly ash on alkali-silica reaction (Section 2.2.13) the need for "suitable quality and quantity," possibly implying a performance basis for selection of amount to use.

Diamond discusses the use of pozzolans to mitigate the effects of alkali-aggregate reactions but does not address the issue that a little could make it worse (*16*). Tuthill wrote

> The amount of pozzolan needed in concrete to control reactive expansion will vary with the individual pozzolan, aggregates, and with the alkali content of the cement. . . . As a safety precaution against the possibility of increased alkali-silica expansion in concretes containing small (pessimum) amounts of certain pozzolans less than 10 percent by weight (sic) of the cement, ACI Committee 212 (Mather, 1971 [*17*]) advises that pozzolans should not be used in amounts less than about 15 percent by weight of total cementitious material (*18*).

The ACI 212 report said, "The use of too small a proportion of pozzolan may actually increase detrimental effects of alkali-silica reaction" (*17*). Its reference is to Stanton, who reported results of tests in which he used finely divided reactive aggregates as pozzolans (*19*). He found that 1½ to 5 percent of ground opaline chert accelerated and magnified the expansion.

In summary, I believe that what this means is never to use fly ash or a natural pozzolan in an amount less than 15 percent by mass of the cementitious material. ASTM Committee C01 should probably revise C595 to delete Type I (PM). Research should be conducted to see whether there are conditions under which small amounts of silica fume (i.e., less than 15 percent by mass of the cementitious materials in concrete) can increase expansion when high-alkali cement is used with reactive aggregate. I am not aware that any research has been reported that shows that this has happened.

1981 STATUS

The 1981 report of ACI 212 (212R-81) discusses the effects of mineral admixtures on expansion caused by alkali-aggregate reaction in 6.10 and chemical admixtures to reduce alkali-aggregate expansion in 7.11. In 6.10 the report says that "almost any pozzolan when used in sufficient quantity is capable of preventing excessive expansion" and cites References 58 and 120: Reference 58 does not deal in any way with alkali-aggregate reaction, and Reference 120 is to Pepper and Mather, who reported results of work using cements of different alkali content and a variety of mineral admixtures, ggbfs, natural cement, and ground quartz (*20*). On the basis of expansion tests of mortar bars with high-alkali cement and Pyrex glass, they found that to reduce expansion by 75 percent at 14 days, the amount of the portland cement that needed to be replaced ranged from 10 to 45 percent by mass. It was shown that the amount of replacement decreased as the silica content, the solubility of the silica in NaOH, and the fineness of the replacement material increased. The Type F fly ashes used required 40 to 44 percent, a very fine synthetic silica glass of 98.6 percent SiO_2 required only 10 percent, and ggbfs needed to be used at 45 percent of the cementitious medium. In 7.11 the committee indicates little change in the state of the art since its 1963 report.

1989 STATUS

In 1989 ACI 212.3R was published, mineral admixtures having been assigned to ACI Committee 232 on Fly Ash and Natural Pozzolans. 212.3R-89 in Section 6.11 speaking of chemical admixtures to reduce alkali-aggregate expansion indicated no change since Committee 212's 1963 report (*7*). ACI 226.3R-87 notes that "some fly ashes . . . may reduce the severity of alkali-silica reactions by reacting with alkali hydroxides that would otherwise be available to attack reactive aggregate constituents." In 2.2.13 the report states: "The use of adequate amounts of some fly ashes can reduce the amount of aggregate reaction and reduce or eliminate harmful expansion" (*21,22*). The effectiveness of a given fly ash can be investigated by using ASTM C441 and C227 or CAN 3-A 23.5-M82. The report notes that some aggregates not regarded as deleteriously reactive by current criteria may be reactive and suggests that "a suitable quality and quantity of fly ash may be used as a general preventive measure." This is one of those rare cases in which taking a "general preventive measure" will almost always reduce rather than increase the cost of the concrete.

CURRENT STATUS

Of the papers in the *Proceedings of the 9th International Conference on Alkali-Aggregate Reaction in Concrete*, the organizing committee classified 22 as dealing with cement replacements and additives. There was one each from China, Egypt, Italy, and the United States (*23*); there were two from France; five each from Canada and Japan; and six from the United Kingdom. The admixtures dealt with included

- Zeolite: 30 percent clinoptilolite blended in the cement is effective (*24*).
- Metakaolin: 10 percent metakaolin replacement of cement is effective (*25*).
- Silica fume: how permanent is the effectiveness? (*26*); combining air entrainment with silica fume decreased expansion more than silica fume alone (*27*).
- Fly ash and silica fume (and ggbfs): a test method involving autoclaving (*28*).
- Fly ash and natural pozzolan (and ggbfs): method for selection of amount used based on expansion at elevated temperature (*29*).
- Fly ash (and ggbfs): cement with 28 percent fly ash was effective (*30*).
- Fly ash: 25 percent or more fly ash was effective (*9*); "fly ash was used (20% replacement) to minimize the risk of [alkali-aggregate reaction] in the Lower Notch Dam built with aggregate proven to be reactive." Rogers was cited: "20% fly ash replacement was used successfully to prevent cracking of concrete containing argillite and greywacke" (*31*). It may be that this is the long-sought-for example of use of a mineral admixture BRYANT intentionally with known high-alkali cement and known reactive aggregate, but I could not find a reported value for the alkali content of the cement used in the Lower Notch Dam.
- Fly ash: all fly ashes studied were effective at 35 percent (*32*).
- Fly ash: two dams were built with reactive aggregate and a cement likely to have been considered low alkali in the United Kingdom: one contained fly ash, not for preventing alkali-silica reaction expansion, although it did; the other did not have fly ash and is showing damage (*10*).
- Silanes: expansion is decreased, most effectively with hexyl trimethoxy silane, which gives the mortar water repellency (*33*).
- Chelation: reaction can be inhibited by chelating the cations adsorbed by the gels (*34*).
- Catalyzed alkali discharge: use of a "crystal breeding type waterproof agent"—sodium silicate, lime, and catalyst—was effective (*35*).
- Nonchloride acclerators: calcium formate, calcium nitrate, sodium benzoate, and sodium nitrite effects were questionable, but future work is indicated (*36*).
- Various chemical admixtures: air-entraining, water-reducing, and high-range water reducing admixtures were tried; there was less expansion due to air entrainment and reduction of cement content (*37*).
- Various chemical admixtures: $CaCl_2$ increased expansion, sucrose decreased expansion but also decreased strength; oxalic acid had little effect (*38*).
- Lithium salts: certain lithium salts are very effective at dosages of about 1 percent (*23*).

I do not comment on the discussions of coatings or the use of ggbfs. As indicated, more attention was given to fly ash than other mineral admixtures. Materials locally available—metakaolin in the United Kingdom and zeolite in China—were reported on favorably, and the chemical admixtures, except for lithium salts, appear to be unlikely candidates.

CONCLUSION

The use of pozzolanic admixtures, especially fly ash, appears to be well established as a means of mitigating or preventing excessive expansion of concrete due to alkali-silica reaction. However, there are few, if any, adequately documented case histories of an owner or engineer deciding to use a known high-alkali cement with a known alkali-silica reactive aggregate plus a pozzolan, relying solely on the pozzolan to prevent damage that would otherwise be expected. The economics and regulatory and environmental benefits of using fly ash are usually such that concrete should contain fly ash in an amount of 25 or more percent of its cementitious medium for reasons unrelated to alkali-silica reaction. Lithium salts are now better understood because of Stark's Strategic Highway Research Program work (*23*) and may well constitute an alternative. The question about silica fume raised by Berubé and Duchesne (*26*) needs to be answered.

ACKNOWLEDGMENT

The author gratefully acknowledges permission from the Chief of Engineers to publish this paper.

REFERENCES

1. T. E. Stanton. Expansion of Concrete Through Reaction Between Cement and Aggregate. *Proceedings*, ASCE, 1940, pp. 1781–1811.
2. Admixtures for Concrete, Report by ACI Committee 212. *ACI Journal*, Vol. 41, 1944, pp. 73–88.
3. T. E. Stanton Jr. and L. C. Meder. Resistance of Cements to Attack by Sea Water and by Alkali-Soils. *ACI Journal*, Vol. 34, 1938, pp. 433–464.
4. B. Tremper. The Effects of Alkalies in Portland Cement on the Durability of Concrete. *ACI Journal*, Vol. 41, 1944, pp. 89–104.
5. Admixtures for Concrete Reported by ACI Committee 212. *ACI Journal*, Vol. 51, 1954, pp. 113–146.
6. W. J. McCoy and A. G. Caldwell. New Approach to Inhibiting Alkali-Aggregate Expansion. *ACI Journal*, Vol. 47, 1951, pp. 693–708.
7. B. E. Foster. Admixtures for Concrete, Reported by ACI Committee 212. *ACI Journal*, Vol. 60, 1963, pp. 1481–1523.
8. W. C. Hanna. Unfavorable Chemical Reactions of Aggregate in Concrete and a Suggested Corrective. *Proceedings*, ASTM, Vol. 47, 1947, pp. 986–1009.
9. B. Q. Blackwell, M. D. A. Thomas, P. J. Nixon, and K. Pettifer. The Use of Fly Ash to Suppress Deleterious Expansion Due to AAR in Concrete Containing Greywacke Aggregate. *Proc., 9th International Conference on Alkali-Silica Reaction in Concrete*, Concrete Society, London, England, 1992, pp. 102–109.
10. M. D. A. Thomas, B. Q. Blackwell, and K. Pettifer. Suppression of Damage from Alkali Silica Reaction by Fly Ash in Concrete Dams. *Proc., 9th International Conference on Alkali-Silica Reaction in Concrete*, Concrete Society, London, England, 1992, pp. 1059–1066.
11. R. Helmuth. *Fly Ash in Cement and Concrete*. Portland Cement Association, Skokie, Ill., 1987.
12. T. C. Powers and H. H. Steinour. An Interpretation of Published Researches on the Alkali-Aggregate Reaction: Part 1—The Chemical Reactions and Mechanism of Expansion; Part 2—A Hypothesis Concerning Safe and Unsafe Reactions with Reactive Silica in Concrete. *ACI Journal*, Vol. 51, 1955, pp. 497–516, 785–812.
13. S. Popovics. *Concrete-Making Materials*. McGraw-Hill, New York, N.Y., 1979.
14. P. K. Mehta and M. Polivka. Use of Highly Active Pozzolans for Reducing Expansion in Concretes Containing Reactive Aggregates. In *ASTM STP-597: Living with Marginal Aggregates*, ASTM, Philadelphia, Pa., 1976, pp. 25–34.
15. H. E. Vivian. The Effect on Mortar Expansion of Amount of Reactive Component in the Aggregate. In *Studies in Cement-Aggregate Reaction. Parts IX–XV*, Bulletin 256, Commonwealth Scientific and Industrial Organization, Melbourne, Australia, 1950, pp. 13–20.
16. S. Diamond. Chemical Reactions Other Than Carbonate Reactions. In *ASTM STP-169B: Significance of Tests and Properties of Concrete and Concrete-Making Materials*, ASTM, Philadelphia, Pa., 1978, pp. 708–721.
17. L. H. Tuthill. Mineral Admixtures. In *ASTM STP-169B: Tests and Properties of Concrete and Concrete-Making Materials*, ASTM, Philadelphia, Pa., 1978, pp. 804–822.
18. Guide for Use of Admixtures in Concrete. *ACI Journal*, Vol. 68, 1971, pp. 646–676.
19. T. E. Stanton. Studies of Use of Pozzolans for Counteracting Excessive Concrete Expansion Resulting from Reaction Between Aggregates and the Alkalies in Cement. In *Symposium on Use of Pozzolanic Materials in Mortars and Concretes*, Philadelphia, Pa., 1950, pp. 178–203.
20. L. Pepper and B. Mather. Effectiveness of Mineral Admixtures in Preventing Excessive Expansion of Concrete Due to Alkali-Aggregate Reaction. *Proceedings*, ASTM, Vol. 59, 1959, pp. 1178–1203.
21. E. R. Dunstan Jr. The Effect of Fly Ash on Concrete Alkali-Aggregate Reaction. *Cement, Concrete, and Aggregates*, ASTM, Vol. 3, No. 2, 1981, pp. 101–104.
22. D. W. Hobbs. Influence of Pulverised-Fuel Ash and Granulated Blast Furnace Slag upon Expansion Caused by the Alkali-Silica Reaction. *Magazine of Concrete Research*, Vol. 34, No. 199, 1982, pp. 83–94.
23. D. C. Stark. Lithium Salt Admixtures—An Alternative Method to Prevent Expansive Alkali-Silica Reactivity. *Proc., 9th International Conference on Alkali-Silica Reaction in Concrete*, Concrete Society, London, England, 1992, pp. 1017–1025.
24. N. Feng, X. Ji, and Z. Yang. Effect and Mechanism of Natural Zeolite for Preventing Expansion Due to AAR. *Proc., 9th International Conference on Alkali-Silica Reaction in Concrete*, Concrete Society, London, England, 1992, pp. 683–689.
25. T. R. Jones, G. V. Walters, and J. A. Kostuch. Role of Metakaolin in Suppressing ASR in Concrete Containing Reactive Aggregate and Exposed to Saturated NaCl Solution. *Proc., 9th International Conference on Alkali-Silica Reaction in Concrete*, Concrete Society, London, England, 1992, pp. 485–496.
26. M.-A. Berubé and J. Duchesne. Does Silica Fume Merely Postpone Expansion Due to Alkali-Aggregate Reactivity? *Proc., 9th International Conference on Alkali-Silica Reaction in Concrete*, Concrete Society, London, England, 1992, pp. 71–80.
27. H. Wang and J. E. Gillott. Effect of Some Chemicals on Alkali-Silica Reaction. *Proc., 9th International Conference on Alkali-Silica Reaction in Concrete*, Concrete Society, London, England, 1992, pp. 1090–1099.
28. J. Duchesne and M.-A. Berubé. Relationships Between Portlandite Depletion, Available Alkalies and Expansion of Concrete Made with Mineral Admixtures. *Proc., 9th International Conference on Alkali-Silica Reaction in Concrete*, Concrete Society, London, England, 1992, pp. 287–297.
29. A. Criaud, C. Vernet, and C. Defossé. Evaluation of the Effectiveness of Mineral Admixtures: A Quick Mortar Bar Test at 150°C. *Proc., 9th International Conference on Alkali-Silica Reaction in Concrete*, Concrete Society, London, England, 1992, pp. 192–200.
30. K. Nakano, I. Ginyama, S. Yoneda, K. Shibasaki, T. Sone, R. Tomita, K. Watada, Y. Murota, Y. Nagao, H. Ushimaya, Y. Tomita, and Y. Murata. Study of Preventive Conditions of Alkali-Silica Reaction. *Proc., 9th International Conference on Alkali-Silica Reaction in Concrete*, Concrete Society, London, England, 1992, pp. 698–705.
31. C. A. Rogers. Alkali-Aggregate Reactions in Ontario. In *Concrete Alkali-Aggregate Reactions*, Noyes Publications, Park Ridge, N.J., 1987, pp. 5–9.

32. M. Berra, T. Mangialardi, A. E. Paolini, and R. Turriziani. Effect of Fly Ash on Alkali-Silica Reaction. *Proc., 9th International Conference on Alkali-Silica Reaction in Concrete*, Concrete Society, London, England, 1992, pp. 61–70.
33. Y. Ohama, K. Demura, and I. Wada. Inhibiting Alkali-Aggregate Reaction with Alkyl Alkoxy Silanes. *Proc., 9th International Conference on Alkali-Silica Reaction in Concrete*, Concrete Society, London, England, 1992, pp. 750–757.
34. L. Hasni and M. Salomon. Inhibition of Alkali-Aggregate Reaction by Non Pozzolanic Treatment. *Proc., 9th International Conference on Alkali-Silica Reaction in Concrete*, Concrete Society, London, England, 1992, pp. 420–431.
35. Y. Kuramoto, Y. Nakamura, and M. Shimamura. Control of AAR by Catalyzed Alkali Discharge. *Proc., 9th International Conference on Alkali-Silica Reaction in Concrete*, Concrete Society, London, England, 1992, pp. 564–569.
36. H. A. El-Sayed and A. H. Ali. Susceptability of Concrete Admixed with Non-Chloride Accelerators to ASR. *Proc., 9th International Conference on Alkali-Silica Reaction in Concrete*, Concrete Society, London, England, 1992, pp. 311–318.
37. M. Nakajima, H. Nomachi, M. Takada, and S. Nishibayashi. Effect of Admixtures on the Expansion Characteristics of Concrete Containing Reactive Aggregate. *Proc., 9th International Conference on Alkali-Silica Reaction in Concrete*, Concrete Society, London, England, 1992, pp. 690–697.
38. H. Wang and J. E. Gillott. Combined Effect of An Air-Entraining Agent and Silica Fume on Alkali-Silica Reaction. *Proc., 9th International Conference on Alkali-Silica Reaction in Concrete*, Concrete Society, London, England, 1992, pp. 1100–1106.

Publication of this paper sponsored by Committee on Chemical Additions and Admixtures for Concrete.

Bond Contribution to Whitetopping Performance on Low-Volume Roads

JAMES D. GROVE, GARY K. HARRIS, AND BRADLEY J. SKINNER

Research was initiated in 1991 as a part of a whitetopping project to study the effectiveness of various techniques to enhance bond strength between a new portland cement concrete (PCC) overlay and an existing asphalt cement concrete (ACC) pavement surface. A 1676-m (5,500-ft) section of County Road R16 in Dallas County, Iowa, was divided into 12 test sections. Techniques used to enhance bond were power brooming, power brooming with air blast, milling, cement and water grout, and emulsion tack coat. As a part of these bonding techniques, two pavement thicknesses were placed, two concrete proportions were used, and two sections were planed to a uniform cross slope. Bond strength was perceived to be the key to determining an appropriate design procedure for whitetopping. If adequate bond is achieved, a bonded PCC overlay technique can be used for design. Without sufficient bond development, an unbonded overlay procedure should be used. The research found that bond was developed in every section, regardless of the bond enhancement technique used. The underlying ACC does contribute to the composite structure and can be considered in the design. The sections on which the underlying ACC contributed the greatest amount of structure to the composite pavement were not the sections with the highest bond strength.

Whitetopping—portland cement concrete (PCC) resurfacing over existing asphalt cement concrete (ACC)—has been used successfully throughout the country. In Iowa, approximately 420 km (260 mi) of whitetopping overlays has been placed, predominantly on the county round system. Projects constructed in 1977 in Boone, Dallas, and Washington counties were regarded as the beginning of whitetopping in Iowa. Nevertheless, an appropriate design methodology has not been determined for the design of the thicknesses of these overlays. The difficulty stems from how to treat the structural contribution of the underlying ACC. If it becomes a part of the monolithic pavement, then a bonded PCC overlay (new PCC bonded to existing PCC) design method using the existing ACC should be appropriate. If no bond is formed, the ACC should be considered as a base and the PCC thickness cannot be reduced. The bond between the PCC and ACC is the key to the way that the two materials act in relation to each other. This interaction determines the appropriate design method. The research investigated that bond and the use of conventional methods to enhance it.

PROBLEM

The whitetopping procedure used in Iowa traditionally has not been concerned with a bond between the old ACC and the new PCC. Current practice is simply to broom the existing ACC surface and then place the new PCC pavement. Past projects have performed very well, but most have been constructed on relatively low volume roads of fewer than 1,000 vehicles a day. To protect against damage to low-volume roads that occasionally experience the extremely heavy loads of large grain wagons and to expand the overlay technique to roads of higher traffic volumes, an appropriate design procedure for whitetopping should be established.

In 1990, four existing county road whitetopping projects were selected and cores tested to determine bond strength. The bond strength was determined through the use of Test Method Iowa 406. This test measures direct shear strength; a photograph of the test collar is shown in Figure 1. Two of the projects were in Boone County (Routes E18 and R18), and two of them were in Dallas County (Routes F31 and P46).

The R18 whitetopping project, constructed in 1981, yielded cores with bond strengths of more than 1380 kPa (200 psi) shear strength. These strengths occurred without special procedures to enhance bonding and established that significant strengths could indeed be achieved. The two projects in Dallas County yielded cores with average shear strengths of about 690 kPa (100 psi). The F31 project was constructed in 1981, and the P46 project was constructed in 1989. As for the cores taken from Boone County E18, constructed in 1982, either they were broken apart at the interface of the ACC and PCC or the ACC was deteriorated to such an extent that testing was not possible.

OBJECTIVE

The primary aim of this research project was to determine what techniques can be used to enhance the bond between the old ACC and the new PCC overlay. If sufficient bond strength is the key to determining an appropriate design technique, the research should also offer a basis for choosing an appropriate whitetopping design procedure.

LOCATION AND EXISTING CONDITIONS

The research project was constructed in Dallas County, Iowa, on County Route R16, from Dallas Center south 7.2 km (4.5 mi) to Ortonville. The original pavement was 6.7-m (22-ft) wide and was built in 1959. It was composed of a 6.4-cm (2.5-in.) ACC surface placed on a 15-cm (6-in.) rolled stone base, over 10 cm (4 in.) of soil base. In 1971 the road received an

J. D. Grove and G. K. Harris, Office of Materials, Highway Division, Iowa Department of Transportation, 800 Lincoln Way, Ames, Iowa 50010. B. J. Skinner, 415 River Street, Adel, Iowa 50003.

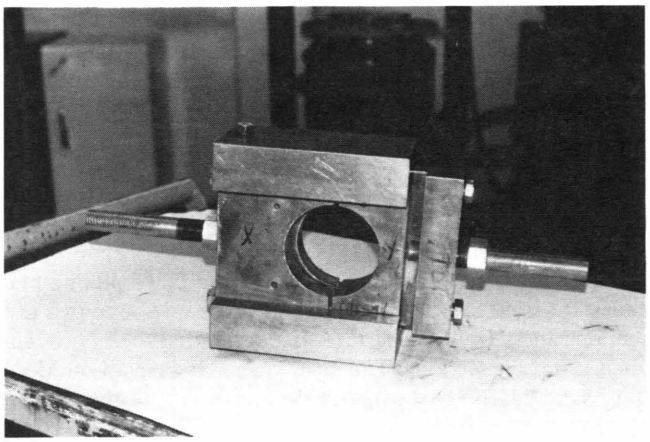

FIGURE 1 Test Method Iowa 406 test collar.

8-cm (3-in.) ACC resurfacing. The traffic on this route ranges from 830 to 1,050 vehicles a day.

The pavement surface was very distorted, with some ruts in excess of 2.5 cm (1.0 in.). There were many cracks in the pavement, both transverse and random, and some areas of alligator cracking.

VARIABLES AND TECHNIQUES TESTED

The research test sections were developed to evaluate several factors. Five variables were tested. Table 1 gives the makeup of each of the 12 sections, and Figure 2 shows the layout of the research.

Surface Preparation

The surface preparation was considered the most important. The current Iowa specification requires only that the surface

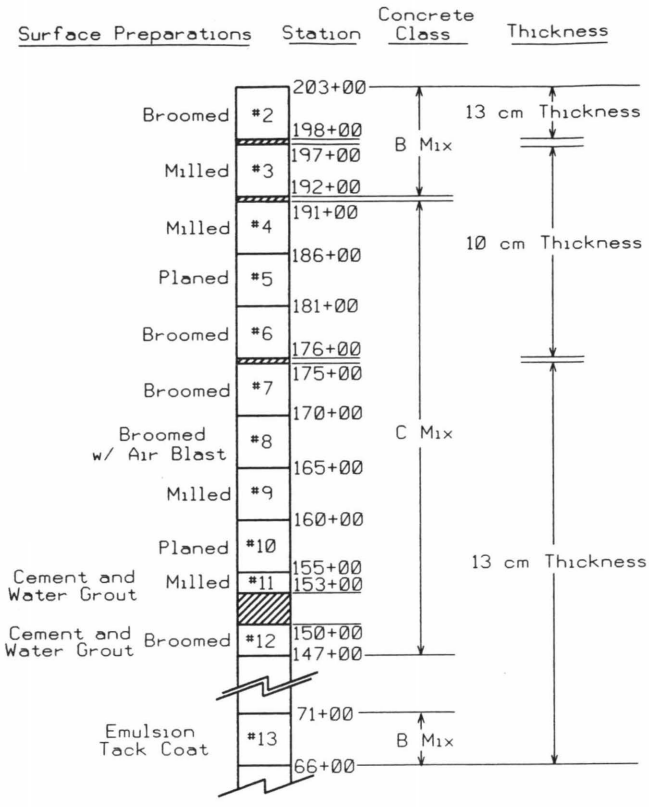

FIGURE 2 Test sections layout (1 cm = 0.394 in.).

of the ACC be power broomed before concrete placement. Therefore, four sections were prepared in that fashion so that the research could be compared with past projects.

Cleanliness is very important with bonded PCC overlays. Therefore, one power-broomed section was also air blasted before concrete placement.

TABLE 1 Section Descriptions

SECTION	SURFACE PREPARATION	BONDING AGENT	PLANING	PCC DESIGN NOMINAL THICKNESS, cm	MIX
2	Broomed	None	No	13	B
3	Milled	None	No	10	B
4	Milled	None	No	10	C
5	Milled	None	Yes	10	C
6	Broomed	None	No	10	C
7	Broomed	None	No	13	C
8	Broomed w/air blast	None	No	13	C
9	Milled	None	No	13	C
10	Milled	None	Yes	13	C
11	Milled	Cement & Water Grout	No	13	C
12	Broomed	Cement & Water Grout	No	13	C
13	Broomed	Tack Emulsion	No	13	B

1 cm = 0.394 in 10 cm = 4 in 13 cm = 5 in

With bonded overlays, the surface is milled or shotblasted to increase the texture of the concrete and help create some mechanical bonding. The same principle was employed, and the surfaces of six sections were milled. The milling was not deep but only roughened the surface.

Bonding Agents

When PCC overlays are bonded to existing PCC in Iowa, a cement and water grout is required. When ACC overlays are placed over existing ACC, a tack coat is used. With this in mind, each of these bonding agents was used on the test sections during placement.

Planing

Whitetopping in Iowa has developed on the premise that rutting in the existing ACC is an advantage. The ruts provide extra PCC thickness in the wheel tracks where the loads are concentrated; they also provide some minor keying action. The resulting lack of uniform overlay thickness has been a point of concern for some. Therefore, two test sections were planed to eliminate the distorted surface and create a uniform cross-section thickness.

Thickness

Dallas County chose to place a nominal 13-cm (5-in.) minimum thickness overlay. If it is assumed that a bond is formed between the old ACC and the PCC overlay, the methodology used for bonded PCC overlays would show that a 10-cm (4-in.) PCC overlay would provide a 20-year life. Sections were constructed of each thickness.

Mix

Two standard Iowa Department of Transportation (Iowa DOT) mixes were used. Traditionally, counties have used a Class B concrete in highway paving. A Class C concrete is required on the primary system, and many counties are now using these proportions for county paving. Therefore, sections with each class of concrete were constructed. See Table 2 for a description of the concrete proportions.

CONSTRUCTION

The contract for this 7.2-km (4.5-mi) PCC overlay was awarded to Cedar Valley Corporation of Waterloo, Iowa. The week of June 17 through 21, 1991, was devoted to preparing the surfaces of the research sections. An Iowa DOT milling machine was used to plane the distorted cross section in two test sections and to mill the surface to a depth that merely roughened it in four sections. The concrete paving began on Monday, June 24, 1991, starting at the north end of the project and progressing southward. The contractor located the batch plant at the south end of the project just north of US-6. The temperature was 28°C (83°F), and winds gusted to 26 km/hr (16 mph).

It was discovered during the construction of Section 6 that the batch trucks tracked dust onto the roadway. The trucks used a rock drive to turn around, and as they backed up to the paver, they tracked dust onto the ACC surface. Unfortunately, the bond strength in this section may have been reduced because of this dust contamination on the surface of the ACC.

The second day of paving, June 25, underwent a considerable change in the weather: the temperature climbed to 31°C (88°F), and wind gusted up to 45 km/hr (28 mph).

A paver malfunction, an intersection at which a high early strength mix was placed, and a section of wet pavement had potential to adversely affect part of Section 10. The portion south of Station 156+00 was not affected and was used for testing.

Sections 11 and 12 involved the use of a cement and water grout as a possible bond enhancer. The grout was delivered in ready-mix trucks, dumped onto the surface, and spread with hand squeegees. In Section 11 the grout was much too dry (like Cream of Wheat), and enough water was not available on site to dilute it to a more fluid consistency. Therefore, only a 61-m (200-ft) section was placed. The grout used in Section 12 was of a proper watery consistency, and placement was much easier. The section was also shortened to 91 m (300 ft) to expedite the paving operation. Tracking of the grout occurred in both sections as the trucks backed into the grouted area as they dumped the concrete. This dried grout from the

TABLE 2 Concrete Proportions

MIX No.	Cement kg per m^3	Fly Ash (Class C) kg per m^3	Fine Aggregate kg per m^3	Coarse Aggregate kg per m^3	Air Entr. Admix. ml/kg	Water Reducer Admix. ml/kg
B-4-C	248	44	952	938	0.54	----
C-4WR-C	298	56	933	914	0.56	2.6

1 kg/m^3 = 1.686 lbs/yd^3

1 ml/kg = 0.015 oz/lb

---- not used

tracking may have actually reduced bond strength in the tracked areas.

Section 13 was placed on Thursday, June 27. The tack coat was applied at approximately 7:30 p.m. on June 26 in an area that would be paved the next morning. Unfortunately, the batch trucks had to back through the tack and it picked up on the tires, and wind had blown dust across the surface during the night. CSS-1H was the only asphalt emulsion available for use.

CONSTRUCTION TESTING

Iowa DOT research personnel performed pre- and postconstruction tests on the project. The tests included rut depth measurements, Road Rater™ (a nondestructive testing device) structural measurements, beam and cylinder strengths, core shear strengths, slump, and entrained air. The air, slump, and strength test results are shown in Table 3. The shear strengths are shown in Table 4.

DISCUSSION OF RESULTS

Testing

The Road Rater was used to determine the structural rating (SR) of the pavement, both before and after the overlay was placed. Two areas of the project were rated before construction, each 1.6 km (1.0 mi) long. The SRs were 2.30 and 2.23. Because these numbers are very similar, it is assumed that they represent the condition of the old ACC on which this project was constructed.

Cores taken from the whitetopped pavement were used to determine the shear strength of the bond at the concrete-asphalt interface. Once this testing was completed, the thickness of the concrete was measured. The shear strengths and the PCC thicknesses are shown in Table 4. The measured SRs of the whitetopped pavement are shown in Table 5.

The 25-ft California profilograph was used to measure the smoothness of the completed overlay. The profile indexes were 4.5 cm/km northbound and 5.0 cm/km southbound.

Structural capacity determination, crack survey, and smoothness measurements will be taken once a year for 3 years and again after 5 years.

Broken Cores

Several cores could not be tested for shear strength because the PCC was not bonded to the ACC or, in some cases, the ACC was broken into pieces. Apparently some cores had been taken over cracks in the ACC or cracked areas. The SRs generally were not measured near these core areas. The Iowa DOT will continue to monitor the overlay for 5 years so that any weakness that may be present, as indicated by the broken cores, will be evaluated. The cores that could not be tested are indicated with a dash in Table 4.

High Bond Strength

The average shear strengths at the bond interface of the cores tested in each test section are given in Table 6. Four sections demonstrated an average shear strength significantly greater than the other sections. Of those, three were milled before PCC placement. The other was the broomed section that was air blasted just before placement. The other three milled sections produced shear strengths in the midrange of all strengths. It appears that milling yielded better shear strength and that air blasting helped to increase that strength.

Lowest Bond Strength

The section on which a tack coat was applied yielded a significantly poorer bond than the other sections. Having like electrical charges, the cationic emulsion and limestone in the concrete may have inhibited bond strength. The tack picked up on the truck tires and the dust blown onto the surface of the tack may also have reduced the bond strength.

TABLE 3 Strength Test Results

Section	Sample ID	Mix	% Air	Conc. Slump (cm)	28-Day Compression Strength (MPa)	28-Day Flexural Strength (MPa)
2	25-1-A	B	7.4	6.5	23.2	4.34
2	25-2-A	B	6.0	5.5	26.8	4.52
3	25-3-A	B	6.3	5.0	26.5	4.60
4	25-1-B	C	7.2	6.5	27.8	4.75
5	25-2-B	C	7.5	6.5	28.4	4.75
6	25-3-B	C	9.5	7.5	26.3	4.56

Flexural Strength is centerpoint loading

1 cm = 0.394 in

1 MPa = 145 psi

TABLE 4 Core Information

Section	Core No.	Lane	Lateral Location	Measured Core Length (cm) ACC	PCC	Shear Strength (kPa)
2	1	SB	1/4 PT	13.5	12.7	----
	1B	NB	OWP	15.0	12.4	950
	2	SB	OWP	13.2	10.2	----
	3	NB	OWP	15.2	13.0	----
3	4	NB	OWP	7.6	11.4	1500
	5	NB	OWP	15.2	10.7	1100
	6	SB	1/4 PT	13.2	11.4	1300
4	7	NB	1/4 PT	14.0	11.2	1350
	8	SB	1/4 PT	13.0	11.2	1250
	9	SB	OWP	13.7	11.7	950
5	10	NB	OWP	14.0	12.2	2350
	11	NB	1/4 PT	12.2	12.4	1050
	12	SB	OWP	14.7	12.4	1100
6	13	SB	1/4 PT	12.4	9.2	650
	14	SB	OWP	17.3	10.9	1000
	15	NB	OWP	2.0	11.2	----
7	16	NB	OWP	15.2	14.5	1300
	17	NB	1/4 PT	15.2	13.3	----
	18	SB	OWP	12.7	13.7	250
8	19	NB	OWP	15.2	13.7	1850
	20	SB	OWP	14.5	12.7	900
	21	SB	1/4 PT	13.5	12.2	750
9	22	NB	OWP	16.0	13.0	1050
	23	NB	1/4 PT	15.2	13.0	950
	24	SB	OWP	14.0	13.0	800
10	25	SB	OWP	15.2	15.2	850
	26	SB	1/4 PT	14.0	16.5	1100
	27	NB	OWP	15.5	15.0	800
11	28	NB	OWP	15.7	14.0	950
	29	NB	1/4 PT	15.2	11.4	1050
	30	SB	OWP	12.4	16.0	----
12	31	NB	OWP	14.5	13.5	1200
	32	SB	1/4 PT	16.8	11.7	650
	33	SB	OWP	16.5	14.0	----
13	34	NB	OWP	14.5	13.0	650
	35	NB	1/4 PT	13.5	12.0	450
	36	SB	OWP	9.7	14.2	700

NOTE: NB = northbound, SB = southbound, 1/4 PT = quarter point, OWP = outside wheelpath

1 cm = 0.394 in 1 kPa = 0.145 psi ---- Broken Core

Structural Contribution of Old ACC

Iowa uses the Road Rater as a nondestructive testing device to measure the pavement structure. Measurements are reported as SRs. During the original calibration of the Road Rater, a calibration coefficient of 0.5 was developed for new PCC pavement. It can be used to convert between SR and effective thickness. The Road Rater measurements are taken along outside wheel tracks. Two of the three sample cores also were taken in this location in each test section. The lengths of the PCC portions of these two cores were averaged and are shown in the second column of Table 5. A theoretical SR was then determined for this average value and is shown in the third column. The average measured SR for the whole test section is shown in Column 4. This is the SR for the total whitetopped section, which includes the PCC overlay and the

TABLE 5 Structural Ratings

Section	Avg. PCC Thickness (wheel path, cm)	Theoretical Structural No. From PCC Thickness	Average Measured Structural Rating of Whitetopped Section	Structural No. of Contribution From Original ACC
2	12.6	2.48	3.86	1.38
3	11.0	2.16	3.31	1.15
4	11.4	2.24	3.38	1.14
5	12.3	2.42	3.50	1.08
6	11.0	2.16	3.70	1.54
7	14.1	2.78	4.03	1.25
8	13.2	2.60	3.95	1.35
9	14.2	2.80	4.31	1.51
10	15.1	2.97	4.76	1.79
11	15.0	2.95	4.21	1.26
12	13.7	2.70	4.16	1.46
13	13.6	2.68	3.65	0.97

1 cm = 0.394 in

TABLE 6 Contribution of Old ACC and Shear Strength by Section

Section	Contribution of Old ACC (SN)	Average Shear Strength (kPa)	Section	Contribution of Old ACC (SN)	Average Shear Strength (kpa)
10	1.79	900	5	1.08	1500
6	1.54	800	3	1.15	1300
9	1.51	950	8	1.35	1200
12	1.46	900	4	1.14	1150
2	1.38	950	11	1.26	1000
8	1.35	1200	2	1.38	950
11	1.26	1000	9	1.51	950
7	1.25	800	12	1.46	900
3	1.15	1300	10	1.79	900
4	1.14	1150	6	1.54	800
5	1.08	1500	7	1.25	800
13	0.97	600	13	0.97	600

1 kPa = 0.145 psi

old, underlying ACC. If the PCC SN is subtracted from the total SR (Column 4 minus Column 3), the result is the theoretical SN for the contribution to the structure by the old ACC. This value is shown in the fifth column.

These values, which represent the contribution of the old ACC, are significant. They demonstrate that in all sections, sufficient bond had been developed for the ACC to contribute to the structure, regardless of bond enhancement.

The SRs for the ACC before construction were 2.30 and 2.23. The contribution of the ACC to the whitetopped section ranged from 1.70 to 0.97. Therefore, not all the ACC structure is used as structure in the new whitetopped pavement. But in all but two sections, the SR of the contribution of the old ACC is more than half the SR of the original ACC pavement.

Design Methodology

One aspect of this research was to determine the appropriate methodology for whitetopping. Iowa's current whitetopping design methodology considers the ACC as support for the PCC pavement. In the research, pavement structure was measured before and after the placement of the overlay. These tests revealed a partial contribution to the structure of the overlaid pavement by the original ACC pavement.

Bonded overlay design methods, on the other hand, consider the original pavement and the overlay to be monolithic. In a bonded overlaid pavement, the structure is the sum of the effective contribution of the original pavement and the overlay.

Neither Iowa's whitetopping design procedure nor current bonded overlay methods are appropriate for whitetopping design. A new design methodology is needed that considers the PCC-to-ACC bond at the interface and that uses the partial contribution of the existing ACC structure.

Bonding Enhancement

The test sections of this research were constructed to determine the most effective bond enhancement techniques. As discussed, milling and air blasting tend to increase the shear strength.

Bond Importance

When the data were analyzed, a very interesting feature became evident. Four sections had superior shear strengths. When the sections that demonstrated the highest use of the underlying ACC were ordered from best to least (Table 6), none of the top four shear strength sections was among the top five in highest contribution of the old ACC. In fact, the section with the best average shear strength yielded the second smallest contribution of effective thickness of the old ACC.

When this research was begun, it was assumed that bond was the key factor in the degree of use of the underlying ACC. Instead, it was discovered that a high structural contribution of the existing ACC does not correspond to a high shear strength at the PCC-ACC interface. The bond enhancing techniques have been evaluated, but they are not necessary to developing adequate bond.

Both the old ACC and new PCC overlay do contribute to the structure. The only bond necessary is that which anchors the PCC to the old ACC in order to use some of the underlying structure. This discovery is important. It provides insight into the reason that the more than 420 km (260 mi) of whitetopping in Iowa, which has not used bond enhancement techniques, has been very successful anyway. Some of these projects are now 15 years old.

CONCLUSIONS

1. The tack coat may reduce bond strength when a cationic emulsion is used.
2. The sections that used cement and water grout showed no significant advantage in bond strength or contribution of the old ACC when compared with all test sections. Thereby, using grout does not justify the extra handling problems and the interference with the paving operation.
3. Milling and air blasting generally produced enhanced bond strengths.
4. Bond strength did not directly relate to the structural contribution of the existing ACC. The bond enhancement techniques evaluated in this research could increase the bond, but that increase did not relate to increased structure.
5. Current bonded overlay design procedures are not appropriate for whitetopping. On the other hand, the existing ACC does contribute to the structure without special surface preparation, and a structural contribution from the ACC should be considered in the overlay thickness design. This research would suggest that, conservatively, half of the existing ACC contributes to the structure of the final composite pavement.

FUTURE RESEARCH NEEDS

This research established that the ACC does contribute to the structure of the final whitetopped pavement. The degree of this contribution can be determined for this project, but further study is needed to determine the contribution to the structure of the final pavement for various thicknesses of existing ACC. This determination will allow proper design techniques to be used for whitetopping design.

Even though bond was achieved in all sections, higher traffic loadings may produce stresses that exceed the stress limits of the bond. Research is needed to determine the limits of traffic loadings as they relate to bond strength, providing an upper limit for traffic loadings past which the ACC could not be used as part of the pavement structure.

ACKNOWLEDGMENTS

The research project was sponsored by the Iowa Highway Research Board and the Iowa DOT. Funding for the project came from the Secondary Road Research Fund. The authors want to extend their appreciation to the Dallas County Board of Supervisors, the Iowa DOT, the Iowa Concrete Paving Association, and Cedar Valley Corporation for their support in the development and implementation of the project.

Publication of this paper sponsored by Committee on Rigid Pavement Construction and Rehabilitation.